G. Ghisellini, G. Tosti, S. Ciprini

Contribution Proceedings of the
4th ENIGMA Meeting

October 6-8, 2004 – Perugia, Italy

Organized by the teams of Brera Observatory and Perugia Observatory

4th ENIGMA Meeting
held in Perugia, Italy, October 6-8, 2004
Local Organisation: Gino Tosti, Stefano Ciprini
Scientific Organisation: Gabriele Ghisellini
Editors of Proceedings: Gabriele Ghisellini, Gino Tosti, Stefano Ciprini
Network Coordinator: Stefan Wagner
Organising Institutions: - INAF Brera Astronomical Observatory (Milano, Italy),
- Perugia University Astronomical Observatory (Perugia, Italy)

The European Network for the Investigation of Galactic nuclei through Multifrequency Analysis (ENIGMA) is a Research Training Network funded within the FP5 program of the European Community

Network Coordinator: Stefan J. Wagner

Summary

Special Session on GRBs and Future Missions (Tasks 3, 6)

- Gabriele Ghisellini: The blazar-GRB connection
- Gino Tosti: The GLAST Gamma Ray Observatory
- Claudia Cecchi: Wavelet Method for Source Detection in GLAST
- Marco Tavani: Gamma-Ray and X-Ray Astrophysics AGILE
- Filippo Zerbi: The REM Observatory
- Gianpiero Tagliaferri: SWIFT a Panchromatic Gamma Ray Burst Mission
- Nicola Masetti: Multiwavelength Afterglows of Gamma-Ray Bursts
- Apostolos Mastichiadis: The Supercritical Pile Model for GRBs

The Multifrequency Campaign on 0716 (Tasks 1, 2, 3, 4)

- Stefan Wagner: Multifrequency Campaigns
- Luisa Ostorero: The ENIGMA-WEBT Campaign on S5 0716+71: Update on the Core-Campaign Multifrequency Observations
- Niall Smith: Fast Optical Variation in 0716+714
- José Gracia: The INTEGRAL View on the 0716+714/0836+710 Field - a First Glimpse
- Silke Britzen: Current Status of the Bonn INTEGRAL Activities
- Johannes Ohlert: 0716 measurements with the Trebur -1 Meter -Telescope

Other Multifrequency Campaigns (Tasks 3, 4)

- Claudia Raiteri: The Multifrequency WEBT-ENIGMA Campaign on AO 0235+16
- Markus Böttcher: The Multifrequency WEBT-ENIGMA Campaign on 3C 66A
- Stefano Ciprini: The ENIGMA Web-Archive

Radio and Optical Observations (Tasks 2, 4)

- Jochen Heidt: 2QZJ 215454.3-305654: a Radio-Quiet BL Lac Object or Lineless QSO ?
- Stefano Ciprini: Optical Behaviour of the Blazar PKS 0735+178 from a Ten-Years Observing Monitoring
- Boris Sbarufatti: Optical Spectroscopy of BL Lac with ESO VLT+FORS1
- Andreas Papageorgiou: Helical Magnetic Fields in Parsec-Scale Radio Jets
- Ilona Torniainen: Long Term Variability of Inverted-Spectrum Sources
- Mirko Tröller: Host Galaxies of Compact Step Spectrum Radio Sources
- Uwe Bach: An Update Study on BL Lacertae
- Emmanouil Angelakis: Elimination of Foreground Sources in the CBI Fields: Status Report and Results
- Lars Fuhrmann: Seasonal Cycles in IDV Blazar Cores and new Projects as ENIGMA Post-doc

High Energies and Theory (Tasks 3, 4, 5, 6)

- Leo Takalo: High Energy Observations and Multifrequency Campaigns
- Dimitrios Emmanoulopoulos: X-ray Variability Studies of TeV Blazars
- Dimitrios Emmanoulopoulos: Update on the October-November 2003 X-Ray Observations of PKS 2155-304
- Krzysztof Katarzynski: Evolution of the Synchrotron Peak in the TeV Blazars
- Fabrizio Tavecchio: Small/Large Scale Jet Connection
- José Gracia: Enigmas from Jet Formation Processes
- Nektarios Vlahakis: Magnetohydrodynamic Interpretation of Superluminal Jet Kinematics
- Massimo Fiorucci: Variability in blazars: Comparison of Mathematical Models with Optical Observations

Tasks legend:
1) Towards Automated, Fast, and Accurate Photometry
2) Separating Intrinsic and Extrinsic Intraday Variability
3) Radiation Processes at High Energies
4) Variations of Source Structure and Flux
5) Particle Acceleration in MHD Outflows
6) The Power of Jets

Pages layout:

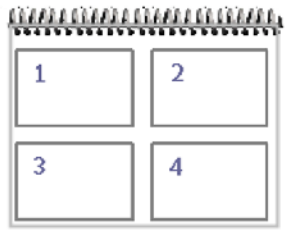

Special Session on GRBs and Future missions

The blazar-GRB connection

gabriele@merate.mi.astro.it - Osservatorio di Brera

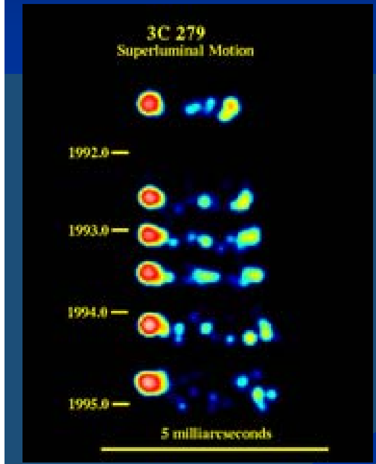

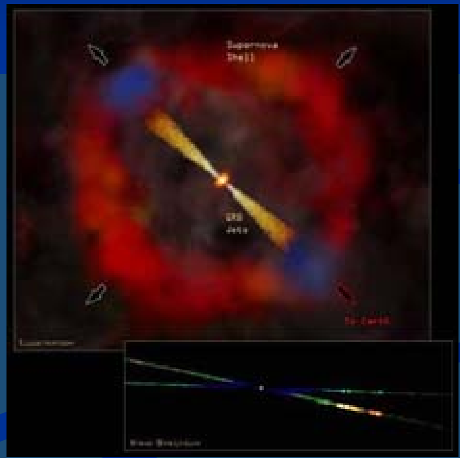

Why to compare GRBs and blazars?

- Relativistic bulk motion
- Transformation of bulk into random energy, and then into radiation
- Collimation
- GRBs are LONG LIVED !...... The prompt emission can last for ~10^4 dynamical times (equivalent to ~300 years for an AGN)

→ Same engine?

GRBs

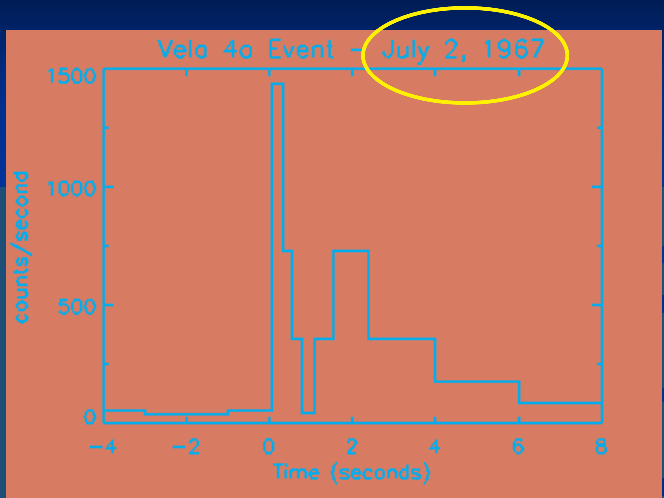

Variability

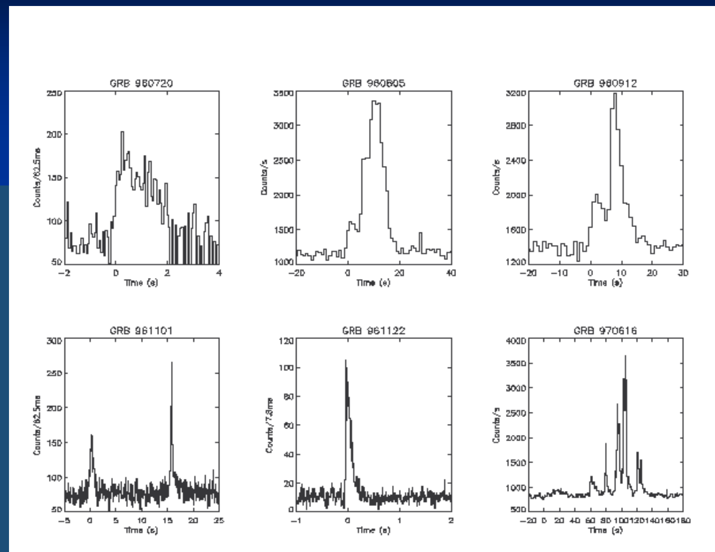

Record holder

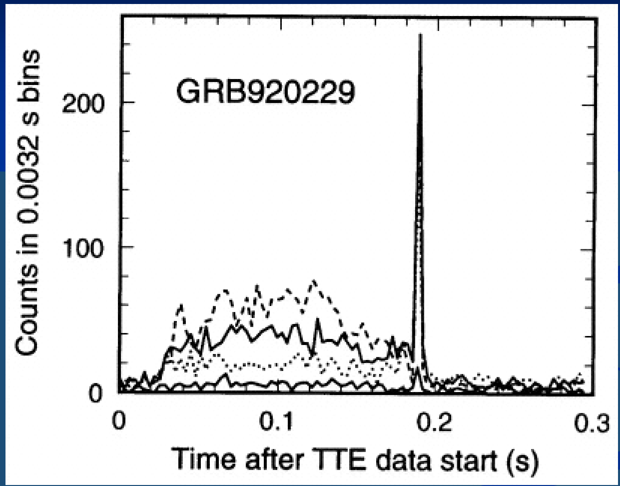

Spike lasting

0.2 millisecond

Schaefer et al. 1999

Long and short

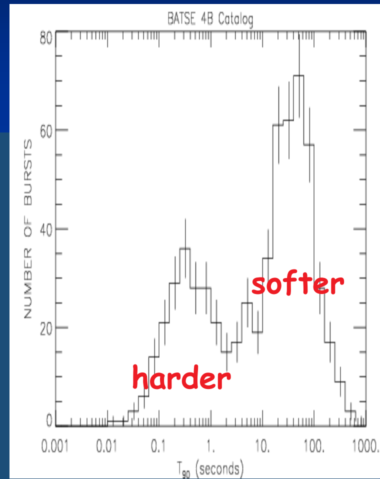

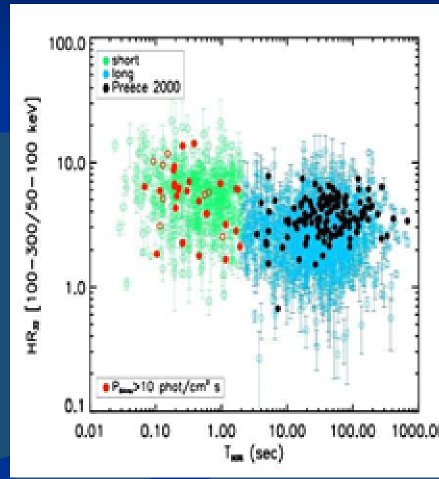

Spectra

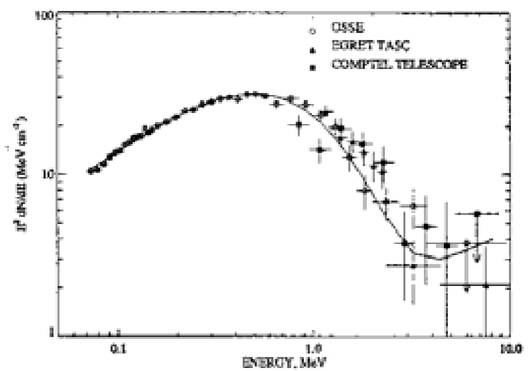

Figure 9 The spectrum of GB 910601 observed over a wide energy range, as measured by three experiments on CGRO (Share et al 1994). A typical broad spectrum with a peak power at about 600 keV is seen. (The fitted spectral up-turn above 4 MeV is not significant.)

Fishman & Meegan 1995

High energy emission

18 GeV

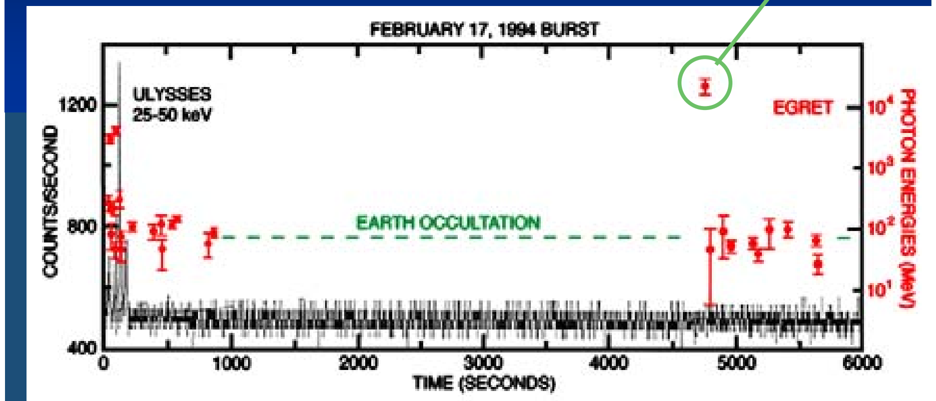

1.5 hours

BeppoSAX breakthrough

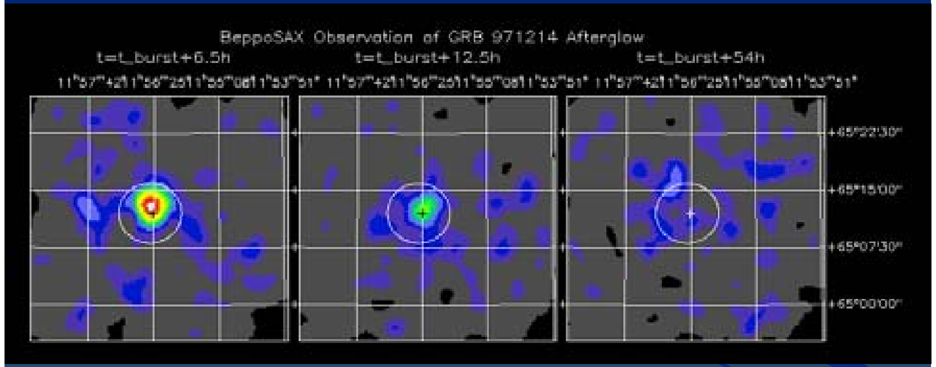

X-ray Afterglow ➡ Precise location

Redshift and Power

If emission is isotropic

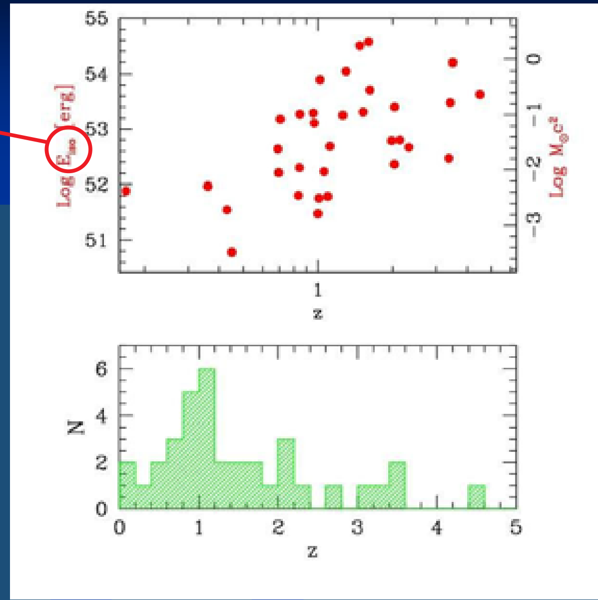

Why Γ >100 ?

1) If not, huge density of gamma-rays: they interact ($\gamma\gamma \rightarrow e^+e^-$), no γ survives

2) If not, fast variability cannot be explained: the source becomes transparent at R~10^{13} cm, corresponding to t_{var}~R/c~300 seconds.
With Γ =100, t_{var} ~ R/(cΓ^2)~30 ms.

3) Theory: huge energy, small volume, large pressure, big acceleration

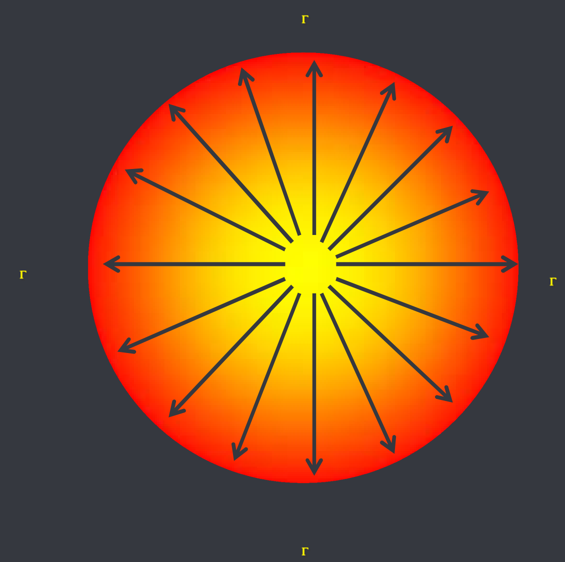

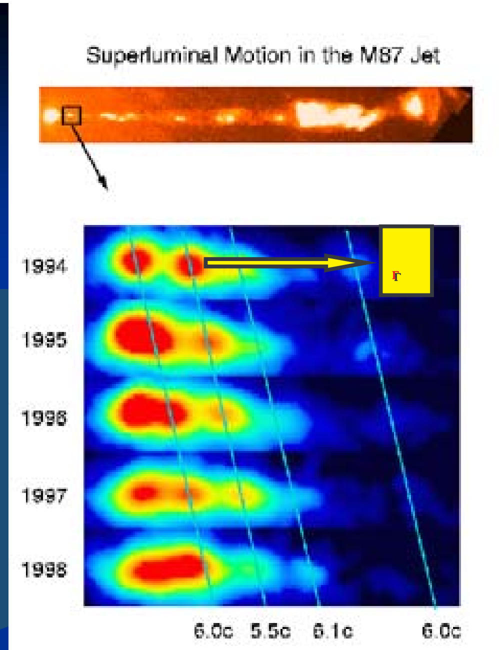

Spheres or jets?

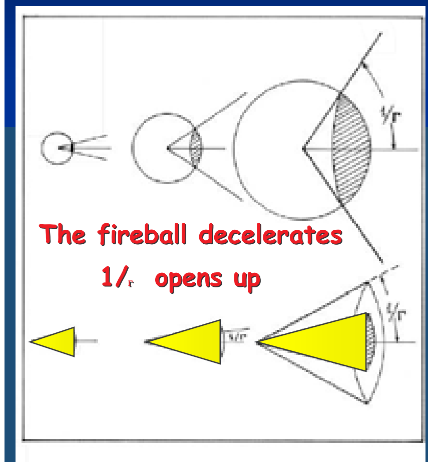

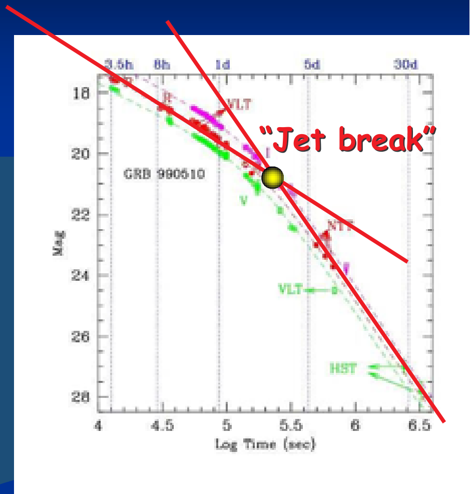

"True" energetics

Frail et al. 2001

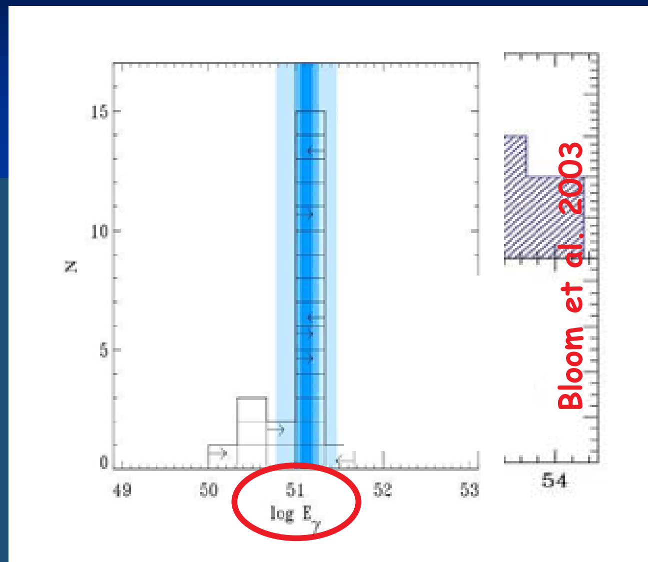

Structured jets?

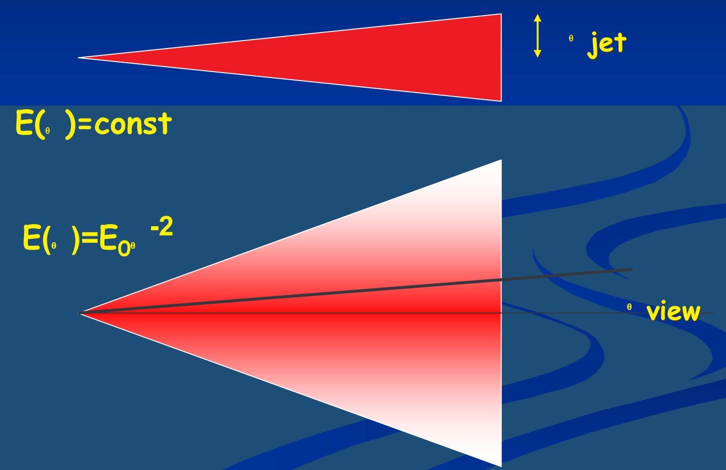

Progenitors: massive star-SN Ic?

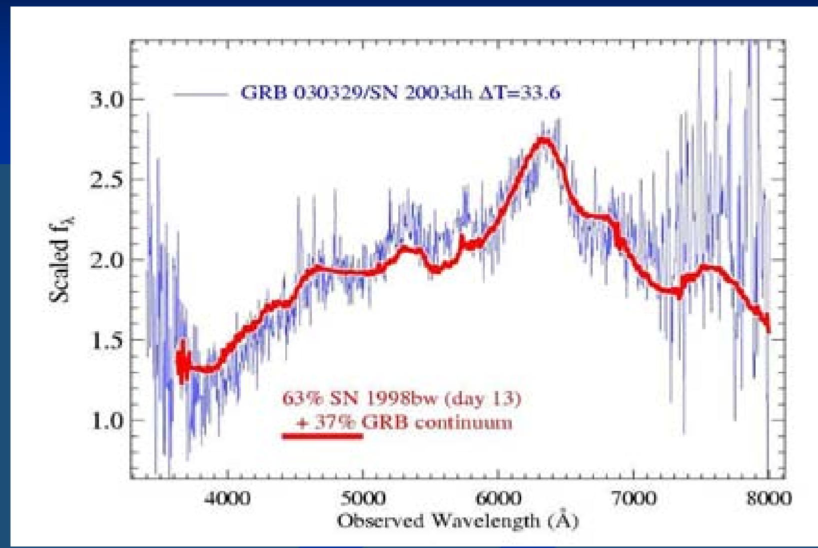

Matheson et al. 2003 (astro-ph/0307435)

Best buy model

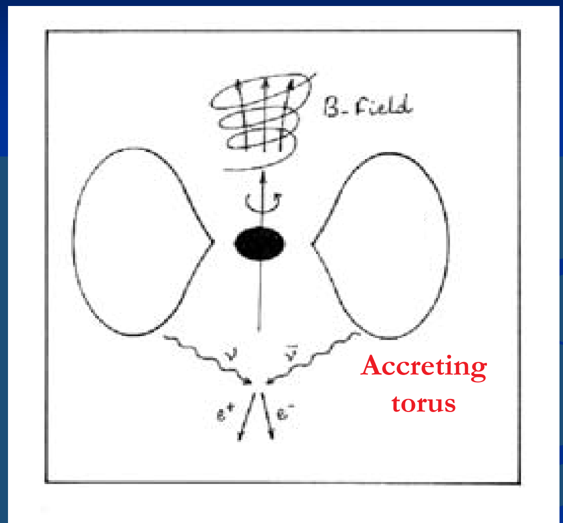

The core collapes. Formation of a BH and a dense torus, sustaining a B-field of order 10^{14}-10^{15} G.

Most of energy: spin of the black hole ($0.29 M_{BH} c^2$)

Outflowing/inflowing mass rate

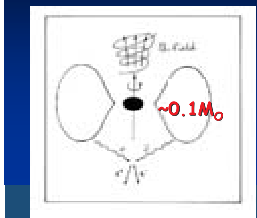

$L_{out} = \dot{M}_{out} \; c^2$

$\dot{M}_{in} \sim M_{Torus} / t_{burst}$

$$\frac{\dot{M}_{out}}{\dot{M}_{in}} \sim \frac{L_{out} \; t_{burst}}{\; M_{Torus} c^2} \sim 0.005 \frac{E_{burst,52}}{\; {}_2 M_{Torus,-1}}$$

For blazars: $L_{disk} = \; \dot{M}_{in} c^2$

$$\frac{\dot{M}_{out}}{\dot{M}_{in}} \sim 0.01 \; {}^{-1} \frac{L_{out}}{\; {}_1 L_{disk}}$$

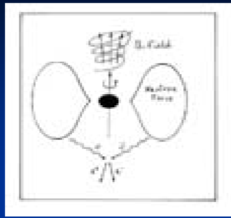

The ultradense torus could sustain a large magnetic field, of the order of 10^{14}-10^{15} Gauss.

With this B-field, B-Z becomes possible

$L_{BZ} \sim 6\times10^{46} a^2\, M_9^2\, B_4^2$ erg s^{-1} (blazars)

$L_{BZ} \sim 6\times10^{50} a^2\, M_1^2\, B_{14}^2$ erg s^{-1} (GRBs)

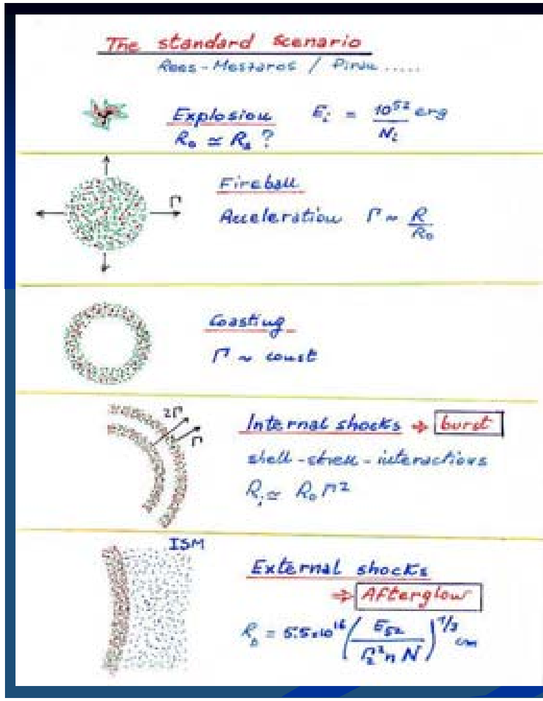

"The" model: Internal/External Shocks

Shell still opaque

Relativ. e^- + B-field: synchrotron??

Relativ. e^- +B-field: synchrotron

Internal shocks for blazars

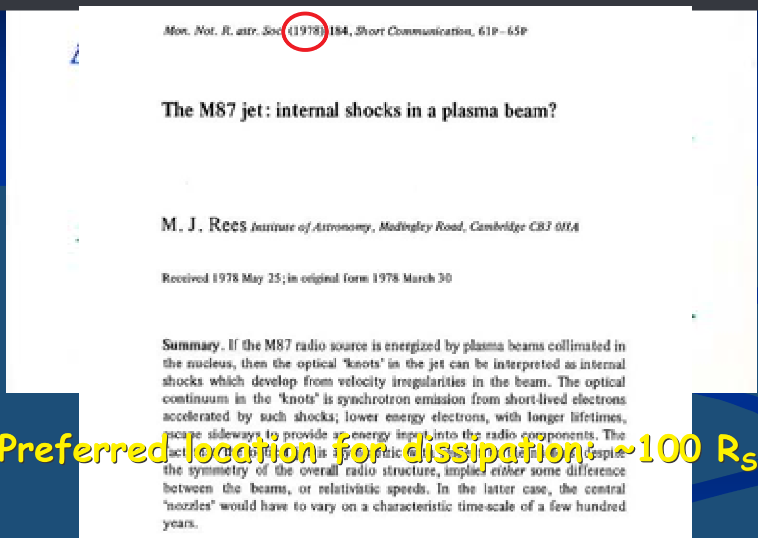

Mon. Not. R. astr. Soc. (1978) 184, Short Communication, 61P–65P

The M87 jet: internal shocks in a plasma beam?

M. J. Rees Institute of Astronomy, Madingley Road, Cambridge CB3 0HA

Received 1978 May 25; in original form 1978 March 30

Summary. If the M87 radio source is energized by plasma beams collimated in the nucleus, then the optical 'knots' in the jet can be interpreted as internal shocks which develop from velocity irregularities in the beam. The optical continuum in the 'knots' is synchrotron emission from short-lived electrons accelerated by such shocks; lower energy electrons, with longer lifetimes, escape sideways to provide an energy input into the radio components. The [...] the symmetry of the overall radio structure, implies either some difference between the beams, or relativistic speeds. In the latter case, the central 'nozzles' would have to vary on a characteristic time-scale of a few hundred years.

Preferred location for dissipation: ~100 R_S

Variability

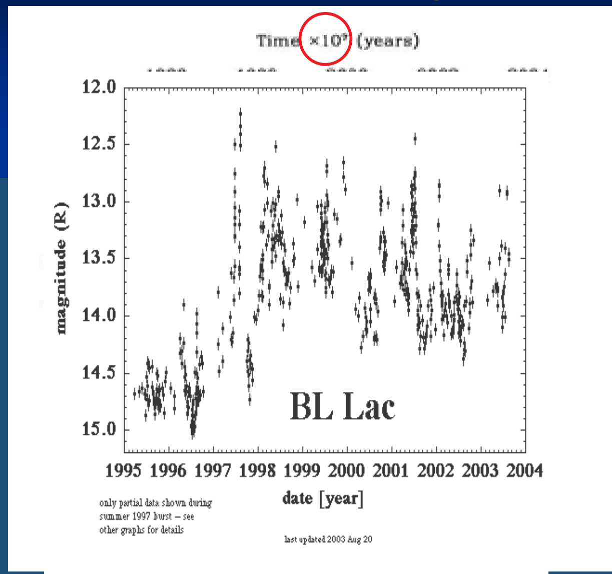

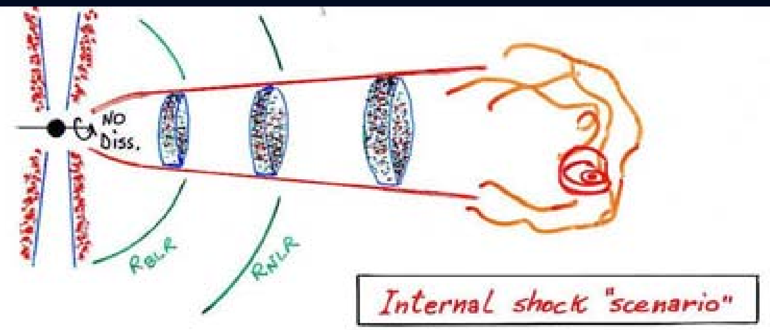

- $R_\gamma \sim R_0 \Gamma^2 \sim 100\ R_s$
- Dissipation : η↓ R↑
- Variability
- Can explain SED
- Requires matter
- $L_K > L_B$ in γ-zone and beyond

Ghisellini 1999, Spada et al. 2001

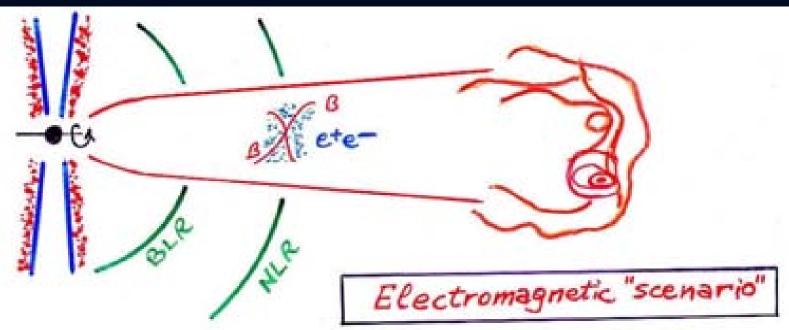

- Almost matter (barion) free
- $L_B > L_K$ everywhere
- Dissipation ⇔ Reconnection

Blandford 2002, 2003, Lyutikov 2003

Jet vs disk power

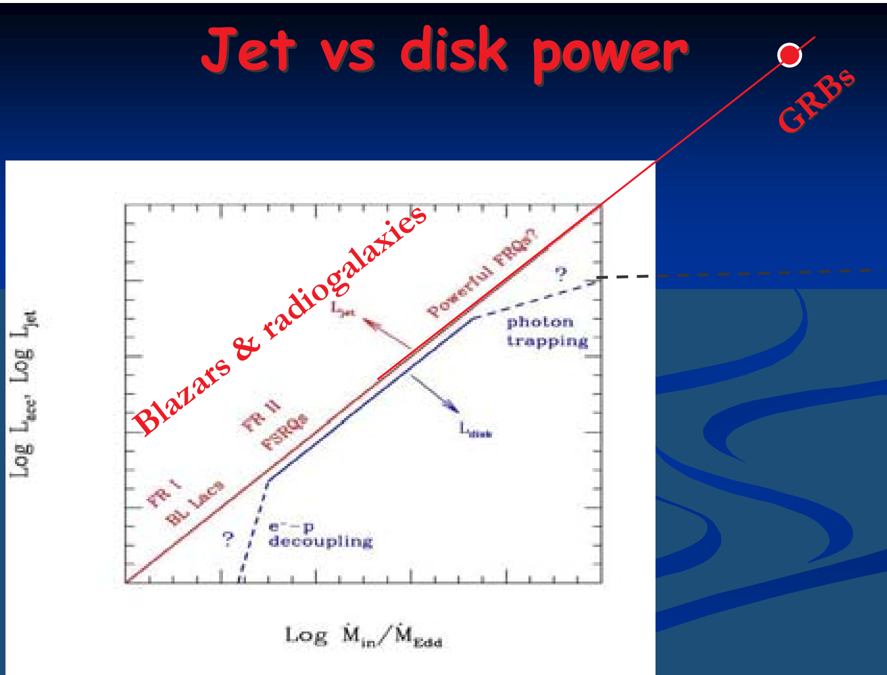

Cosmology with GRBs

28 GRB +2 XRF

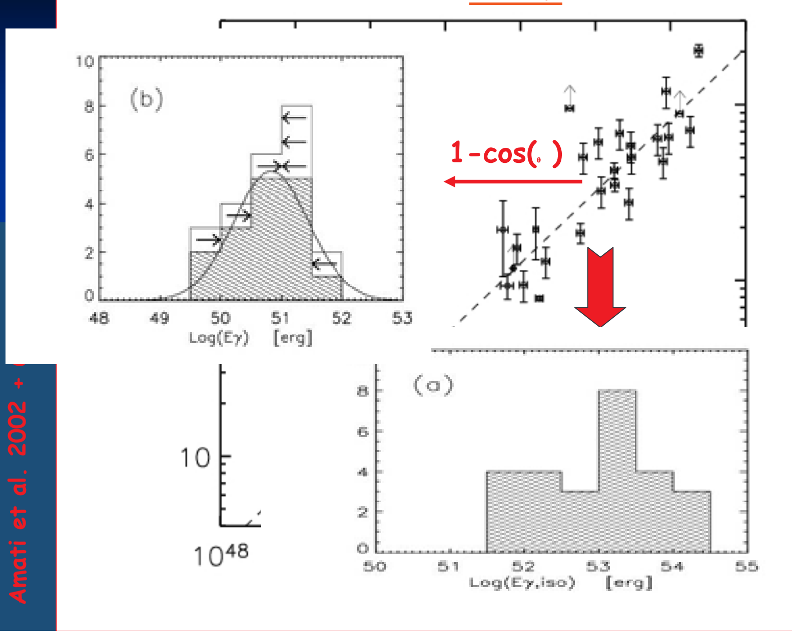

Amati et al. 2002 +

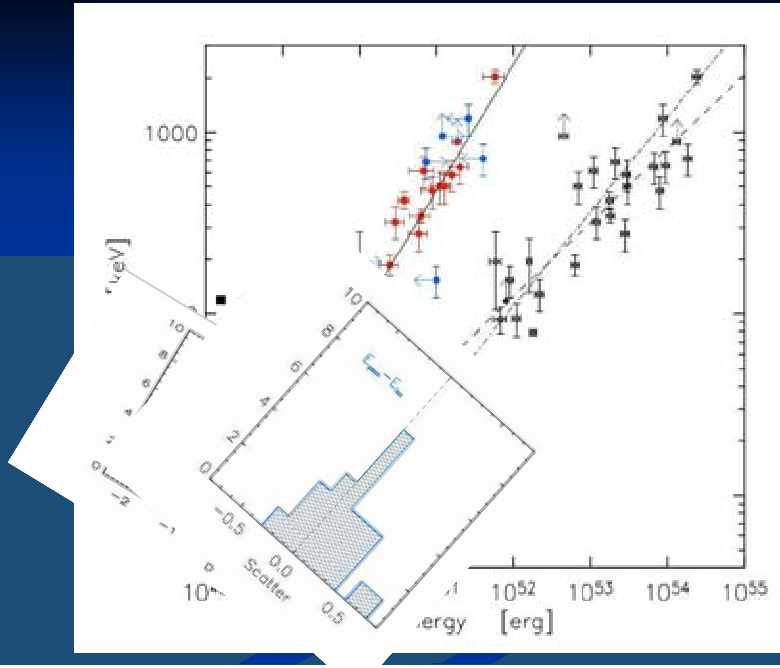

Ghirlanda, Ghisellini & Lazzati 2004

Similar to Supernovae Ia

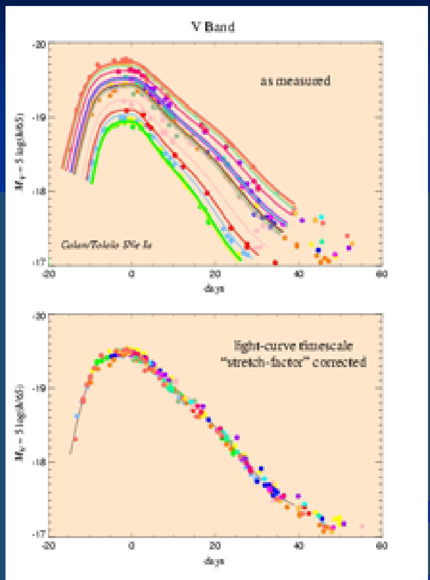

"Stretching": the slower the brighter

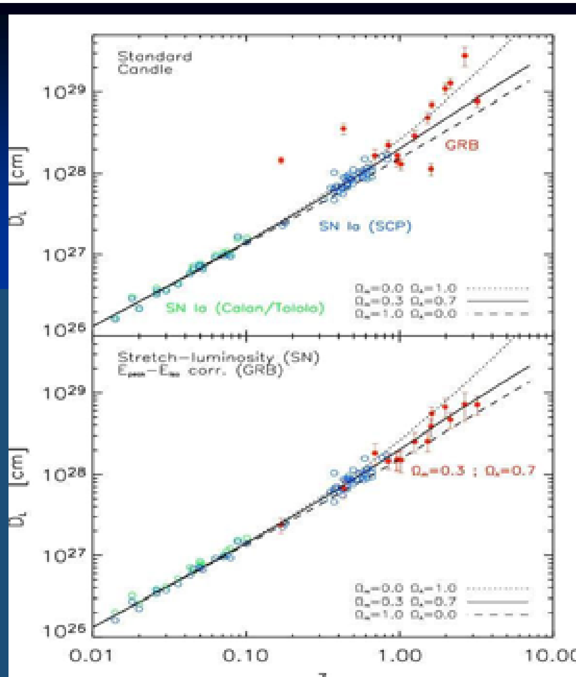

Ghirlanda, Ghisellini, Lazzati & Firmani 2004

Ghirlanda, Ghisellini, Lazzati & Firmani 2004

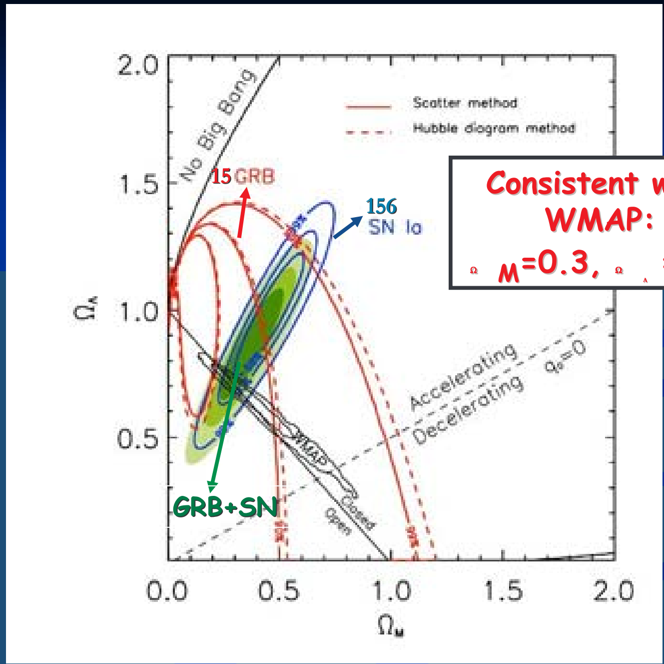

Consistent with WMAP: $\Omega_M=0.3$, $\Omega_\Lambda=0.7$

Flat Universe: $\Omega_{tot}=1$

$P=w_0 \rho c^2$

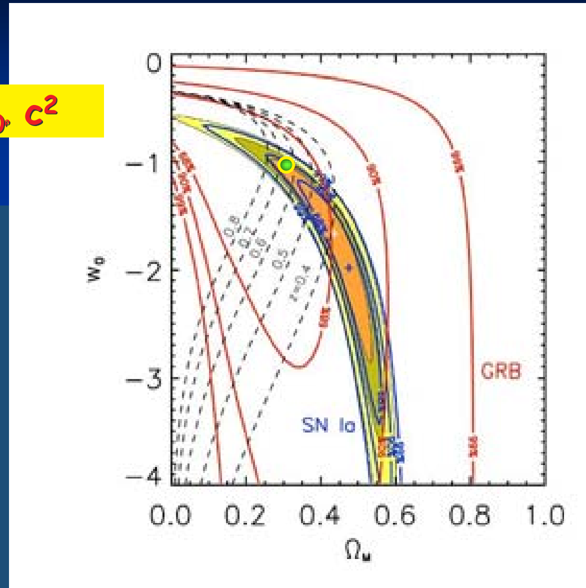

Firmani, Ghisellini, Ghirlanda & Avila-Reese, 2004

Flat Universe: $\Omega_{tot}=1$, $\Omega_M=0.27$

$P=(w_0+w'z)\rho c^2$

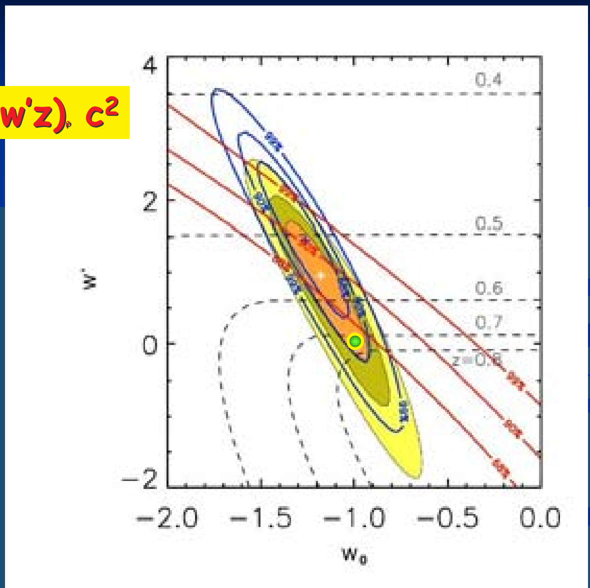

Firmani, Ghisellini, Ghirlanda & Avila-Reese, 2004

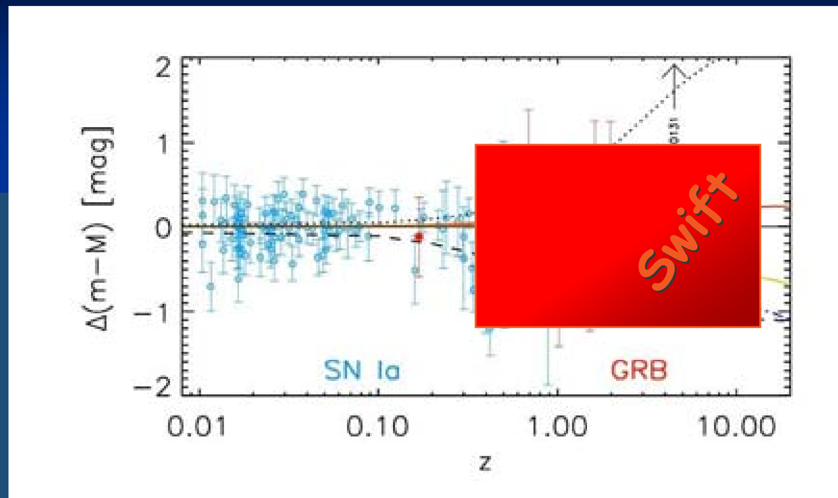

Firmani, Ghisellini, Ghirlanda,& Avila-Reese, 2004

Conclusions

- Most relativistic objects in the Universe
- Jets and/or collimation in both
- Jets can be more powerful than disks
- Jet energy: matter or magnetic field?
- GRBs are standard candles!

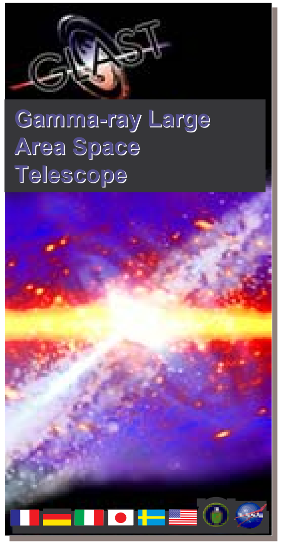

The GLAST Gamma Ray Observatory

Gino Tosti
Department of Physics and INFN, Perugia, Italy
gino.tosti@pg.infn.it

http://www-glast.slac.stanford.edu/

GLAST OBSERVATORY

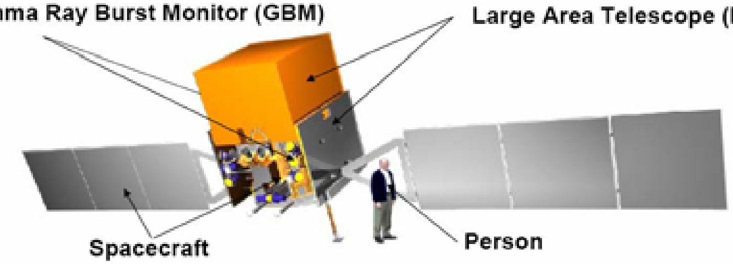

Launch Vehicle	Delta II – 2920-10H
Launch Location	Kennedy Space Center
Orbit Altitude	575 Km
Orbit Inclination	28.5 degrees
Orbit Period	95 Minutes
Orientation	+X to the Sun

GLAST Instruments

Large Area Telescope (LAT)
PI: Peter Michelson
Stanford University

GLAST Burst Monitor (GBM)
PI: Charles Meegan
Marshall Space Flight Center

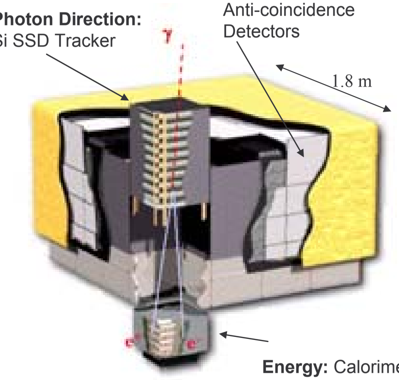

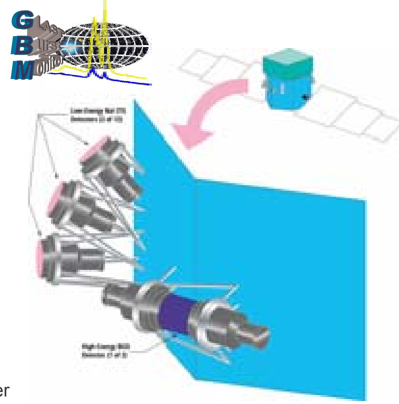

The International Collaboration

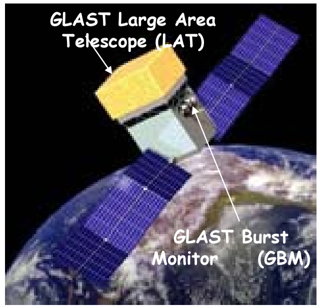

NASA - DoE Partnership on LAT

LAT is being built by an international team
- Si Tracker: Stanford, UCSC, Japan, Italy
- CsI Calorimeter: US - NRL, France, Sweden
- Anticoincidence: GSFC
- Data Acquisition System: Stanford, NRL

GBM is being built by US and Germany
- Detectors: MPE

•GLAST-LAT Italian Collaboration: PI-Ronaldo Bellazini (INFN-Pisa)

INFN Bari, Padova, Perugia, Pisa, Trieste, Udine (59)
35 Astrophysicists belonging to various Institutions
(IASF, ASI, Arcetri, Brera, Bologna, Torino, and several Universities)

Supported by INFN and ASI

GBM

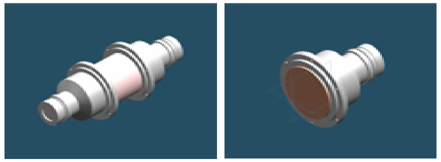

2- Bismuth germanite (BGO) Detectors

12- Sodium iodite(NaI) Detectors

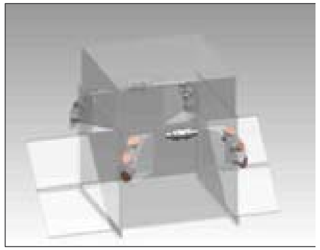

Energy range: 10 keV - 25 MeV
FOV of 8 sr
Notify observers world-wide:

Recognize bursts in realtime
Positions to few degree accuracy
Transmit (within seconds) GRB coordinates to the ground
Re-point the main instrument to GRB positions within 10 minutes

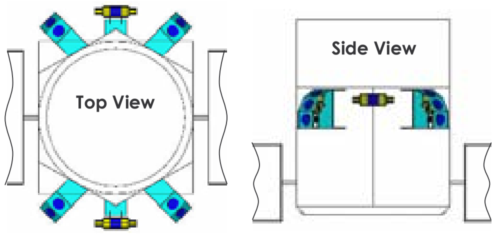

GBM Capabilities

	BATSE	GBM - Requirement	GBM - Current Design
Energy Range	25 keV – 10 MeV	<10 keV – >25 MeV	6 keV - 30 MeV
Field of View	All sky not occulted by Earth	>8 sr	8.7 sr
Energy Resolution	<10%	<10% (0.1-1.0 MeV, 1s on-axis)	7% (100 keV) 5% (1 MeV)
Deadtime		< 10 ms/event	2.5 ms/event
Burst Sensitivity - Ground (5s, 50-300 keV)	0.2 cm^{-2} s^{-1}	<0.5 cm^{-2} s^{-1}	0.45 cm^{-2} s^{-1}
Burst Sensitivity - On-board (5s, 50-300 keV, 50% efficiency)		<1.0 cm^{-2} s^{-1}	0.78 cm^{-2} s^{-1}
GRB Alert Location	~25°	-	<15°
GRB Final Location	1.7°	-	<1.5°
GRB Notification Time to Spacecraft		<2s	2s (arbitrarily selectable, trade-off between speed & accuracy)

GLAST Burst Monitoring

- LAT and GBM work synergistically to make new GRB observations

- GBM provides low-energy context measurements with high time resolution
  - Broad-band spectral sensitivity
  - Contemporaneous low-energy & high-energy measurements
  - Continuity with current GRB knowledge-base (GRO-BATSE)

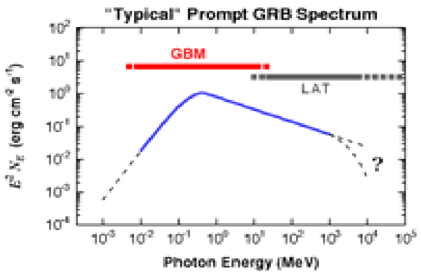

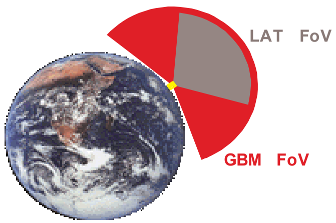

- Provides rapid GRB timing & location triggers w/FoV > LAT FoV
  - Improved sensitivity and response time for weak bursts
  - Follow particularly interesting bursts for afterglow observations
  - Provide rapid locations for ground/space follow-up

LAT Instrument

Tracker: 18 xy planes

Si-strips: fine pitch: 228 µm, high efficiency

12 x 0.03 X_0 front-end ⇒ reduce multiple scattering

4 x 0.18 X_0 back-end ⇒ increase sensitivity > 1 GeV

2 blank planes to locate calorimeter entry position

16 [4x4] towers ⇒ modularity
height/width = 0.4
⇒ large field-of-view

Calorimeter: 1536 CsI(Tl) crystals in 8 layers

CsI: wide energy range 0.1-100 GeV

hodoscopic ⇒ cosmic-ray rejection
⇒ shower leakage correction

8.5 X_0 ⇒ shower max contained < 100 GeV

Anti-Coincidence Detector

segmented [89 tiles] plastic scintillator

⇒ minimize self-veto

> 0.9997 efficiency & redundant readout

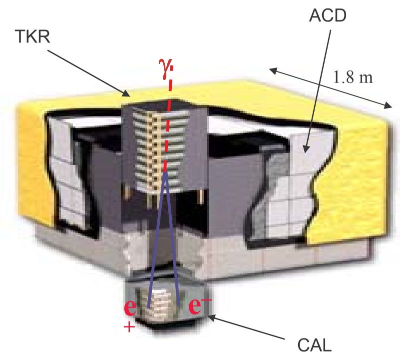

LAT Large FOV

EGRET (Spark Chamber) vs. GLAST/LAT (Silicon Strip Detector)

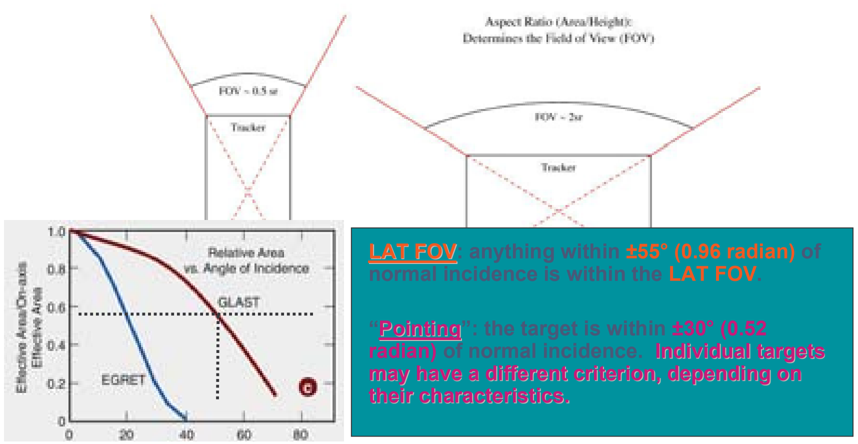

LAT FOV: anything within ±55° (0.96 radian) of normal incidence is within the LAT FOV.

"**Pointing**": the target is within ±30° (0.52 radian) of normal incidence. **Individual targets may have a different criterion, depending on their characteristics.**

LAT γ detection technique

Instrument must measure the direction, energy, and arrival time of high energ

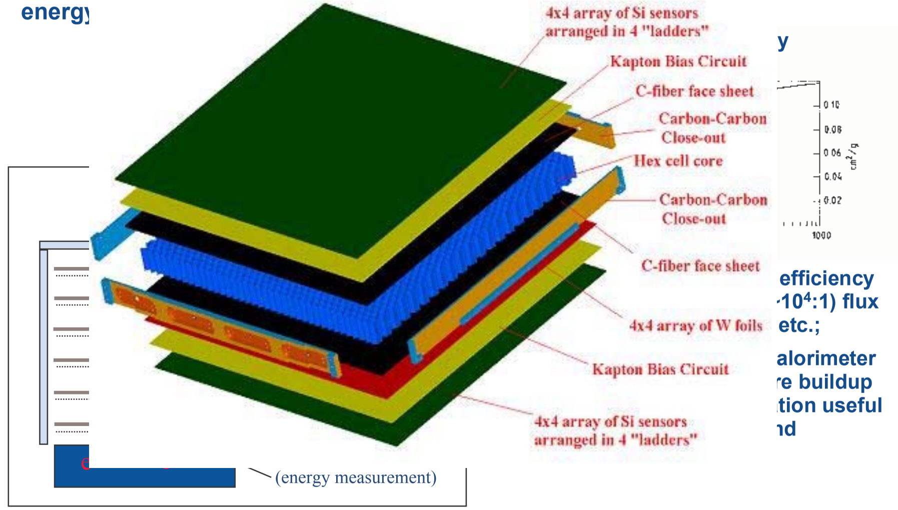

y efficiency ·10⁴:1) flux etc.; alorimeter re buildup tion useful nd

The Tracker Detector

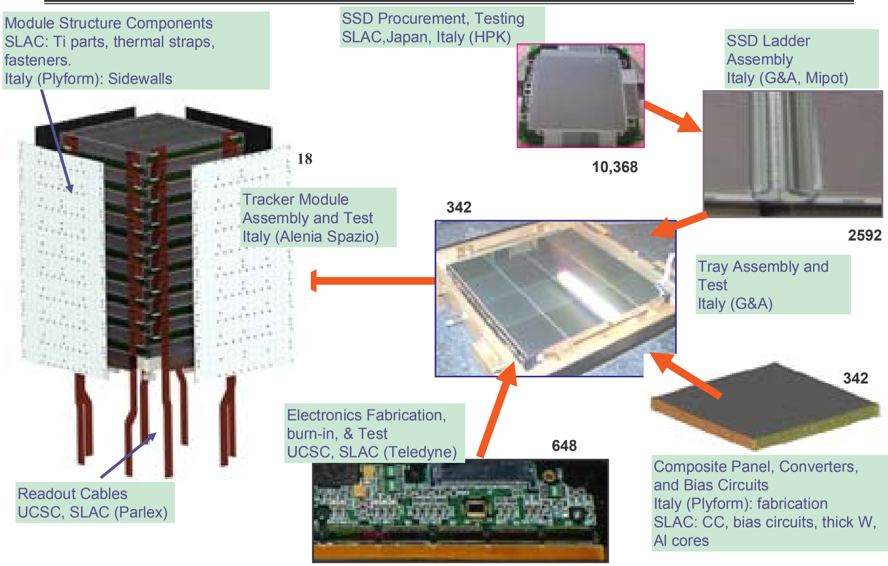

LAT Capabilities

	EGRET	LAT - Requirement	LAT - Current Design
Energy Range	20 MeV – 30 GeV	20 MeV – 300 GeV	20 MeV - 300 GeV
Energy Resolution	10 %	<10%, 0.1–100 GeV (1s, on-axis)	~9%, 0.1–100 GeV
Effective Area	1500 cm^2	>8000 cm^2 (maximum value, 1-10GeV)	10,000 cm^2 at 10 GeV
Point Source Sensitivity (5s, >100 MeV)	~1 × 10^{-7} cm^{-2} s^{-s}	<6 × 10^{-9} cm^{-2} s^{-2} (at high gal. latitude for 1-year sky survy, for photon index of -2)	3 × 10^{-9} cm^{-2} s^{-2}
Angular Resolution	5.8° (100 MeV)	<3.5° (100 MeV) <0.15° (>10 GeV)	3.4° (100 MeV) 0.086° (>10 GeV)
Source Location Determination	15 arcmin	<0.5 arcmin (1σ radius, flux 10^{-7} cm^{-2} s^{-1} at 100 MeV, high gal latitude)	0.4 arcmin
Field-of-view	0.5 sr	>2 sr	2.4 sr
Timing Accuracy	100 µs	<10 µs	TBD
Deadtime	100 ms/event	<100 µs/event	TBD
GRB Location Accuracy On-Board		<10 arcmin	5 arcmin
GRB Notification Time to Spacecraft		<5 s	TBD

LAT Capabilities

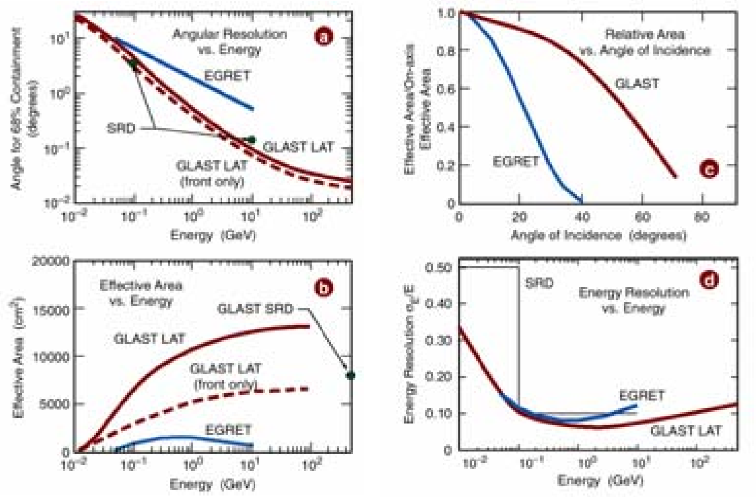

Astrophysics with GLAST

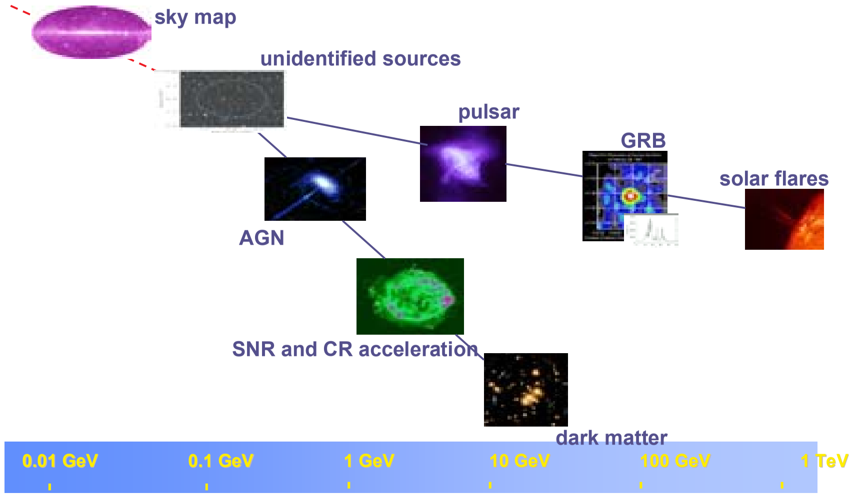

GLAST Survey: ~10,000 sources (2 years)

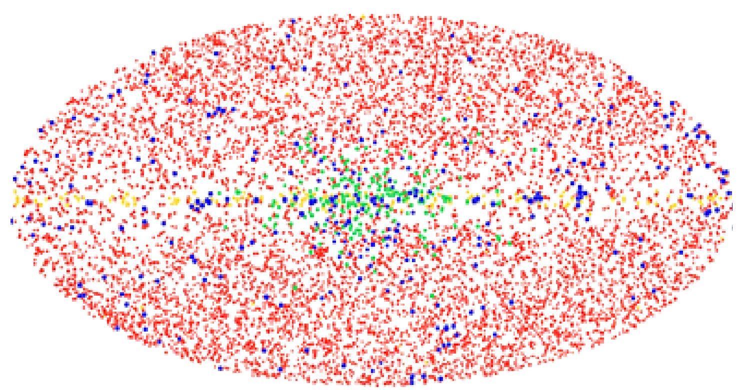

GLAST science capabilities - resolution

source identification requires a multiwavelength approach
- **localization**
- **variability**

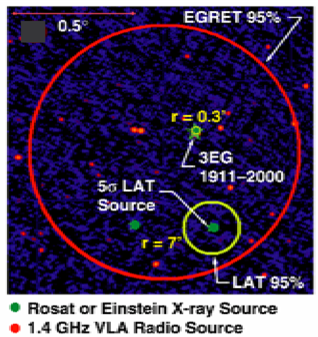

source localization (68% radius)
- γ-ray bursts: 1 to tens arcminutes
- unid EGRET sources: 0.3' – 1'

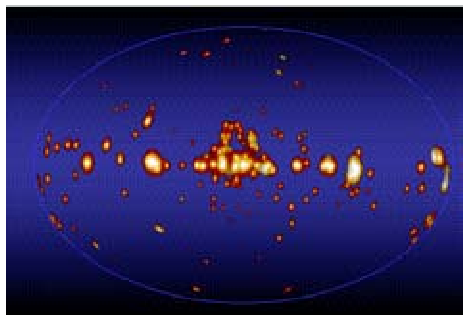

Unidentified EGRET sources

LAT Transient Sensitivity

enabling capabilities
- wide field-of-view
- low deadtime (for light curve)

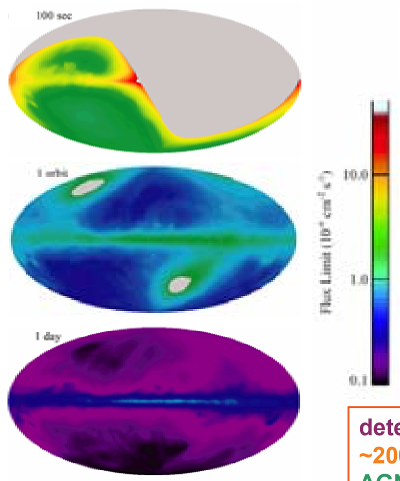

- GRB940217 (100sec)
- PKS 1622-287 flare
- 3C279 flare
- Vela Pulsar
- Crab Pulsar
- 3EG 2020+40 (SNR γ Cygni?)
- 3EG 1835+59
- 3C279 lowest 5σ detection
- 3EG 1911-2000 (AGN)
- Mrk 421
- Weakest 5σ EGRET source

detect all EGRET sources after ~day
~200 γ-bursts/year
AGN flares >few minutes

AGNs in the GLAST era

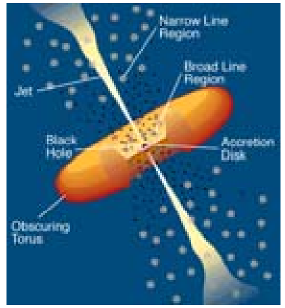

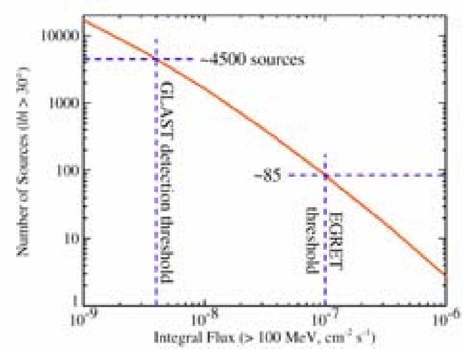

- EGRET detected ~ 70-90 AGN. Extrapolating, GLAST should expect to see dramatically more – many <u>thousands.</u>

The GLAST energy range is broad, overlapping those of ground-based experiments for good multiwavelength coverage.

AGNs in the GLAST era

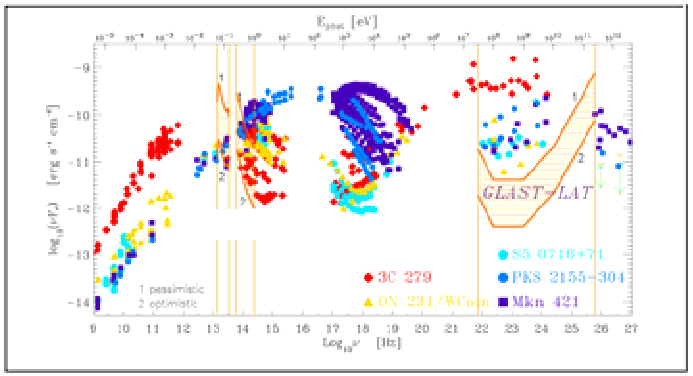

Joining the unique capabilities of GLAST with other detectors will provide a powerful tool to study the SED of blazars.

AGNs in the GLAST era: GeV – TeV Connection

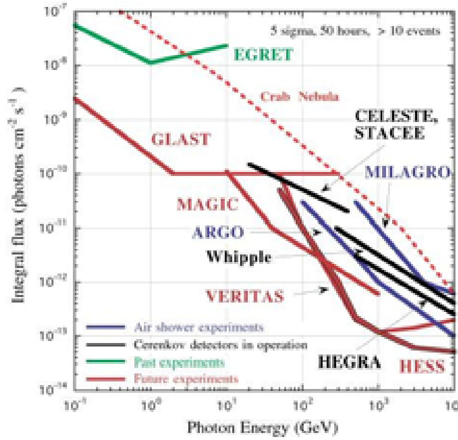

<u>Complementary capabilities</u>

	ground-based		space-based
	ACT	EAS	Pair
angular resolution	good	fair	good
duty cycle	low	high	high
area	large	large	small
field of view	small	large	large+can reorient
energy resolution	good	fair	good, w/ smaller systematic uncertainties
limiting factor	background		photon statistics

The next-generation ground-based and space-based gamma-ray telescopes are well matched.

Blazar Spectra

Mrk 501

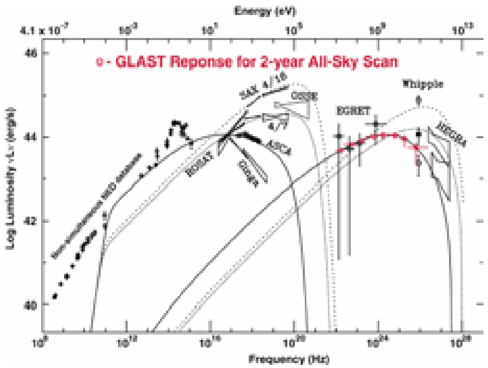

- GLAST combined with TeV observatories will probe the complex spectra of blazars.

Large FoV allows GLAST to monitor AGN over the whole sky for variability on many timescales.

AGN: Multiwavelength Variability

- Strength and phasing of flaring at different wavelengths is a powerful tool for modeling emission.
- Observations before and after a flare to be sure it is the same flare.
- Improved sensitivity will allow measurements of flares to shorter time scales and lower flux values.

3C279

Gamma rays

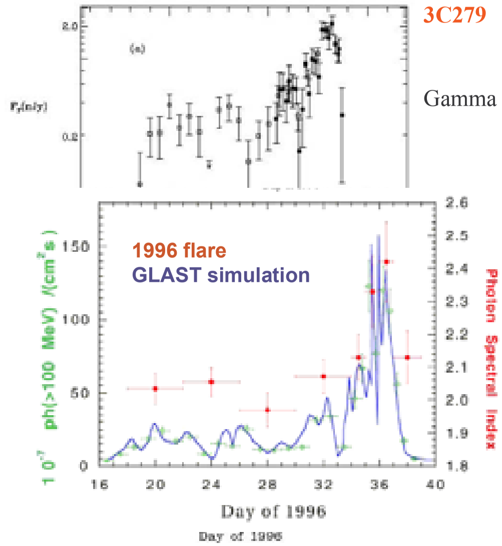

Mission Requirements – Observing Plan

- Spacecraft
  - Pointing knowledge < 10 arcseconds (1 s)
  - Observatory is designed to "point anywhere, anytime"
    - Operate without pointing at the Earth
    - Reorient quickly and autonomously to follow a transient
  - 3 normal operational modes
    - Scan (baseline)
    - Inertial pointing
    - Scan pointing - takes advantage of the wide field of view to optimize time on sky

Mission Requirements – Observing Plan

- After the initial on-orbit checkout, verification, and calibrations, the first year of science operations will be an all-sky survey.
  - first year data used for detailed instrument characterization, refinement of the alignment, and key projects (source catalog, diffuse background models, etc.) needed by the community
  - data on transients will be released, with caveats
  - repoints for bright bursts and burst alerts enabled
  - extraordinary ToO's supported
  - limited first-year guest observer program
  - workshops for guest observers on science tools and mission characteristics for proposal preparation
- Observing plan in subsequent years driven by guest observer proposal selections by peer review. All data released through the science support center (GSSC).

GLAST MASTER SCHEDULE

- LAT complete and tested — July 2005
  - To NRL for environmental testing
- Delivery to Observatory Integration — December 2005
  - Mate with spacecraft and GBM and test
- Launch — February 2007
  - Kennedy Space Flight Center
- Science operation begins — May 2007

GLAST Data Challange

- Fall 2003 - DC1
- 1 day's data through full instrument simulation and first look at Science Tools
- Summer 2005 – DC2
  - 1 month's background/1 year signal
  - Test more Science Tools; improved Pipeline
- Spring 2006 – DC3
  - run up to flight – test it all!

DC1 - GLAST Simulation Infrastructure

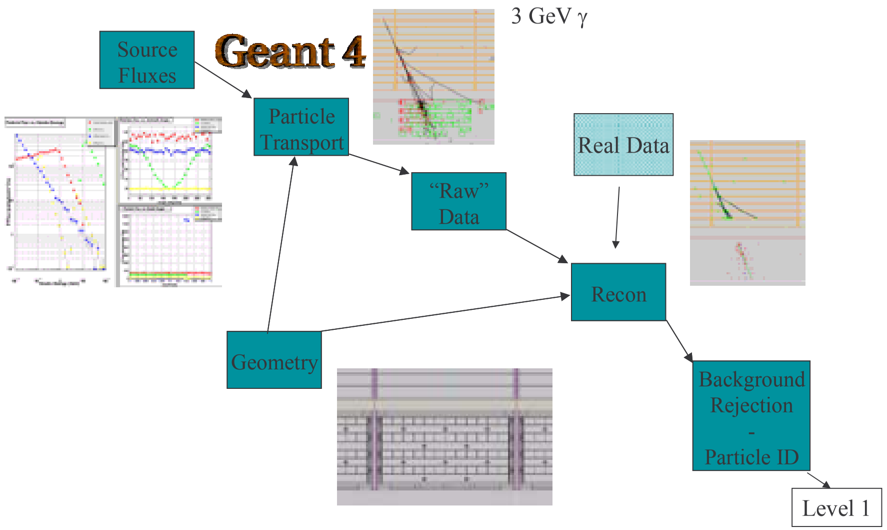

DC1 – Exposure Map

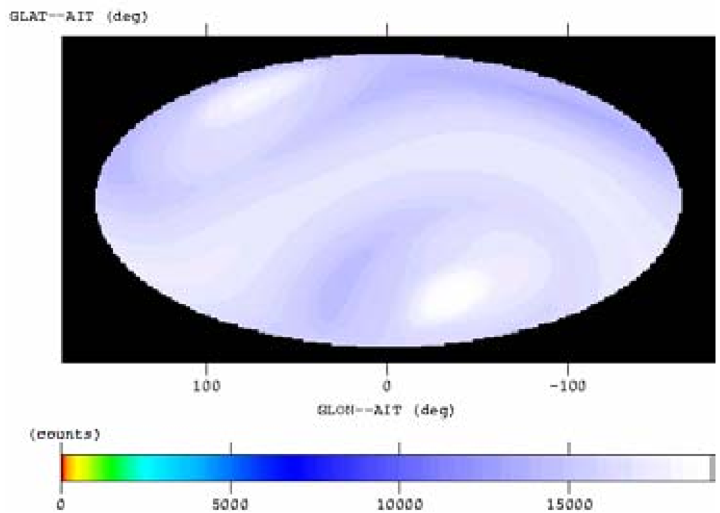

DC1 – Sky Map

Gamma rays in 1-day scanning observation (~150k >30 GeV), color coded by energy

Annual rate (all energies) ~10^8 gamma rays/year

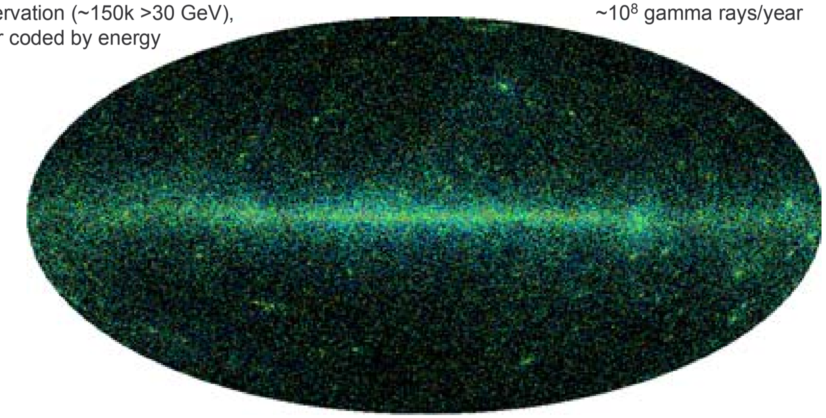

Bright diffuse emission of the Milky Way + Galactic and extragalactic point source populations

Hundreds of sources even in this short time: What are their fluxes? Which are flaring?

GLAST Science Tools

The big picture:
Details are changing, but still basically right

Standard Analysis Environment

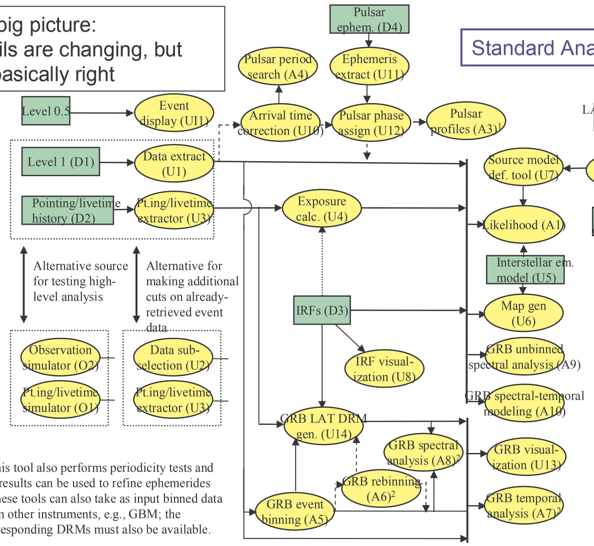

User Interface aspects of the standard analysis environment, such as Image/plot display (UI2), Command line interface & scripting (UI4), and GUI & Web access (UI5) are not shown explicitly.

[1] This tool also performs periodicity tests and the results can be used to refine ephemerides
[2] These tools can also take as input binned data from other instruments, e.g., GBM; the corresponding DRMs must also be available.

DC1- Main Science Tools

Package	Description
Likelihood	Workhorse model fitting for detection & characterization of cosmic gamma-ray sources
Level 1 database access	Extracts desired event data
Exposure calculation	Uses IRFs, pointing, livetime etc. for deriving calibrated source fluxes
Source identification (Perugia Contribution)	Identifies gamma-ray sources with cataloged counterparts at other wavelengths
GRB analysis	Temporal and spectral analyses of burst profiles
Pulsar analysis	Phase folding & period searching of gamma-ray pulsars and candidates
Observation simulator (Perugia Contribution)	High level simulation of observations of the gamma-ray sky with the LAT

Wavelet method for source detection in GLAST photon-counting images

Claudia Cecchi
Francesca Marcucci
Gino Tosti
University and INFN, Perugia, Italy

Why do we need to apply wavelet method and to study new algorithm?

What do we have?
GLAST: maps containing signal from astrophysical sources..but..
convoluted with the spatial and spectral instrument response

In most astronomical gamma-ray images a large fraction of sources is near the detection limit → careful statistical treatment is needed to determine their existence and properties (accurate position, flux, size, etc.)

Many tools (parametric methods) need a priori model to fit the data and estimate their parameters

No model or hypotesis on the data are requested by the wavelet method

Comparison with other methods

• **SLIDING CELL method (ROSAT and CHANDRA) :**
non parametric method to search for excess of intensity in a map
- due to the presence of a source
- not realated to poissonian fluctuation of the background
fast but poor in signal discrimination

• **LIKELIHOOD ANALYSIS (EGRET and ROSAT) :**
assume a relatively simple model described by a finite number of parameters and fit data maximizing a function representing the probability of observed data
slow and model dependent
→A blind detection by Likelihood analysis would require long computing time (while the characterization will be more precise)

• **WAVELET (ROSAT and XMM)**
Allows to distinguish between signal and background
gives a *precise* and *fast* localization of points and extended hidden sources

What is a wavelet transform (WT)?

• similar to 2-D filter

• multiscale transform providing a representation of data proper to extract both position and shape of features (for images or light curves)

• decomposes the signal in translated and scaled versions of an original function (the mother wavelet)

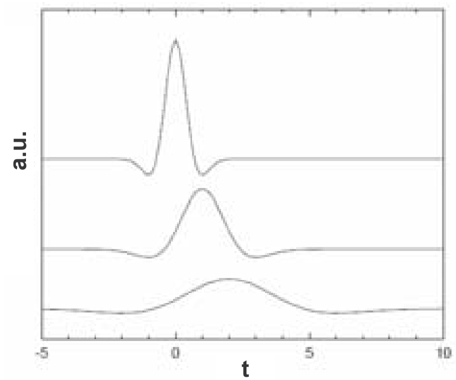

$\psi(t)$: mother wavelet

$\psi_{a,l}(t)$: derived wavelets

$\psi_{a,l}(t) = 2^{a/2}\,\psi(2^a t - l)$ $\quad a,l \in Z$

a controls the scaling allowing to study the local details

l controls the translation allowing a full coverage of analysed region

2-d wavelet

Def.: $w(x,y,a) = \iint \psi(\frac{x-x'}{a}, \frac{y-y'}{a}) f(x',y') dx' dy'$

The Mexican Hat Wavelet:

a) $\psi(\frac{x}{a}, \frac{y}{a}) = \psi(\frac{r}{a}) = (2 - \frac{r^2}{a^2}) e^{-\frac{r^2}{2a^2}}$

$(r^2 = x^2 + y^2)$

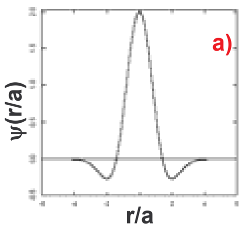

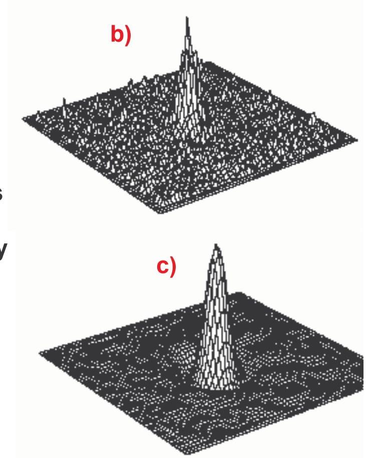

Why the Mexican Hat ??

✓ choose ψ as a function having a similar shape as observed sources
✓ gamma-ray detectors have **PSF** well described by one or more gaussian functions (b)
✓ *WT enhances the signal contribution and attenuates the background (c)*

ALGORITHM :

requirements
- allows fast blind localization of **point** sources (by WT)
- *efficient detection → small number of spurious detections*
- allows characterization of sources (position, spectral index and flux)

Structure Iterative procedure

WT of input count map → computation of a threshold → acceptance test (S/N density) → source fitted and subtracted → re-analyse output image

Estimation of background map → computation of a threshold

Source characterization: position estimated from fit on intensity map + intensity maps at different E fit of sources and α estimation

Application to simulation GLAST data

Method tested on 6 days all sky data

Bin size: 0.25 deg	2 iterations are sufficients
Projection = -TAN , -SIN (at poles)	4 sigma threshold analysis

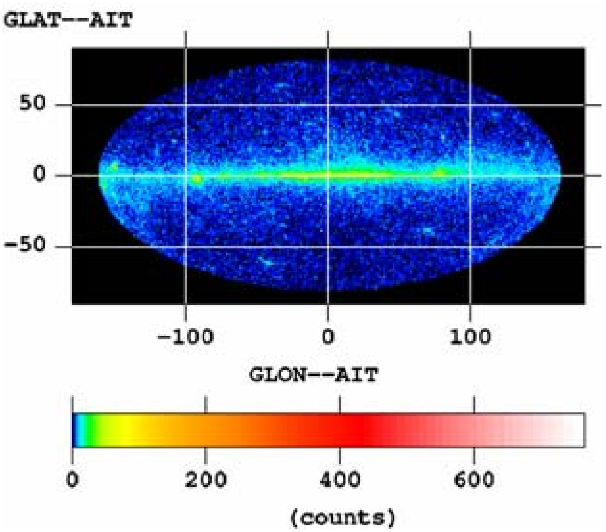

172 detected sources

139 d<0.5 deg
19 d<1.0 deg
2 d<1.5 deg

24 associated to faint blazars
7 associated to *unid-halo*
6 associated to GRB's
the rest with 3EGC

12 spurious detection

4 because of bad fitting/subtraction

Results

GC region and zoom on Galactic Plane

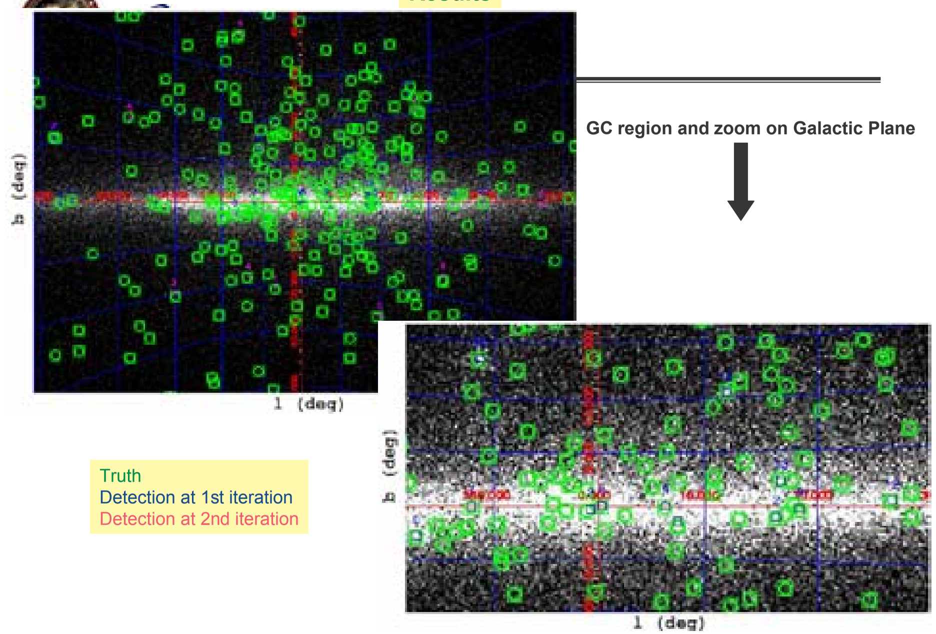

Truth
Detection at 1st iteration
Detection at 2nd iteration

Results

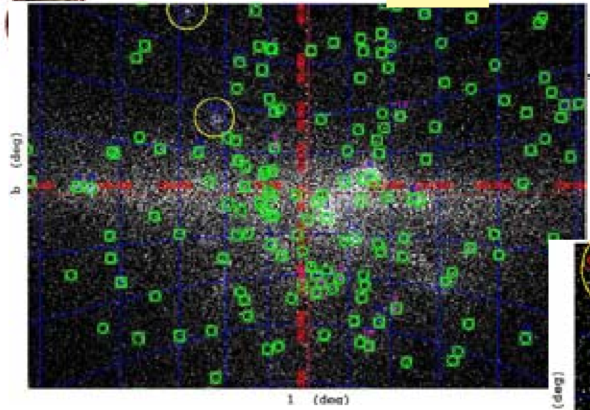

AC region and zoom on region with GRB's

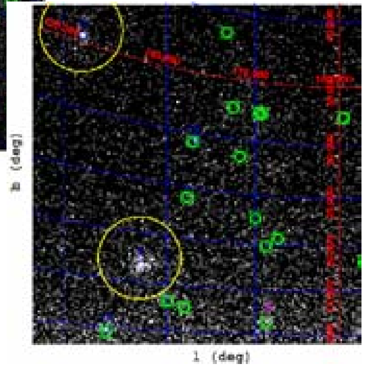

Truth
Detection at 1st iteration
Detection at 2nd iteration

Finer analysis of source parameters

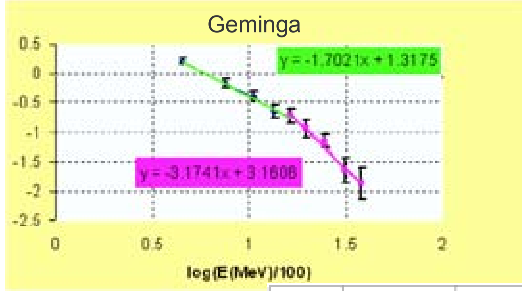

NAME	l	b	counts (C)	α_1	α_2
3C 273	290.878 ± 1.6 (289.834)	64. 76 ± 1.9 (64.47)	240 ± 15	-2.17 ± 0.21 (-2.58)	
Vela	263.719 ± 0.14 (263.527)	-2.69 ± 0.14 (-2.86)	4558 ± 68	-1.76 ± 0.04 (-1.69)	-3.71 ± 0.11 (-3.69)
Crab	184.7 ± 0.5 (184.53)	-5.70 ± 0.5 (-5.84)	514 ± 23	-2.22 ± 0.11 (-2.19)	
Geminga	195.17 ± 0.2 (195.06)	4.45 ± 0.2 (4.32)	1558 ± 39	- 1.70 ± 0.08 (-1.66)	- 3.2 ± 0.2 (-3.1)

Comparison light_sim / DC1

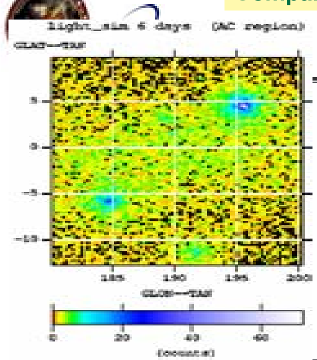

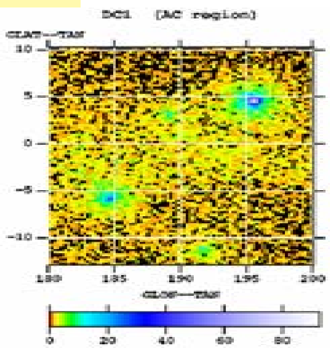

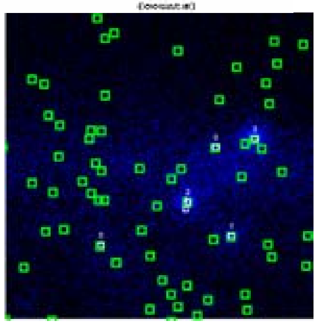

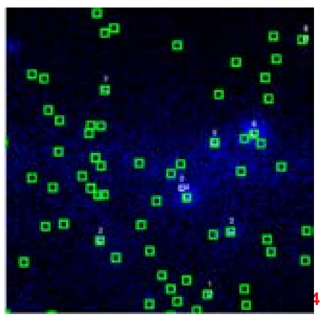

Simulation of 1 month data with light_sim

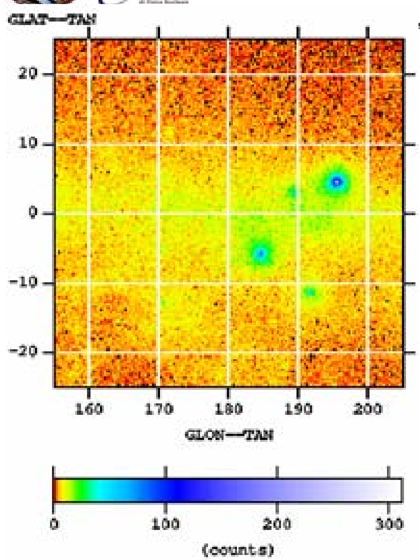

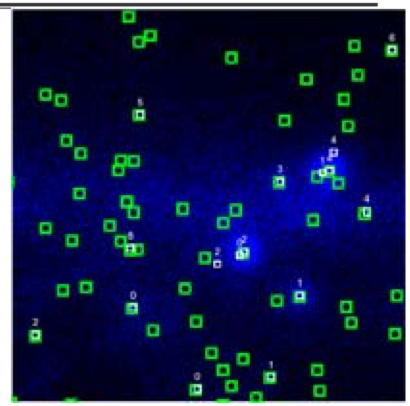

16 sources detected, 4 spurious

Application to EGRET data

4 regions: Vela, Cygnus, 3C279, AC for the first four observation periods

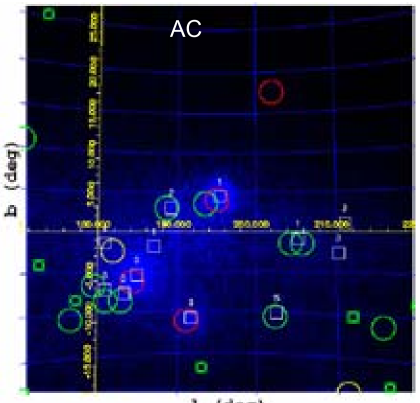

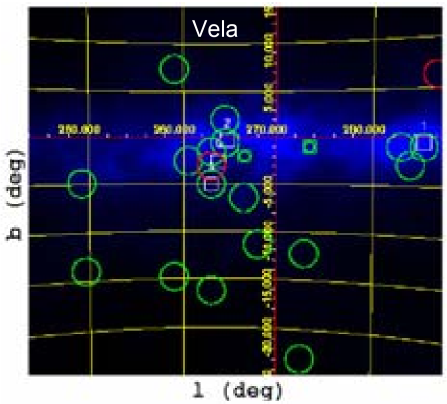

Wavelet detection
Identified 3EGC
Unidentified 3EGC

- -All identified 3EGC sources in the analysed regions have been detected except a faint Blazar near 3C379 (improve fit/subtraction)
- -Half of detected sources associated with identified + unidentified 3EGC
- -All undetected sources are unidentified sources of the 3EGC

Finer analysis of source parameters

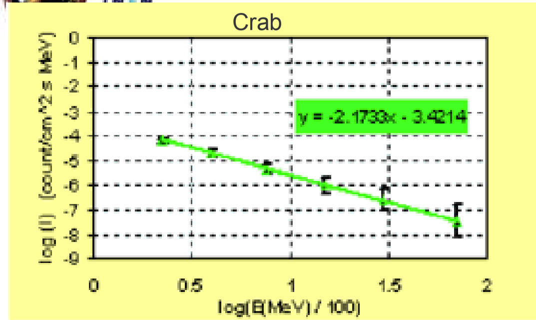

NAME	l	b	counts (C)	α_1
3C 279	305.7± 0.5 (304.982)	57.5± 0.5 (57.03)	1452 ± 38 1487	-1.90 ± 0.06 (-1.96 ± 0.04)
Vela	263.9± 0.3 (263.527)	-2.5± 0.3 (-2.86)	10432 ± 102 (10320)	-1.71 ± 0.03 (-1.69 ± 0.01)
Crab	185.0± 0.4 (184.53)	-5.5± 0.4 (-5.84)	5513 ± 74 (5314)	-2.17 ± 0.02 (-2.19 ± 0.02)
Geminga	195.5± 0.3 (195.06)	4.7± 0.3 (4.32)	6531 ± 80 (6329)	- 1.70 ± 0.10 (-1.66 ± 0.01)

Details on spurious detection in EGRET data

-Peaked around local maxima in count maps

→ Identification with radio/X counterparts?
(based on *position* within 30 arcmin = 0.5 deg) ...but...
possible only for bright sources

Correlation between γ-ray fluxes and X-ray fluxes or radio fluxes are needed
(R. Mukherjee on multifrequency strategies for γ-ray source identification)

Most of the found candidates are radio sources, Galaxy clusters, QSO, X-ray or Infra Red sources

→ GLAST will be very important!!!

First application to extended sources: CenA

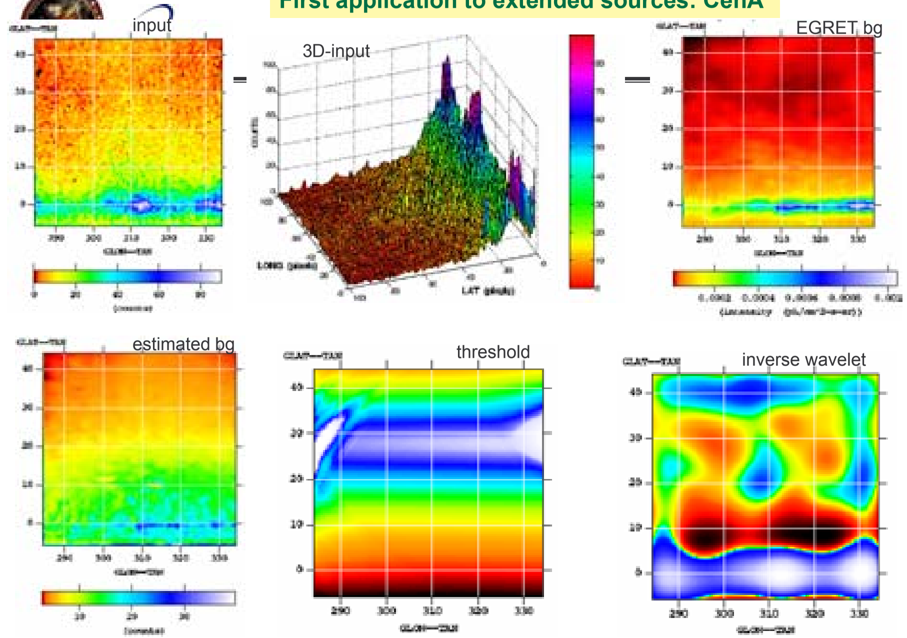

First application to extended sources: CenA (cont'd)

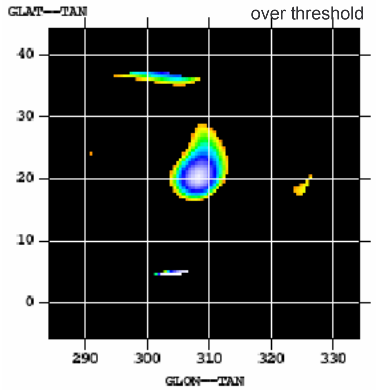

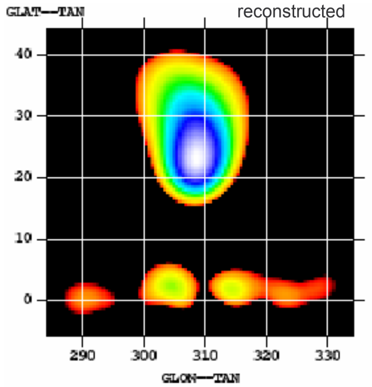

Conclusions

- Wavelet method perform **fast and blind source detection** (quick look of transient and bright signals)
- It gives source location used as input for a more detailed analysis for their description (flux, spectral index)
- With only 6 day of GLAST data localization of several sources and the characterization of the brightest ones is possible
- Analysis of EGRET data gives localization of all identified sources + some of the unidentified (about 50%) + possible identification of unknown sources
- Extended sources can be studied looking at over threshold contributions at large scales

Gamma-Ray and X-Ray Astrophysics with AGILE

M. Tavani

ENIGMA Meeting, Perugia

6 October, 2004

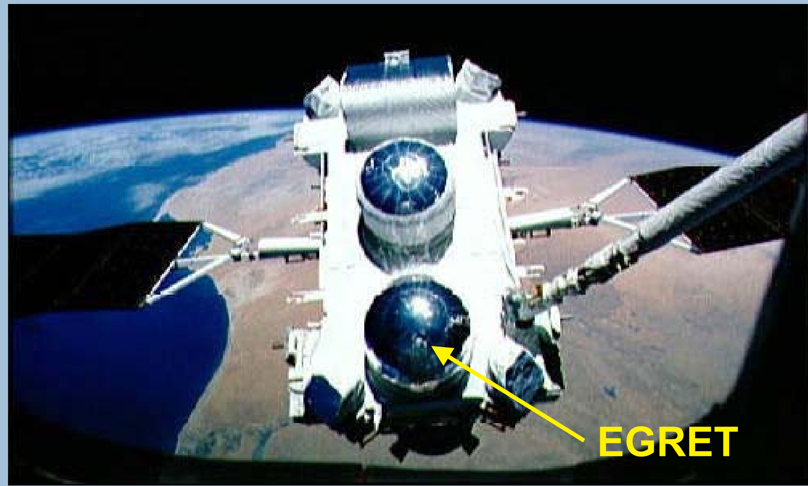

EGRET/GRO gamma-ray sky map, E > 100 MeV

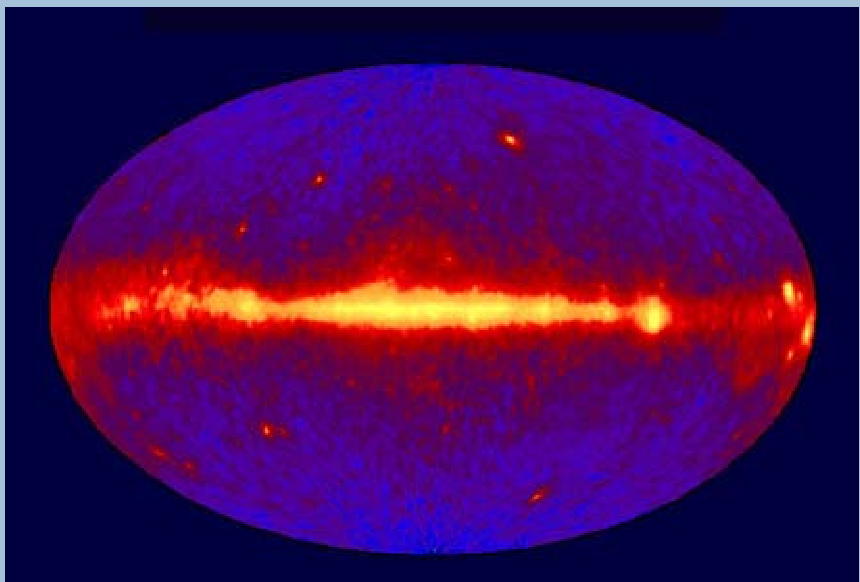

challenges

- AGNs
- Gamma-Ray Bursts
- Pulsars
- Unidentified gamma-ray sources
- SNRs and origin of cosmic rays
- Fundamental physics

The mystery of the unidentified gamma-ray sources

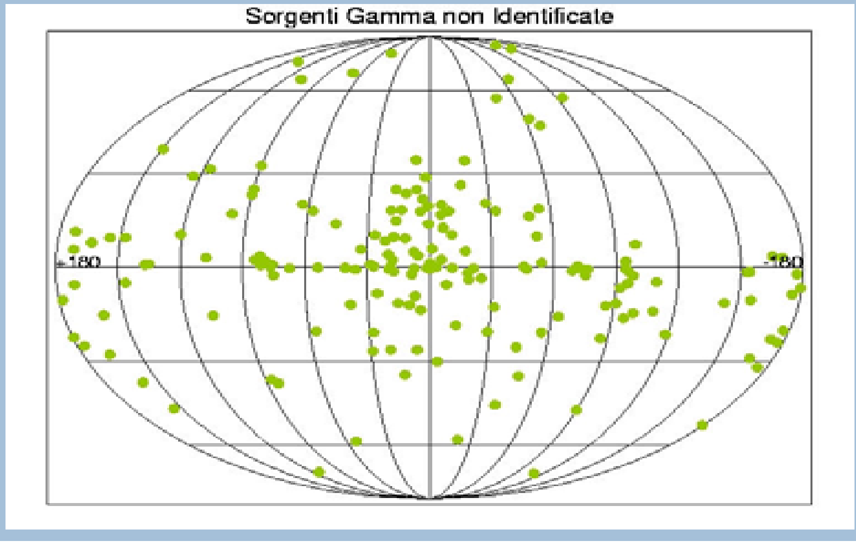

7 isolated gamma-ray pulsars

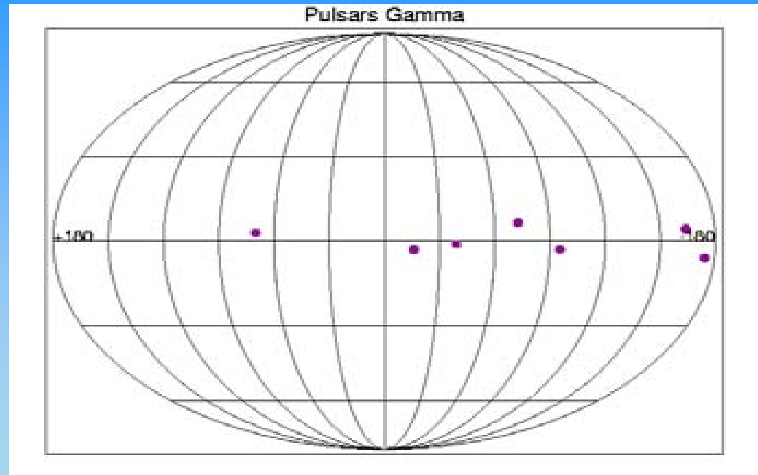

AGNs detected above 30 MeV by EGRET

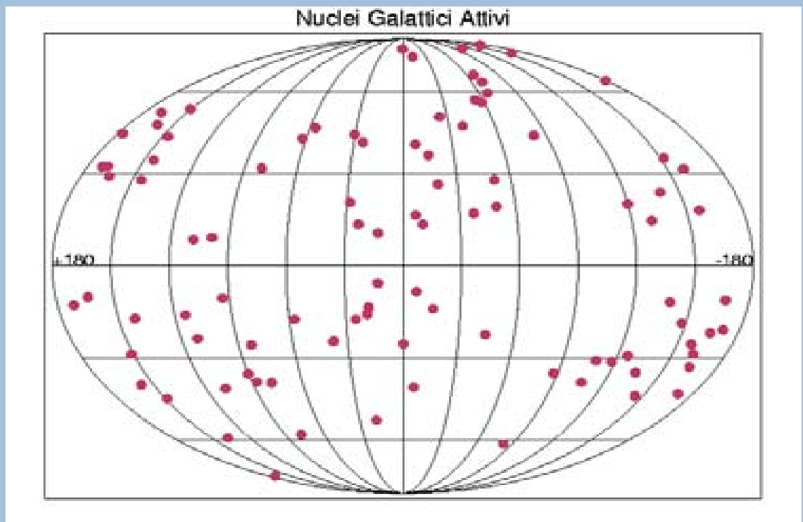

Ψ_{-7} vs. M_{BH}

(Vercellone et al. 2004)

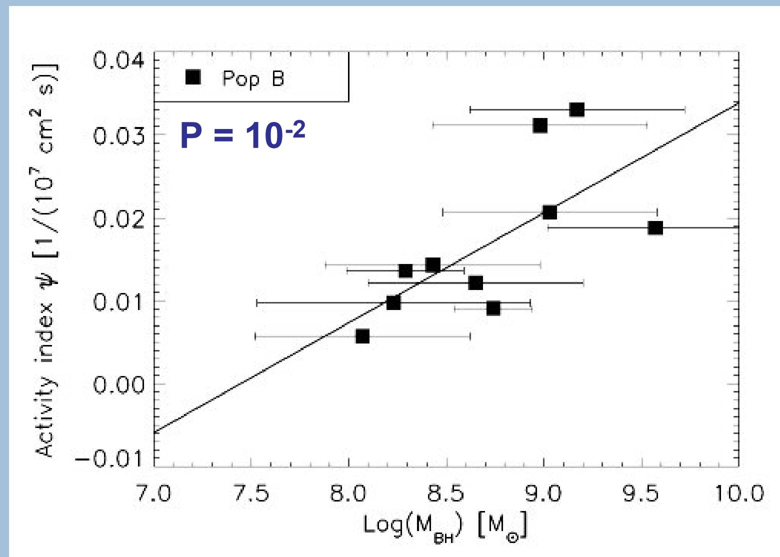

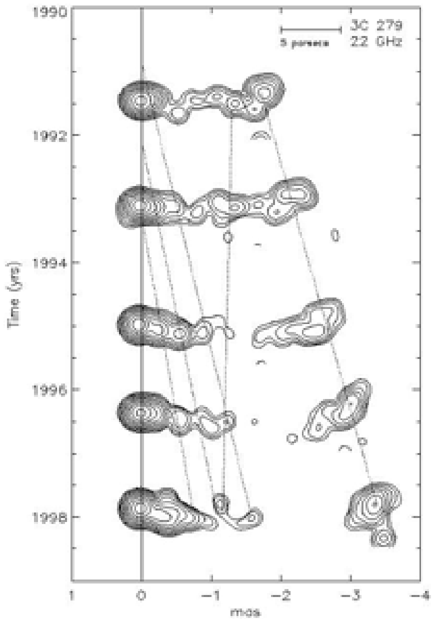

3C 279 radio-plasmoid ejections (associated with γ-ray flares ???)

VLBA radio maps

Are γ-ray blazars more strongly beamed ?

(Kellermann et al., astro-ph/0403320)

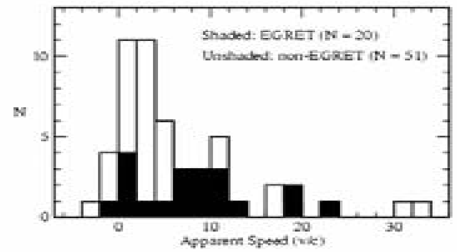

<v>/c = 3.9 ± 1.1 (53 sources, no EGRET detections)

<v>/c = 8.0 ± 1.6 (18 sources, EGRET detections)

Fast variability (< 1 day) !

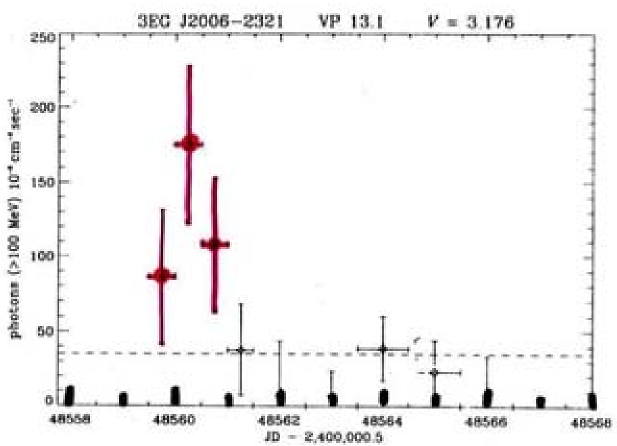

Strongest AGN γ-ray flare, but…

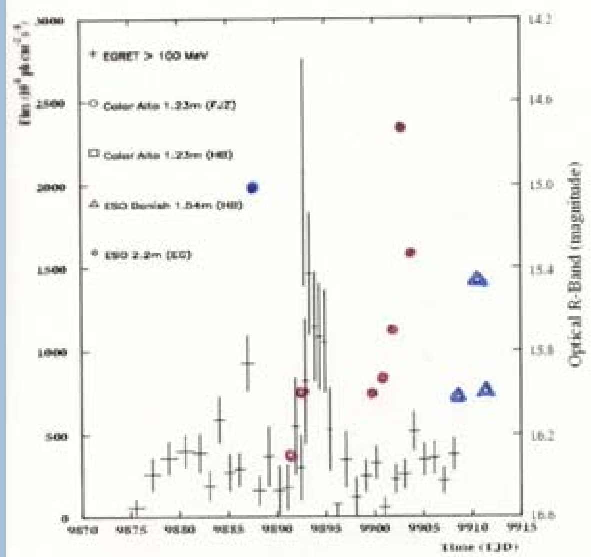

PKS 1622-287

- In “desperate” need of simultaneous multiwavelength data to study source variability.

GRB 930131

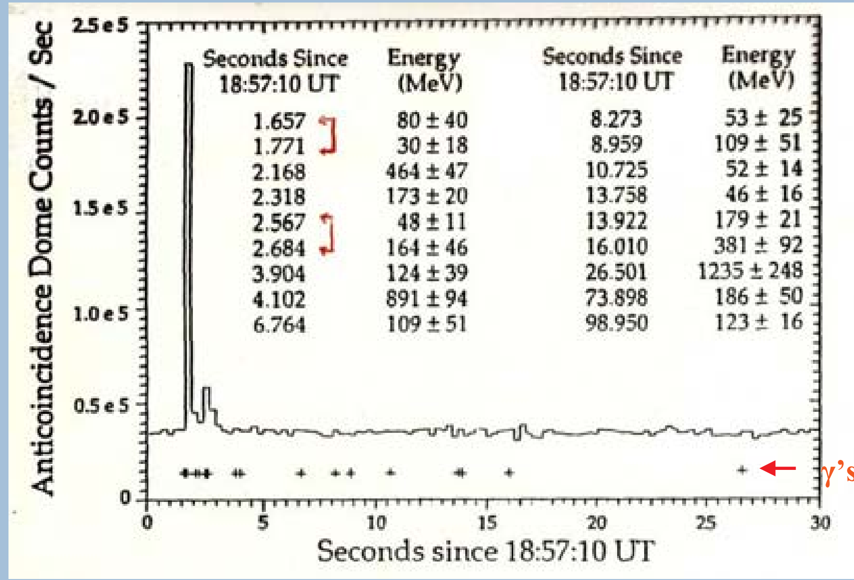

- Need fast timing for gamma-ray detection (improving EGRET deadtime, 100 msec → 100 microsec or less).
- What is the ultimate mechanism of particle acceleration in GRBs ?

The future

- AGILE (2005-2007)
- GLAST (2007-2011 and beyond)

To make progress we need:

- Excellent gamma-ray imaging with a large Field-of-View
- Simultaneous broad-band spectral information
- Microsecond timing
- Efficient transient detection and alerts

For both AGILE and GLAST the goal is

"arcminute" γ-ray astrophysics

employing two very different methods:

1. Using the simultaneous imaging information in the 15-45 keV and 30 MeV-30 GeV (by AGILE)
2. Using a large collecting area for imaging in the 30 MeV-100 GeV range (by GLAST)

AGILE

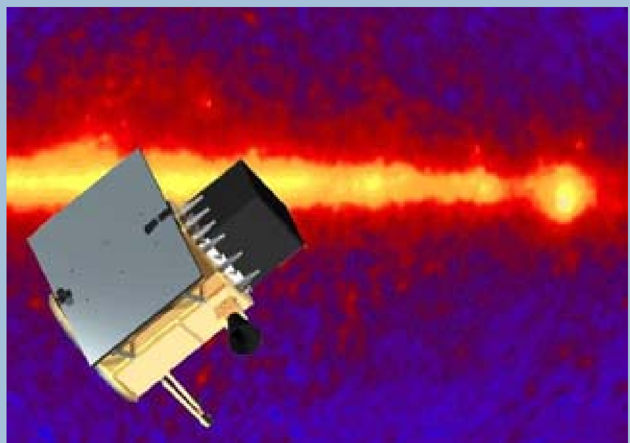

- AGILE, is an ASI Small Scientific Mission with crucial participation by IASF/INAF, INFN, CIFS
- Total satellite mass ~ 330 kg
- Scientific Instrument mass 120 kg

Scientific Institutes involved in the development of AGILE

PI: M. Tavani, IASF-Roma e Univ. Tor Vergata
co-PI: G. Barbiellini, INFN e Univ. Trieste

- IASF – CNR / INAF, sez. Milano
- IASF – CNR / INAF, sez. Bologna
- IASF – CNR / INAF, sez. Roma
- INFN- Sez. Trieste
- INFN- Sez. Roma I
- INFN- Sez. Roma II
- Università di Trieste
- Università di Roma "Tor Vergata"
- Università "La Sapienza"
- CIFS - Consorzio Interuniversitario per la Fisica Spaziale (Torino)

Main industrial contractors

- Carlo Gavazzi Space
- Laben
- Oerlikon Contraves
- Telespazio

AGILE Mission currently in Phase D.

Launch planned in second half of 2005 (PSLV, equatorial orbit 0-3 degree).

Use of Ground Station in Malindi (Kenya).

Mission Operations Center at TZP-Fucino.

Quicklook and data archiving at ASDC.

EGRET

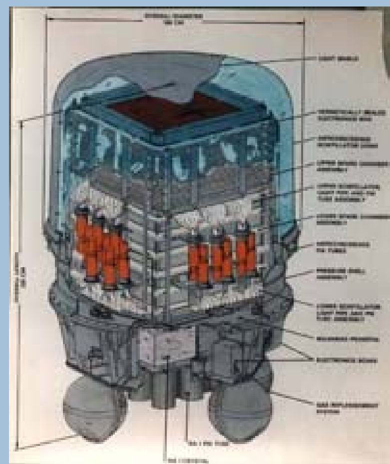

AGILE

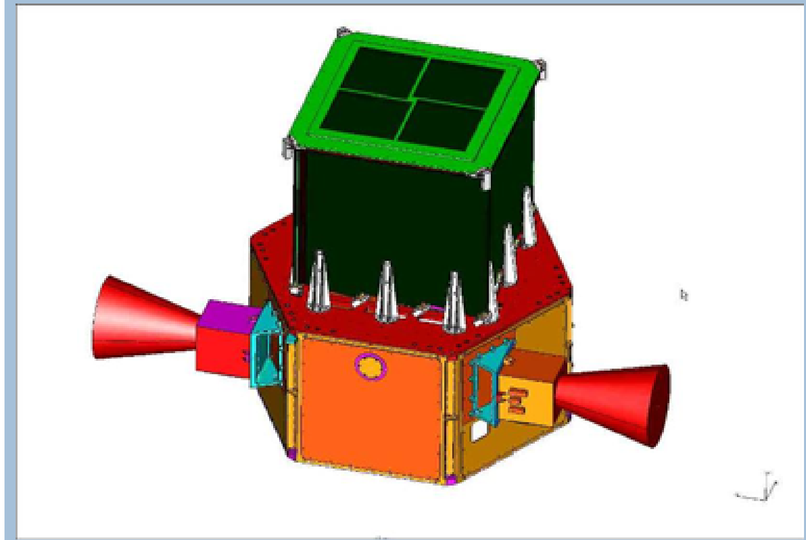

AGILE Instrument

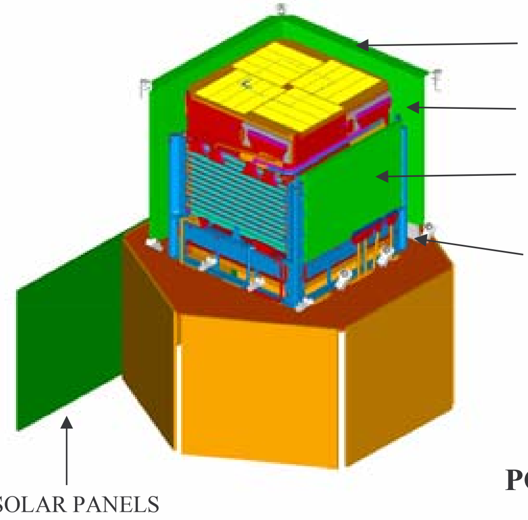

3 innovative features of AGILE:

(1) optimal imaging capabilities and large FOV in the energy bands:

* 15 keV - 45 keV (Super-Agile)
* 30 MeV - 50 GeV (GRID: Tracker+MCAL)

(2) Excellent X-ray/γ-ray timing (GPS)

(3) Burst search with large dynamic range (sub-milliseconds-60 seconds) and independent triggering of the Mini-Calorimeter (300 keV-100 MeV).

AGILE EM Vibration Tests (ENEA, Casaccia, 2-5 dec. 2003)

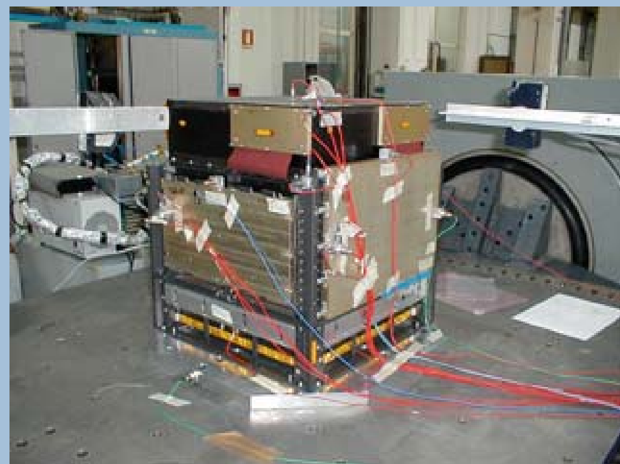

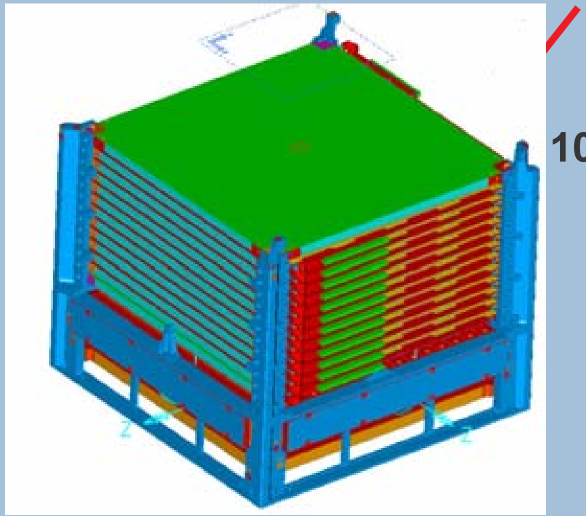

10 planes with
* $0.07\ X_0$

* 40 micron resolution

Total: $0.8\ X_0$

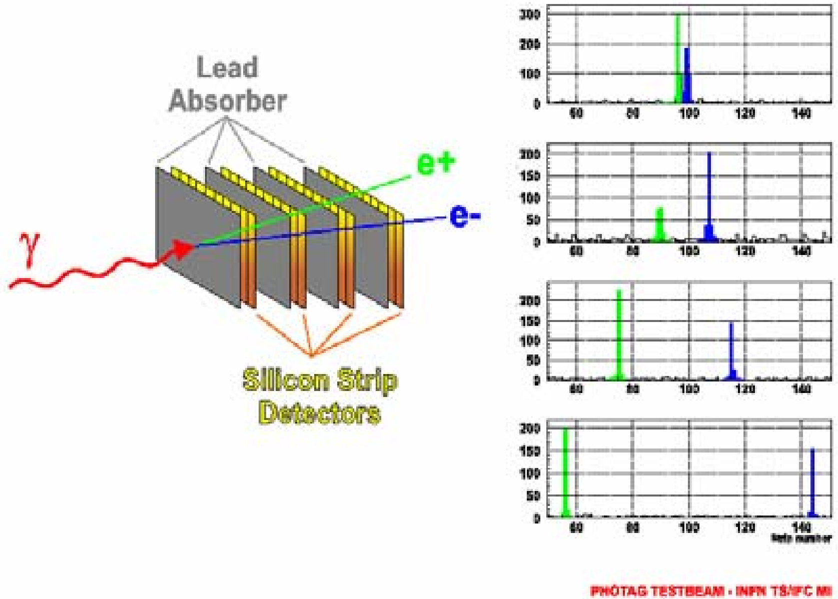

AGILE Tracker trays
(INFN-Ts, G. Barbiellini, M. Prest et al.)

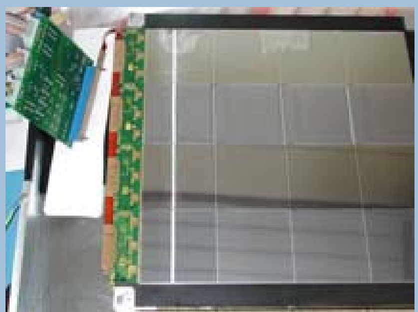

AGILE Tracker, TA A1 chip
(INFN-Ts, G. Barbiellini, M. Prest et al.)

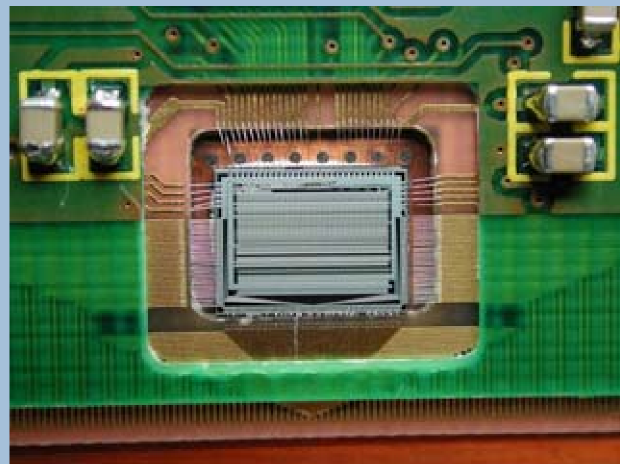

La stesura della colla sul vassoio 12 side bottom (tempo di stesura ≈ 4 min per ladder)

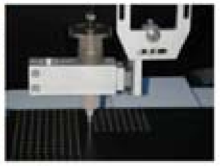

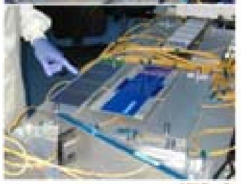

Il montaggio delle ladder sul sistema di trasporto

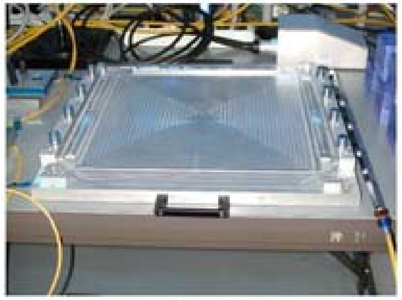

Il montaggio delle ladder sul vassoio e il vassoio completo

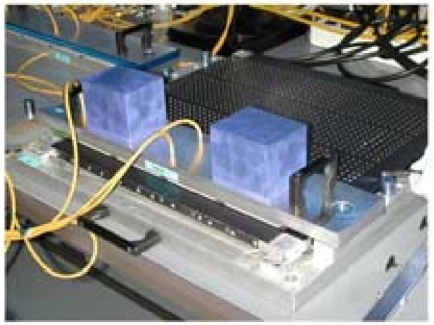

AGILE Tracker trays
(INFN-Ts, G. Barbiellini, M. Prest et al.)

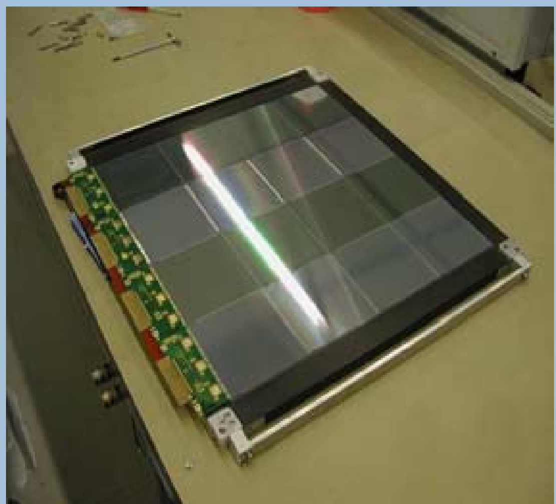

AGILE photon tagged beamtests at CERN (2002-2003)

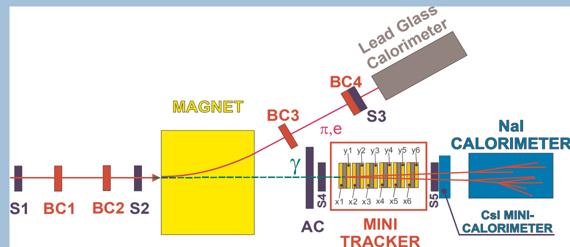

E_{photon} = 107 MeV
(Agile Beam Tests, CERN 2002-2003)

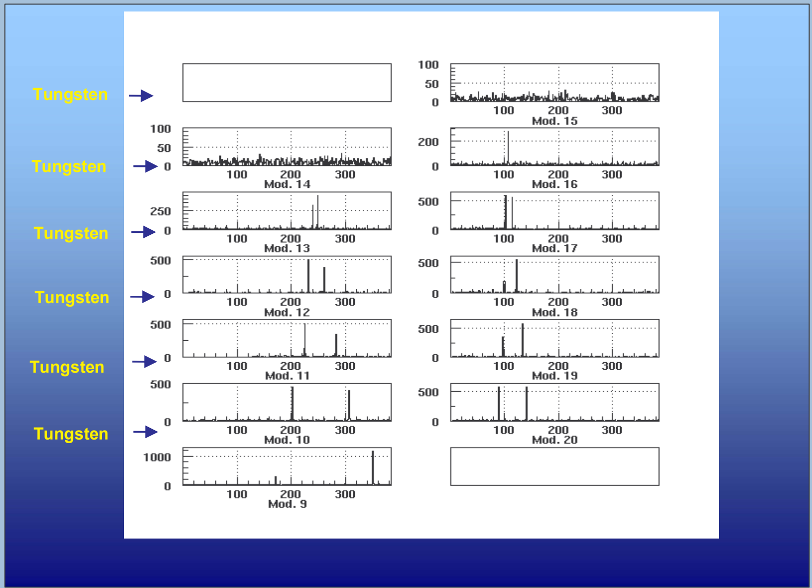

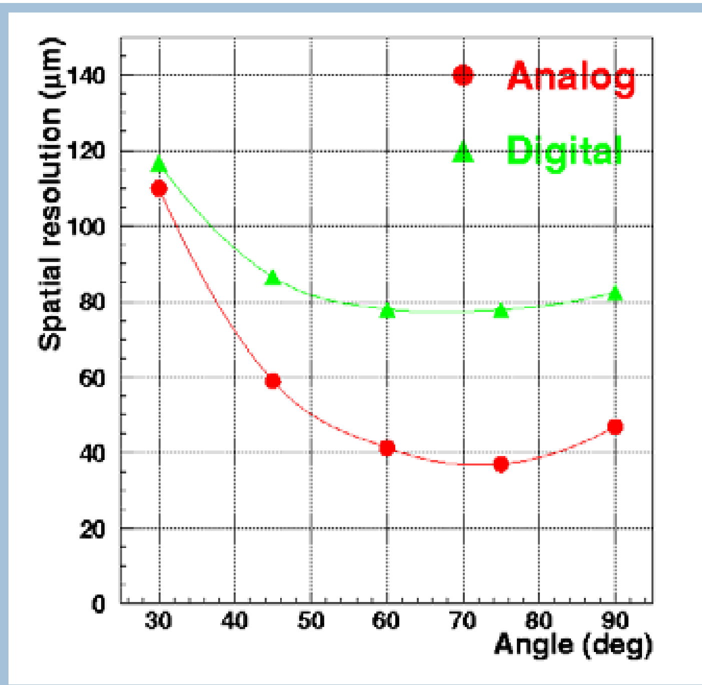

MINI-CALORIMETER

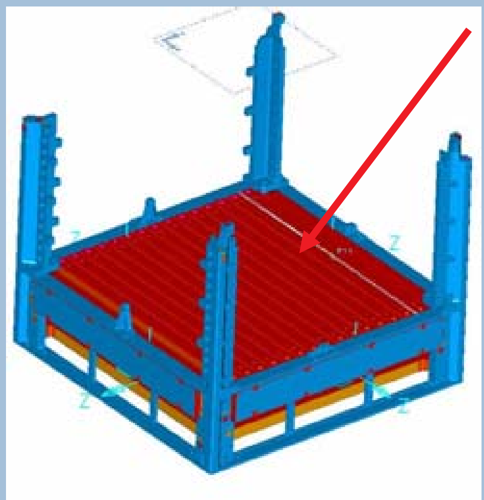

2 layers

30 CsI bars

300 keV-

100 MeV

A_{eff}~ 400 cm²

(@1-10 MeV)

GRID Effective Area

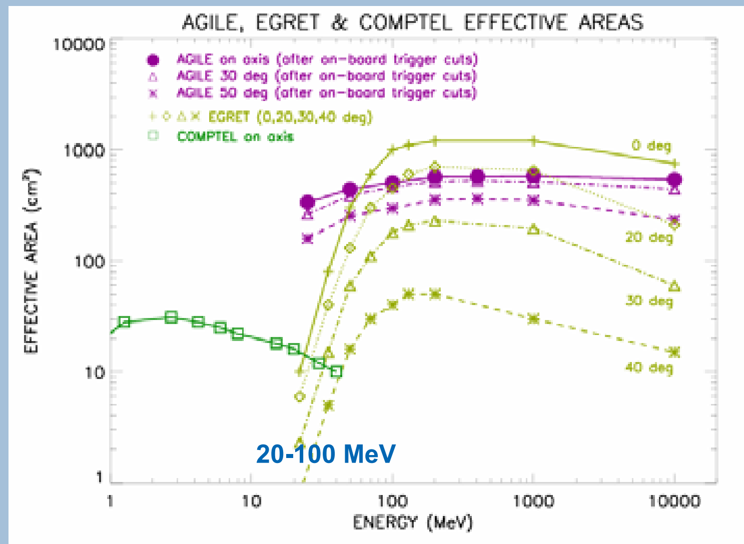

GRID angular response vs. EGRET

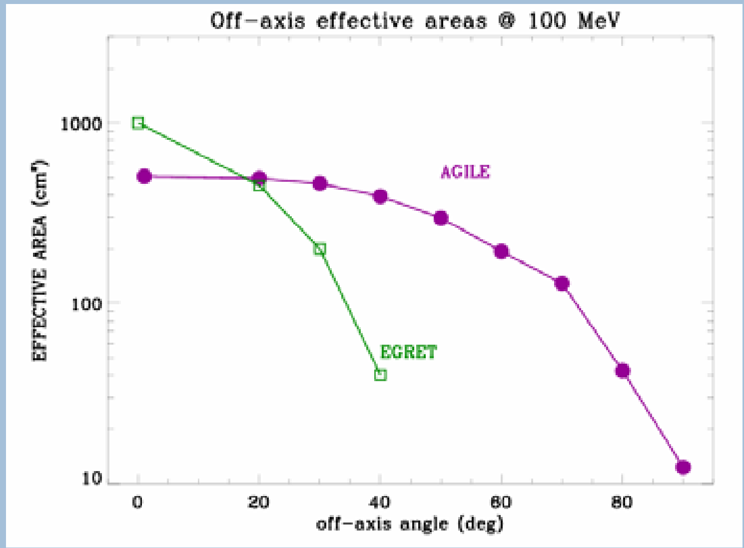

AGILE-GRID angular resolution

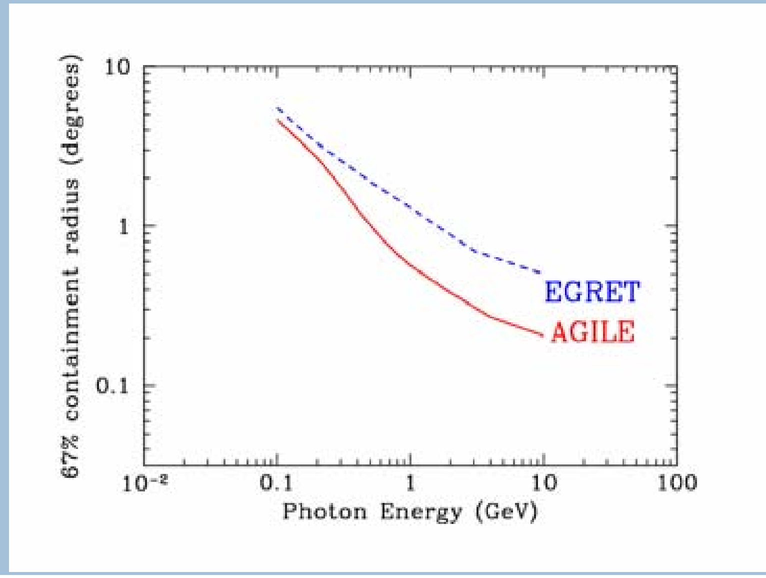

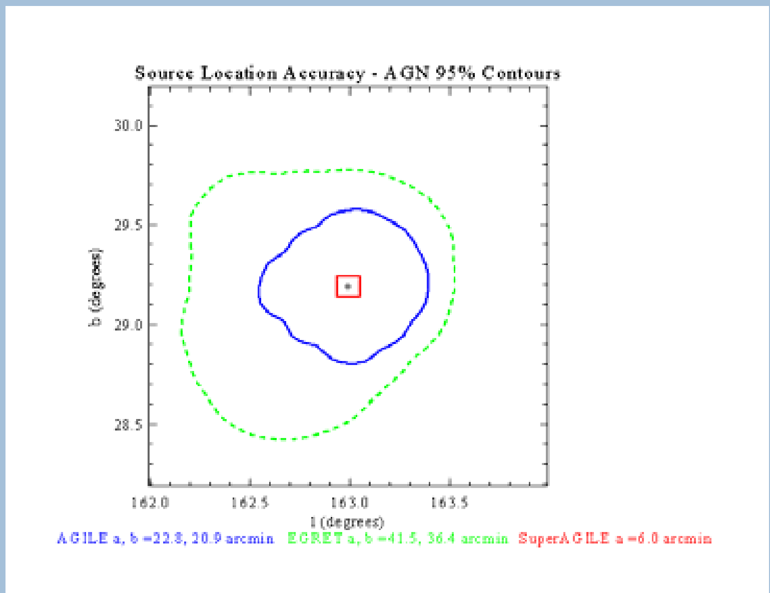

The X-Ray Imager (Super-AGILE)

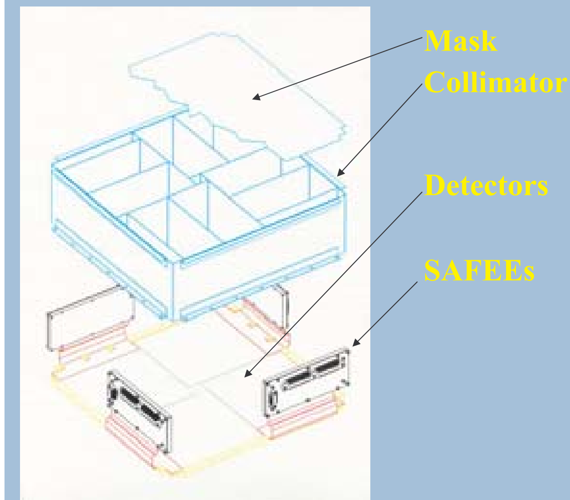

arcmin resol.

imager

15- 45 keV

Super-Agile: X-ray imager (15-45 keV)

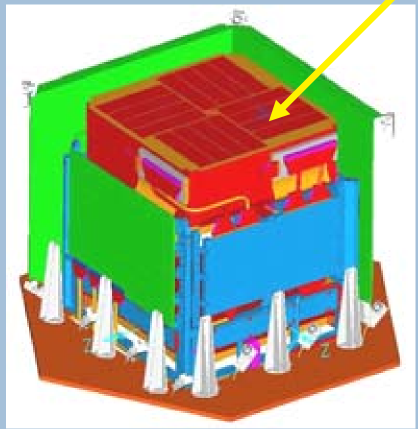

AGILE Engineering Model

Super-Agile detection capability for

Galactic sources

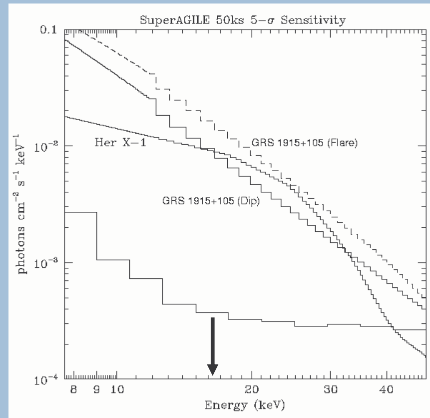

Extragalactic sources

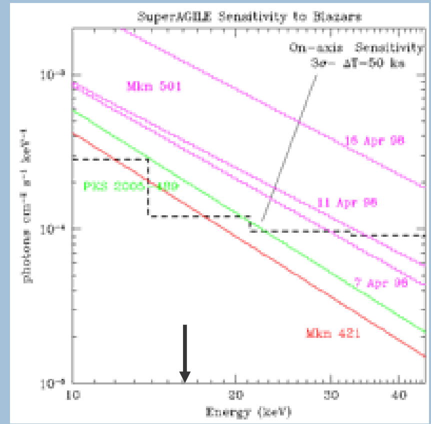

Super-Agile: GRB detection capability

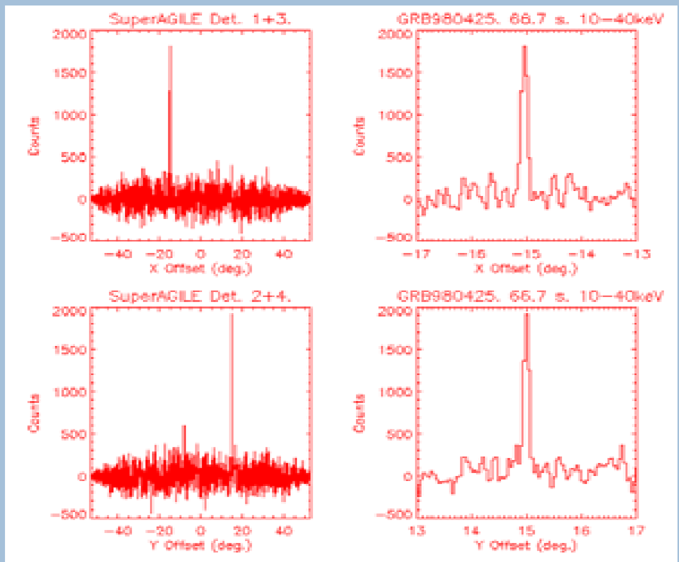

Alerts for GRB and other transients: AGILE Fast Link (ORBCOMM)

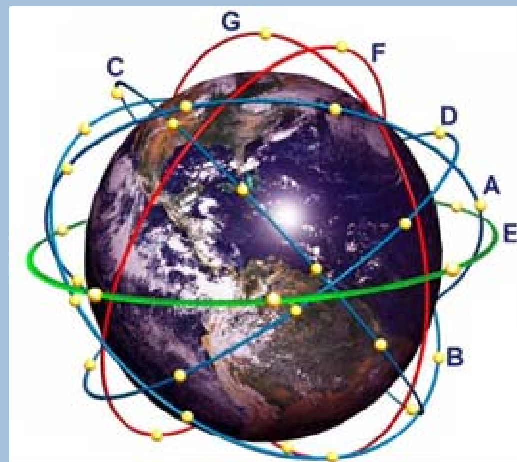

Alerts for GRB and other transients: AGILE Fast Link (ORBCOMM)

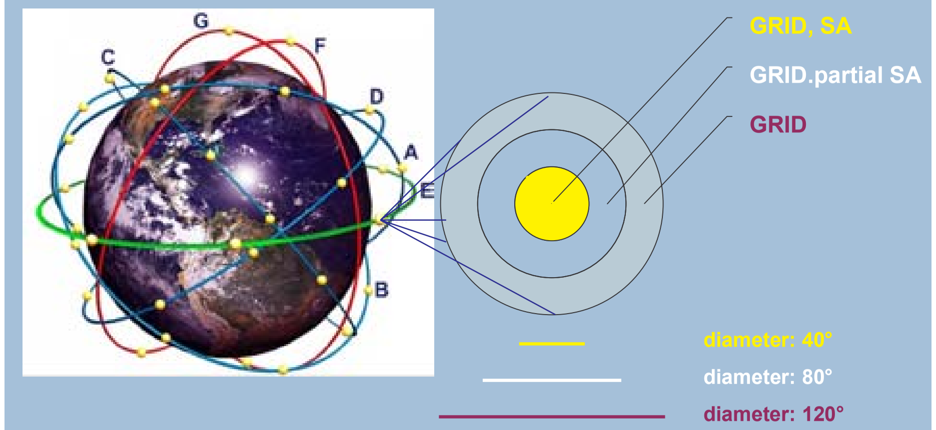

Gamma-ray exposure

EGRET | **AGILE**

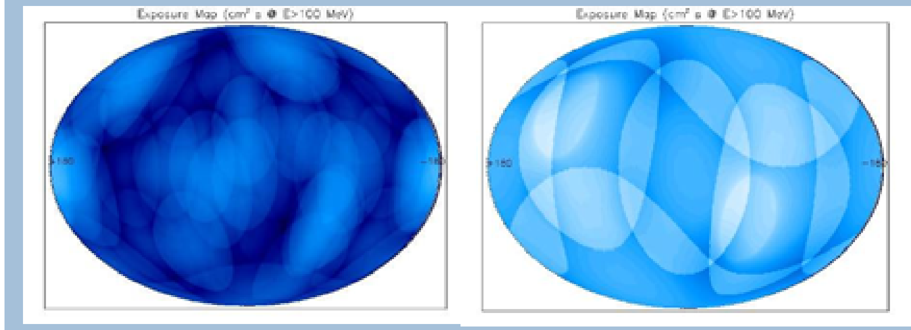

EGRET: ~ $3 \cdot 10^8$ cm² s sr (~1 yrs)

AGILE: ~ $3 \cdot 10^9$ cm² s sr (~1 yrs)

AGILE pointing strategy optimized with ground based observations (radio, optical, TeV)

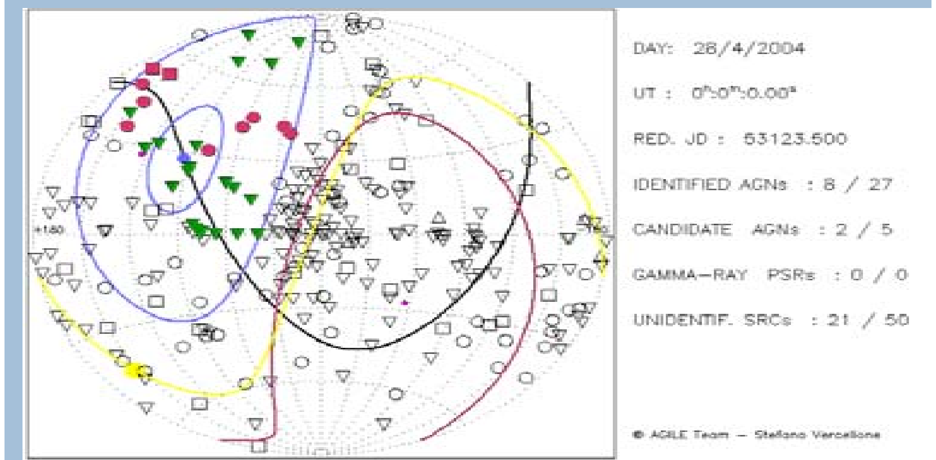

AGILE performance in AGN monitoring

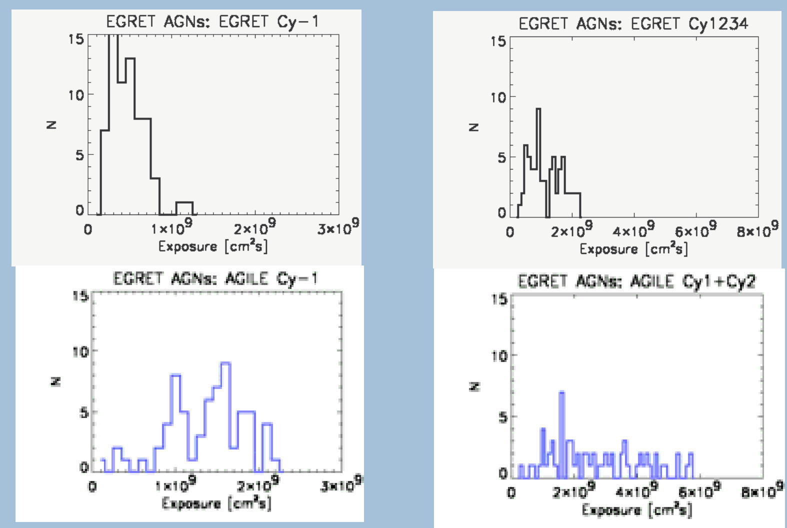

What about all the other AGNs...

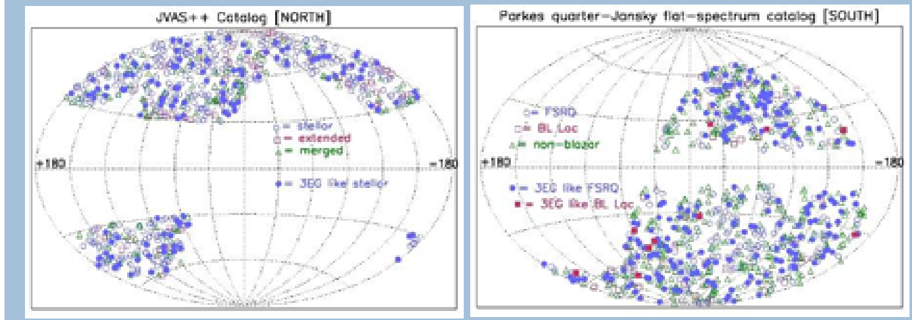

123 candidates in Northern em.
$F_{5\,GHz} > 0.497$ Jy
$z < 2.172$

225 candidates in Southern em.
$F_{5\,GHz} > 0.406$ Jy
$z < 2.286$

Assuming a ~10% duty cycle, AGILE will observe at each pointing about 10 AGN candidates for γ– ray emission

EGRET Galactic Sources (>100 MeV)

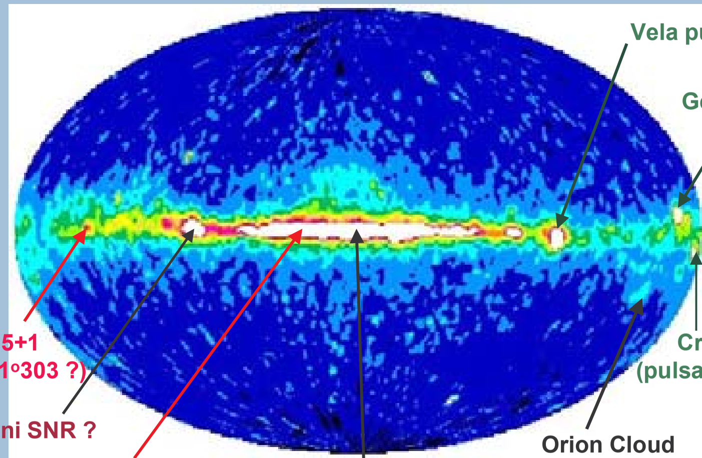

AGILE pointing simulation of the Galact. Center

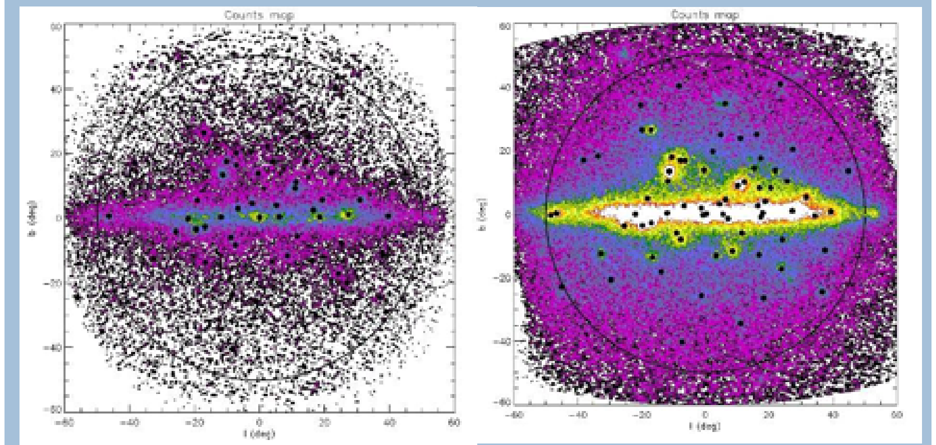

CHALLENGING SOURCE MONITORING (Likelihood simulations)

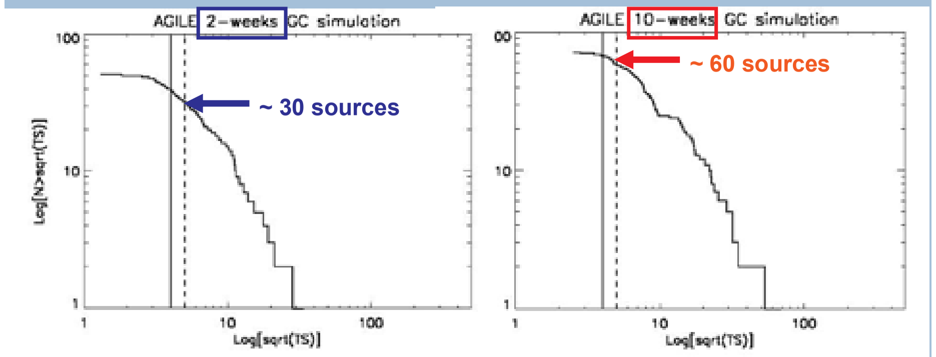

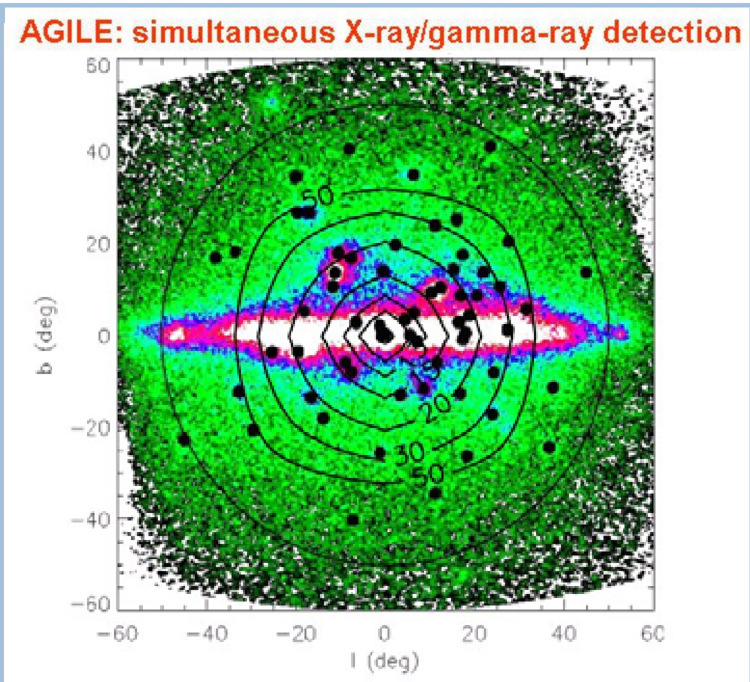

X-rays + Gamma-rays !!!

	X-rays (20-100 keV)	γ-rays
PSRs	yes	yes
Cyg X-1	> 100 mCrab	?
GRS 1915+104	10-100-1000 mCrab	?
PSR 1259-63	1-10 mCrab	no, ?
2CG 135+01	0.1-1 mCrab	yes

New prospects for AGILE: X-ray/γ-ray detection/monitoring of Galactic sources

- Discovery of hundreds of hard X-ray sources by INTEGRAL (Revnivtsev et al. 2004, Bird et al. 2004)
- LMXBs and BHCs flaring above 20 keV, more than 1/3 with fluxes 10-100 mCrab
- "Compton thick" sources…how many ?

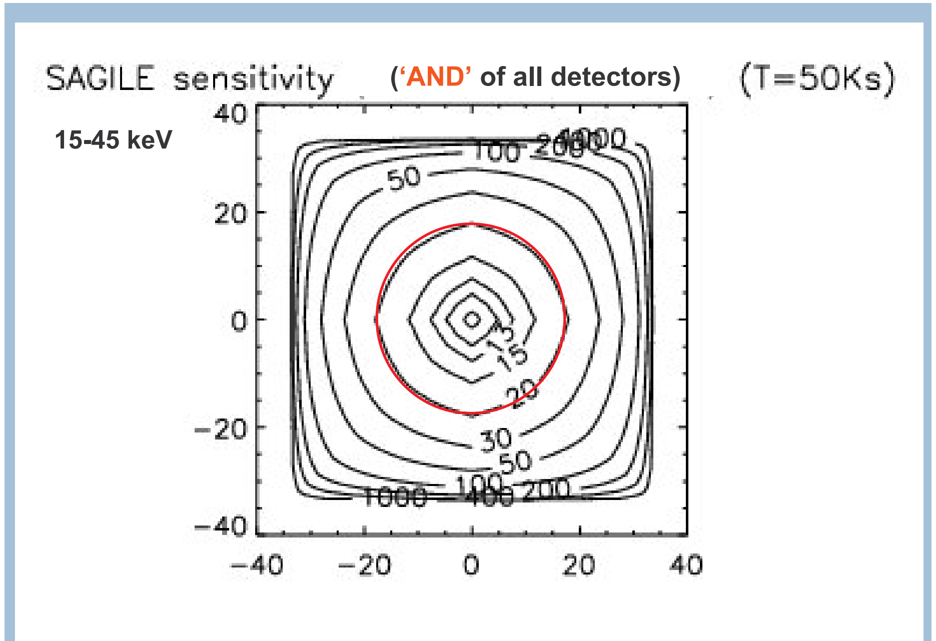

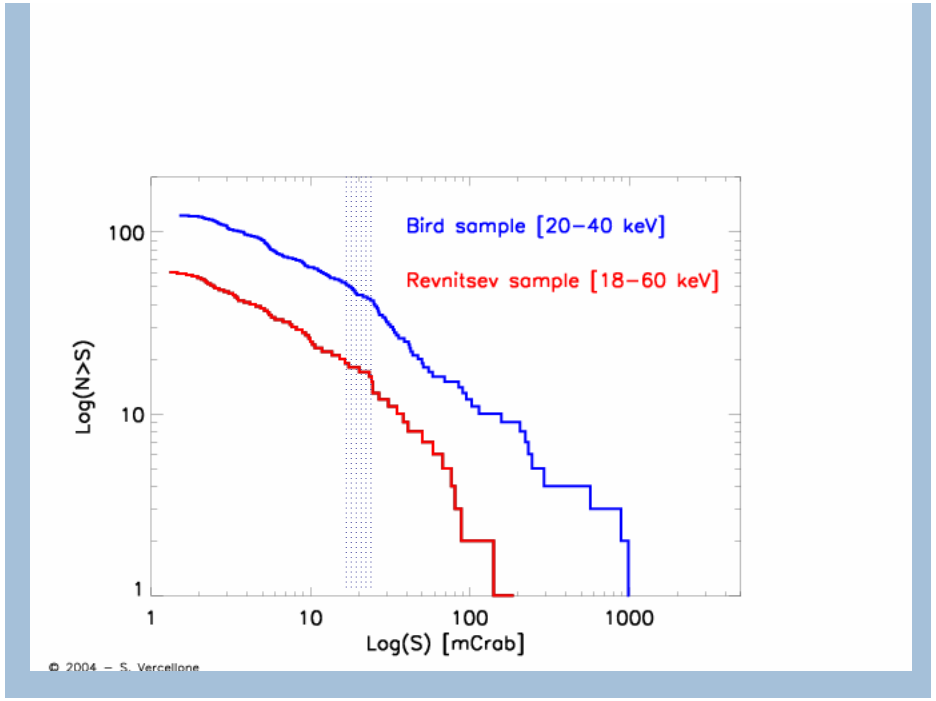
Bird sample [20–40 keV]
Revnitsev sample [18–60 keV]
Log(N>S)
Log(S) [mCrab]
© 2004 – S. Vercellone

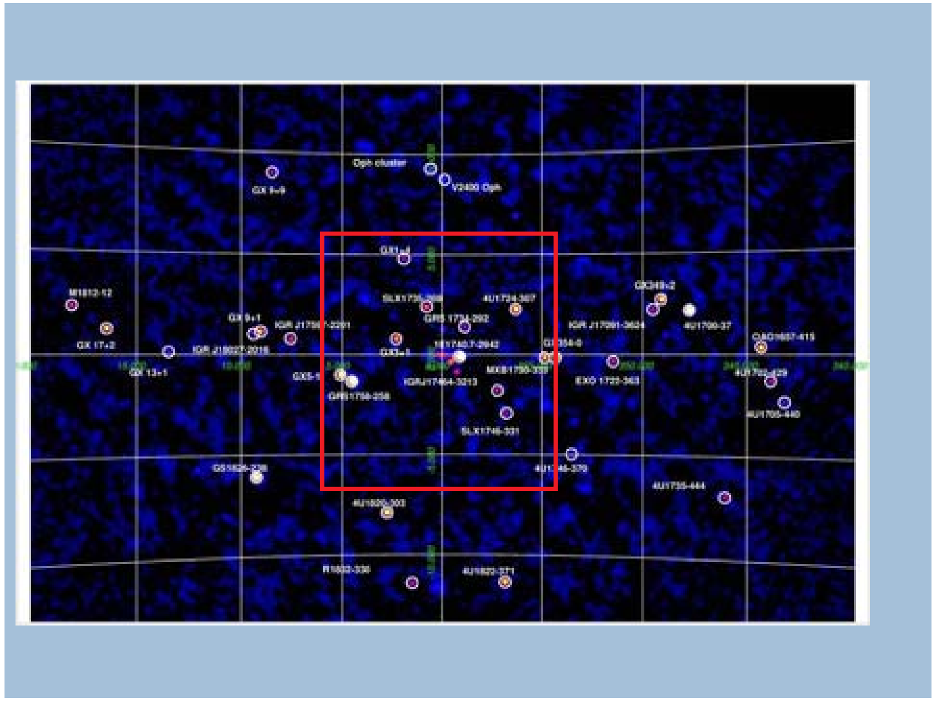

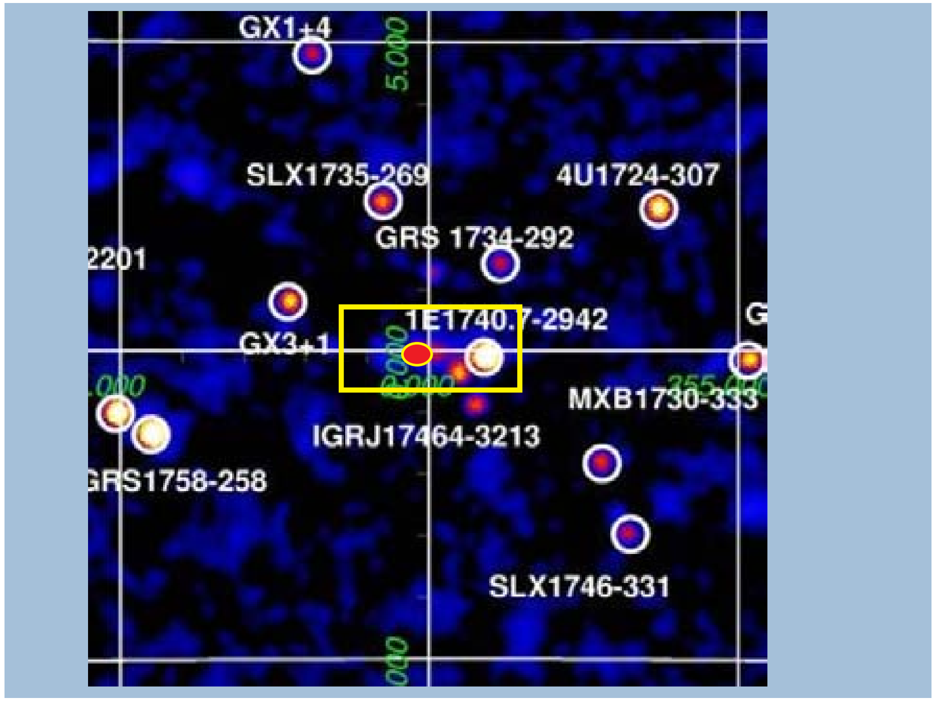
GX1+4
SLX1735-269
4U1724-307
GRS 1734-292
GX3+1
1E1740.7-2942
MXB1730-333
IGRJ17464-3213
GRS1758-258
SLX1746-331

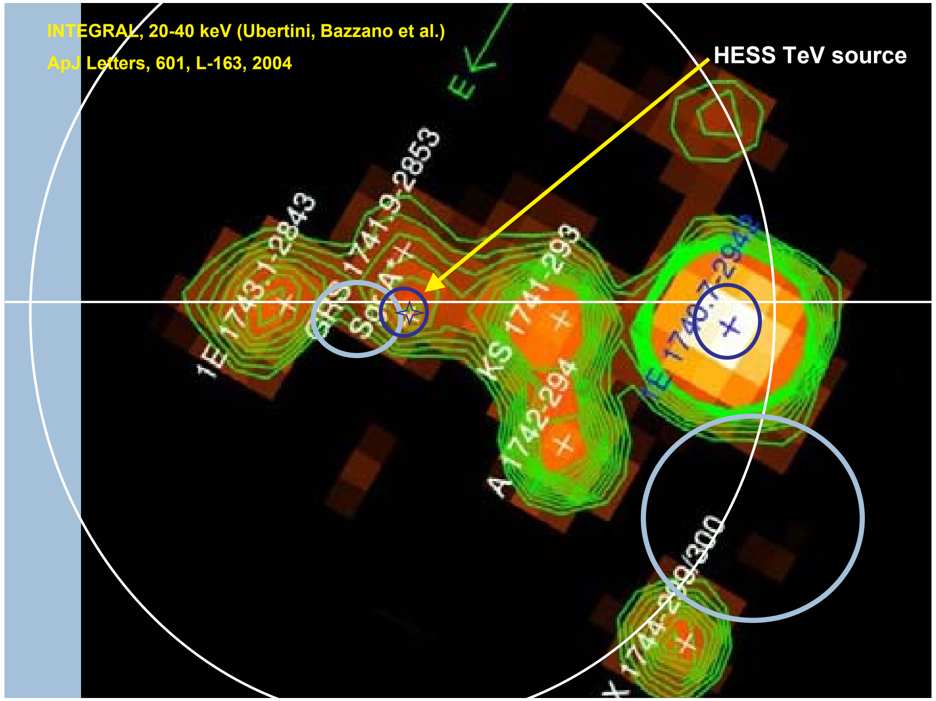
INTEGRAL, 20-40 keV (Ubertini, Bazzano et al.)
ApJ Letters, 601, L-163, 2004
HESS TeV source
1E 1743.1-2843
1E 1740.7-2942
KS 1741-293
A 1742-294
1E 1741.9-2853

- Simultaneous imaging and monitoring in the 15-45 keV and 30 MeV-30 GeV bands is the unique plus of AGILE.
- GRB on-board search with a large dynamical range of timescales and independent self-triggering in the energy ranges 15-45 keV, 300 keV-100 MeV, 30 MeV-30 GeV.
- GRB on-board positioning within 3-6 arcmin and GRB alerts within 1-3 minutes.

- Equatorial orbit (0-3 degrees): low-bkg !
- Quicklook Analysis results available to the community.
- Guest Observer Program.
- AGILE Science Group: multiwavelength program.

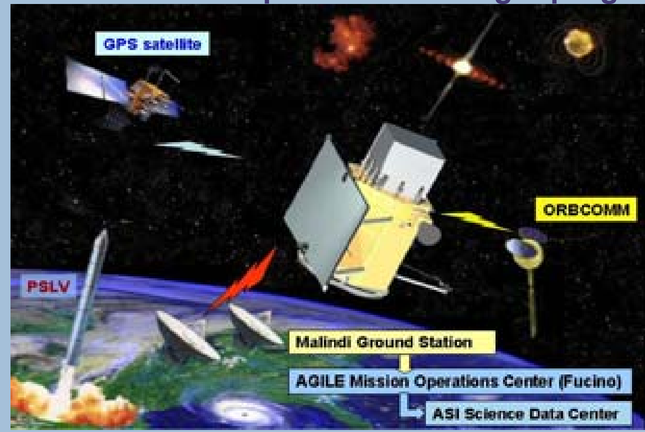

Forthcoming AGILE Science Workshops

- Fall 2004, tbd
  "The Galactic Center"

- Spring 2005, tbd
  "Selected topics in GRB high-energy modelling"

The REM Observatory:

Filippo Maria Zerbi
INAF Osservatorio di Brera
On behalf of the REM/ROSS team

Menu of the meal

Science with REM

How you can Access REM

A fast moving telescope …
- Alt-az 60 cm f/8 RC silver-coated
- 2 Nasmyth foci (one idle)
- 60 deg 5 sec – to any α,δ in 60 sec

… with a high throughput NIR Camera…
- 10x10 am^2 FoV
- 1.2 as pixel scale (diff.limited)
- 0.9-2.3 microns (Z',J,H,Ks)
- 512x512 HgCdTe chip @77 Kelvin
- Wobbling plate for dithering

… and a Visible Imaging-Spectrograph
- 10x10 am^2 FoV
- 0.55 as pixel scale
- 30 bins between 0.45-0.9 μm (Amici Prism)
- 1024x1024 Marconi CCD in Apogee head

The Telescope

- Alt AZ mount
- Direct Torque Motors 12 deg/sec max speed both axis.
- IR-optimized Mech. Structure
- Derotated Nasmyth Focal Station
- Etel/Heidenain – Profibus control system
- F/2.2 primary F/8 RC optical system
- Protected Silver Coating

The Instrument Flange

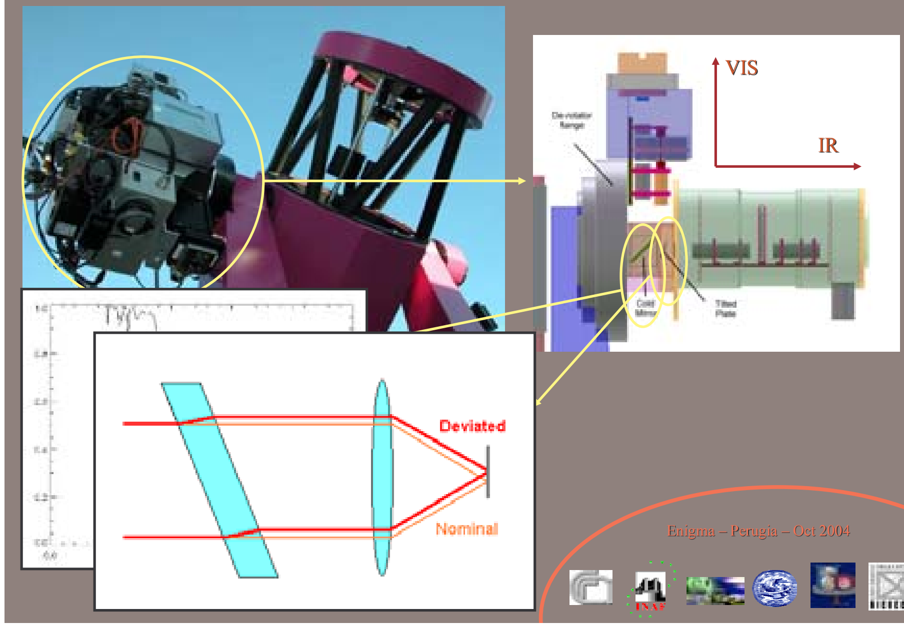

The IR Camera

- Focal Reducer Configuration
- Thick easy-to-align lenses
- Stirling cryocooled – no bath no helium lines
- Light self-cooled dewar

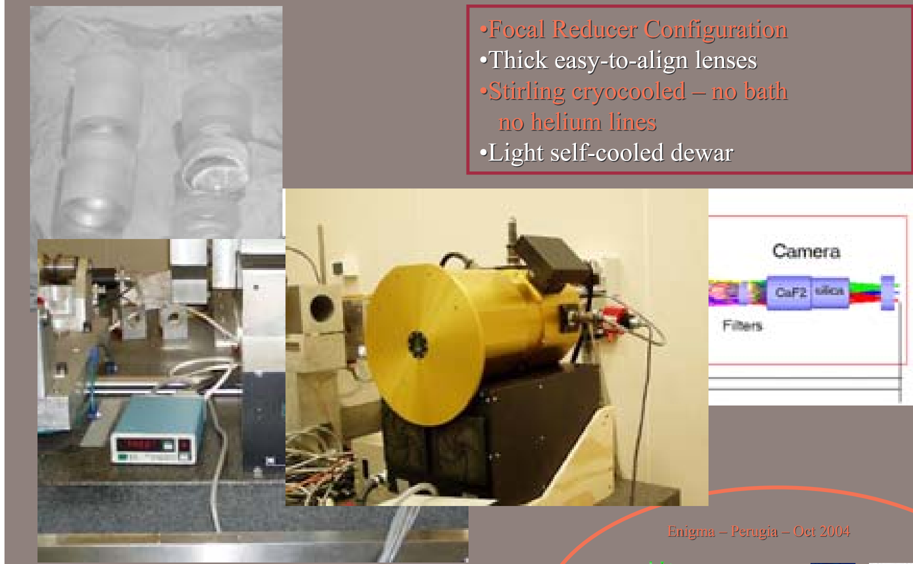

The ROSS Spectrograph

- Focal Reducer Configuration
- AMICI prism for slitless spec.
- Thick filters to match AMICI
- Mounted orthogonal to IR axis

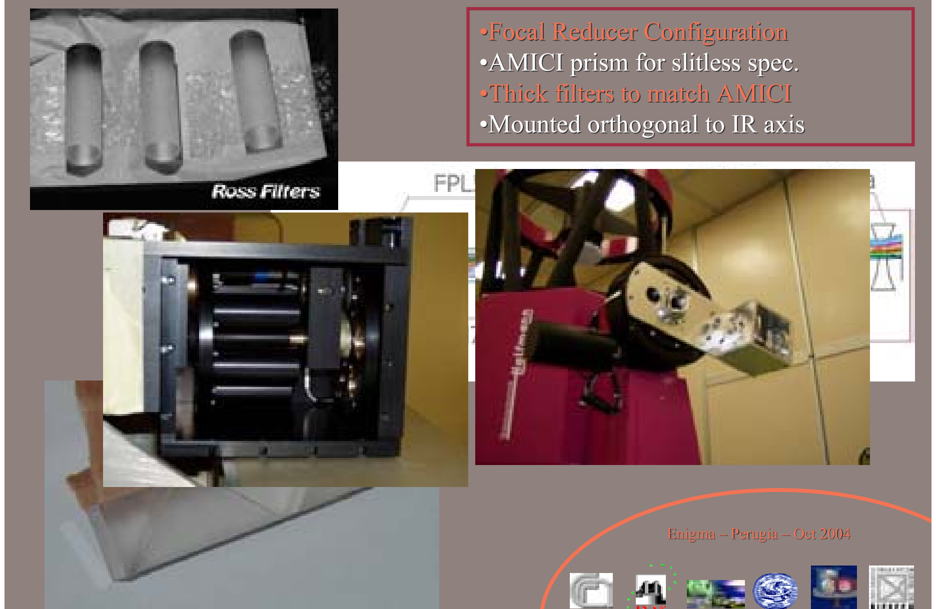

Nôtre Dome de la Silla

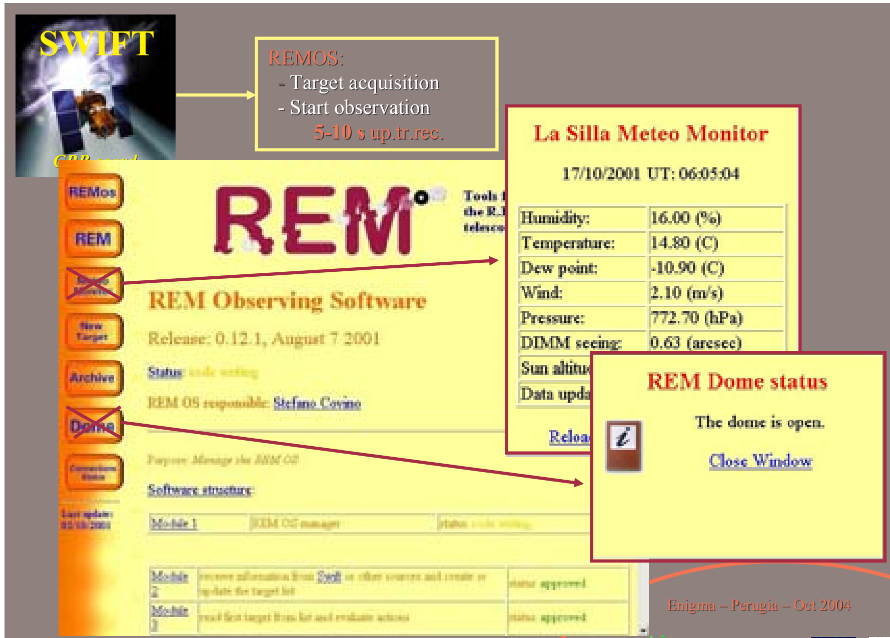

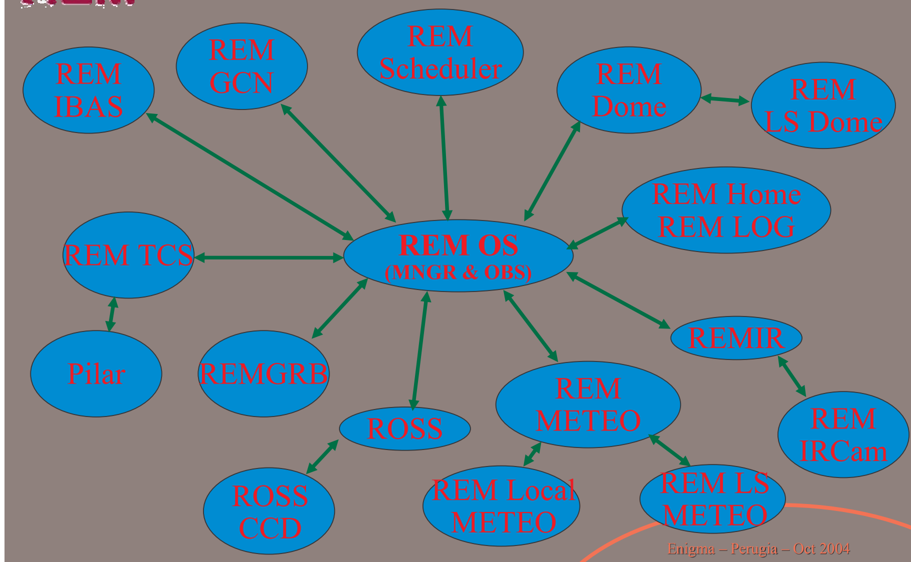

What is REM for ?

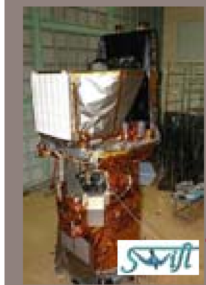

REM is conceived as a **link** between transient phenomena detected at high energy from space AND Large ground-based facilities on the ground → **Gamma Ray Bursts**

Such a link is needed for:

- Transient Coordinate determination

High Energy detections have large error-boxes

- Pre-screen of transient characterisitics

Cases selection for further observations

In both Cases crucial are:

a) Coverage up to NIR

b) Fast response

REM

Who triggers REM ?

SWIFT

What SWIFT gives us is

- Position of the GRB - [15 sec] (4 am)
- Position of the XT [20-70 sec] (5 as)
- Position of the OT [20-70 sec] (n/10 as) (if there)
  Color Information 0.15-0.65 μm[600 sec]

What SWIFT does not give us

- Position of the Red-T (above 0.65 μm) and NIR-T

>150 trigger per year !

REM

50% of the known GRB do not show an Optical AG.
It could be **dust** or it could be Ly-α if the GRB is high-z

→Fast – NIR←

REM

ROSS acquires 30 simultaneous calibrated data points between 0.45 and 0.9 microns

This allows to:

- Correlate the time of the optical peaks with the distribution of Lorentz Factors in the original cataclysm.
- Detect the possible time dependent obscuration of optical transients associated with GRBs.
- Possibly detect the peak energy that goes from gamma to optical within few hours.

REM

Any possible optimization of the Space-borne trigger source will let free REM observing time

INTEGRAL-AGILE few bursts
SWIFT-HETE II more bursts but
latitude/longitude constraints

- Housekeeping and calibration
- Other Observing programs

Anywhere Rapid multi-frequency observations are needed

1. Multifrequency monitoring of AGNs
2. Black Hole Candidates –X-ray Novae
3. Flare Stars

Other Programs Proposed by
The community

REM

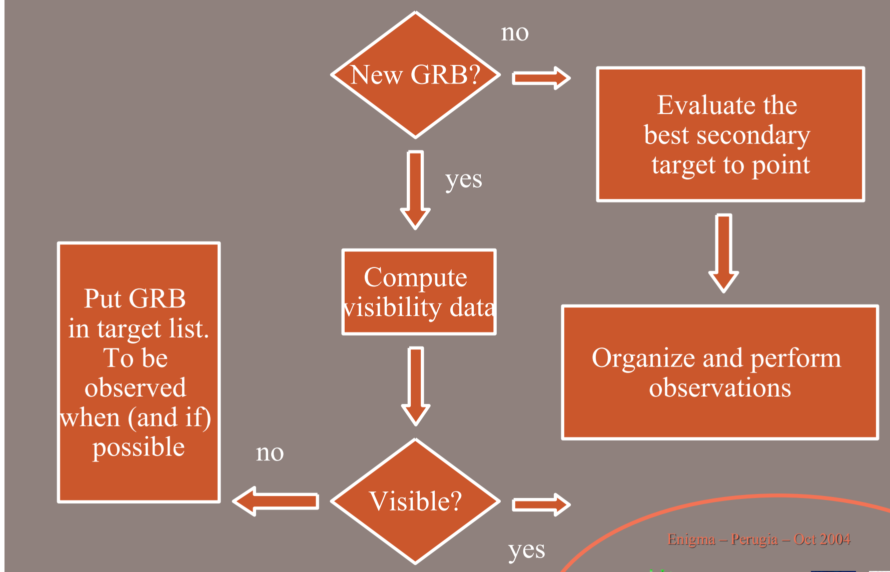

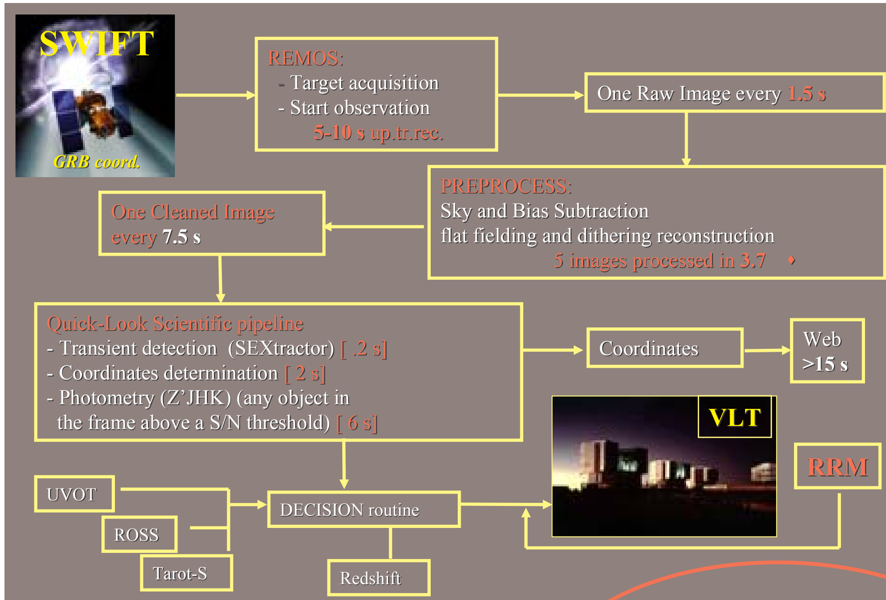

REM

What has REM done so far?

Flat
Calibration
Flat
Calibration
Flat
Calibration
Flat
Calibration
Flat
Calibration

Error
Debugging
Error
Debugging
Error
Debugging
Error
Debugging
Error
Debugging

Modify the cable
Tune the motor
Change the port
UPS
Firewall
Redundancy
Etc.

- No degradation of expected performances
- Acceptable (and improving) duty cycle
- Acceptable reliability

REM

All happened during La Silla day time!

Most of the "visible" GRBs from starting of operation have been observed.

GRB 031203	(Zerbi et al. 2003)
GRB 040106	(Palazzi et al. 2004)
GRB 040223	(Israel et al 2004)
GRB 040416	(not a real GRB!)
Some SGRs!	
GRB 040511	(Testa et al. 2004)
GRB 040624	

GRB 040511

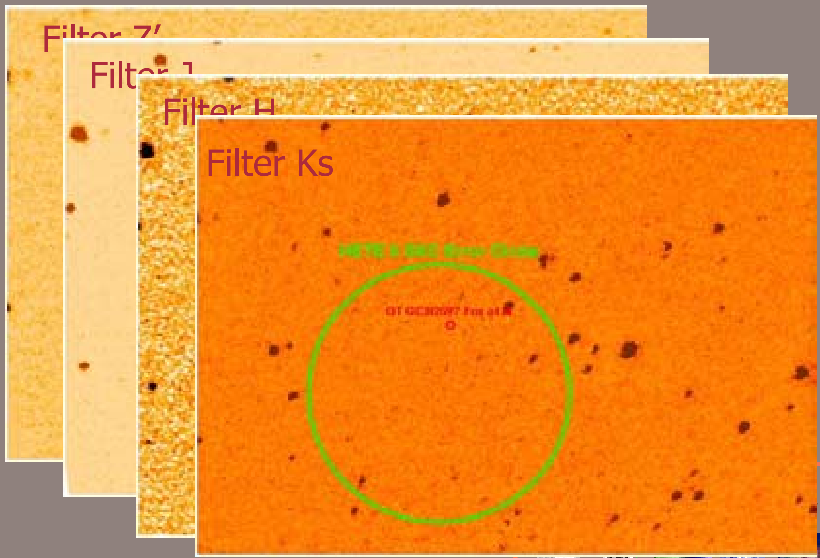

GX339-4 :
a BH candidate

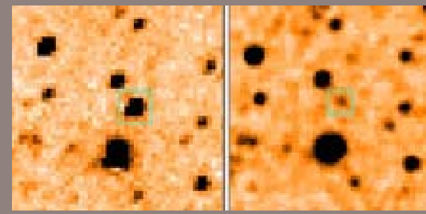

The bright status discovered
by comparison with the
2mass catalogue

Some SGRs…

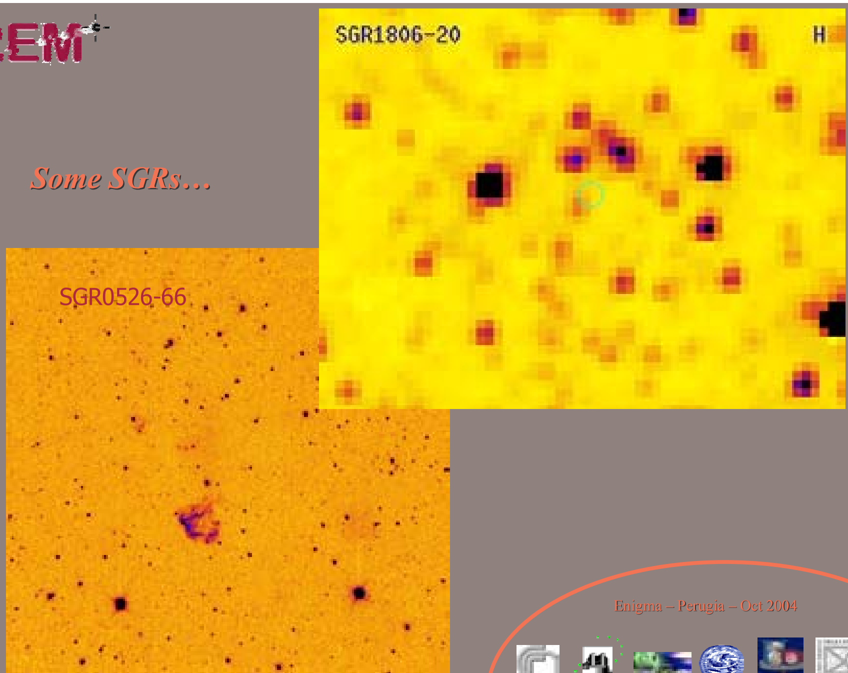

HMXB IGR16318-4848
High Mass X-Ray Binary.

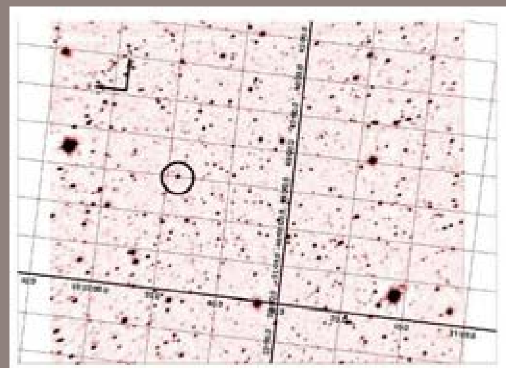

The first new gamma source discovered
by the INTEGRAL IBIS/ISGRI
imager on 2003, January 29

REM

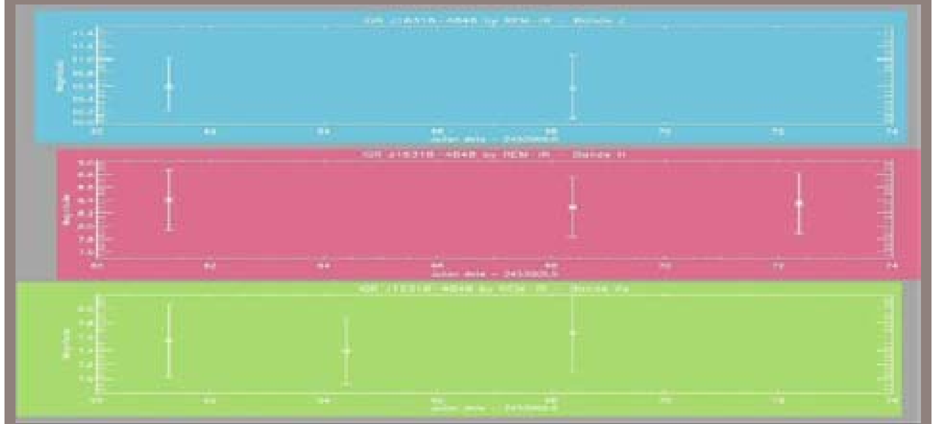

Looking for variability of the source to check then nature of the collapsed object

REM

ROS

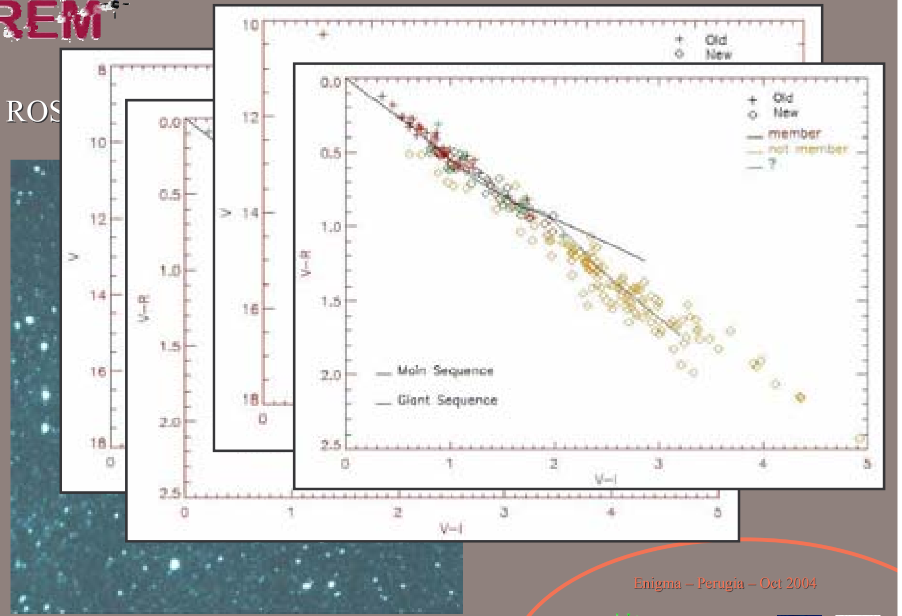

REM

VCC Galaxies

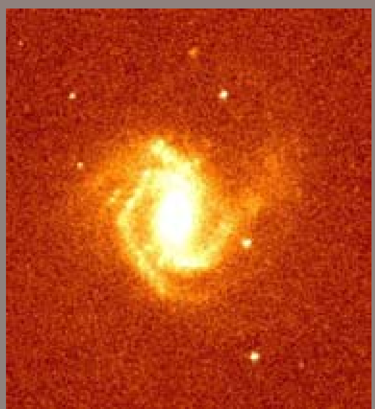

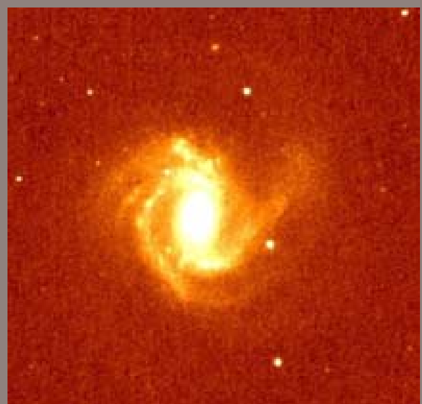

Extended object surface NIR photometry.

REM

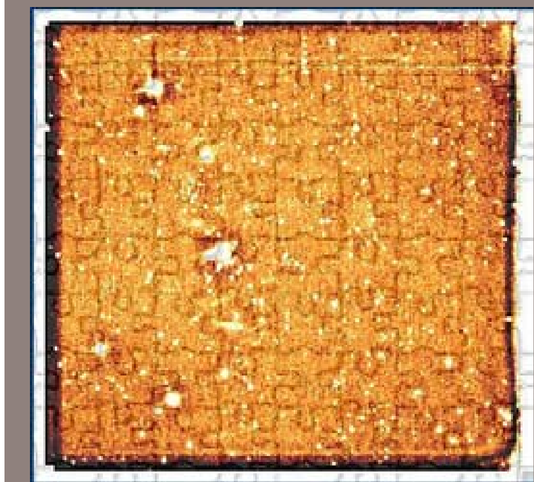

IRS 17

Mosaicing H2 images of Molecular Clouds

REM

Even Something Amusing…

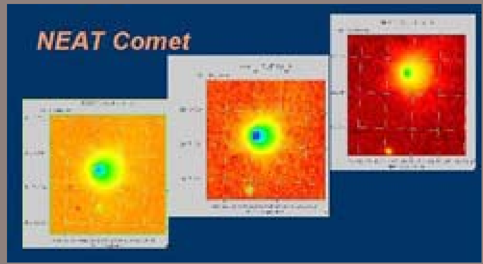

…. The NEAT comet

REM

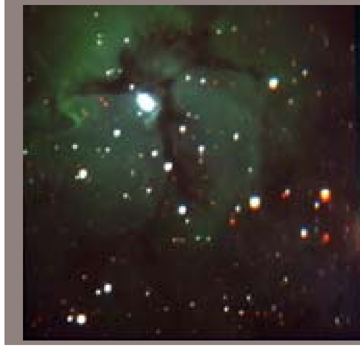

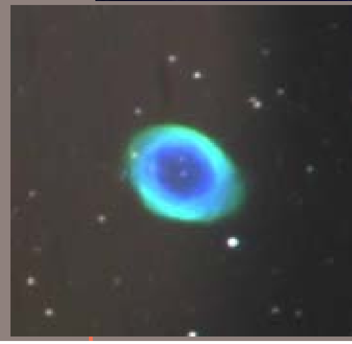

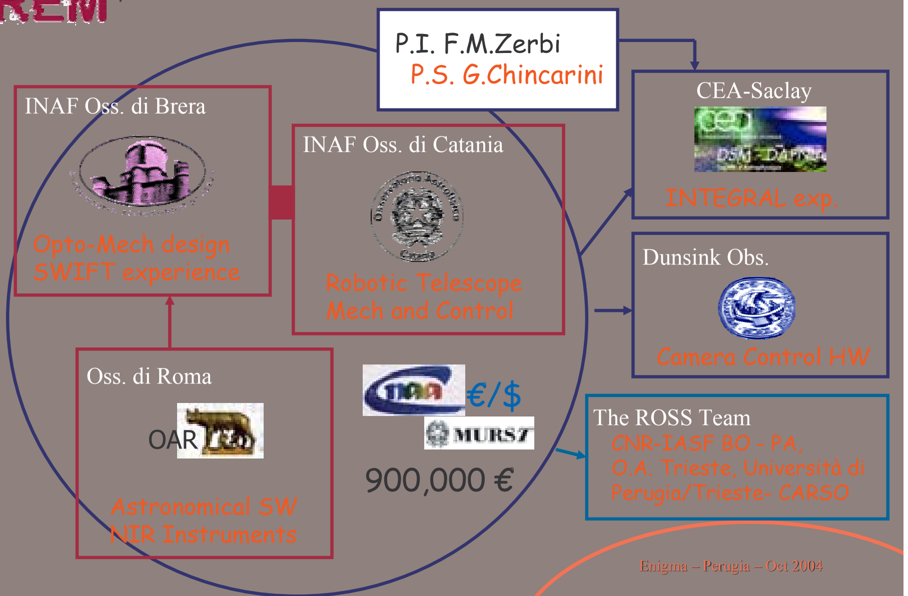

REM

Intellectual property rules

3.4 Secondary "individual projects " results

A minor amount of telescope *idle time* will be dedicated to "individual projects" initiated by members of the REM team or other astronomers in the community. A call for prop[…] issued and a number of referees selected in the REM-ST will judge the proposal and […] time.

The Intellectual property of the data belongs to the whole REM-Team but the access to […] be reserved to the proponent team until publication. The proponent team have the resp[…] analyze the data and publish the results in a correct and timely manner. After publica[…]

As described in ***Annex A***, the Consortium is fully responsible for the use and handling of idle time data and results. Such responsibility includes receiving proposals for the use of such idle time from the ESO community.

A Panchromatic Gamma Ray Burst Mission

Gianpiero Tagliaferri

October 7, 2004

Perugia

Swift Overview

Catching Gamma Ray Bursts on the Fly

- Selected by NASA on October 14, 1999 for flight in 2003
- Objectives
  - Determine origin of GRBs
  - Use GRBs to probe the early Universe
  - Perform hard X-ray survey
  - Its multiwavelenght capability and fast reaction are very effective also for various other research fields (BLAZARS …)
- International collaboration:
  - GSFC: lead institution
  - PSU: lead university partner
  - UK & Italy: key hardware collaborators
  - Spectrum Astro: spacecraft provider

Italian Contributrion & Responsibility

- Mirror Module of the XRT Telescope
- Malindi Ground Station (ASI)
- XRT Data Analysis software
- BA responsibility
- XRT calibration & operation support

The discovery of Gamma Ray Bursts

- 1967-1973 Vela 4,5,6 satellites: look for X and gamma rays in order to monitor compliance with the Geneva Limited Nuclear Test Ban Treaty of 1963 (no nuclear tests in space and atmosphere)
- Discovered intense flashes of Gamma-rays of cosmic origin:

  GAMMA RAY BURSTS (GRBs)

  (Klebesadel et al. 1973; Strong et al. 1974)

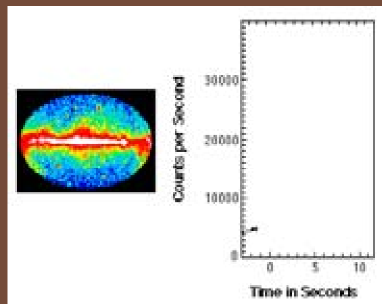

-Hundreds GRBs discovered from satellite networks through the 80's.

- No clue on source distance

-Early models often involved neutron stars

- Remarkably little is known about gamma- ray bursts (Harwit 1984 in "Cosmic Discovery")

Are there different Gamma-Ray Bursts types ?

- GRBs duration distribution is bimodal (e.g. Briggs et al. 2002)
  - 0.1-1 s -> Short bursts
  - 10-100 s -> Long bursts
- Short GRBs are harder than long GRBs
  (e.g. Fishman & Meegan, 1995;Tavani 1996).

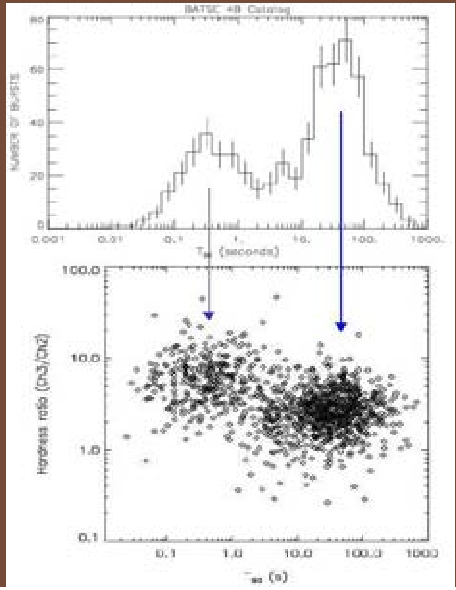

BeppoSAX & GRBs Afterglows

- Italian-Dutch satellite for X-ray astronomy (1996 -2002)
- Wide energy range (from Gamma to soft X-rays)
- Good positional accuracy (~ 1 arcmin)
- Relatively fast repointing capabilities (down to 3-4 hours)

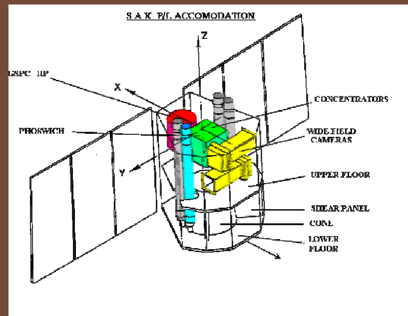

GRB970228: the 1st X-ray and Optical afterglow

- Fast follow up with the BeppoSAX-NFIs (8hr) led to the discovery of a bright unknown X-ray source.
- A second pointing 3 days after showed that source had faded.

(Costa, et al., 1997)

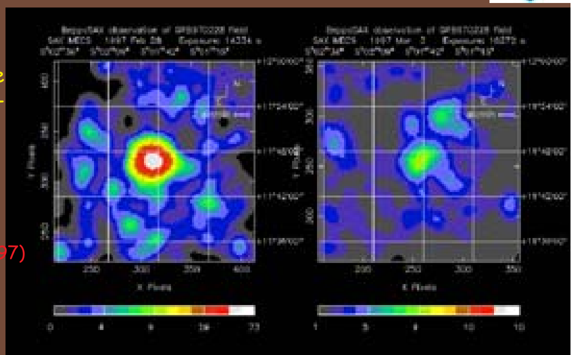

- Accurate (~1 arcmin) X-ray position led to the identification of a fading optical source from ground based telescopes

(Van Paradijs, et al., 1997)

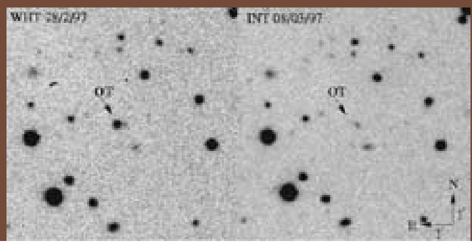

GRB970508: the 1st redshift

- Images in the 2-10 keV range by the BSAX WFC (10-200 sec after the GRB) and by the BSAX MECS (6 hrs and 3 days).
- The BSAX observation led the Caltech group to the measurement of the first redshift and Frail et al to the discovery of the 1st radio afterglow and direct measurement of relativistic expansion

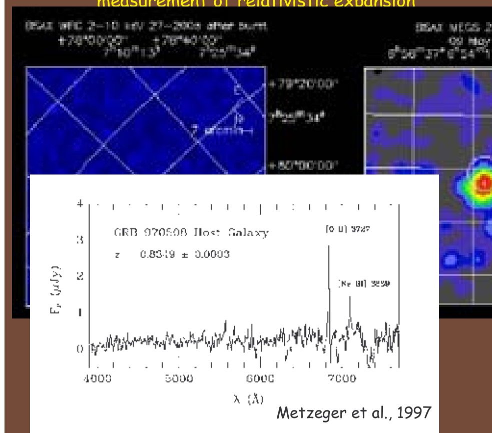
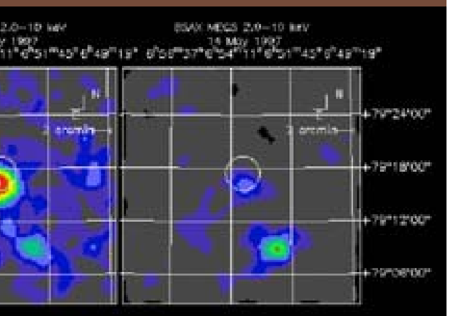

Metzeger et al., 1997

GRBs are at cosmological distances !

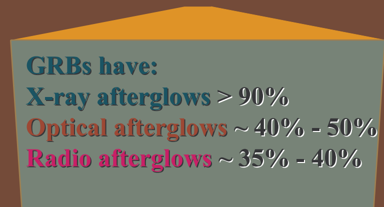

Requirements for Discovery

- Afterglow observations immediately following GRB when emission is brightest
- Multiwavelength afterglow observations for > 200-300 GRBs
- Arcsec positions immediately to ground for spectroscopy when emission is bright
- Sub-arcsec positions for hundreds of GRBs for host galaxy ID and GRB origin determination
- Redshifts for hundreds of GRBs

Swift Instruments

Instruments

- Burst Alert Telescope (BAT)
  - New CdZnTe detectors
  - Detect >100 GRBs per year depending on logN-logS
  - Most sensitive gamma-ray imager ever
- X-Ray Telescope (XRT)
  - Arcsecond GRB positions
  - CCD spectroscopy
- (UVOT) UV/Optical Telescope
  - Sub-arcsec imaging
  - Grism spectroscopy
  - 24th mag sensitivity (1000 sec)
  - Finding chart for other observers
- Autonomous re-pointing 20 - 70 sec
- Onboard and ground triggers

Spacecraft

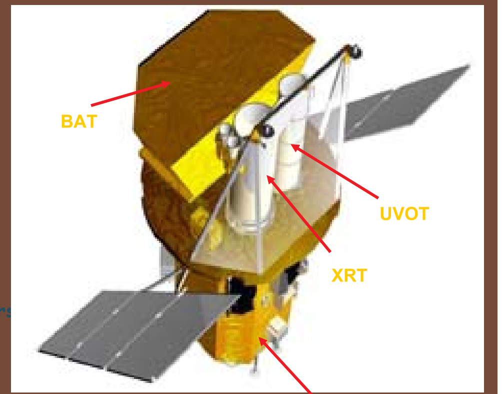

Burst Alert Telescope (BAT)

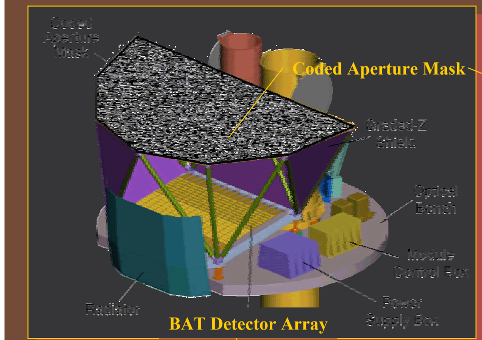

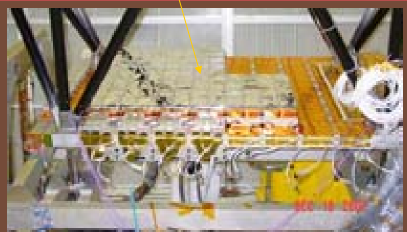

BAT Characteristics

Telescope	Coded Aperture
Telescope PSF	17 arcmin FWHM
Position Accuracy	1-4 arcminutes
Detector	CZT
Detector Format	32768 pixels
Energy Resolution	7 keV FWHM (ave.)
Timing Resolution	100 microseconds
Field of View	2 Steradians, partially-coded
Energy Range	15 – 150 keV
Detector Area	5200 cm^2
Sensitivity	0.2 $photons/cm^2/s$
Max Flux	195,000 cps (entire array)
Operation	Autonomous

BAT Hardware

The BAT Cave

Spectral Resolution

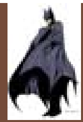

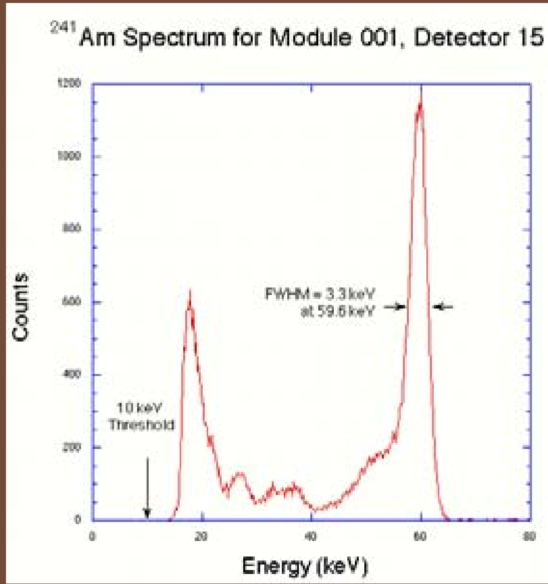

BAT survey

- Large field of view → good sky coverage

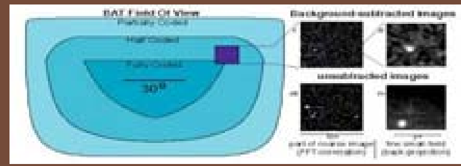

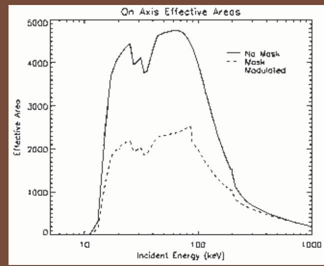

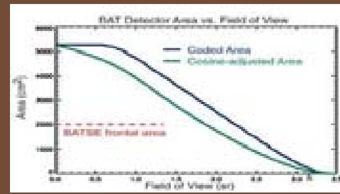

- Effective area up to 1 MeV but not coded

Mirror Module Properties

Panter, July 2000 calibration results

Half Power Diameter

Energy (keV)	1996 arcsec	2000 arcsec	Req arcsec
0.53 keV		15.3	<20
1.49 keV	15.6	14.1	<20
4.50 keV		17.2	
8.05 keV	18.8	20.4	<30

Mirror Effective Area

Energy (keV)	1996 cm^2	2000 cm^2	Theory cm^2	Req cm^2
1.49	162.5	161.4	164.6	>140
4.50		107.5	117.9	
8.05	69.6	68.3	72.9	> 45

The off axis observations: the vignetting

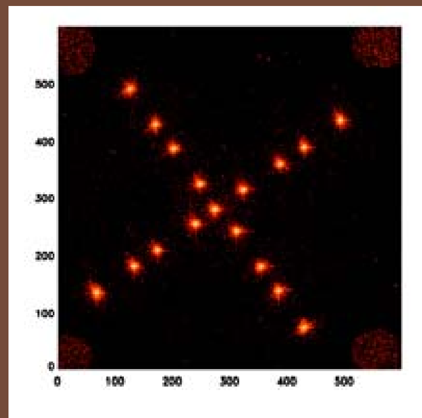

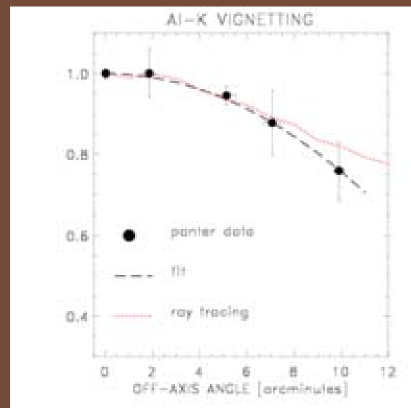

The image quality: off-axis HEW

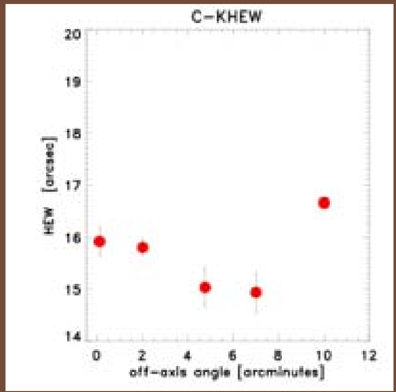

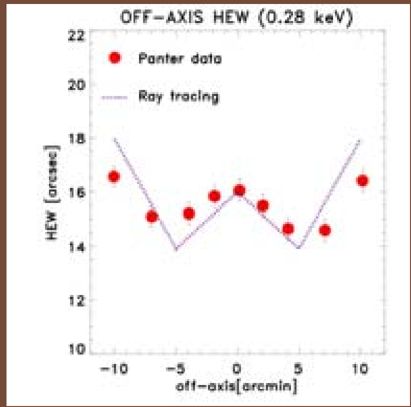

XRT Hardware

XRT Calibration Verification

Automatic switching between readout modes

Response to Simulated GRB/Afterglow decaying as $t^{-1.3}$

Detected "Count Rate"

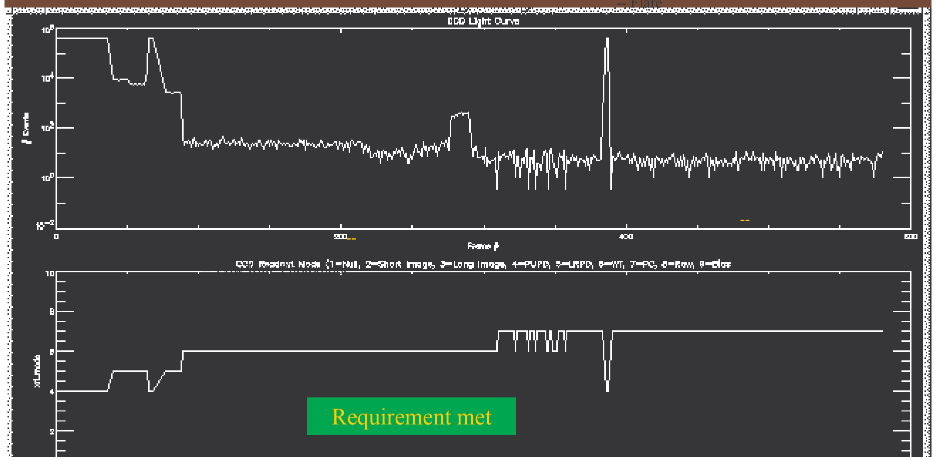

XRT Calibration Verification

Centroid Accuracy vs Flux

Centroid to 1 arcsec for 0.2 to 15 Crab source

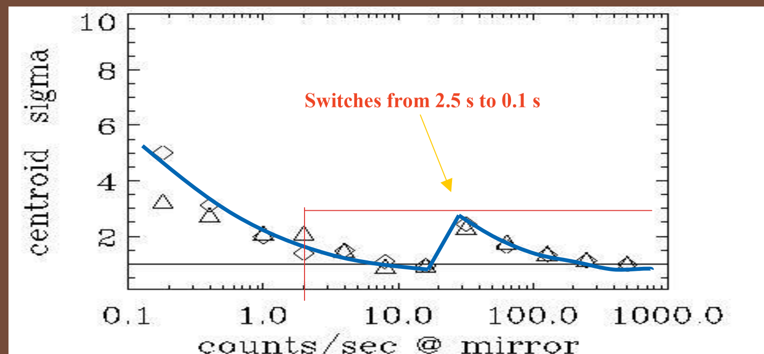

UVOT Hardware

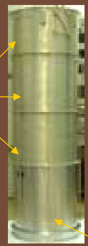

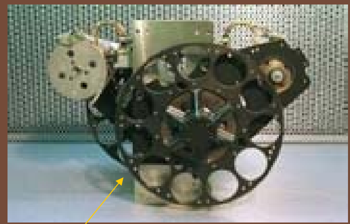

Baffle tubes

Telescope tube

Filter Wheel

UVOT Performance

- Positions to 0.3 arc-seconds using onboard image registration
- Filters give spectral/color information and allow redshift determination from Lyman edge detection

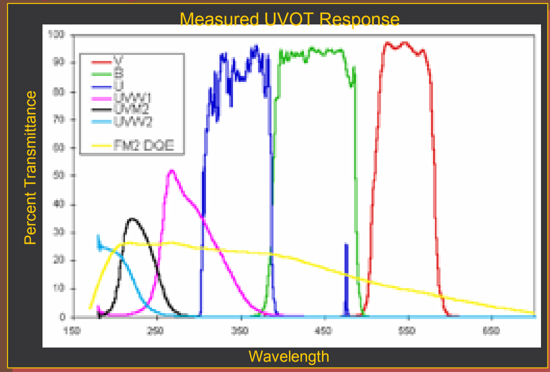

UVOT Sensitivity

For V = 20 B star in 1000 s get:

UVW2	680 cts
UVM2	800 cts
UVW1	1000 cts

Sensitivity to Ly-α cutoff:

UVM1 - UVM2	z ~ 1.5
UVM1 - UVM1	z ~ 2
U - UVW1	z ~ 2.7
B - U	z ~ 3.5

UV and optical grisms with Δλ of 0.5 nm and 1.0 nm, respectively, for $M_b < 17$

- IUE type resolution

Spacecraft with XRT & UVOT Installed

Spacecraft with BAT, XRT & UVOT Installed

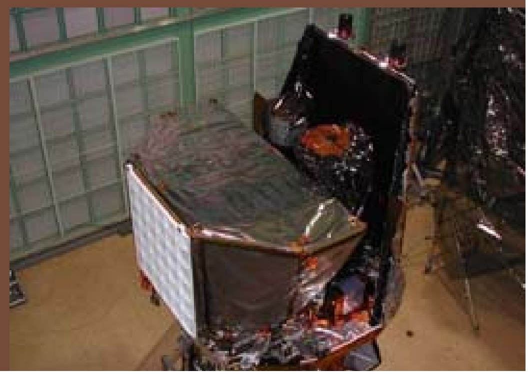

Mission Status

Hanger AE

Swift Science

> What causes GRBs?
> What is the origin of subclasses of GRBs?
> What physcis can be learned about BH formation and jets?

Mission Capabilities:

- Arcsec positions and counterparts for 100's of GRBs
- Identify host galaxies and measure offsets
- Sensitive to short and X-ray bursts
- 5X more sensitive than BATSE
- Multiwavelength observations on all timescales
- X-ray and UV/optical spectroscopy
- Rapid GRB notifications via GCN

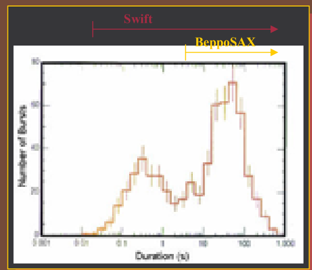

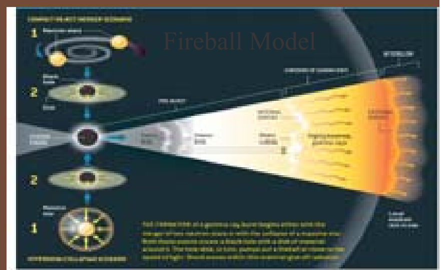

Swift Science

> What can GRBs tell us about the early Universe?

Mission Capabilities:

- Higher sensitivity than previous missions
- Measure hundreds of redshifts
- Measurements immediately after bursts when afterglow is brightest

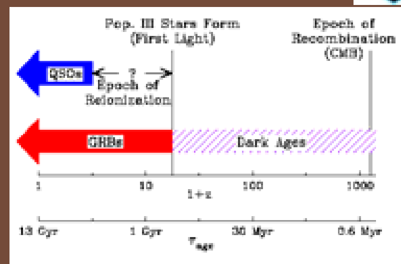

Lamb & Reichart (2000)

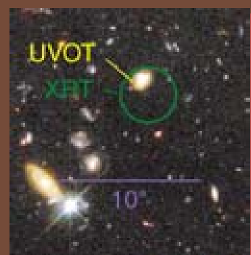

- Star formation history
- Re-ionization of IGM
- Metallicity history
- Epoch of first stars
- Dust and gas content of early galaxies

Observing Scenario

1. Burst Alert Telescope triggers on GRB, calculates position to < 4 arcmin
2. Spacecraft autonomously slews to GRB position in 20-70 s
3. X-ray Telescope determines position to < 5 arcseconds
4. UV/Optical Telescope images field, transmits finding chart to ground

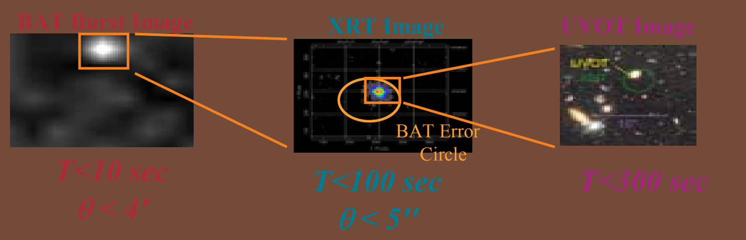

Swift Mission

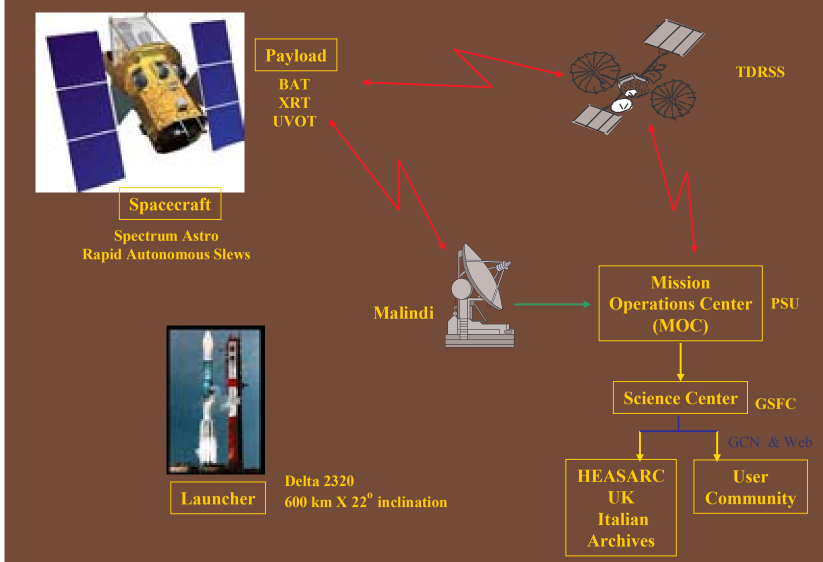

How fast do we get there

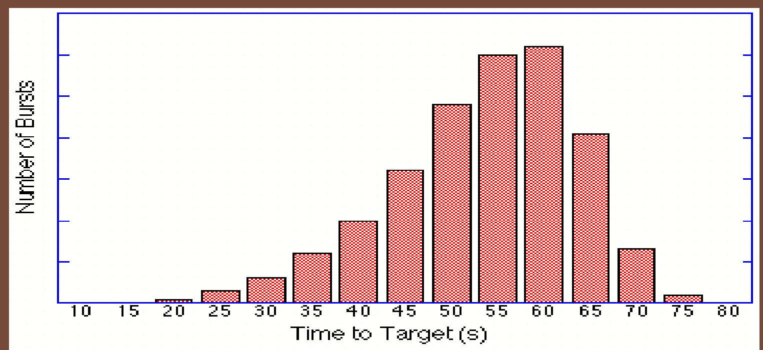

GRB monitoring as foreseen so far

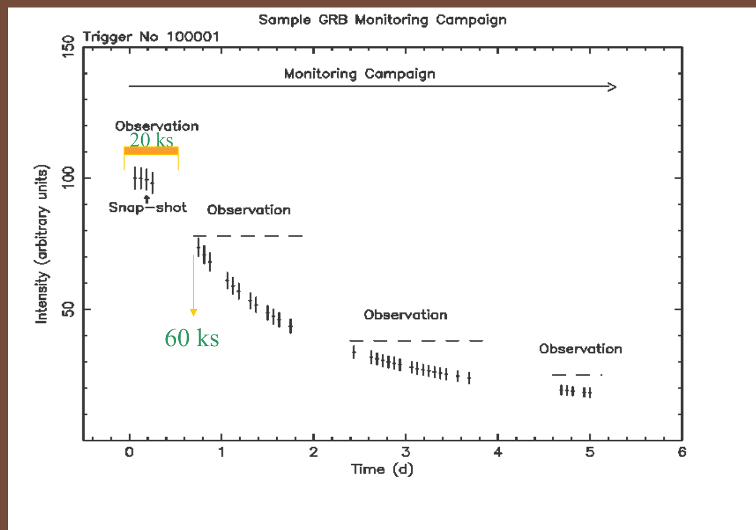

Operation Base Line

- GRBs:
  - Integration 2x10^4 s – Frequency 150/365
  - Time to Target 60s
  - Duration – Gamma Max 700s – X ray <Δt> ~ 5 days
  - FoM decision.
- Interesting Objects:
  - 15 position to cover all sky – 1 orbit/day
  - Selcted on various criteria – Variable objects.
- Hard X ray Survey:
  - Random Coverage of all the sky
  - TBD Check every 4 months

Swift Data Dissemination

- Rapid dissemination of burst positions and data to the world community via GCN and WWW
- *All data to everyone, immediately*
- Triggers provided for ground-based photon, neutrino and gravitational wave instruments, robotic telescopes and space telescopes
- Swift follow-up team
- Upload capability for re-pointing Swift at GRBs and other transients detected by other missions

Swift Non-GRB Capabilities

- Hard x-ray survey of sky
  - ~1 mCrab* sensitivity (high latitude)
  - 20 times better than HEAO-4 (1979)
  - Search for predicted class of absorbed Seyfert 2 AGN
- Monitor sky for transients
  - ~50% sky coverage on each orbit
  - ~10 mCrab sensitivity per orbit
  - 15 - 150 keV
- Response to transient detection
  - Community notification, minutes timescales
  - Observatory repointing, hour timescales

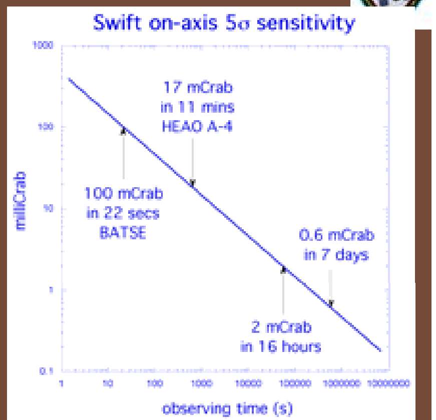

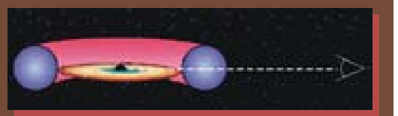

* 1 mCrab = 2x10^{-11} erg cm^{-2} s^{-1}

Swift Non-GRB Capabilities

- Swift multiwavelenght capability: Optical-UV, 0.2-10 keV X-ray, 15-150 hard X-ray (better if > 10 mCrab for the spectrum)
- Fast reaction (few seconds to re-point)
- Capability to automatically change its operation mode in the X-ray band

Very good for multiwavelenght-variability studies => BLAZARS

First year (2?) fully devoted to GRB (and ToO) than if (as we hope) the mission will be extended it will probably be partially (e.g. 50% of the time) opened to observing proposals


Swift
OSSERVATORIO ASTRONOMICO DI BRERA
NASA
GSFC
PENNSTATE
1855
UCL
MSSL
University of Leicester
agenzia spaziale italiana
SRI
SPECTRUMASTRO
eV PRODUCTS
SWALES AEROSPACE
OMITRON INC.
Los Alamos
NATIONAL LABORATORY

Multiwavelength afterglows of Gamma-Ray Bursts

Nicola Masetti

IASF/CNR, Sezione di Bologna, Italy

GRB RTN GROUP

Leader: Prof. E.P.J. van den Heuvel
(Univ. Amsterdam, NL)

Nodes:

- Denmark (Copenhagen)
- France (Toulouse)
- Germany (Munich)
- Israel (Jerusalem)
- Italy (Trieste + Rome)
- Netherlands (Amsterdam)
- Sweden (Stockholm)
- United Kingdom (Leicester)

HEADLINES

- What is a Gamma-Ray Burst (GRB)?
- The discovery of afterglows
- Observational results – GRB/SN connection
- The theory behind afterglows
- The genesis of GRBs
- The early GRB phases
- Conclusions: what have we learnt then?

GRB SKY DISTRIBUTION (2704 BATSE GRBs)

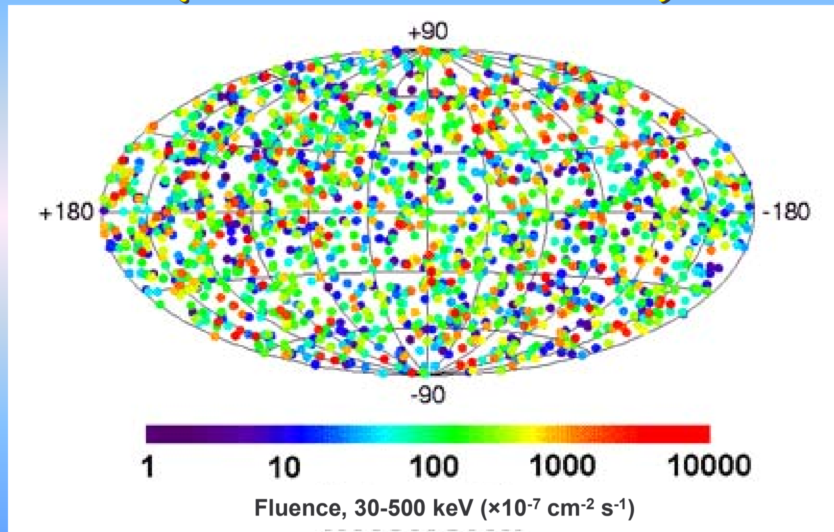

GRB LIGHT CURVES

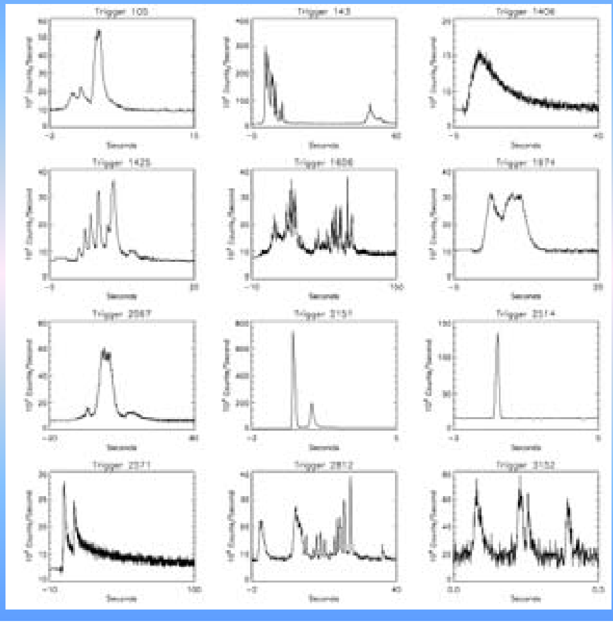

LONG AND SHORT GRBs

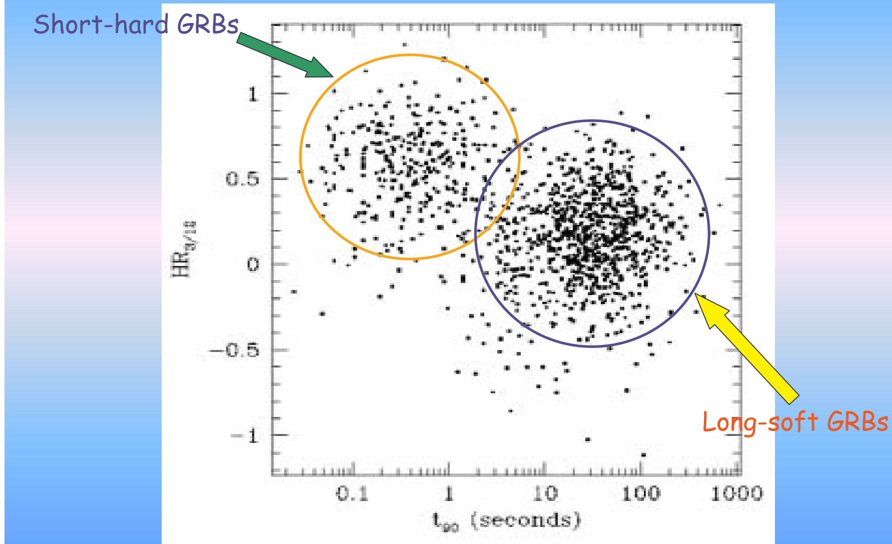

THE BEPPOSAX REVOLUTION

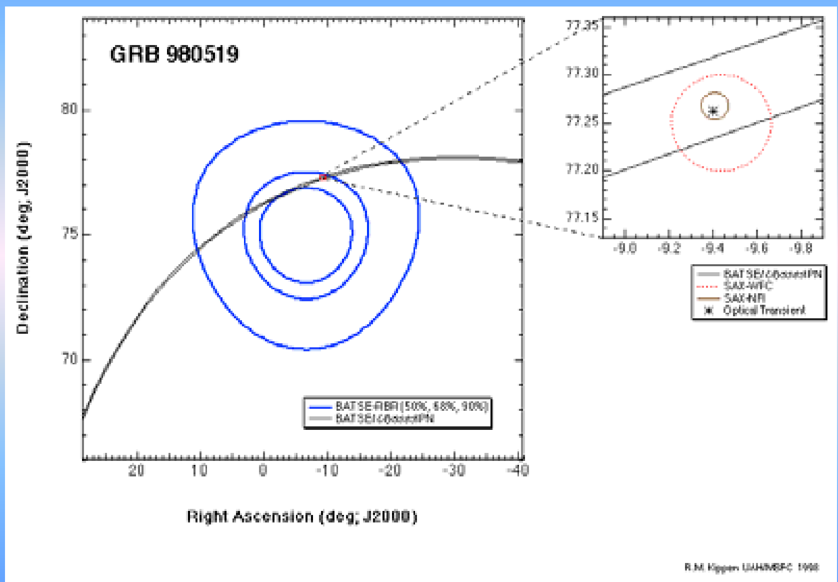

X-RAY AFTERGLOWS

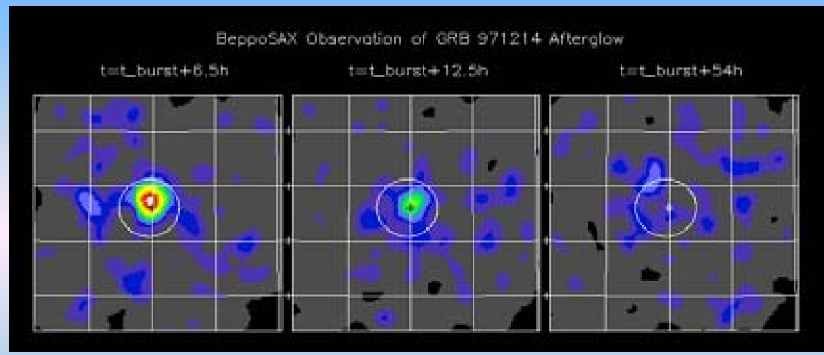

BeppoSAX Team (1997)

They appear as uncatalogued, relatively bright and fading X-ray sources, with powerlaw-shaped spectrum of photon index Γ~2

X-RAY AFTERGLOWS: SPECTRAL FEATURES

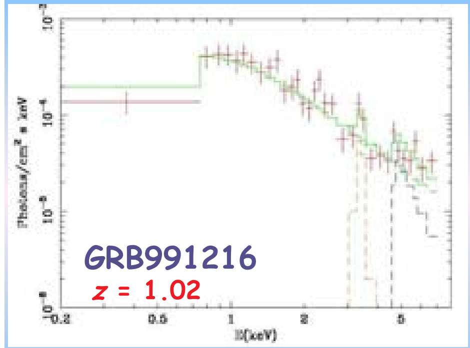

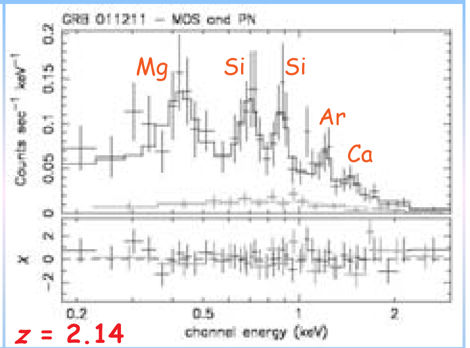

Piro et al. (2000)

Reeves et al. (2002)

Ionized Fe or light metals emissions in the X-ray spectra of some afterglows may indicate metal-rich environment or ejecta (but see Sako et al. 2004).

GRB X-RAY ECHO: A PRETTY PICTURE

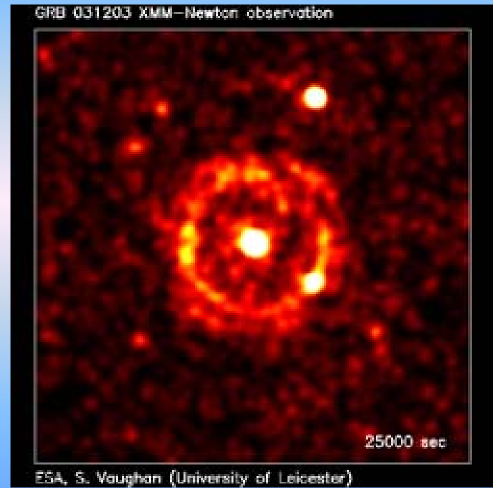

Vaughan et al. (2004)

RADIO AFTERGLOWS

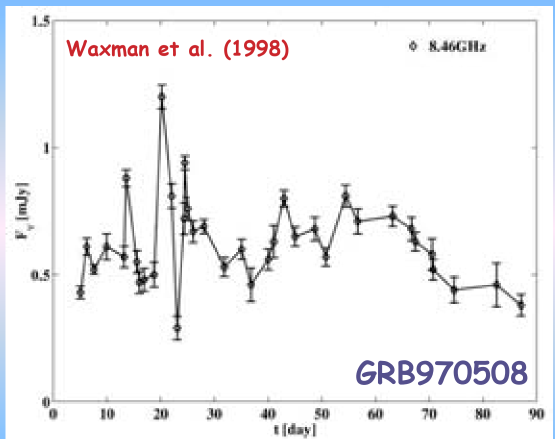

Flickering due to interstellar scintillation; indirect measure of blastwave size and expansion velocity (e.g., Frail et al. 1997).

HOW TO RECOGNIZE AN OPTICAL TRANSIENT (OT)?

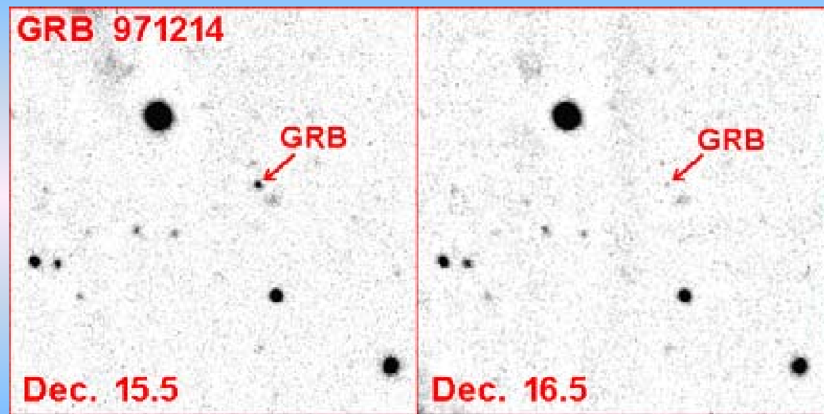

By looking for strongly variable objects in the error box...

OTs ARE QUITE BLUE…

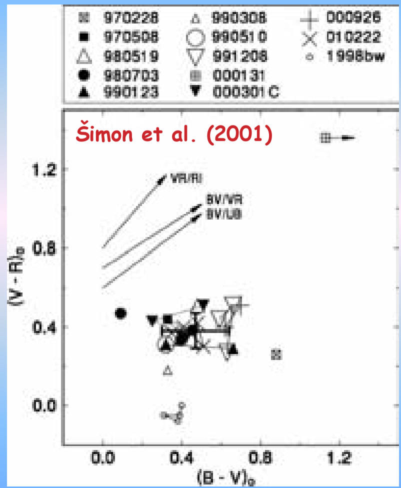

…AND SHOW A NONTHERMAL SPECTRUM

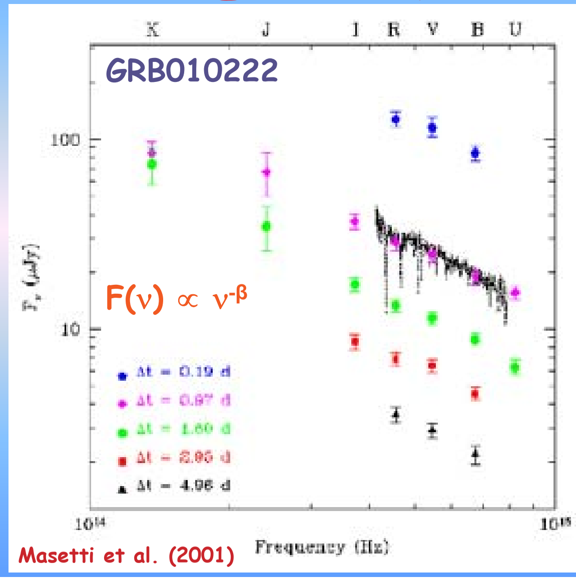

HOW TO MEASURE THEIR DISTANCE?

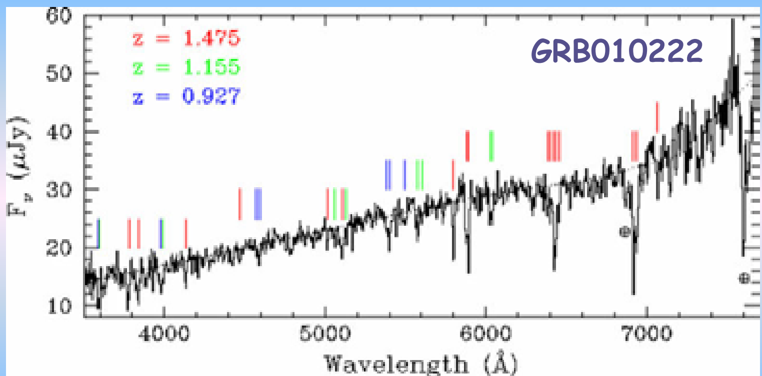

Masetti et al. (2001)

By taking its optical spectrum and by finding its redshift.
GRB are among the farthest objects of the Universe.

GRB030323 – DLA CASE STUDY

OTs can be used as probes to measure the metallicity yield of high-z objects and its evolution with time

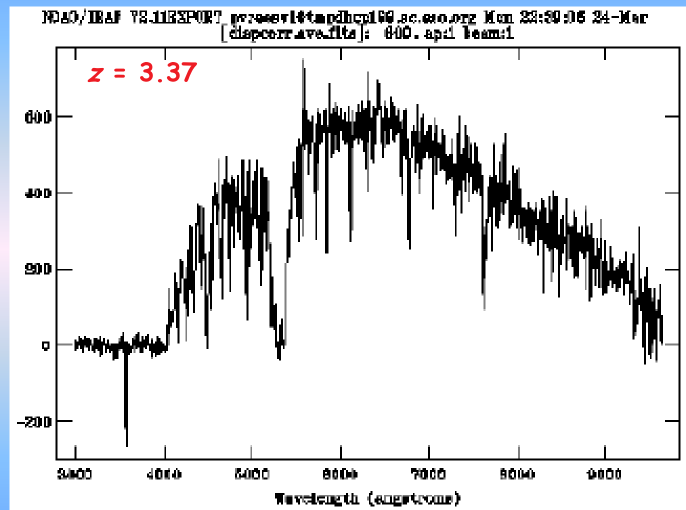

Vreeswijk et al. (2004)

OPTICAL POLARIMETRY

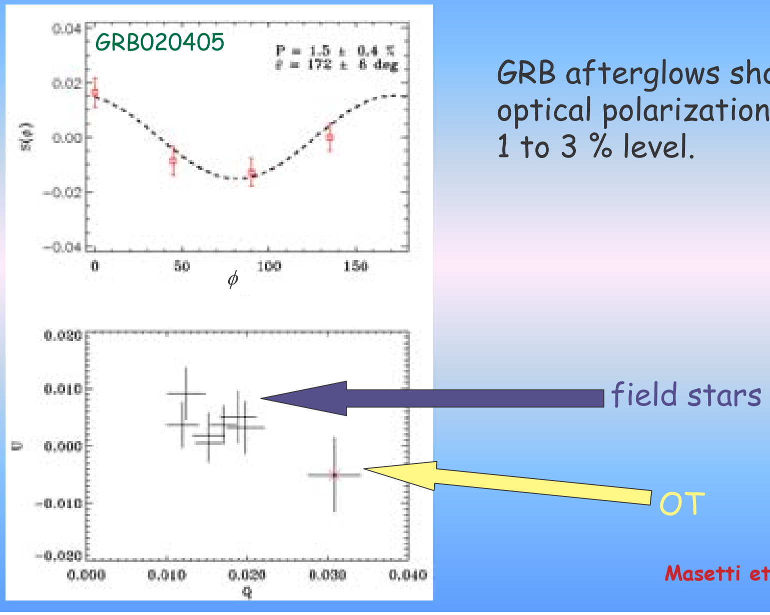

GRB afterglows show optical polarization at 1 to 3 % level.

Masetti et al. (2003)

AFTERGLOW LIGHT CURVES

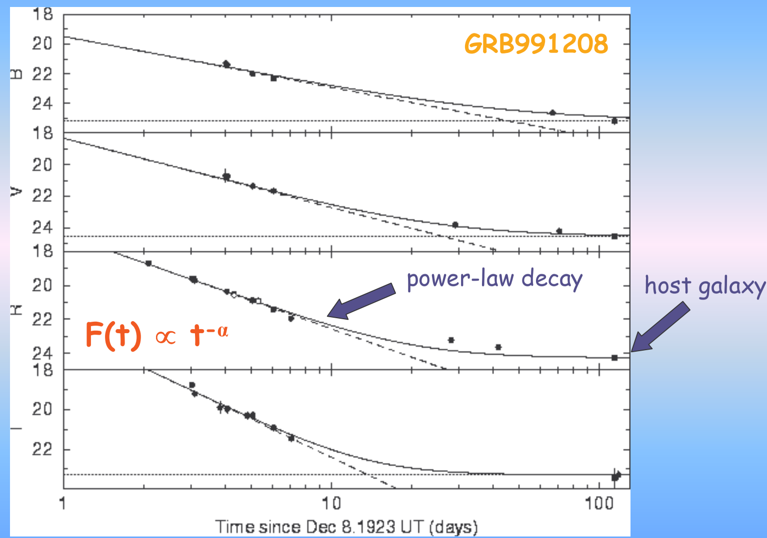

Castro-Tirado et al. (2001)

BREAKS...

collimation break

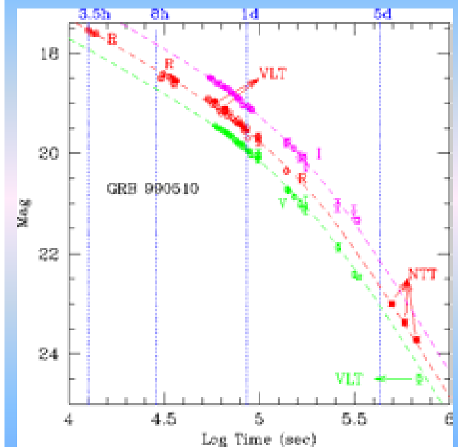

Israel et al. (1999)

subrelativistic transition break

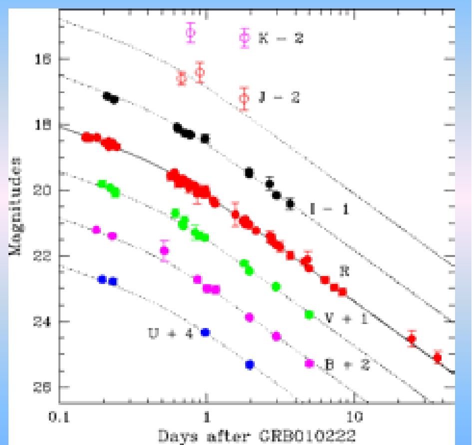

Masetti et al. (2001)

BUMPS...

shock re-energization?

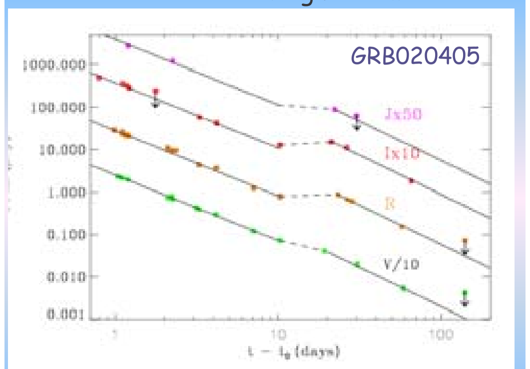

Masetti et al. (2003)

microlensing?

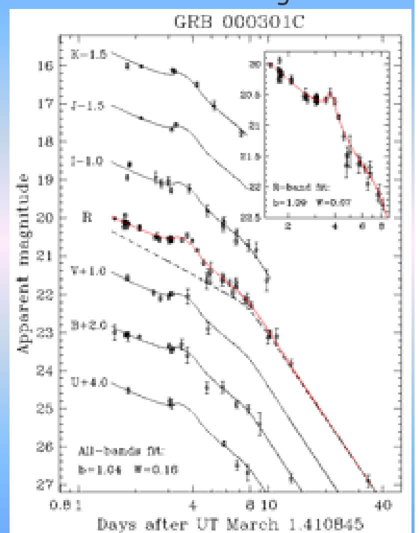

Garnavich et al. (2000)

JUMPS…

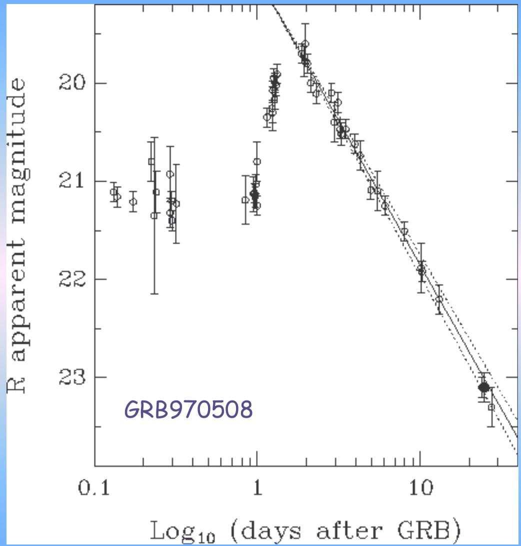

Pian et al. (1998)

GRB030329 - WOW!!!

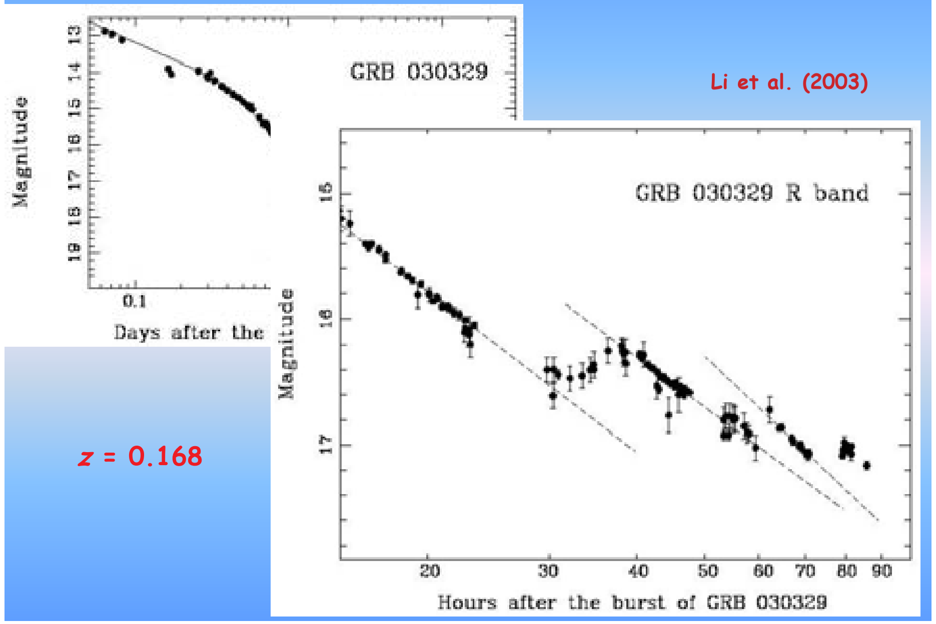

Li et al. (2003)

z = 0.168

EXPONENTIAL DECAY

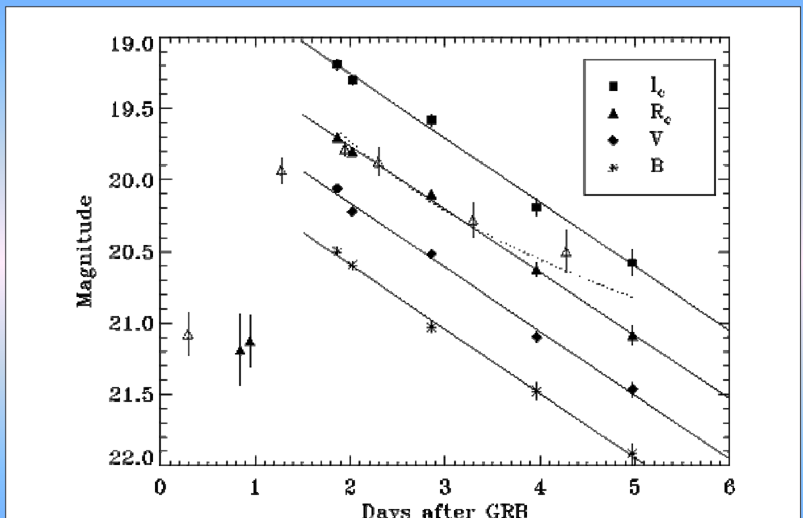

GRB970508

Sokolov et al. (1997)

SN 1998bw / GRB980425

Galama et al. (1998)

z = 0.0085

SUPERNOVA RISING

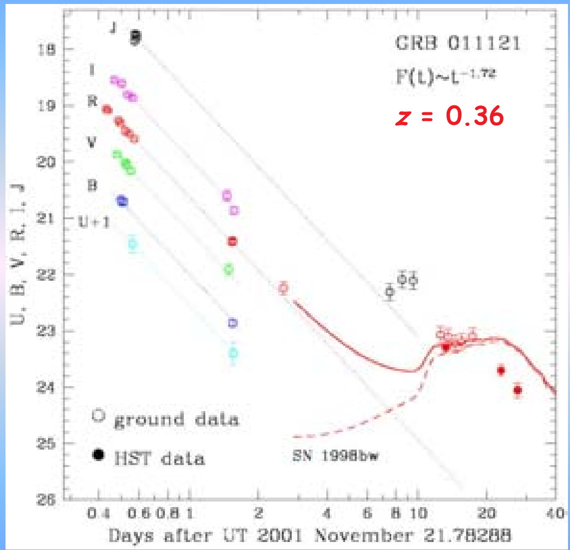

Garnavich et al. (2003)

BUT WHICH SN?

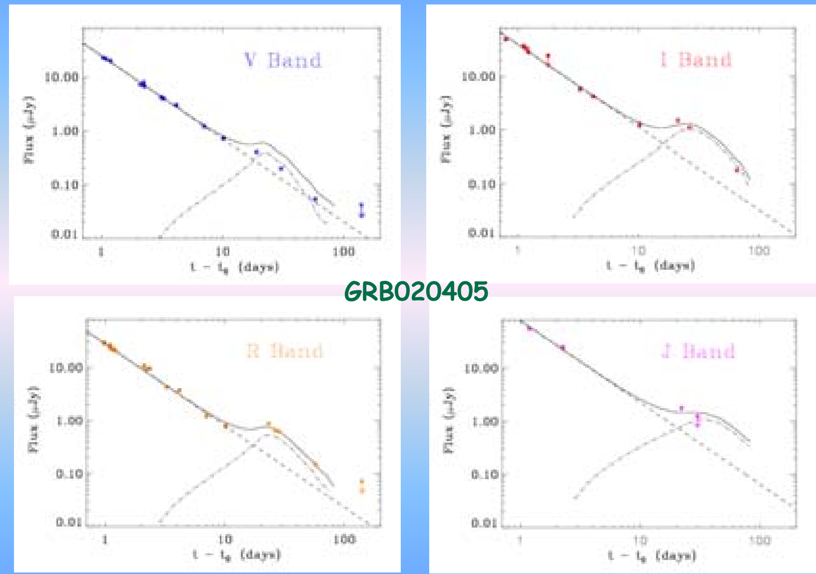

GRB020405

Fits made with a SN 2002ap

Masetti et al. (2003)

GRB030329 – A HYPERNOVA

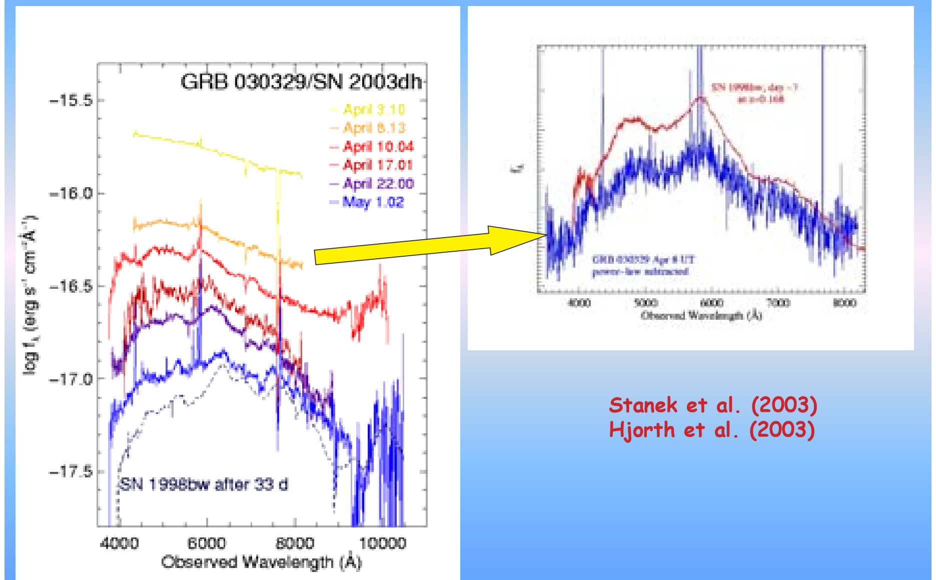

Stanek et al. (2003)
Hjorth et al. (2003)

THE ARCHAEOPTERYX

An animal which bears both bird and reptile features.

GRB030329 has the characteristics of both a GRB afterglow and a supernova (SN2003dh).

This "Archaeopterhypernova" helped us in catching the missing link between (some) GRBs and SNe.

"Given that GRBs typically occur at z = 1-2, the probability that the source of an observed burst should be as close as GRB 030329 is one in several thousand.
It is therefore unlikely that HETE-2, or even Swift, will see another such event."

[astro-ph/0310414]

GRB031203 – A HIDDEN SN

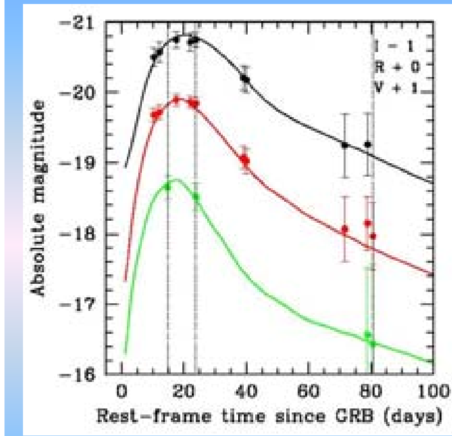

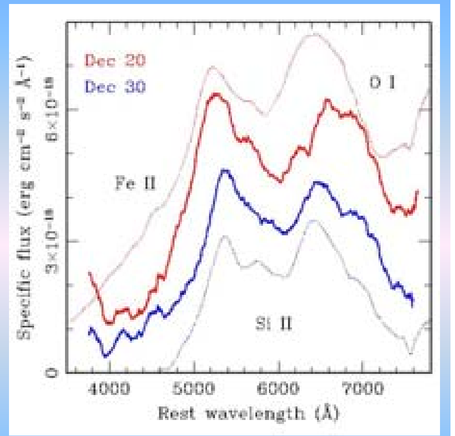

Malesani et al. (2004)

z = 0.105

GRB (closer than 030329) detected by INTEGRAL...
No OT, but a bright SN was found in this case.

XRFs: VARIATIONS IN A SOFTER KEY

XRF020903

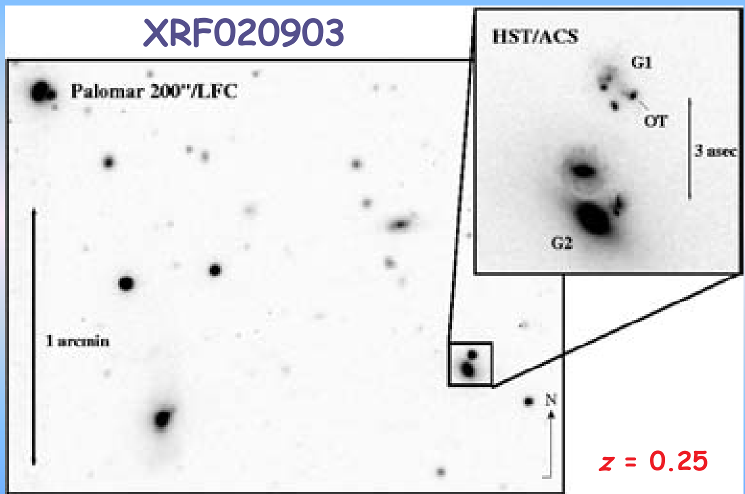

z = 0.25

Soderberg et al. (2004)

XRF030723: SNe EVERYWHERE?

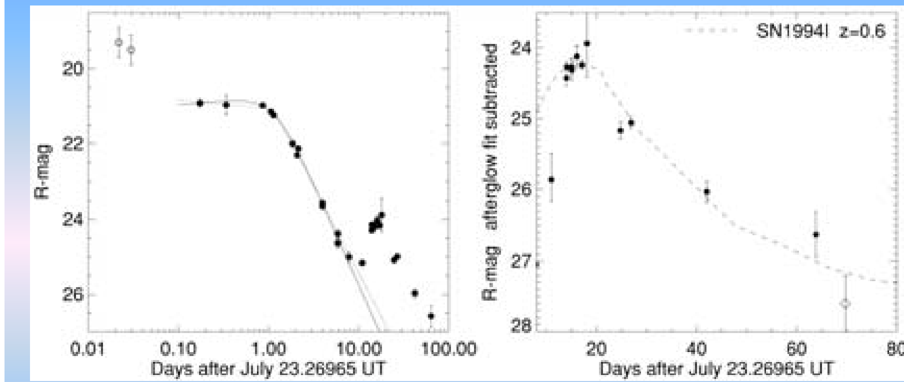

Fynbo et al. (2004)

This time the best template is the Type Ic SN 1994I at z =0.6, scaled up by 1 mag.

HOST GALAXIES

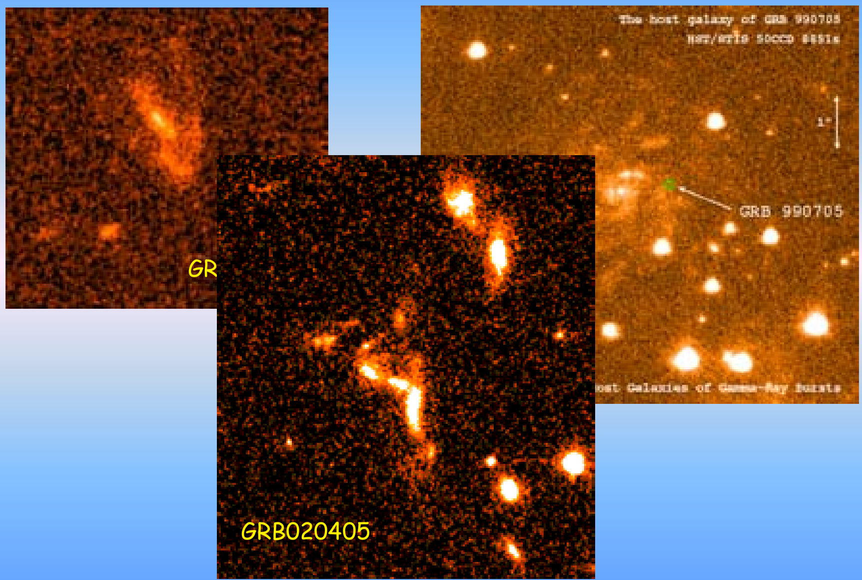

THE FIREBALL MODEL

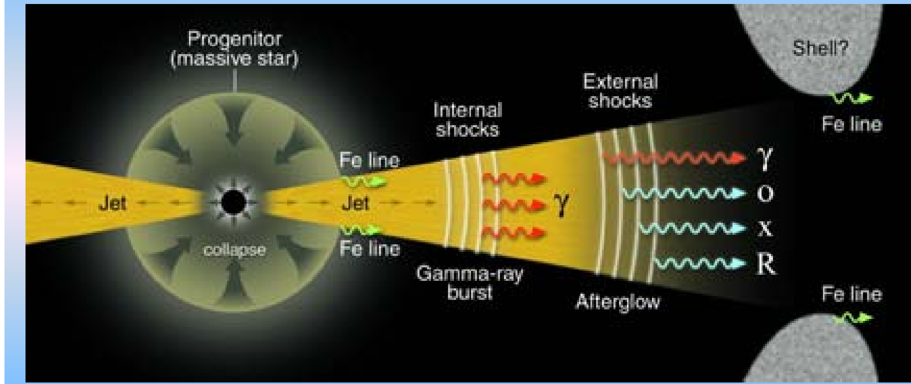

AFTERGLOW EMISSION

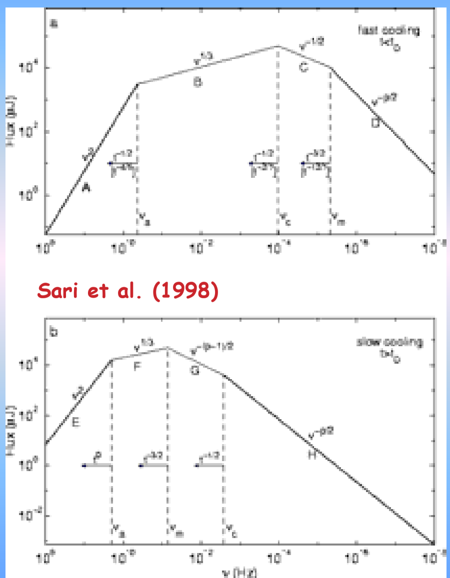

Sari et al. (1998)

The afterglow emission is modeled as due to synchrotron.

$$F(t,\nu) \propto t^{-\alpha}\,\nu^{-\beta}$$

with α and β depending on p, where

$$N(\gamma) \propto \gamma^{-p}$$

is the electron energy distribution.

STATISTICS

To date (October 2004) about 200 GRBs with fast, arcmin-sized error box localizations have been detected. Among these, those reobserved in various spectral passbands presented the following statistics:

- almost all (~95%) showed an X-ray afterglow;
- ~50% showed an optical afterglow;
- ~30% showed a radio afterglow.

Besides, practically all transients localized with arcsecond precision at optical, radio or X-ray wavelengths are associated with a host galaxy.

STATISTICS - II

The values of the main parameters which can be determined for the OTs from optical observations are reported below:

- $0.10 < z_{GRB} < 4.5$ — $\langle z_{GRB} \rangle \sim 1.4$
- $1 < \alpha < 2$ — $\langle \alpha \rangle \sim 1.3$
- $0.5 < \beta < 1.5$ — $\langle \beta \rangle \sim 1$
- $1.5 < p < 3$ — $\langle p \rangle \sim 2.5$
- $P_{opt} \sim 1 - 3$ %
- $\langle R_{host} \rangle \sim 25$

Up to now, redshifts were measured for ~40 GRBs.

WHY SO FEW IN THE OPTICAL?

- dusty environment in the host galaxy
- high redshift ($z > 4$)
- crowded fields
- foreground Galactic absorption
- shallow and/or late-response observations
- field problems (bright saturated stars, wide galaxies, etc.)
- intrinsically faint optical afterglows

A NICE PICTURE...

- The GRB afterglow can be modeled with the 'fireball' model
- Synchrotron emission
- Host galaxies with high redshift: (long) GRBs are cosmological objects
- GRB positions likely associated with star-forming regions inside the hosts

All this would suggest that GRBs are produced by sudden and violent death of stellar-mass object(s).

GRB PROGENITORS

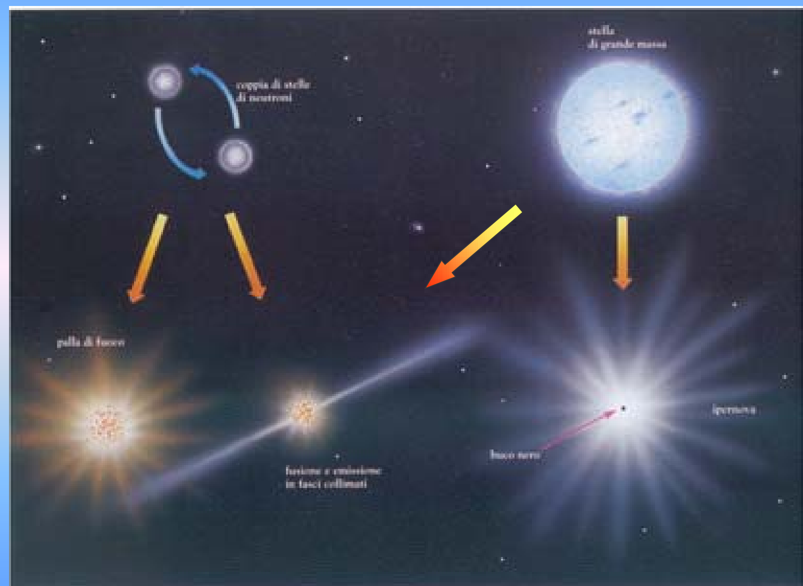

…WITH DEVIATIONS!

- Bumps and/or plateaus in the light curve
- A Supernova in the GRB error box! (SN1998bw/GRB980425)
- Light curve breaks (i.e. changes in the decay slope)
- Fast decay (with α > 2)
- Other pathologies (exponential decay, rising branch, etc…)

GOING FOR THE FIRST PHASES

ROTSE-I data of the first GRB "optical flash"

Akerlof et al. (1999)

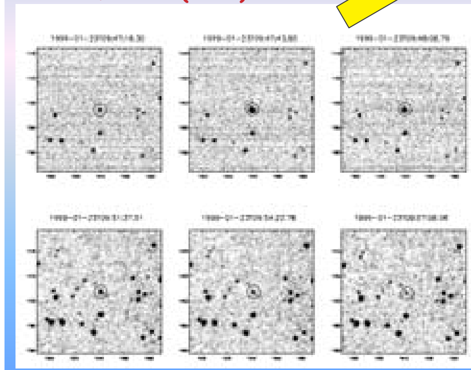

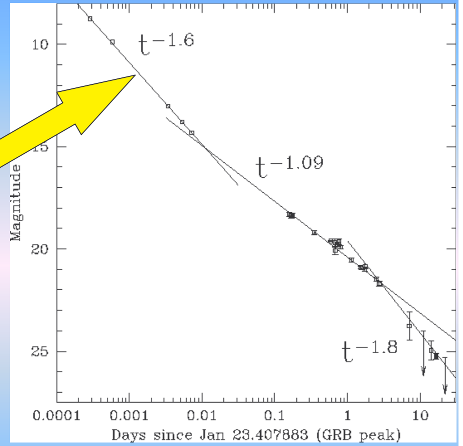

GRB990123

OTHER EXAMPLES

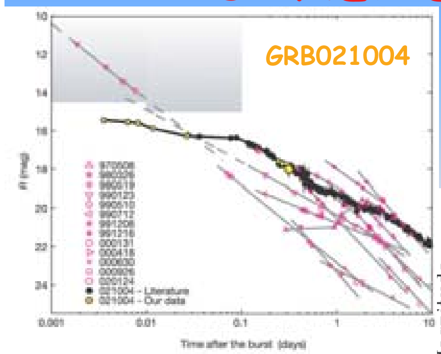

Li et al. (2003)

Fox et al. (2003)

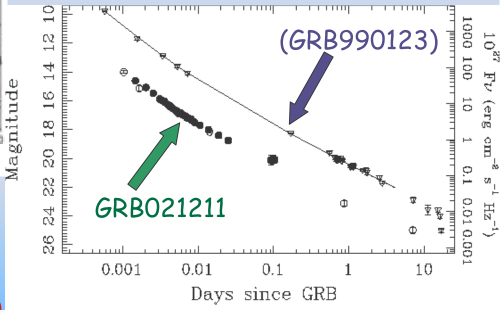

We thus need fast and precise GRB localizations and fast (robotic) telescopes able to quickly point the GRB spot.

THE OPTICAL FLASH

It is therefore important to monitor the very first phases of the GRB in the optical also, in order to:

- test the current models;
- understand and map the broadband spectral variations during the "optical flash";
- understand the physical and emission mechanisms at work in the early GRB phases;
- compute the optical to high-energy emission ratio and see how it varies from burst to burst;

Thanks to the real-time localizations provided by *HETE-2* and *INTEGRAL* (and, in the near future, by *Swift*), robotic telescopes will be able to catch the optical counterpart of the GRB proper.

REM, THE ROBOTIC TELESCOPE

- Diameter: 60 cm
- Location: La Silla (Chile)
- first light: June 2003
- IR camera (J, H, K, z filters)
- ROSS optical camera (V, R, I, Hα filters; 400-900 nm slitless spectroscopy)
- Fast repointing (10 s for 90° slew)
- Now in science verification phase

HOW ROSS CAN SEE THEM

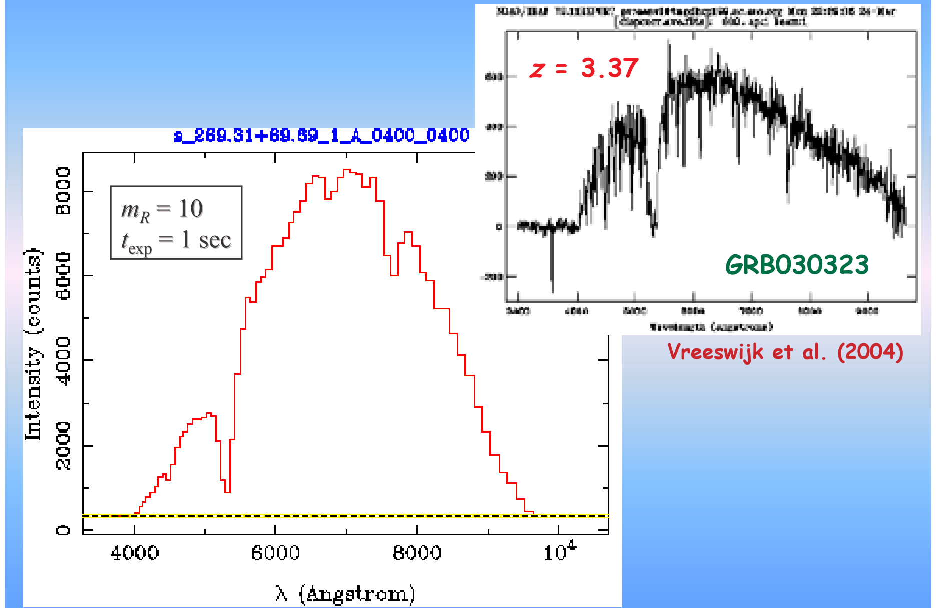

Vreeswijk et al. (2004)

THE NEXT STEP

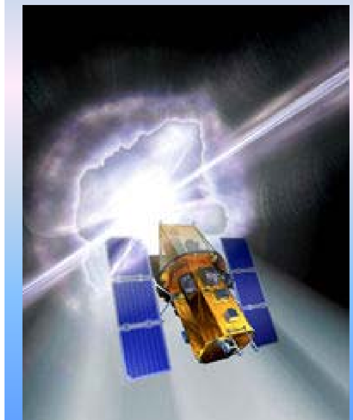

- 2 GRB localizations per week
- Real-time trigger distribution
- High-precision (arcmin to arcsec) localizations
- X-ray and UV telescopes
- Optical (U,B,V) camera

Conclusions...?

- We know the GRB spatial distribution;
- We developed a simple theory for the GRB afterglow emission;
- We have (a lot of) theories – some convincing, some not – to explain peculiar behaviours of GRB afterglows
- We know where GRBs are originated (at least the long ones).

BUT:

- We do not have a clear theory for the early GRB emission;
- We do not know anything about short GRBs.

And, most importantly...

- We still do not exactly know what the GRB progenitor is (but we are getting close).

THE SUPERCRITICAL PILE MODEL FOR GRBs:

Getting the luminosity at 1 MeV

Apostolos Mastichiadis
Physics Dpt
University of Athens

TALK OUTLINE

- Relativistic protons in compact sources
- Supercriticality in static plasmas
- Generalization to moving plasmas
- Application to GRBs

AN ONGOING WAR: ELECTRONS vs PROTONS

For high energy sources (AGN, GRB)

- **Electrons radiate efficiently**
  need continuous acceleration
- **Protons do not radiate as efficiently,**
  EM ~(m/M)^2
  hadronic – small cross sections or inelasticities
  they are good for storing energy

- **Favoured by the astrophysical community**
- **Favoured by the Cosmic Ray community**

ULTRARELATIVISTIC PROTONS IN COMPACT OBJECTS

1. **Photopair Production (Bethe Heitler)**

$$p + \gamma \rightarrow p + e^{\pm}$$

- Threshold of $2m_e c^2$
- Cross section $\sigma = \alpha r_0^2 \left(\frac{28}{9} \ln(2\gamma\varepsilon) - \frac{218}{27} \right)$
- Inelasticity $\kappa \approx 2 \frac{m_e}{m_p}$

2. Photo-pion Production

$$p + \gamma \rightarrow p + \pi^0 (\rightarrow 2\gamma)$$

$$p + \gamma \rightarrow n + \pi^+ (\rightarrow \mu^+ \rightarrow e^+)$$

Threshold of $m_\pi c^2$
Cross section $\sigma = 10^{-28} cm^2$
Inelasticity $\kappa \approx .5$

- Energy loss rate $t^{-1} \approx n(\varepsilon)\kappa\sigma c$

- For target photons with $n \propto \varepsilon^{-2}$
  $t_e^{-1} \approx t_p^{-1} \approx\sim 3.10^{-15} \gamma U_{rad} \sec^{-1}$

- Usually protons are assumed to cool on some external photons (disc radiation, etc)
- However, can protons cool on their own radiation? (Rough analogy to SSC)

THE PAIR PRODUCTION – SYNCHROTRON LOOP

Kirk & Mastichiadis 1992

Concept:

- Assume a stationary proton distribution,
  e.g. a power law $n_p(\gamma_p) = n_o \gamma_p^{-\beta}$ (for $\gamma_p \le \gamma_{p,max}$)

- Consider the processes
  1. Photopair production ($p\gamma \rightarrow pe^+e^-$) --Bethe Heitler
  2. Electron synchrotron radiation

- Possibility of loop:

$$(A)\ p\gamma \rightarrow pe^+e^- \rightarrow pe^+e^-\gamma \rightarrow (A)$$

- For the $p\gamma \rightarrow pe^+e^-, Be \rightarrow Be\gamma$ reaction network to be self-contained, the threshold condition

$$\gamma_p \varepsilon_s = \gamma_p(\gamma_e^2 b) = \gamma_p^3 b = 2$$

  must be met

Kinematic threshold (feedback)

$$\gamma_{p,max} \ge \left(\frac{2}{b}\right)^{1/3}$$

- This criterion should be matched with another one about the probability of such collision to be occuring

CRITICALITY (1)

- The blob will be 'critical' if at least one of the synchrotron photons pair produces before it escapes.

  O.o.M.
- 'Optical depth' $n_0 \gamma_p^{-(\beta-1)} N_s \sigma_{p\gamma} R \geq 1$

  where $N_s \sim \gamma_e / b\gamma_e^2 = 1/b\gamma_e$ are the photons emitted per electron. Using the threshold condition

$$\therefore n_0 \geq n_{crit} \approx b^{1-\beta/3} \big/ \sigma_{p\gamma} R$$

CRITICALITY (2)

- Kinetic equations for electrons

$$\frac{\partial n_e(\gamma,t)}{\partial t} - \frac{4}{3}\ell_B \frac{\partial}{\partial \gamma}\left[\gamma^2 n_e(\gamma,t)\right] -$$
$$-2n_p(\gamma)\int_0^\infty dx n_\gamma(x,t)\sigma_{BH}(x\gamma) = 0$$

- Kinetic equation for photons

$$\frac{\partial n_\gamma(x,t)}{\partial t} + n_\gamma(x,t) - \frac{2}{3}\ell_B b^{-3/2} x^{-1/2} n_e(\sqrt{x/b},t)$$

where $\ell_B = \sigma_T R \frac{U_B}{m_e c^2}$ the magnetic field compactness

---

- Assume protons stationary
- Assume no initial electrons or photons in the system
- Perform a stability analysis on the two equations: System becomes unstable ($n_e \propto n_\gamma \propto e^{st}, s \geq 0$) when

$$n_{p0} > n_{crit} = \left(\frac{2}{3}\beta - 1\right) b^{1-\beta/3} \left[\int_0^{b\gamma_{mx}^2} dy \sigma_{p\gamma}(y) y^{-1-\beta/3}\right]^{-1} \Big/ \sigma_T R$$

Dynamical threshold (marginal stability)

- When both criteria satisfied the protons become unstable to Pair Production – Synchrotron (PPS) loop and photons/pairs grow exponentially in the system

---

s=0, marginal stability (full line)

s=1, photon/pair growth time=crossing time (dashed line)

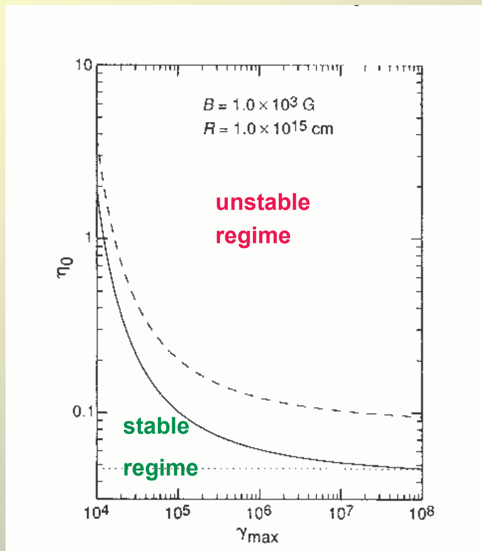

THE NEXT STEP

- PPS loop leads to explosive outgrowth of pairs/photons, then what?
- Study numerically the behaviour of the system using the kinetic equation approach
- Protons

$$\frac{\partial n_p(\gamma_p,t)}{\partial t} + \text{(Rate of proton losses – Bethe Heitler)} =$$

$$= \text{(Rate of proton injection – if any)}$$

- Similar equations for electrons/positrons and photons (use usual processes: synchrotron, ICS, photon-photon absorption, etc)

SOME FACTS ABOUT THE KINETIC EQUATIONS

- Coupled partial integro-differential equations
- They conserve energy (e.g. energy lost by protons is injected to electron eqn and if cooling is fast it is radiated)
- Without the Bethe-Heitler pair production, protons decouple and the system becomes identical to the ‘one-zone’ time-dependent leptonic models, so, by analogy, the full system constitutes the ‘one-zone’ time dependent hadronic model
- First effort: M&K 95 – simplified rates
- Second effort: AM, Protheroe & Kirk (2005) (an ENIGMA publication!)
- Main difficulty: Bethe-Heitler rates

BETHE-HEITLER PAIR PRODUCTION

- Electron/positron production spectra were modeled from Monte Carlo simulations (Protheroe & Johnson 1996) → electron equation (relaxes the delta function approximation)
- Total inelasticity was used to calculate the proton losses → proton equation

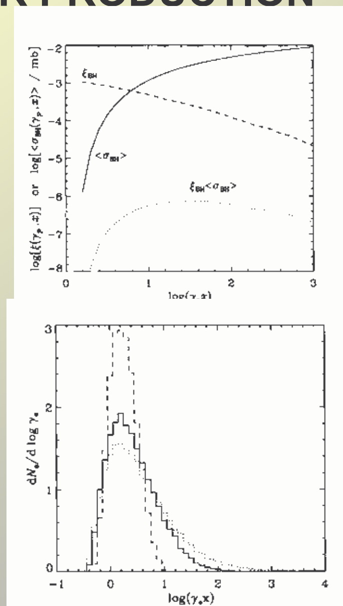

ONE OF THE FIRST TASKS: VERIFY THE PPS LOOP

- Starting with a stationary proton distribution and using its normalisation as a free parameter we observe that photons grow spontaneously

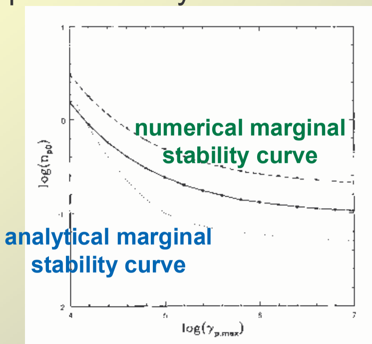

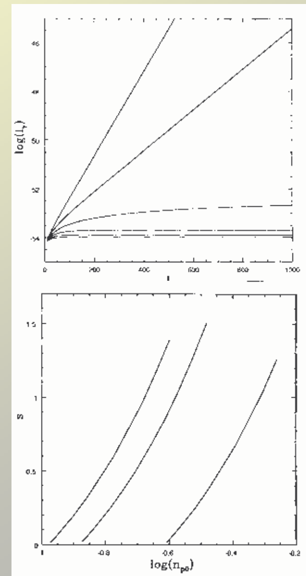

PHOTON OUTGROWTH OK. THEN WHAT?

- Question: How protons react to the outgrowth of photons? (Ans: By losing energy!)
- Different behaviour of the system for various initial conditions.
- For continuous injection of protons sometimes oscillatory behavior: Energy is slowly stored into protons and once they become supercritical is released into pairs and (bursts of) radiation

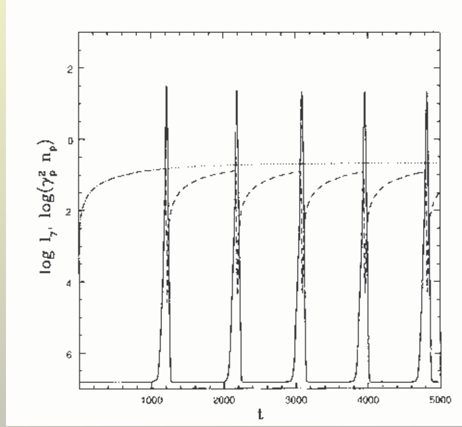

Light show courtesy of protons

SUPERCRITICALITY AND GRBs

- Can outflows related to GRBs become supercritical?
- 'Straight' PPS loop requires proton densities in excess of the densities usually associated with GRBs.
- However: Assume that the plasma described earlier is in relativistic motion with bulk Lorentz factor Γ. Assume also the presence of a 'mirror' upstream.
- Upstream mirroring enhances the synchrotron photons energy by Γ^2 and their energy density by $\propto \Gamma^3$ (Ghisellini & Madau 96, Boettcher & Dermer 98)
- Modified PPS loop!

$$(A)\ p\gamma \rightarrow pe^+e^- \rightarrow pe^+e^-\gamma \rightarrow \Gamma^2\gamma \rightarrow (A)$$

MODIFIED CRITERIA

- Perform a stability analysis on the modified loop
- Kinematic threshold

$$\gamma_{p,max} \geq \left(\frac{2}{\Gamma^2 b}\right)^{1/3}$$

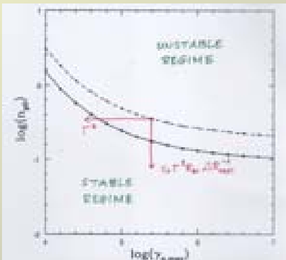

- Dynamical threshold

$$n_{p0} > n_{crit} = \left(\frac{2}{3}\beta - 1\right) b^{1-\beta/3} \left[\int_0^{b\gamma_{mx}^2} dy\sigma_{p\gamma}(y) y^{-1-\beta/3}\right]^{-1} \Gamma^{-1-2\beta/3} \Big/ \sigma_T R$$

- Both criteria are relaxed by the combination of relativistic motion + reflection

APPLICATION TO GRBs (I)

- Assume that the particles in (or swept by) the RBW are isotropised and obtain Lorentz factors similar to that of the flow $\gamma_p = \Gamma$, i.e. no extra acceleration is required.
- The kinematic threshold becomes

$$b\Gamma^5 \geq 2 \Rightarrow \Gamma \geq 466 B_G^{-1/5}$$

- Radiated spectra characteristics (RBW frame)
  1. Synchrotron peak at $\varepsilon'_s \quad b\Gamma^2$
  2. IC on reflected photon targets of energy $\varepsilon'_R \quad \Gamma^2\varepsilon'_s \quad b\Gamma^4$ at $\varepsilon_c \quad \Gamma$ (KN)

APPLICATION TO GRBs (II)

- Observed spectra characteristics
  1. Synchrotron peak at ε_s $\delta b \Gamma^2$
  2. IC on reflected photon targets at ε_c $\delta\Gamma$
  - Reflected component will not be seen as it is directed away from us. However if cold plasma accumulates in the RBW (as a result of the PPS loop) then Compton scattering on it will shift the reflected peak at
  3. ε_R $\delta\varepsilon'_R$ $\delta b\Gamma^4$

If loop operates close to threshold $(b\Gamma^5 = 2)$, then

ε_R □ $2(\delta/\Gamma)$ and if δ~Γ, then ε_R 1 MeV, irrespective of the value of Γ

NUMERICAL APPROACH

- Rewrite kinetic equations as to treat reflection
  1. Zone I: RBW outside the reflection zone
  2. Zone II : RBW inside the reflection zone Reflected component is calculated taking light travel effects into account (Boettcher & Dermer 98). At each instant t, the reflected photon energy density depends on the RBW emissivity at all $t' < t$.

$$U'_R \approx 4\Gamma^3 \tau_{T,ext'} \frac{R_b}{\Delta R_{ext}} U'$$

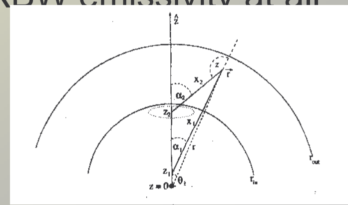

- **Does the PPS(R) loop operate?**
- **Set delta-function of protons (at γ=Γ=400) as initial condition.**
- **Assume no initial electrons or photons.**
- **Two free parameters: Proton number density and magnetic field.**
- **Zone I: Nothing happens**
- **Zone II: Growing solutions**

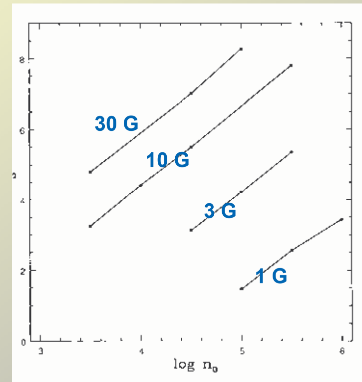

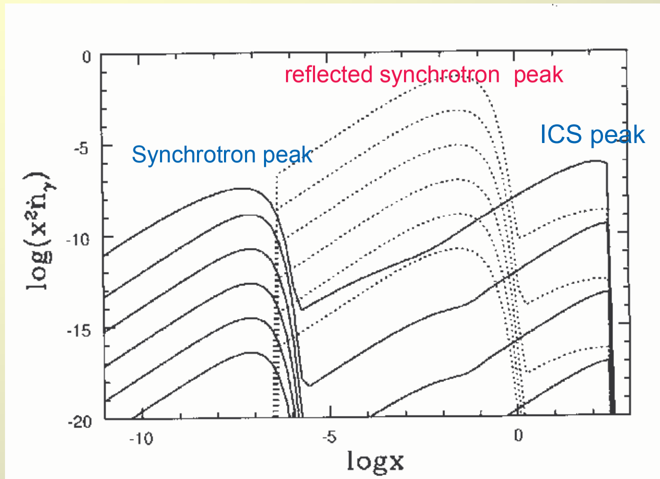

RBW photon spectra snapshots during the outgrowth phase. RBW consists only of protons

A SAMPLE

- Photons grow until protons cool below the critical conditions, then they decay, i.e. a burst.
- For the particular example

Γ=400

B=10 G

N=10^4 pr/cc

tcross=6 sec

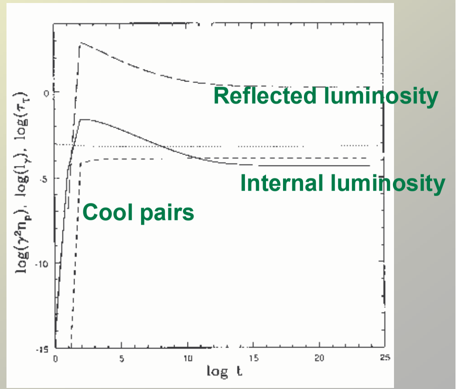

- Photons grow -> protons lose energy -> move to stable regime-> photons decay -> A burst

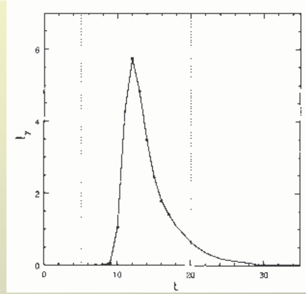

- The view from Earth during the decay phase
- Γ=400
- B=10 G
- N=10^4 pr/cc
- tcross=6 sec
- $\delta=\Gamma$

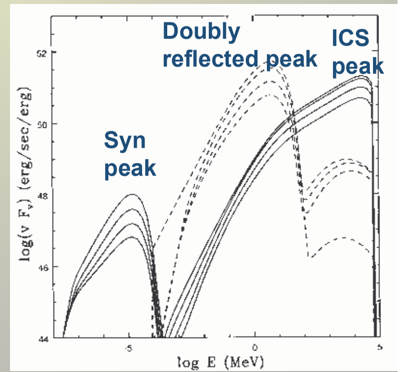

- Both outgrowth and decay phases show varied behaviour depending on the initial conditions (proton number density, B-field)
- Systematics?

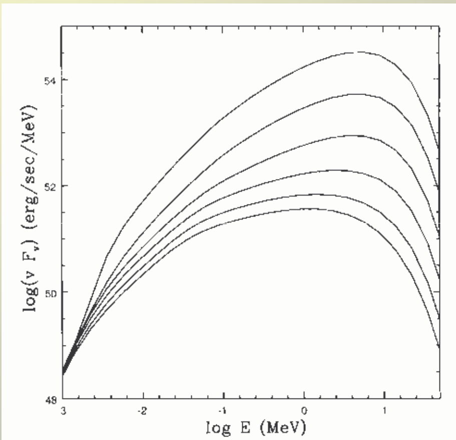

- Peak energy of the doubly reflected component (at max of the burst) versus total energy radiated in 10 crossing times (~1 min) (both as measured in the observer;s frame)

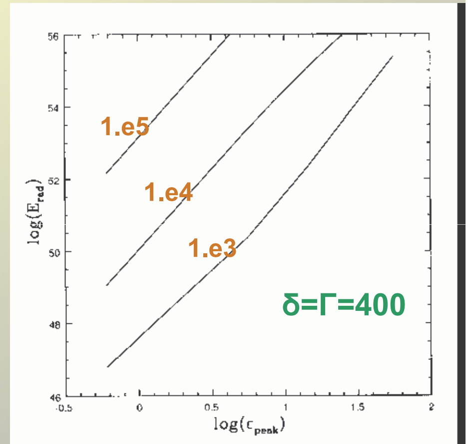

CONCLUSIONS

- Proton loops can effectively transfer energy stored in protons into radiation producing a burst
- GRB-like parameters can support such a picture provided that some mirroring occurs (wind of progenitor?)
- Thorough study of the parameters is required

- Assume

1. $\gamma_e = \gamma_p$ (pairs are produced with the Lorentz factor of the protons)

2. Emission of photons at synchrotron critical energy $\varepsilon_s = b\gamma_e^2$ where $b = B/B_{cr}$

($B_{cr} = m_e^2c^3/e\hbar$=4.4e13 G, the critical magnetic field, ε_s in m_ec^2 units)

The Multifrequency Campaign on 0716

Multifrequency campaigns

ENIGMA campaigns 2003-2004...

...and a look into the future.

Stefan Wagner, LSW

Multifrequency campaigns

- Campaigns on:
- 0716+714 (INTEGRAL, see special session for the core and extended campaigns)
- 0235+164 (XMM, see talk by Claudia Raiteri)
- 3C66 A (see talk by Claudia Raiteri)
- PKS 2155-304 (HESS)

PKS 2155-304

- Campaign in August to September 2004, involving HESS, XTE, ground-based telescopes
- ENIGMA: KVA Monitoring from La Palma, and
- MH
- SW
- DE
- GP

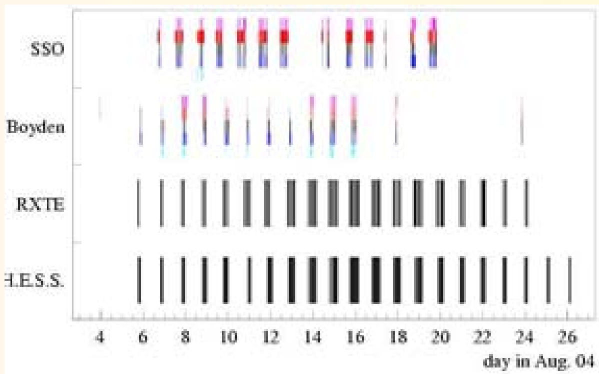

S5 0716+714

- INTEGRAL campaign:
- IDV infers high intrinsic photon densities
- IC signature of 2[nd] order scattering
- Broad MeV bump
- Multifrequency campaign required and carried out.
- Contemporaneous campaign on 0836+71 (see contribution from Jose Gracia)

The future:

- INTEGRAL AO3
- AGILE
- TeV experiments: HESS, MAGIC

THE ENIGMA-WEBT CAMPAIGN ON S5 0716+71: UPDATE ON THE CORE-CAMPAIGN MULTIFREQUENCY OBSERVATIONS

Luisa Ostorero[1] & *Stefan Wagner*[2]

on behalf of the *ENIGMA 0716 collaboration*

(1) *Tuorla Observatory, Finland*
(2) *Landessternwarte Heidelberg, Germany*

Outline of the talk

- Summary of the campaign
- Data collection and archiving
- Analysis and calibration of optical-NIR data
- Core campaign: first results
- Conclusions

Summary of the campaign

Summary of the campaign

- INTEGRAL observations of S5 0716+71 (PI: S.Wagner; Δt=450 ksec) — NOV 10 - NOV 17, 2003

- First plan: simultaneous multi-λ coverage with ground-based telescopes during the period — NOV 06 - NOV 20, 2003
- Several radio-mm-optical observatories involved during Sep-Oct 2003
- WEBT campaign proposed on Oct 01, 2003

Summary of the campaign

- Exceptional brightening of the source in the radio-mm bands during Sep-Oct 2003

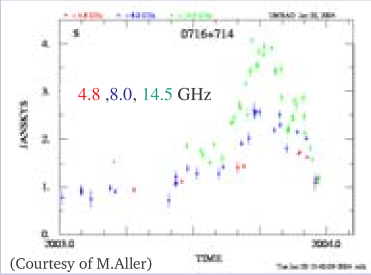

(Courtesy of M.Aller)

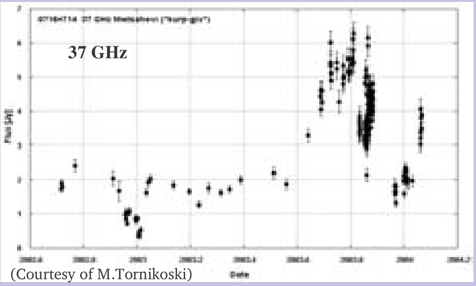

(Courtesy of M.Tornikoski)

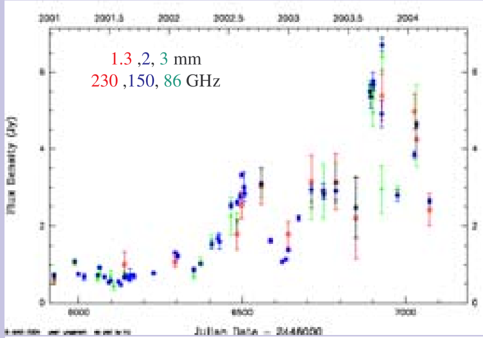

(Courtesy of T.Krichbaum)

Summary of the campaign

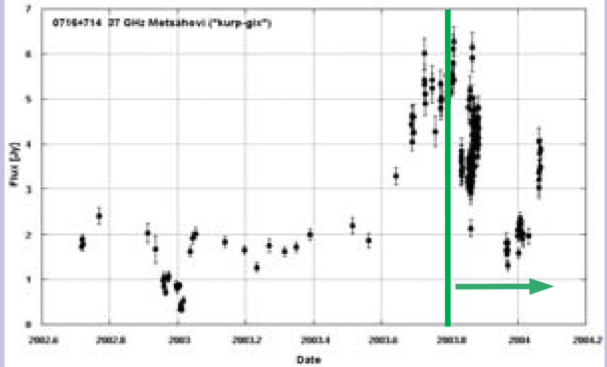

- New plans for the campaign

Extended campaign – I :	OCT 06 - NOV 05, 2003
Core campaign (sim. INTEGRAL):	NOV 06 - NOV 20, 2003
Extended campaign – II :	OCT 20 - DEC 20, 2003

Summary of the campaign

- WEBT campaign announced on Oct 08, 2003 (WEBT news 29)

WEBT News 29 - **October 8, 2003**

WEBT campaign on 0716+714

A new WEBT campaign starts today on the BL Lac object S5 0716+71.
The campaign announcement by the Campaign Manager is appended below.

All observers interested in participatingin the campaign are invited to send a message to the Campaign Manager (Stefan Wagner) and the WEBT President (Massimo Villata), providing information on their instrumentation and observing plans.

Massimo Villata

Summary of the campaign

- Telescopes involved

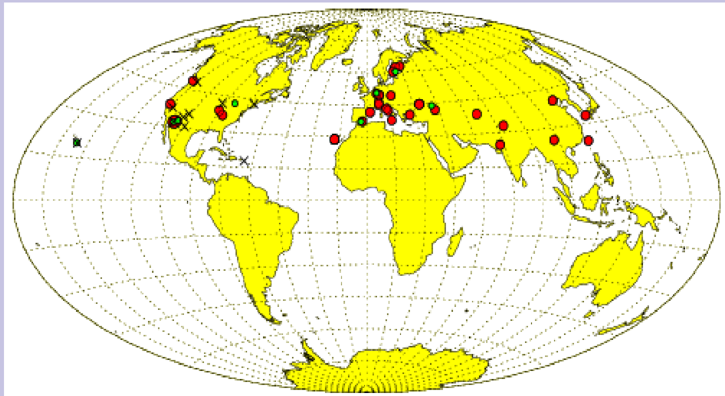

- ● Optical/IR telescopes (38; 28 cm – 4.2 m)
- ● Radio/mm/submm telescopes (9)
- X VLBA antennas

lon = (-123.22 ÷ 128.46) deg

http://www.lsw.uni-heidelberg.de/users/lostorer/0716/0716-nov2003.html

Summary of the campaign

Optical-NIR Observatory list (E ⇒W)

E → W

Observatory (telescope/s) and location	Telescope diam. (cm)	People involved
Mt Sobaek, Korea	N/A	Sohn,Gu
Lulin Observatory,Taiwan	100	Chen,Lin,Hojaev,Takahashi,Chen
Xinglong China	80; 60; 60/90	Peng,Wu,Jiang,Wei
Yunnan, China	100	Dai
Hanle, Ladakh, India	200	Shastri,Baliyan
GIRT, Mt. Abu, India	120	Baliyan, Joshi
Mt. Maidanak, Uzbekistan	60 or 150	Ibrahimov
Abastumani, Georgia	70	Kurtanidze, Nikolashvili
SAI Crimean, Ukraine	60	Goranskij
Crimean, Ukraine	70	Larionov,Efimova,Hagen-Thorn, Doroshenko,Arkharov,di Paola
Jakokoski, Finland	50	Paakkonen,Karppanen,Itkonen
COMU Ulupinar, Turkey	30; 40	Erdem,Bakis,Cicek
Nyrola, Finland	40	Oksanen
Tuorla, Finland	100	Takalo,Sillanpaa,Nilsson,Lindfors,Pasanen
Monte Boo, Czech Republic	60	Hroch,Sixtova,Munz
Catania, Italy	91	Frasca,Marilli,Sodyugan
Campo Imperatore, Italy	110	Larionov
Perugia, Italy	40	Tosti,Ciprini,Nucciarelli

Summary of the campaign

Optical-NIR Observatory list (E ⇒W)

E → W

Observatory (telescope/s) and location	Telescope diam. (cm)	People involved
LSW Heidelberg, Germany	70	Wagner,Strub,Hauser,Tapken,Ostorero, Kachel,Emmanoulopoulos
Trebur, Germany	100	Ohlert
TIRGO, Gornergrat, Switzerland	150	Tozzi
Torino, Italy	105	Villata, Raiteri,Lanteri,Crapanzano
Hoher List, Bonn, Germany	106	Krichbaum,Bach
Sabadell, Spain	50	Ros,Coloma
Calar Alto, Spain	220	Kurtanidze
Roque (NOT), La Palma, Spain	256	Pursimo
Roque (KVA), La Palma, Spain	35; 60	Takalo,Sillanpaa,Nilsson,Lindfors,Pasanen
WHT with ULTRACAM, La Palma, Spain	420	Smith
Bell, Kentucky, USA	60	Carini
St. Louis, Missouri, USA	35	Wilking,Tartar
Mt. Lemmon, Arizona	N/A	Sohn,Yim,Lee
Kitt Peak (WIYN), Arizona, USA	90	Rector
Lowell, Arizona, USA	180	Miller
Kitt Peak (RCT), Kitt Peak, Arizona, USA	130	Mattox
Coyote Hill, California, USA	28	Pullen
University of Victoria, Canada	50	Robb

4th ENIGMA Meeting - Perugia (Italy), October 06-08, 2004

Summary of the campaign

Radio-mm-submm Observatory list

Observatory and and location	Antenna diameter	People involved
Effelsberg, Germany	100 m	Krichbaum et al. *
IRAM, Pico Veleta, Spain	30 m	Krichbaum et al. *
JCMT, Mauna Kea, Hawaii, USA	15 m	Tornikoski
Metsahovi, Finland	14 m	Tornikoski,Lahteenmaki, Torniainen, Terasranta
Steward KP, Kitt Peak, Arizona, USA	12 m	Krichbaum et al. *
Heinrich Hertz, Mt. Graham, Arizona, USA	10 m	Krichbaum et al. *
UMRAO, Michigan, USA	26 m	Aller, Aller
RATAN-600, Zelenchukskaya, Russia	576 m	Kovalev
Westerbork, Hooghalen, Germany	14 ant., 25 m	Krichbaum et al.*
VLBA, Socorro, New Mexico, USA	27 ant., 25 m	Krichbaum et al. *

* Krichbaum, Agudo, Angelakis, Bach,Beckert,Britzen,Friedrichs, Fuhrmann, Impellizzeri,Kadler,Klare,Kraus,Pagels,Sohn,Witzel,Zensus

4th ENIGMA Meeting - Perugia (Italy), October 06-08, 2004

Summary of the campaign

- S5 0716+71 *bright* in the optical band (R~ 12.8) before the core campaign, but *faint* during the core campaign (R ~ 13.5-14.2)

optical band

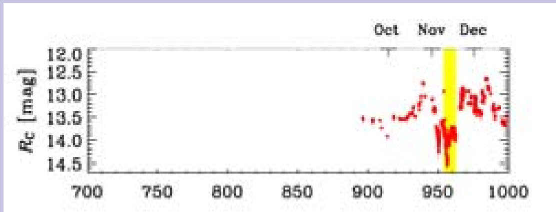

radio band

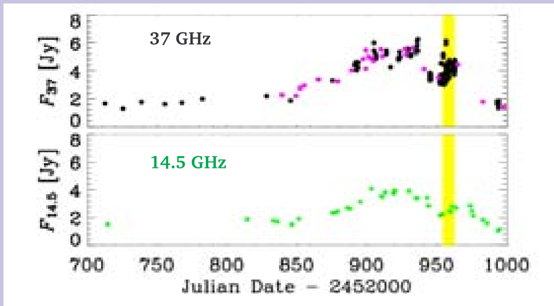

INTEGRAL observation: Nov 10-17, 2003

4th ENIGMA Meeting - Perugia (Italy), October 06-08, 2004

Summary of the campaign

- Brightening of S5 0716+71 in the optical band *after* the INTEGRAL pointing: 2 unprecedented outbursts recorded in
  - late January 2004 (R ~ 12.2)
  - late March 2004 (R ~ 12.1)

RXTE ToO (PI: S.Wagner)

2 observations performed on March 27 and March 28-29
$\Delta t \sim 5$ ksec

INTEGRAL ToO (PI: E.Pian)

April 02-06, 2004
$\Delta t \sim 280$ ksec
(Pian et al. 2004, astro-ph/0408580)

Summary of the campaign

- Preliminary long-term UBVRI optical light curves and the high-energy pointings

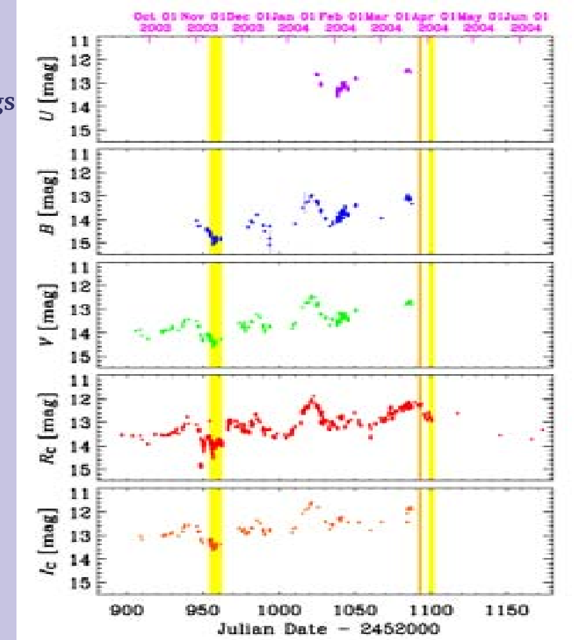

INTEGRAL observation: Nov 10-17, 2003 (PI: S.Wagner)

RXTE ToO Mar 27 + 28/29, 2004 (PI: S.Wagner)

INTEGRAL ToO: Apr 02-04, 2004 (PI: E.Pian)

Summary of the campaign

- Preliminary long-term R-band optical light curves and the high-energy pointings

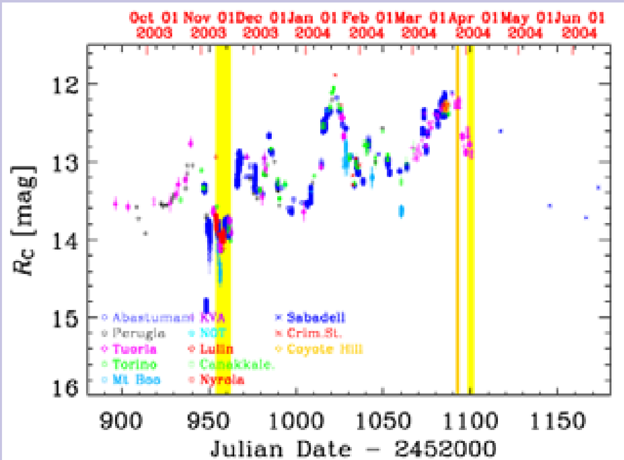

INTEGRAL observation: Nov 10-17, 2003 (PI: S.Wagner)

RXTE ToO Mar 27 + 28/29, 2004 (PI: S.Wagner)

INTEGRAL ToO: Apr 02-04, 2004 (PI: E.Pian)

Summary of the campaign

- Final long-term radio light curves and high-energy observations

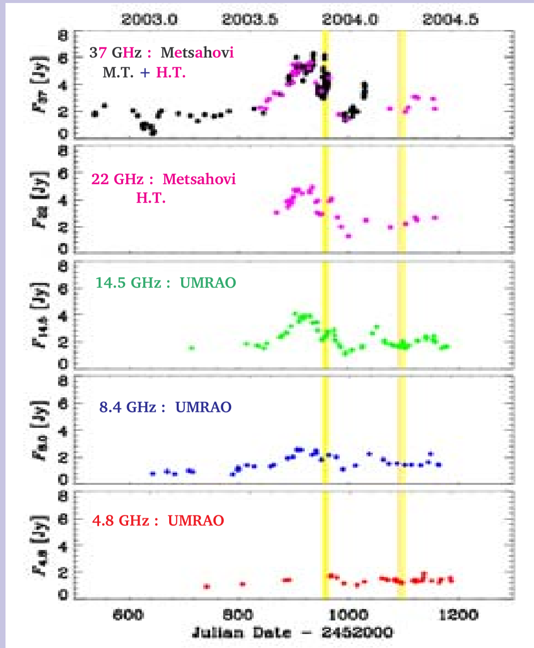

INTEGRAL observation: Nov 10-17, 2003 (PI: S.Wagner)

RXTE ToO Mar 27 + 28/29, 2004 (PI: S.Wagner)

INTEGRAL ToO: Apr 02-04, 2004 (PI: E.Pian)

Summary of the campaign

- Further extension of the campaign till May 2004 (~end of the observability window)

- Total duration of the campaign: ~ <u>8 MONTHS</u>

Extended campaign – I :	OCT 06 - NOV 05, 2003
Core campaign (sim. INTEGRAL):	NOV 06 - NOV 20, 2003
Extended campaign – II :	OCT 20, 2003 - MAY 31, 2004

Data collection and archiving

Data collection and archiving

- Communication with the campaigners

  - Campaign WEB page (general information, telescopes involved, observing strategies, news, instructions for data submission, preliminary light curves, ...)
    http://www.lsw.uni-heidelberg.de/users/lostorer/0716/0716-nov2003.html
    also
    http: //www.to.astro.it/blazars/webt/
    --> *Campaigns* --> *0716+71 during an INTEGRAL observation*

  - Intensive e-mail exchange: ~ 850 messages (~750: opt-NIR; ~50: rad-mm-submm) sent/received during the whole campaign, on
    - general information on the campaign
    - observing strategies
    - technical information on telescopes/CCDs used
    - people involved and contact persons
    - location of new observatories joining the collaboration
    - coordination among different telescopes during intensive follow-up of high-energy pointings
    - observing reports
    - check on preliminary data/frames
    - submission of preliminary and final data

Data collection and archiving

DAY BY DAY...

- Storage of information and data
  - Campaign WEB page
  - Our 0716+71 archive:
    - spreadsheets (data statistics)
    - technical notes
    - preliminary and final data files
    - images (FITS files)

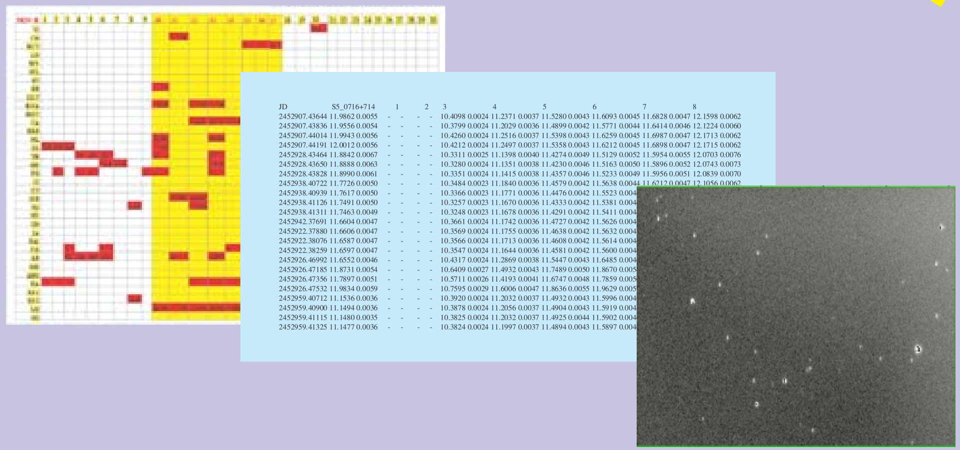

Data collection and archiving

- Format of optical-NIR data
  - ♦ We aimed at collecting
    - when possible: reduced frames (bias/dark and flat-field corrected)

→ *ftp://ftp.lsw.uni-heidelberg.de/incoming/lostorer/*

→ CD-ROM/DVD delivered via mail

- when not possible: instrumental mags of the source and 8 comparison stars in order to apply the same analysis and calibration procedures to all the datasets

Suggested format for instrumental data (WEBT format)
http://www.lsw.uni-heidelberg.de/users/lostorer/0716/0716-nov2003.html

```
JD-2452000   0716+71      1            2            ..... 8
961.37406    11.824 0.007 9.564 0.002  10.053 0.002 ..... 12.6796 0.0123
```

Data collection and archiving

♦ We got:

- reduced frames
- non-calibrated data (instr. mags of the source and comparison stars)

as requested

as well as:

- non-calibrated data in SEVERAL DIFFERENT FORMATS (often unobvious and unexplained)
  format=format (observatory, observer, time, ...)
- data already calibrated with different calibration sequences
- non-reduced frames +biases/darks + flatfields

format conversion: time – consuming !

Data collection and archiving

- Optical-NIR data statistics (updated to Oct 03, 2004)

Whole campaign: 13497 data-points

Filter	Frames	Data	Total
U	0	135	135
B	372	652	1024
V	883	401	1284
R	3876	5151	9027
I	746	201	947
J	1	354	355
H	1	366	367
K	1	357	358

Nov 2003 (core campaign): 4015 data-points

Filter	Frames	Data	Total
U	0	0	0
B	172	158	330
V	152	109	261
R	1071	1727	2798
I	174	41	215
J	1	123	124
H	1	138	139
K	1	147	148

Analysis and calibration of optical-NIR data

Analysis and calibration of optical-NIR data

- Steps of the optical- NIR data analysis and calibration

1) Frame photometry — performed with a C-code of aperture photometry developed by K. Nilsson (Tuorla Observatory)

2) Homogeneization of the non-calibrated data sets — both the photometry output files and the submitted data sets are converted in WEBT format

3) Choice of a calibration sequence

4) Calibration of the data

4) Light curve assembling

→ discussed in the following

Analysis and calibration of optical-NIR data

- Choice of the calibration sequence: available data

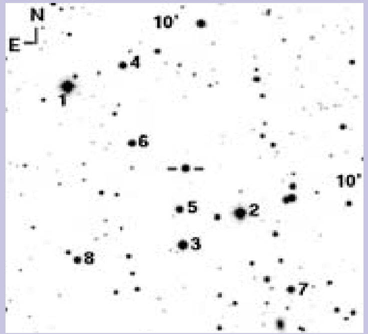

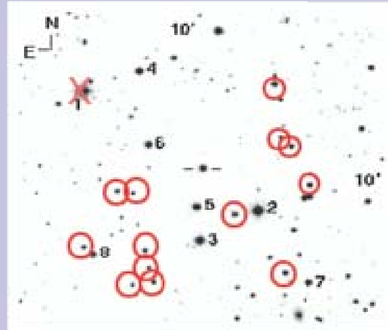

B,V,R : Villata et al. 1998, A&AS, 130, 305
I : Ghisellini et al. 1997, A&A, 327, 61
U,I : Gonzáles-Pérez et al. 2001,AJ,122,2055

UBVRI: Gonzáles-Pérez et al. 2001,AJ,122, 2055

20 comparison stars (13 new, fainter stars): Field "not well observed" by the authors, but stars 234678 claimed to be in agreement ~ 2-3 % with Villata et al. 1998

Analysis and calibration of optical-NIR data

- Choice of the calibration sequence: agreements

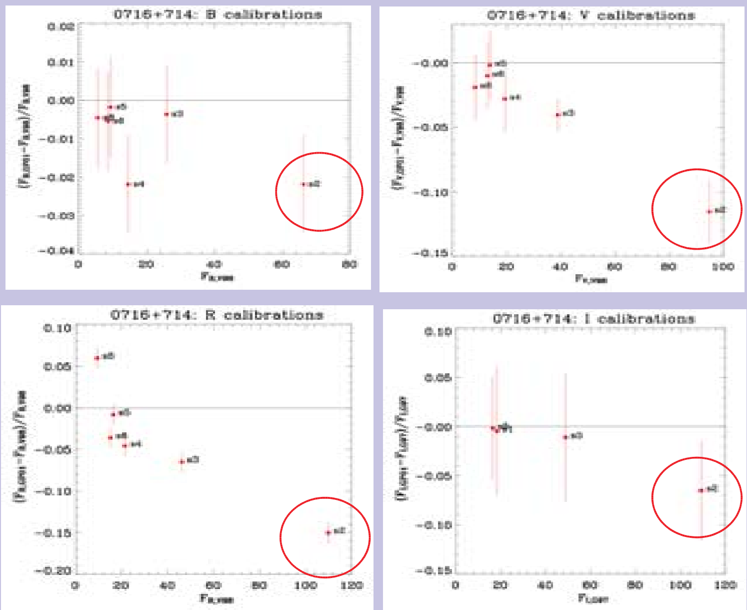

Agreement bw GP01 and V98,G97

B: 2.2%
V: 11.5% (4% excl. #2)
R: 15% (6.5% excl. #2)
I: 6.5% (1% excl. #2)

Analysis and calibration of optical-NIR data

- Choice of the calibration sequence: R band

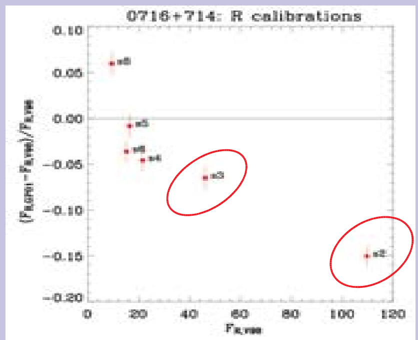

R band: -strong disagreement bw GP01 and V98
-big uncertainties on the absolute calibration of stars 2 and 3
#2 : R=11.297 ± 0.105
#3 : R=12.133 ± 0.051
which are useful (bright, close to the source)

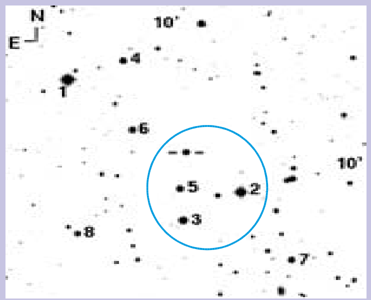

Analysis and calibration of optical-NIR data

- Choice of the calibration sequence:
  tests on R-band intranight light-curves

Light-curve of 0716+714 calibrated with different reference stars (different colours)

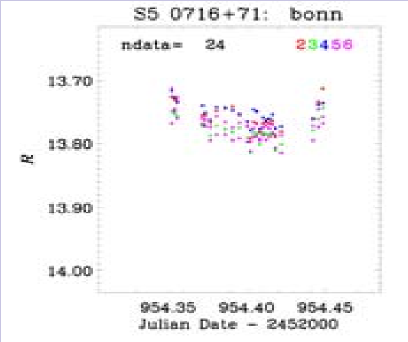

Villata et al. 1998

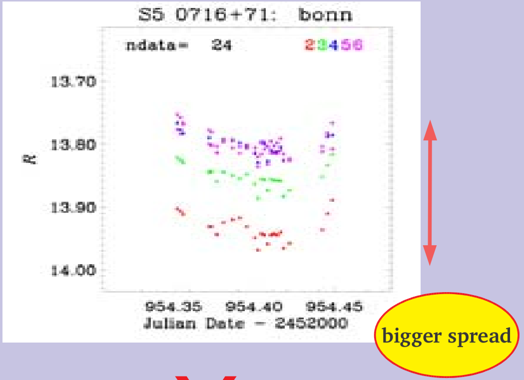

Gonzáles-Pérez et al. 2001

Analysis and calibration of optical-NIR data

- Choice of the calibration sequence

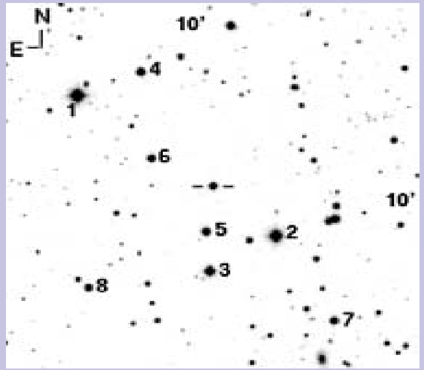

Adopted sequence:

B,V,R	Villata et al. 1998, A&AS, 130, 305
I	Ghisellini et al. 1997, A&A, 327, 61
U,I	Gonzáles-Pérez et al. 2001, AJ, 122, 2055
JHK	2MASS (http://www.ipac.caltech.edu/2mass/)

Star	U	B	V	R	I	J	H	K
1	N/A	11.54 (0.01)	10.99 (0.02)	10.63 (0.01)	N/A	10.050 (0.018)	9.813 (0.017)	9.750 (0.020)
2	12.089 (0.005)	12.02 (0.01)	11.46 (0.01)	11.12 (0.01)	10.92 (0.04)	10.515 (0.021)	10.301 (0.017)	10.228 (0.020)
3	13.199 (0.007)	13.04 (0.01)	12.43 (0.02)	12.06 (0.01)	11.79 (0.05)	11.319 (0.020)	11.063 (0.017)	10.978 (0.022)
4	13.629 (0.006)	13.66 (0.01)	13.19 (0.02)	12.89 (0.01)	12.656 (0.001)	12.275 (0.023)	12.045 (0.021)	12.039 (0.025)
5	14.246 (0.003)	14.15 (0.01)	13.55 (0.02)	13.18 (0.01)	12.85 (0.05)	12.341 (0.021)	12.066 (0.019)	12.010 (0.026)
6	14.360 (0.004)	14.24 (0.01)	13.63 (0.02)	13.26 (0.01)	12.79 (0.04)	12.479 (0.023)	12.212 (0.021)	12.166 (0.027)
7	15.002 (0.021)	14.55 (0.01)	13.74 (0.02)	13.32 (0.01)	13.306 (0.038)	12.453 (0.021)	12.071 (0.021)	12.006 (0.025)
8	14.804 (0.004)	14.70 (0.01)	14.10 (0.02)	13.79 (0.01)	13.419 (0.007)	13.072 (0.021)	12.778 (0.025)	12.736 (0.034)

Analysis and calibration of optical-NIR data

- Calibration of the data

♦ Calibration procedure : performed on each "data unit"
⇓
data set produced by a given telescope/detector during a given observing night (or part of that night when the sky condition are variable)

I) Identification of a subset S of comparison stars common to all the elements of the data unit (S depends on : telescope size, CCD dimensions, exposure times,...)

II) Computation of the calibrated mag of 0716+714 with a suitable subset of S: S1 (brightest stars, but non saturated!)

III) Computation of the errors with a suitable subset of S: S2 (mag~mag_0716)

Analysis and calibration of optical-NIR data

- Light curve assembling

I) Exclusion of bad isolated photometric data points

II) Binning of noisy data sets

III) Computation of the *offsets* among different data units

IV) Application of the offsets and assembling of the data units

Core campaign: first results

Core campaign: first results

- Core campaign: November 06-20, 2003

Source faint in the optical band

Optical band

Radio band

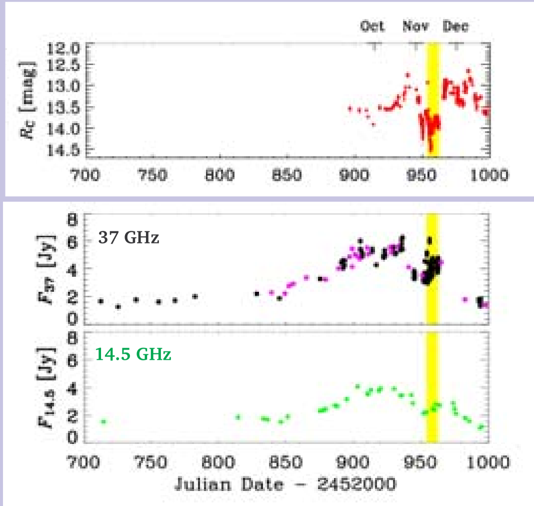

INTEGRAL observation:
Nov 10-17, 2003

Core campaign: first results

- Boundary conditions …

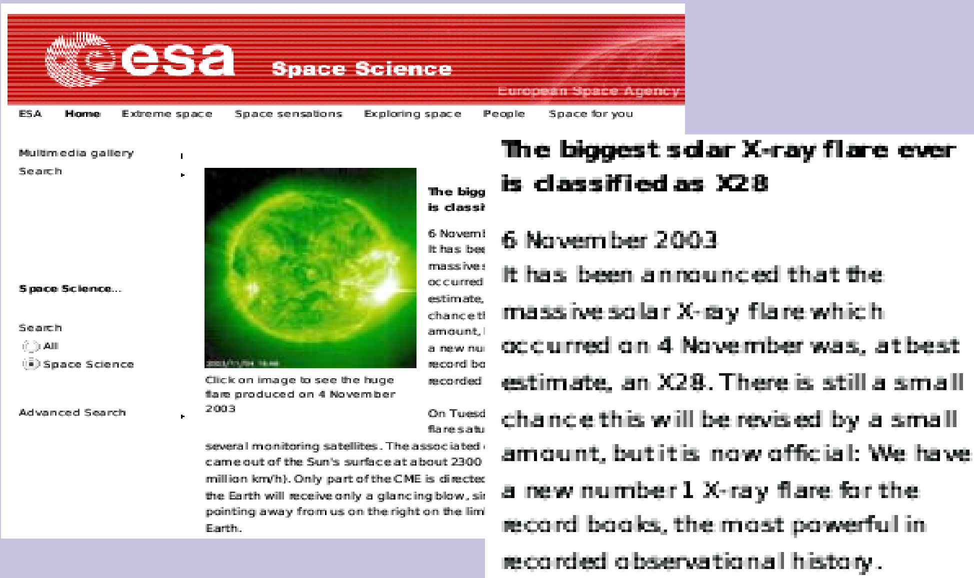
esa Space Science
European Space Agency
ESA Home Extreme space Space sensations Exploring space People Space for you
Multimedia gallery
Search
Space Science...
Search
All
Space Science
Advanced Search
Click on image to see the huge flare produced on 4 November 2003

The biggest solar X-ray flare ever is classified as X28

6 November 2003

It has been announced that the massive solar X-ray flare which occurred on 4 November was, at best estimate, an X28. There is still a small chance this will be revised by a small amount, but it is now official: We have a new number 1 X-ray flare for the record books, the most powerful in recorded observational history.

several monitoring satellites. The associated … came out of the Sun's surface at about 2300 … million km/h). Only part of the CME is directe… the Earth will receive only a glancing blow, … pointing away from us on the right on the lim… Earth.

Core campaign: first results

- Boundary conditions …

unprecedented solar flare, space storm, ~full moon, clouds, auroras …

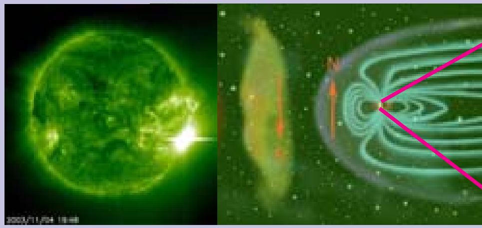

INTEGRAL data strongly affected by enhanced background

Ground-based optical-to-radio observations affected by bad weather.
Enhanced background in optical-NIR frames (moon, clouds, auroras,…)

Core campaign: first results

Rc band: ~2800 data collected up to now for Nov 2003 (~2000: core campaign)

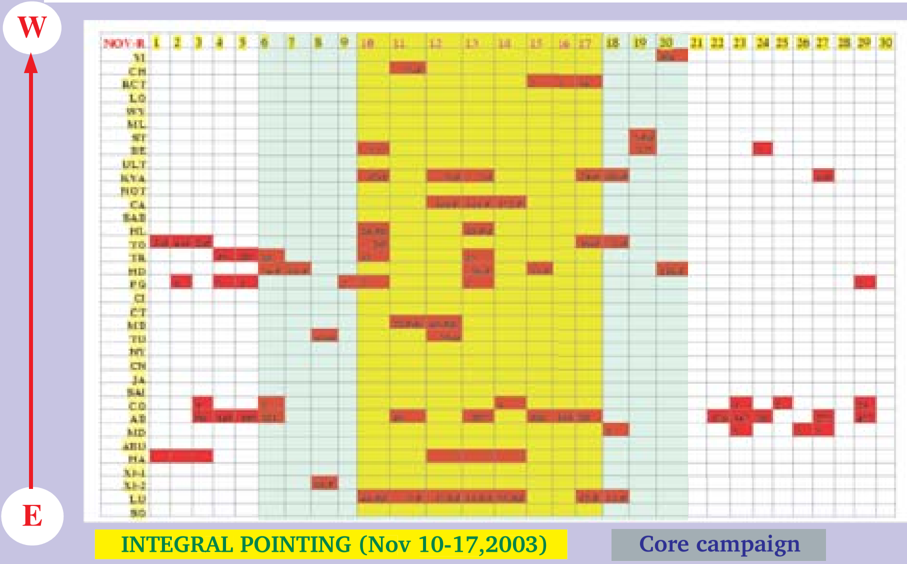

Core campaign: first results

- Optical R-band light curve

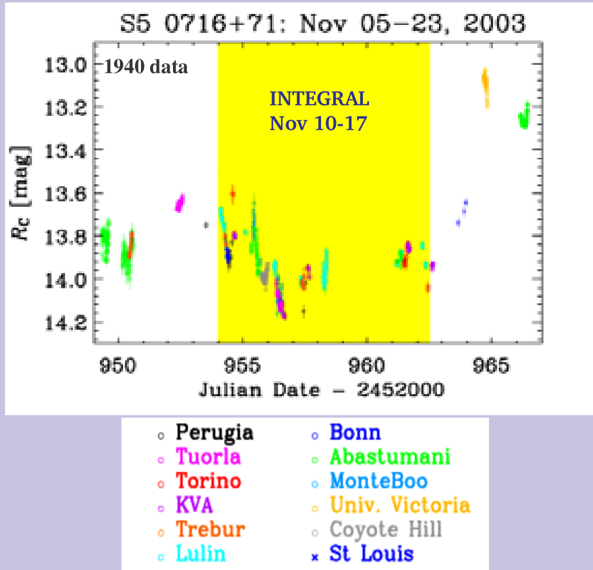

Applied offsets:

Lulin	0.000
Univ. Victoria	0.000
Tuorla	0.000
Coyote Hill	0.000
Trebur – Lulin	–0.007
Bonn – Lulin	+0.120
Torino – KVA	+0.030
MonteBoo – Abastumani	+0.080

Core campaign: first results

- Optical R-band light curve: rough estimate of the variability

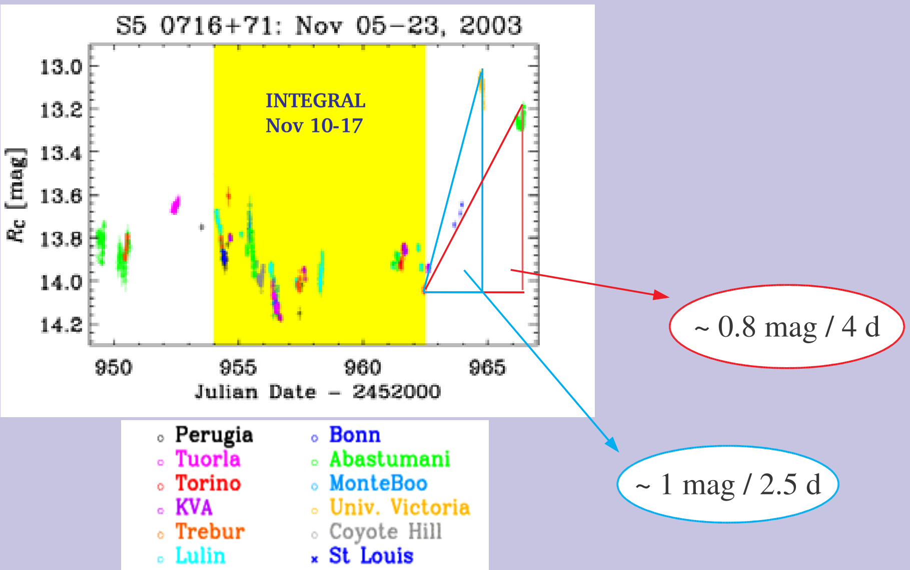

Core campaign: first results

- Optical R-band light curve: zoom on the core-campaign period

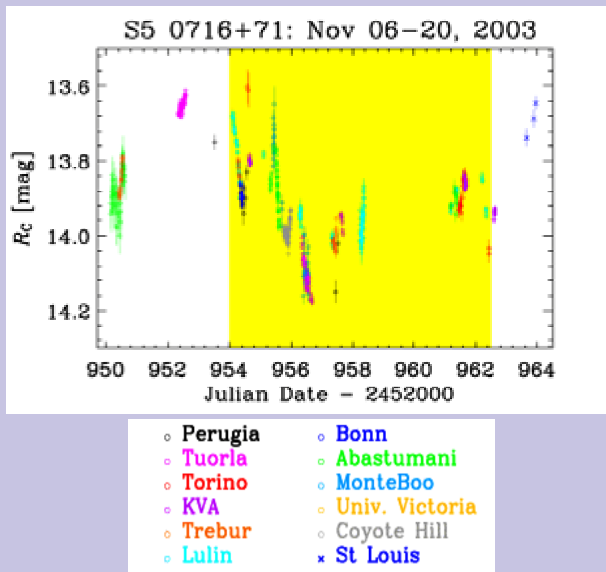

Core campaign: first results

- Optical R-band light curve: zoom on the core-campaign

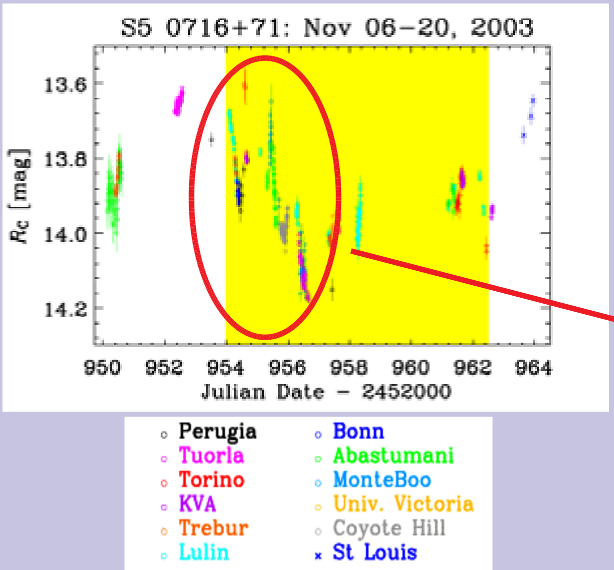

Best sampling:
Nov 10-13
(current status
of the analysis)

Core campaign: first results

- Optical R-band light curve: zoom on Nov 10 -13, 2003

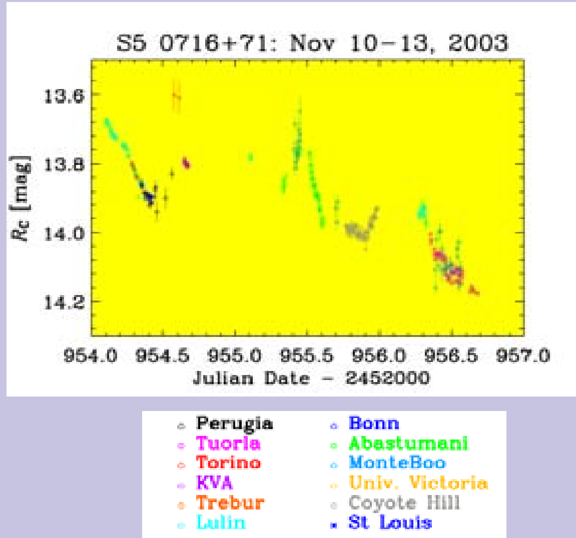

Core campaign: first results

- Optical R-band light curve: zoom on Nov 10 -13, 2003

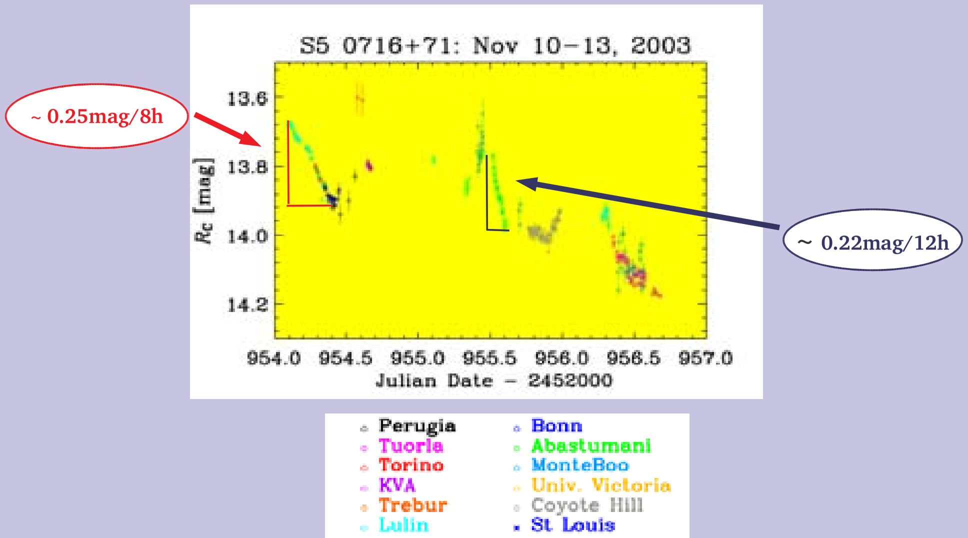

Core campaign: first results

- INTEGRAL – OMC: Optical Monitoring Camera

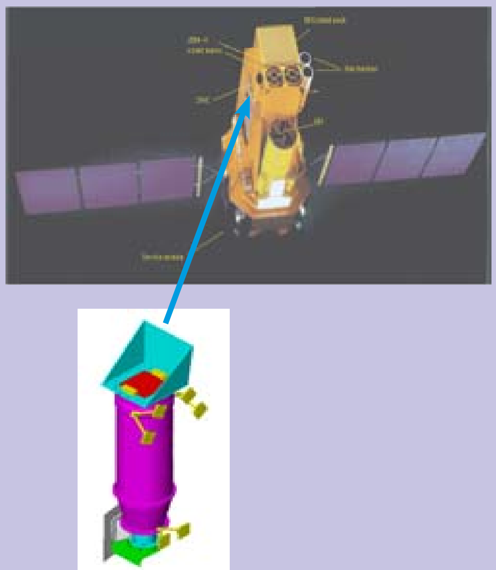

Parameter	Value
Wavelength range	500 - 600 nm (Johnson V-filter)
Detector	50 mm lens + CCD (2055 x 1056 pixels), imaging area = 1024 x 1024 pixels
Pixel size	(13 x 13) micrometer^2 = (17.5 x 17.5) arcsec^2
Field of view	5 x 5 deg
Angular resolution	23"
Typical integration times	10 s - 50 s - 200 s
Sensitivity (3 sigma in 10 x 200 s)	18.1 mag (V)
Photometric accuracy	< 0.3 mag for < 16 mag and > 300 s
Typical source location accuracy	6"

Core campaign: first results

- OMC V-band light curve

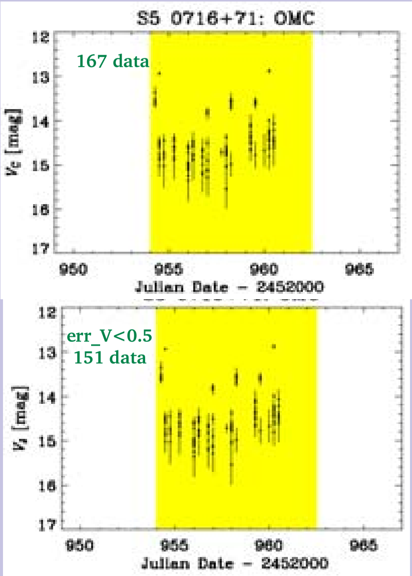

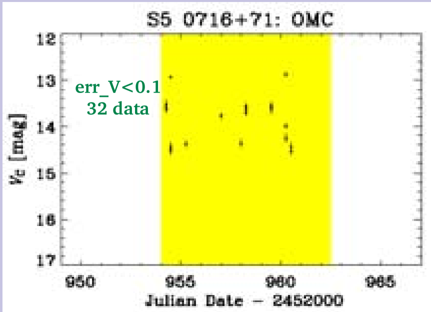

photometric accuracy
err_V = 0.03 – 0.96

Preliminary

Core campaign: first results

- OMC and ground-based R-band light curves

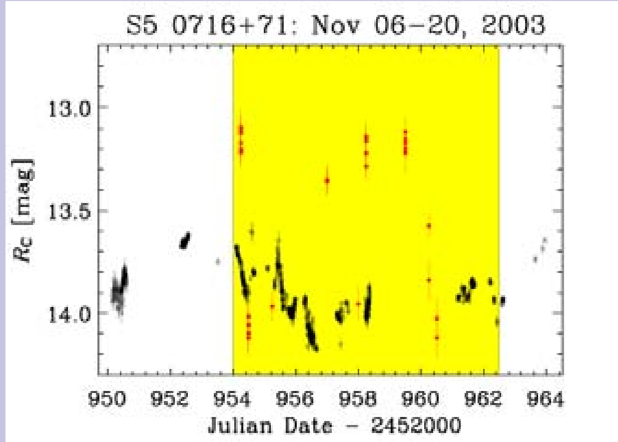

- OMC R-band data (V-R=0.420 ; Raiteri et al. 2003)
- ground-based R-band data

Disagreement

Core campaign: first results

- Next step: quantitative estimate of variability and cross-correlation with radio-mm-submm data

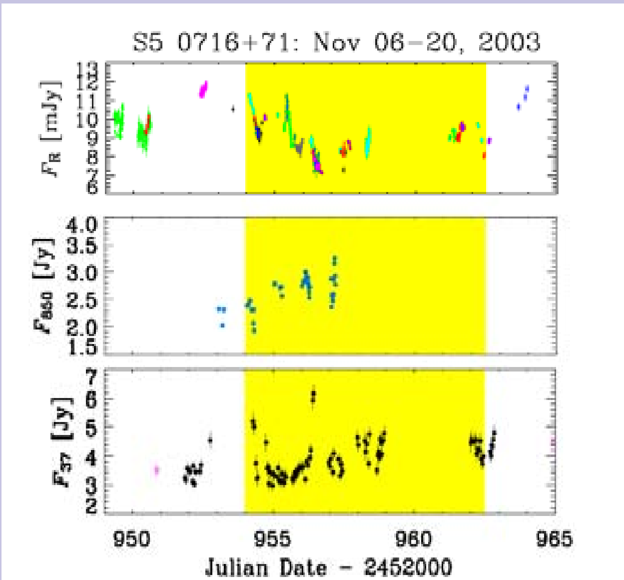

Perugia, Tuorla, Torino, KVA, Trebur, Lulin, Bonn, Abastumani, MonteBoo, Univ. Victoria, Coyote Hill, St Louis

JCMT
850 microns

Metsahovi
(M.T. + H.T.)

Conclusions

- General remarks on the 0716 campaign:
  - An 8-month multiwavelength campaign was carried out on the BL Lac object 0716+714, from October 2003 to May 2004.
  - Optical-to-radio ground-based observations were performed continuously and intensified during the high-energy observations by INTEGRAL, RXTE, XMM.
  - A big multiwavelength database on this source is under construction.
- Update on the 0716 core-campaign:
  - A suitable optical-NIR calibration sequence was identified.
  - The core-campaign optical light curve is almost completely assembled.
  - Optical IDV was detected during the core campaign (up to 0.25mag/8h)
  - The OMC camera onboard INTEGRAL detected 0716+714, and some variability was recorded, but the uncertainties on the photometry are big . Estimate of the variability still in progress.
  - IDV was detected in the radio and sub-mm bands.
  - A quantitative estimate of the core-campaign optical variability and the radio-to-optical cross-correlation analysis will be the next step of this work.

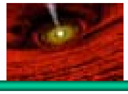

Fast Optical Variations in 0716+714

4th ENIGMA Meeting, Perugia, October 2004

N. Smith, A. Giltinan, A. O'Connor, S. O'Driscoll
Cork Institute of Technology

S. Wagner, M. Hauser
LSW, Heidelberg

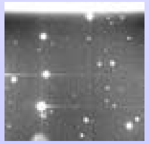

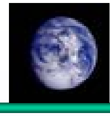

Why search for fast optical variations?

- Optical wavelengths remain the best regime to search for small-amplitude variations on short timescales (<1% in minutes)
- Previous campaigns have strongly hinted at small-amplitude, rapid variability
- Rapid variations reveal discrete substructures on small spatial timescales (minutes?)

This regime of angular diameters cannot be probed directly.

Even space-borne mm-interferometers will fall short by three orders of magnitude

L3 CCD ENIGMA Campaigns

- L3 = Low Light Level
- 2.2m telescope at Calar Alto
- 7 nights Jan/Feb 2003
- 6 nights Sept 2003
- Approx. 70,000 science frames in January
- Approx. 340,000 science frames in September

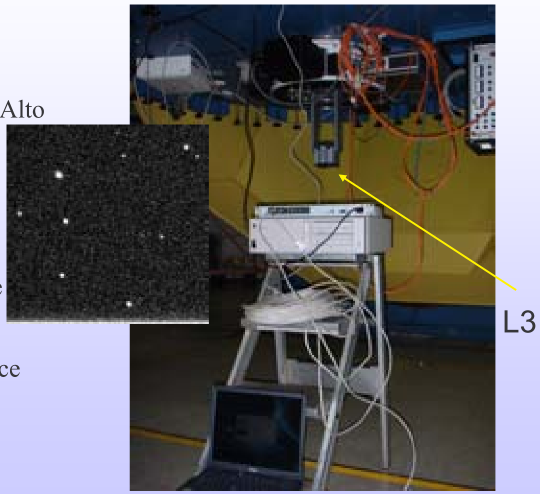

Ultracam "Mini-Campaign"

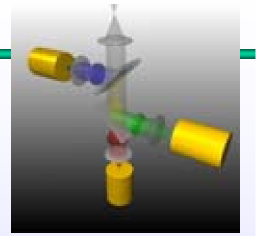

- 3-channel camera capable 4 Mb/s readout
- Three 1k x 1k frame-transfer CCDs
- Observations taken in November 2003 on 4.2m WHT at La Palma in Service Mode
  - Windowed to 100x80 pixels
  - 46,000 science frames per filter = 138,000 frames of data
  - 2 hours of data
- Only one reference star selected by service astronomer
- Similar follow-up observations taken in May 2004

L3 Data Results on 0716+714 – January 2003

Night 6

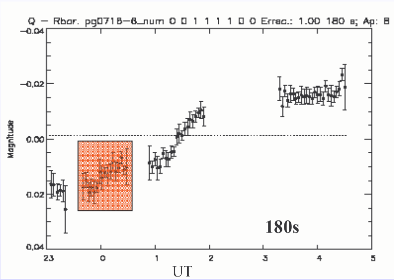

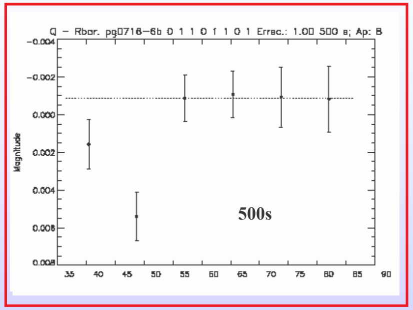

Note:

Reference stars statistically flat

$\Delta m \; \alpha \; t^{0.5}$

L3 Data Results on 0716+714– January 2003

Night 6

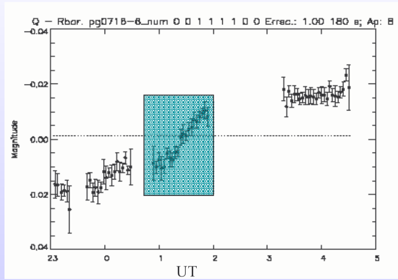

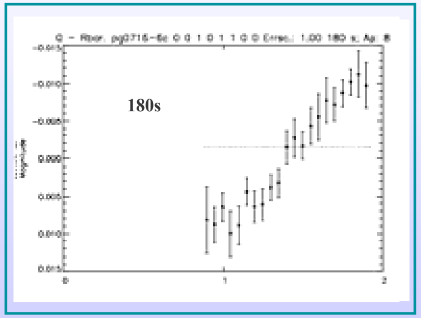

L3 Data Results on 0716+714– January 2003

Night 7

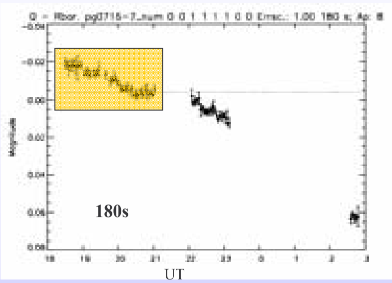

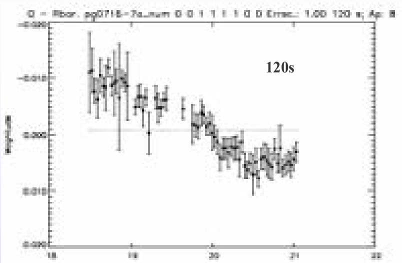

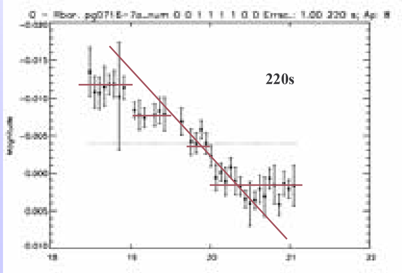

L3 Data Results on 0716+714– January 2003

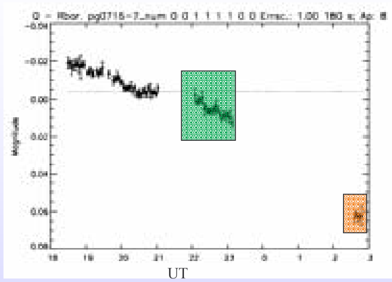

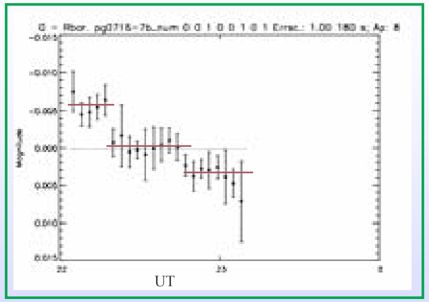

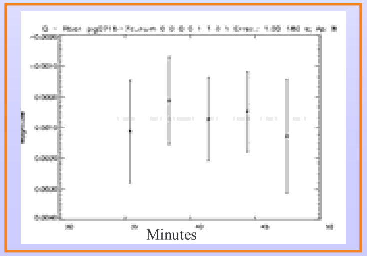

0.47 *mmag* rms scatter

L3 Data Results on 0716+71 – September 2003

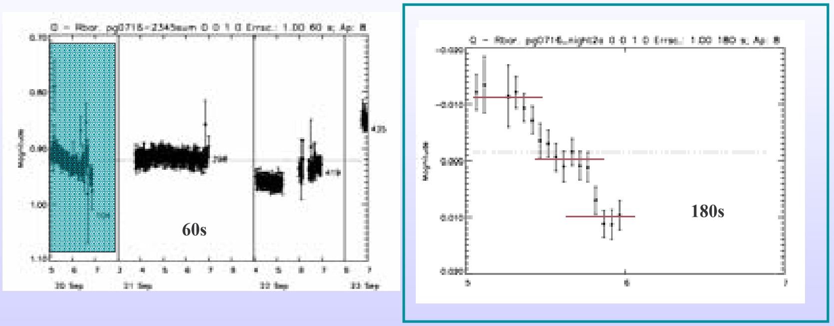

L3 Data Results on 0716+71– September 2003

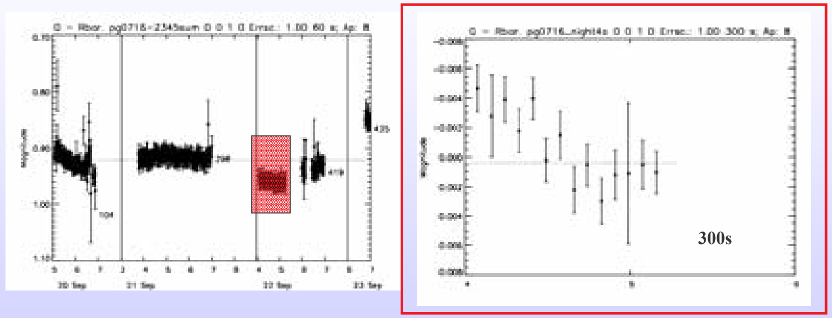

Ultracam Results – November 2003

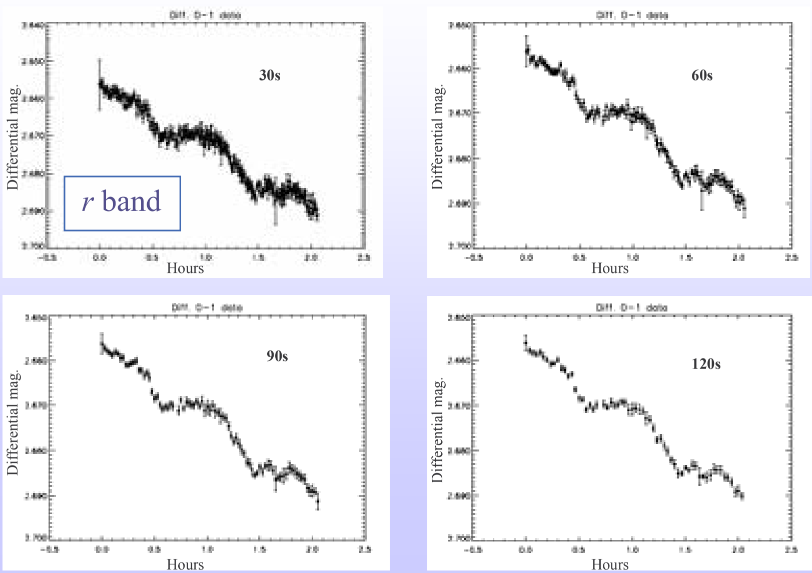

Ultracam Results – November 2003

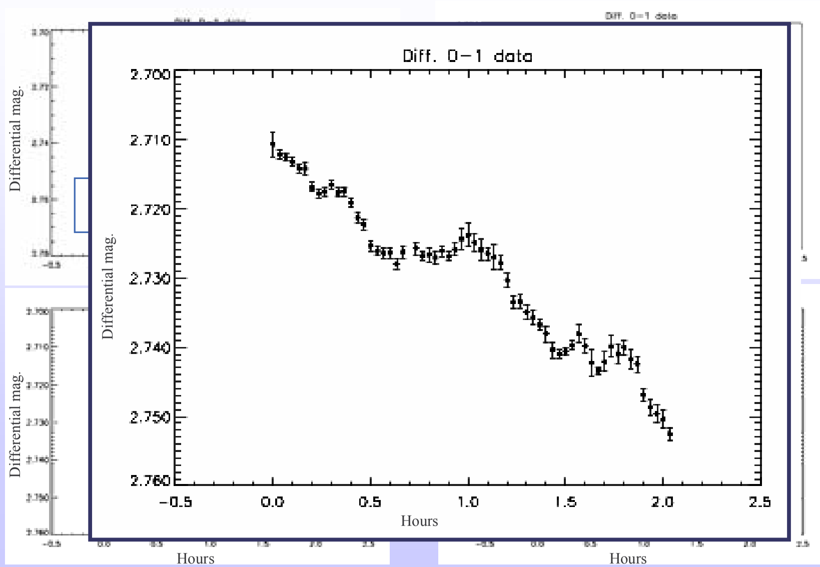

Ultracam Results – November 2003

(r – g) spectral evolution

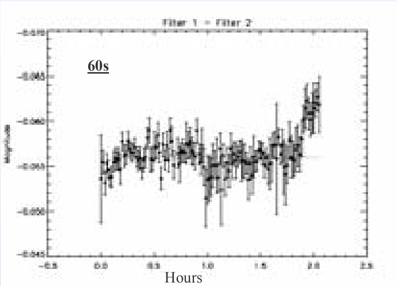

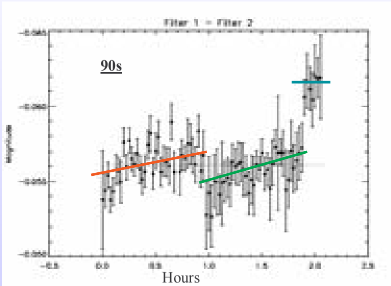

Conclusions

- Photometric precision of +/-1 *mmag* on either 2.2m or 4.2m
- Evidence for <u>step-like</u> brightness variations, especially on falling edges of lightcurves
- Step-like behaviour also visible in light-curves of BL Lac (not shown)
- Ultracam data difficult to interpret on short timescales due to presence of only one reference star

BUT

- <u>suggests</u> colour variations with step-like behaviour on falling edge

The INTEGRAL view on the 0716+714/0836+710 field – a first glimpse

José Gracia, IASA Athens
Stefan Wagner, LSW Heidelberg
Dimitrios Emmanoulopoulos, LSW Heidelberg
Luisa Ostorero, Observatory Tuorla

Enigma Meeting 6-8 Oct 2004, Perugia

Outline

What are secondments?

"EU Research *Training* Network ENIGMA"

Supported training instruments:

- workshops
- schools
- *secondments*

Young researchers are asked to visit foreign nodes 1-2 times per year to work on a joint project *not necessarily* related to their own work.
→ Visited Heidelberg during July 2004 to work on "timing analyses of high energy instrument data."

Why 0716+714 or 0836+710?

... or the problem of high photon densities:

- Intraday Variability (IDV) → compact sources
- high intrinsic luminosity → high photon density

→ brightness temperature $T_B > 10^{17}\,\mathrm{K}$
But:

- IC cooling / synchrotron emission $\sim \rho^{10}$
- inverse Compton limit $\approx 10^{12}\,\mathrm{K}$

→ inverse Compton catastrophe:

- short-term flashes of Compton scattered radiation
- limit-cycle
- boost photons into $10^{18} - 10^{20}\,\mathrm{Hz}$ (Integral)
- correlation through all energy bands

The 0716+710 campaign INTEGRAL observations

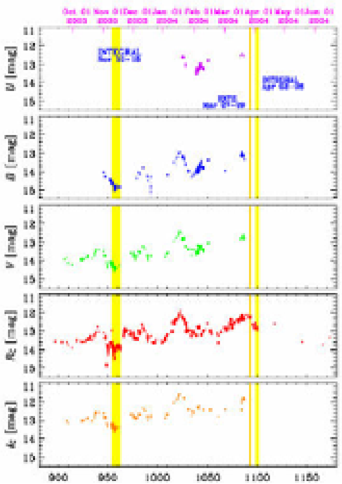

- 400 ksec allmost continously during orbits 131,132,133
- target instrument IBIS: Isgri 15-1500 keV, PICsIT 200-6000 keV
- optical monitoring with OMC (Luisa Ostorero)
- too faint for JEMX (X-rays)?
- SPI was not functional

Coded mask dispersion

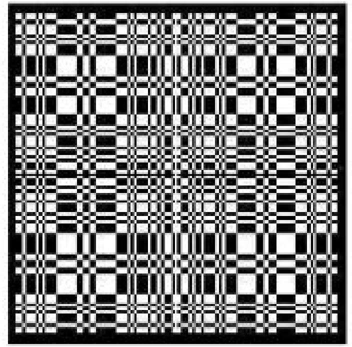

- Building an image is basically the same as determining the incident direction.
- How to get information on direction?
  → Casting shadows with the coded mask

The field ...

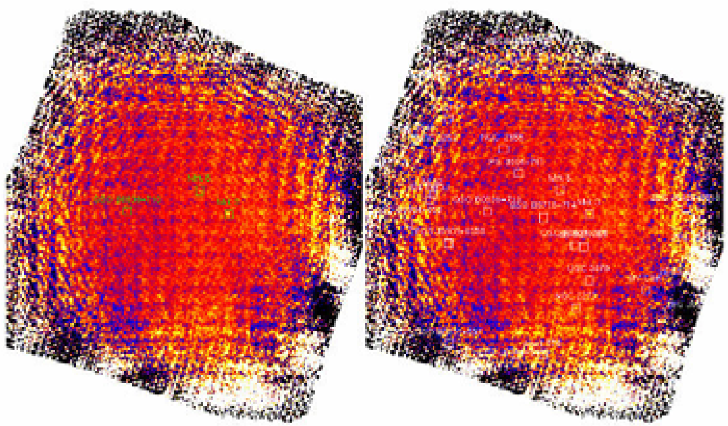

Intensity

The field ...

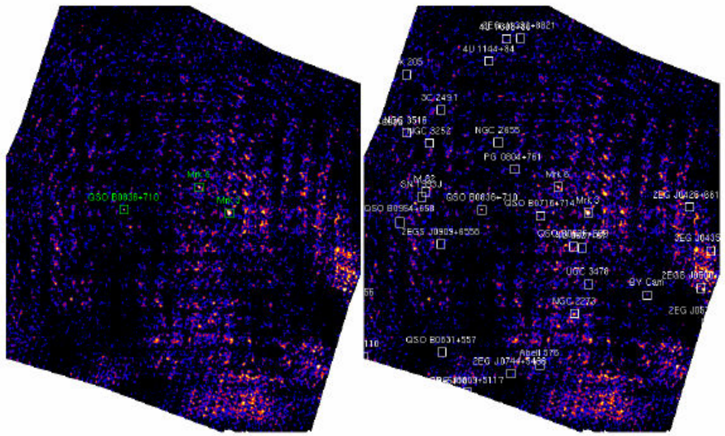

Significance

The field ...

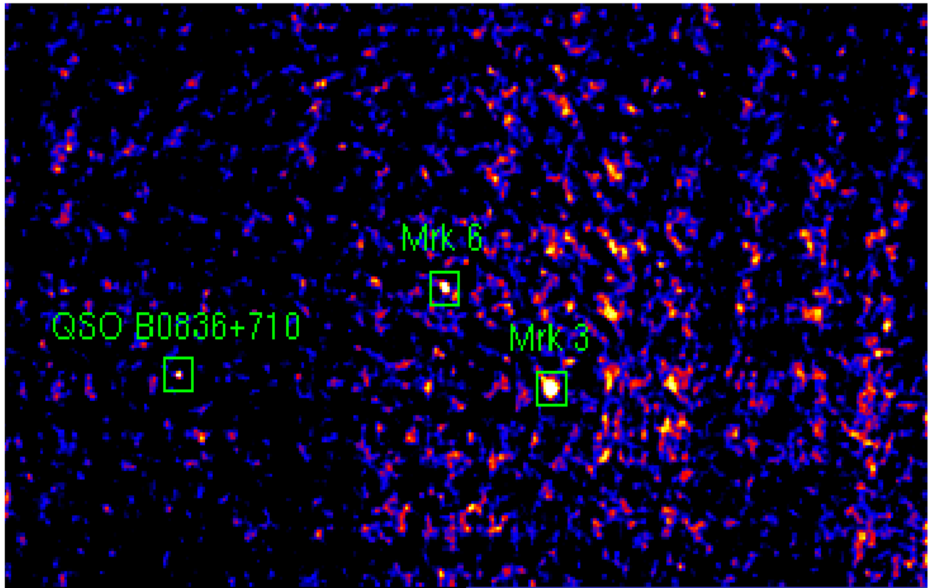

The field ...

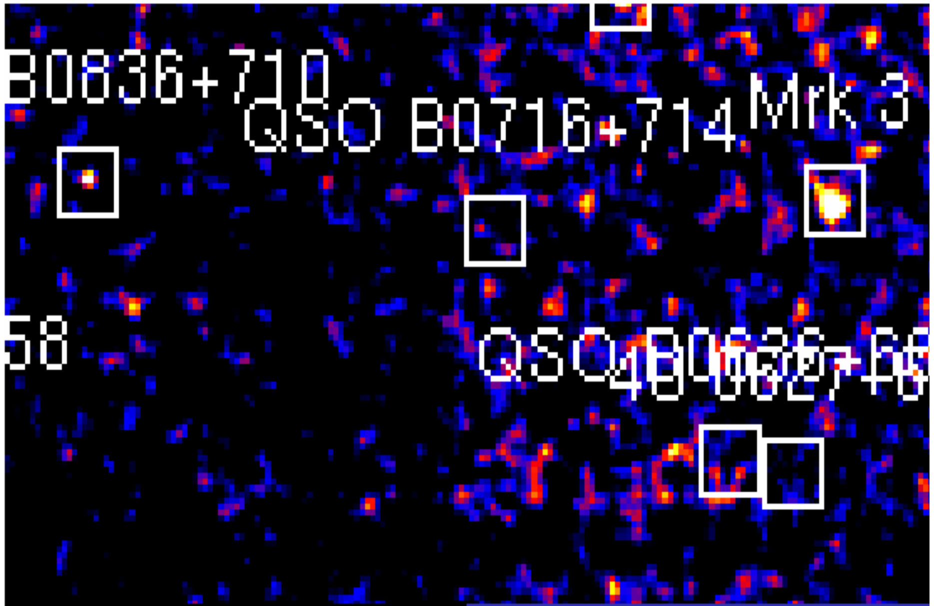

... at different energies

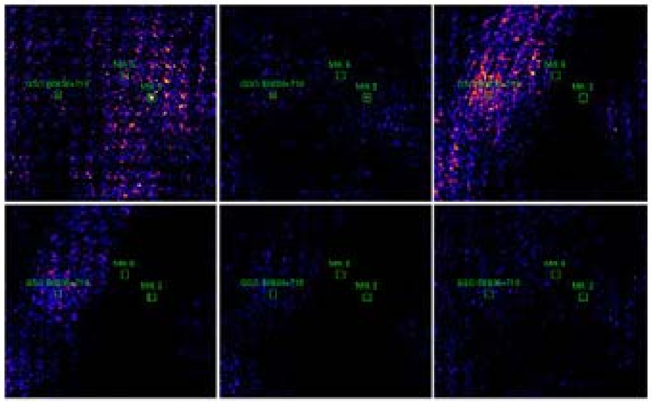

energy bins [keV]: 15-40, 40-100, 100-200, 200-400, 400-700, 700-1500
bad background correction for > 100keV

Raw spectrum

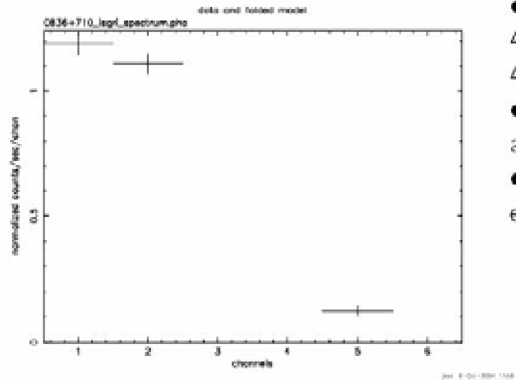

- energy bins [keV]: 15-40, 40-100, 100-200, 200-400, 400-700, 700-1500
- bad bkg correction around 100-400 keV?
- count rates lower than expected

Spectral folding

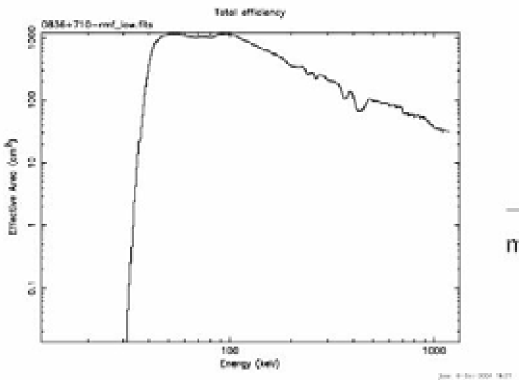

- effective area is function of energy
- blending between different energy bins

→ complicated response matrix

Unfolded spectrum

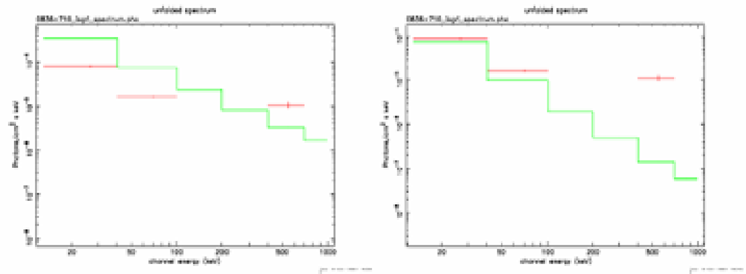

- fluxes very sensitive to the model and response matrix
- response matrix still bad

Other sources

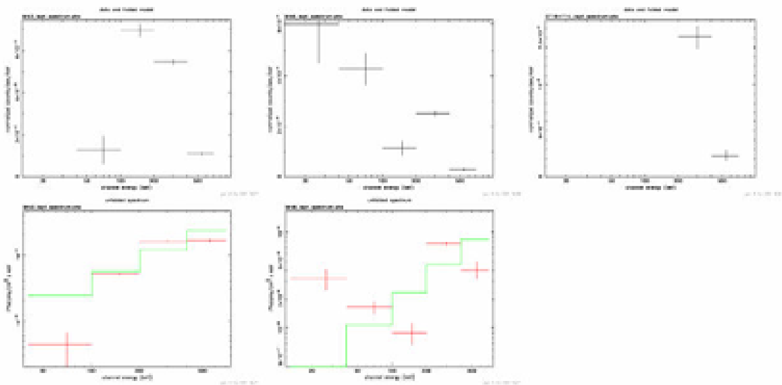

Is there anything else?

ISGRI sources with significance > 5

J0500+5902(?)	5.3
Mrk 3	16,3
NGC2273	6.5
Mrk 6	11.2
PG 0804+761	6.9
0836+710	10.0
0954+556	5.3
NGC 3516	5.2
4U 1308+86	5.0
J1332+8821(?)	5.1

PICsIT

- PICsIT pipeline crashes, only results on individual frames
- 0716+714, 0836+710 to faint

ENIGMA meeting, Perugia

Current status of the Bonn INTEGRAL activities

A broad band flux density monitoring of 0716+714 -
Data and first Results

Involved Scientists at MPIfR:

Max-Planck-Institut für Radioastronomie

I. Agudo, M. Angelakis, U. Bach, T. Beckert,
S. Bernhart (Friedrichs), L. Fuhrmann, V. Impellizzeri,
J. Klare, E. Körding, A. Kraus, T.P. Krichbaum,
A. Pagels, B.W. Sohn, A. Witzel, J.A. Zensus

Other Partners:

H. Ungerechts, M. Grewing (*IRAM*)

A. Apponi, B. Vila-Vilaro, P. Strittmatter, L. Ziurys (*Steward Obs.*)

R. Strom (*ASTRON*)

H. & M. Aller (*Michigan*)

Participating observatories

Radio:

Effelsberg (5 GHz I+P, 10.7 GHz I+P, 32 GHz I),

Michigan (5, 8, 15 GHz, I+P)

Westerbork (1.4 & 2.2 GHz, I),

VLBA (6 x 8 hrs, 1.6 - 43 GHz, dual pol.)

Millimeter:

Pico Veleta (90 & 230 GHz), Kitt Peak (90 GHz),

Heinrich-Hertz (345 GHz)

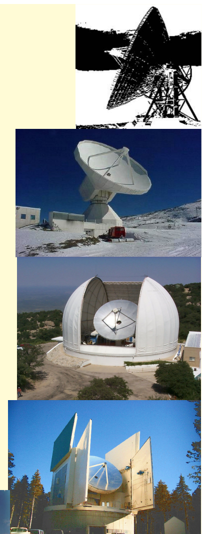

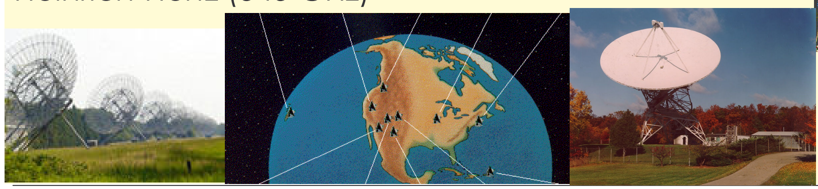

From all the analysis performed up to now, the most general findings are:

Intensity

- We have improved the initial technical goal of reaching a 5% accuracy in flux density measurements. A rms~3% has been obtained.
- The 0716+714 data does not seem to present a clear IDV Type II pattern.
- The 3mm total flux density of 0716+714 increased by ~1.5 Jy in 4 days.

Polarisation

- For the first time, we have showed that 0716+714 is strongly polarized at 3mm.
- The mean *P* over the seven observing days is 0.69±0.02 Jy. The degree of polarization is m ~10-15%

Polarisation angle

- The mean *EVPA* over the seven observing days is 32±1°.
- The polarized emission from 0716+714 at 3mm show evidences of variation during our observing time range:
  - *P* changed from ~0.4±0.1 Jy (during the first observing day) to ~0.8±0.05 Jy (during the fourth one).
  - The *EVPA* changed from ~25±4° (during the first observing day) to 36±1° (during the fourth one).

analysis: Agudo



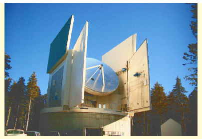
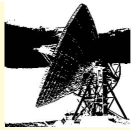

Conclusions

- 0716+714 varied in the radio to mm-bands on time scales of days
- in Nov. 2003 only mild IDV was detected at cm-wavelengths
- in July 2004 IDV was strong again
- at mm-wavelengths the source is highly polarized & variable
- first detection of $T_B > 10^{12}$ K at mm-wavelengths, consistent with superluminal motion and normal (d=10-20) Doppler-factors
- the radio spectrum peaks near 100 GHz
- two periodicity time scales in the long-term light curve

Will be interesting to compare all this with the data from the other wavelengths.

0716 measurements with the Trebur - 1 Meter - Telescope

Johannes M. Ohlert
Astronomie Stiftung Trebur
Trebur, Germany

Where ?

Trebur
Rhein-Main region
Germany

with clouds

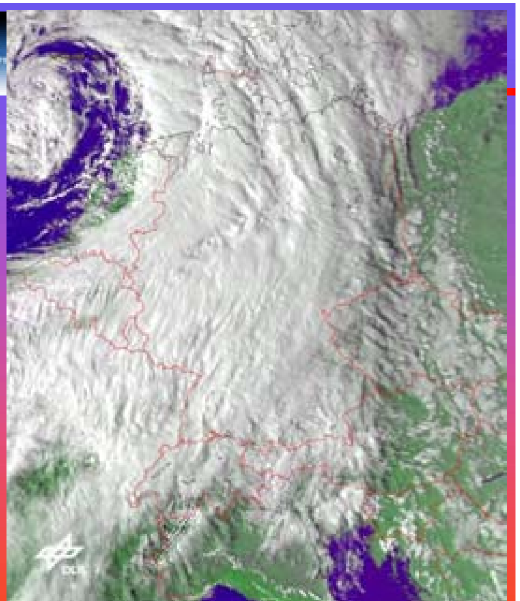

Where ?

Trebur
Rhein-Main region
Germany

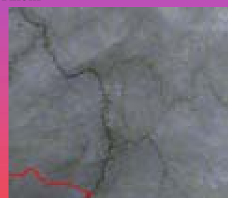

w/o clouds

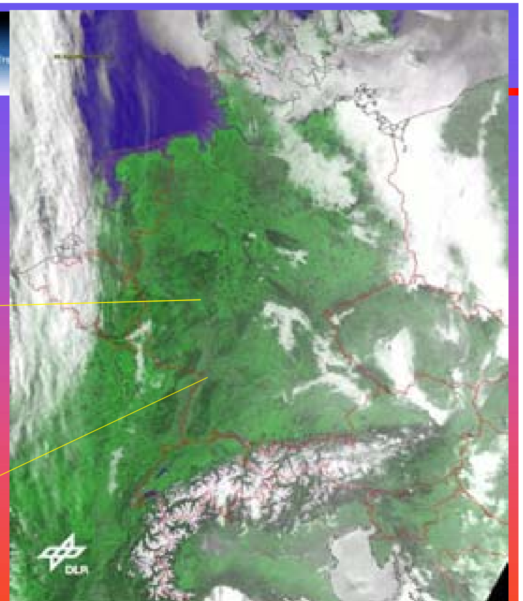

Observatory

Code 239 MPC Lo: 8.4114 E La: 49°55'32" N

Foundation

since July 1997

Astronomie Stiftung Trebur

Michael Adrian Observatorium

Board: 6 members
T1T-team: 8 members

Johannes M. Ohlert   4th ENIGMA meeting in Perugia   Oct. 6-8, 2004

Objectives

* Public relations work

Constitution:

... Information to the public;
... especially to interest young people for Astronomy and Astrophysics;
... to support the new generation of academics.

Johannes M. Ohlert   4th ENIGMA meeting in Perugia   Oct. 6-8, 2004

Lecture hall

* more than 70 seats
* Internet

Johannes M. Ohlert   4th ENIGMA meeting in Perugia   Oct. 6-8, 2004

Public relations work

Guided tour of
our observatory

Objectives

* Scientific work

Constitution:
Aim in view of the foundation is the promotion of science and research in the field of Astronomy and Astrophysics.

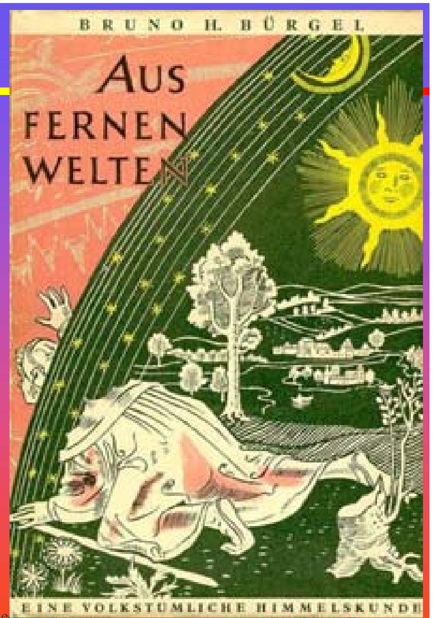

Mai 1997:

T1T
Trebur **1** Meter **T**elescope

one of the biggest telescopes in Europe open to the public for visual observations!

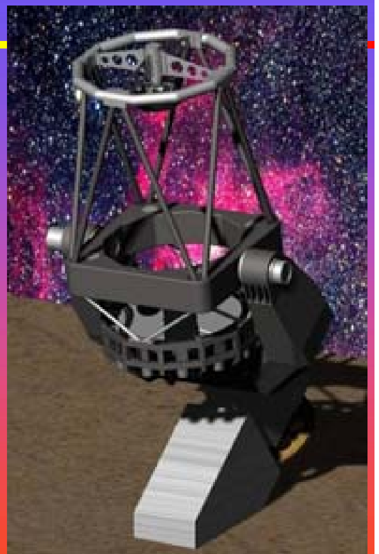

August 1995, Michael Adrian:

"Which telescope should I buy"
"Could You please help me"

?

Construction

shells of
the
unfinished
buildings
1996

peace
negotiations
1996

T1T Trebur 1 Meter Telescope

(the first one)

RA axis and fork

Mirror in its cell

flying T1T
above Trebur

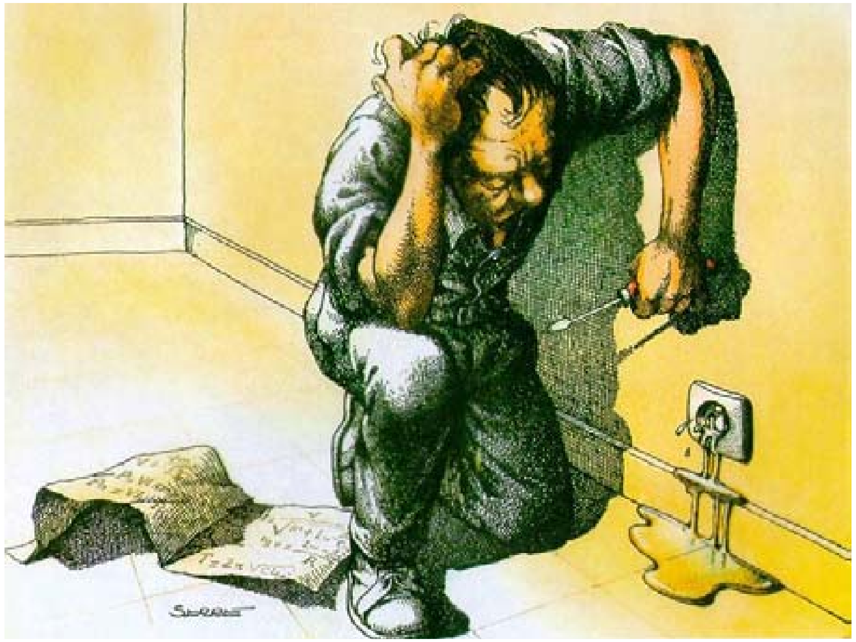

T1T 2nd

Aug. 2004

T1T Trebur 1.2 Meter Telescope

mirror material:	1st Grade Sital
protective coating:	Al-SiO_2-ZrO_2

Geometry:

* primary mirror-∅:	1235±2 mm
* border thickness:	160 mm
* central bore-hole-∅:	340 mm
* primary focus:	3600±5 mm
* sekundary mirror-∅:	430±1.5 mm
* border thickness:	60 mm

Total focal length: 9550±100 mm

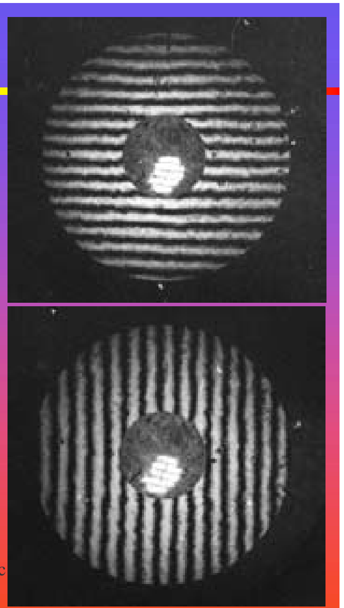

Interferometric measurements

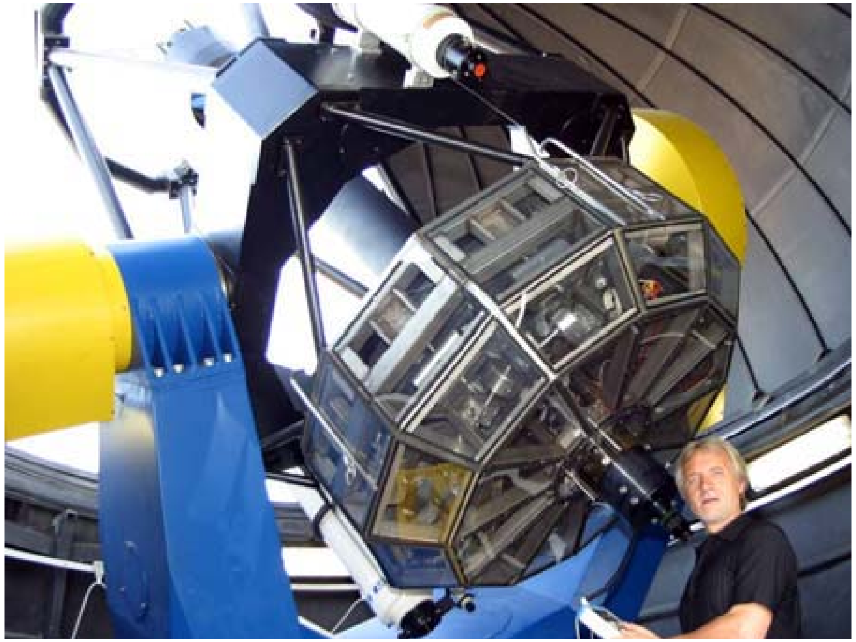

First Light for 1.2m-T1T
Jan. 4./5., 2002

M82

M1

Within the control room for the T1T and CCD

CCD camera

Roper Scientific VersArray 1300 EB

CCD-Chip
1340 x 1300 Pixels
20 x 20 µm²

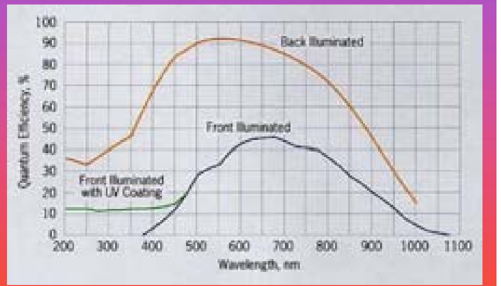

Quantum Efficiency

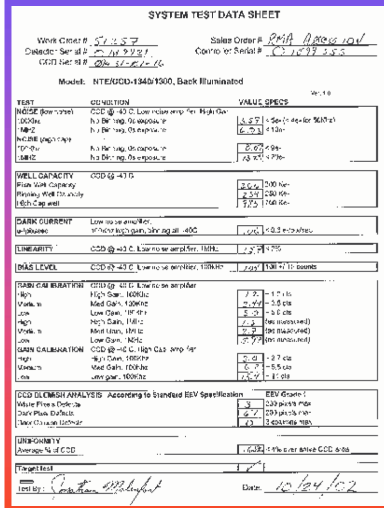

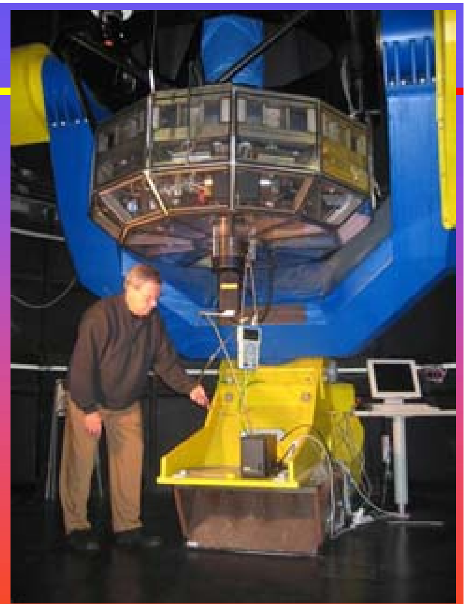

Linearity of CCD

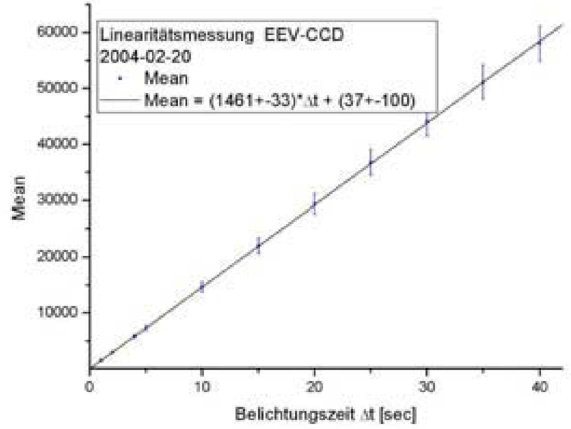

The dreams of Jochen

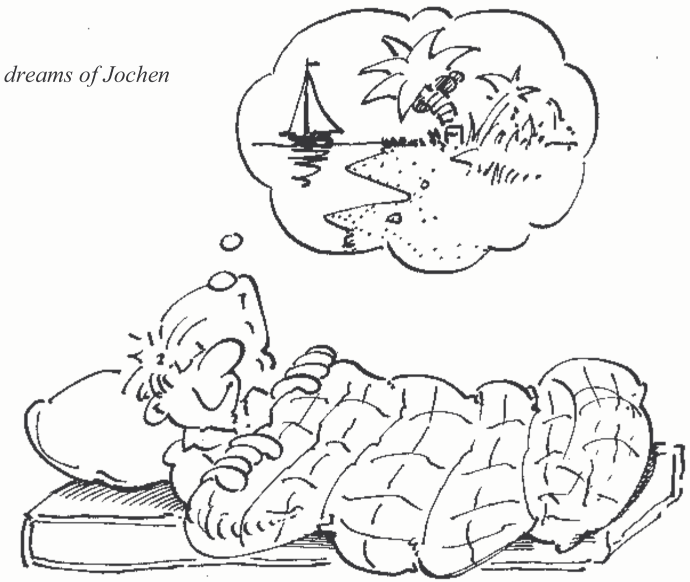

Statistics

Date	Time UT	0716 frames
2003-11-04	18:50 – 22:31	31
05	22:49 – 01:31	20
06	21:40 – 01:50	28
10	18:40 – 19:50	12
13	20:31 – 23:30	30
12-07	18:04 – 01:36	50
08	22:57 – 02:22	31
09	17:56 – 00:28	60
10	19:33 – 20:44	20
2004-01-23	18:46 – 01:08	67
02-20	19:48 – 01:55	41
03-26	22:03 – 03:57	52
27	22:47 – 23:38	16
28	19:35 – 01:41	132
29	19:33 – 01:40	70
30	19:32 – 23:23	56
05-18	22:22 – 23:42	15
Total:	105.4 h	599

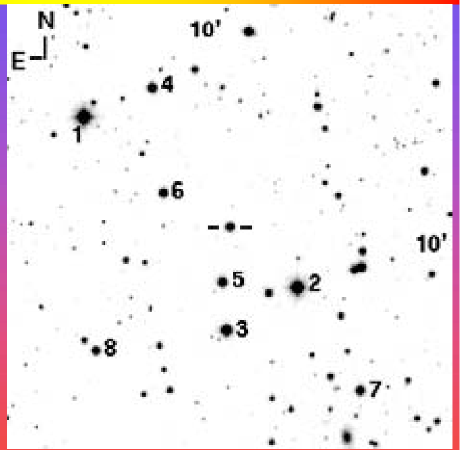

Software

Full-featured scientific image processing application for the Microsoft Windows platform

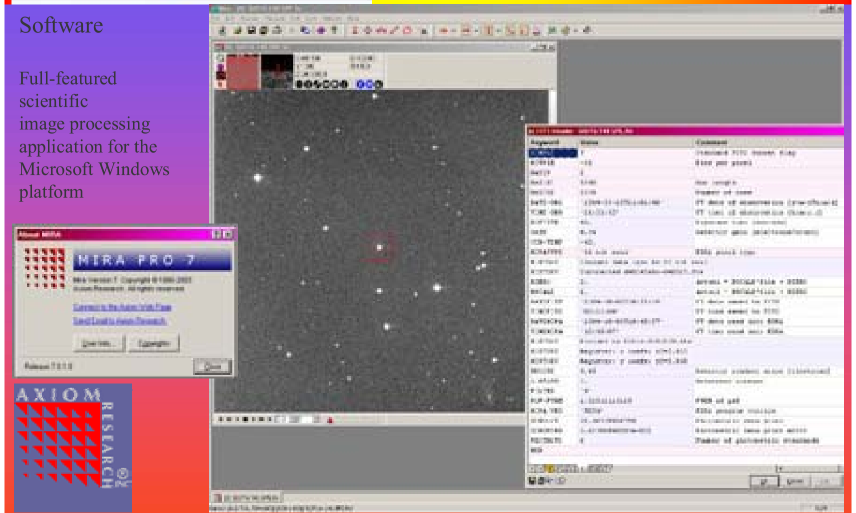

Data analysis

Measuring the FWHM

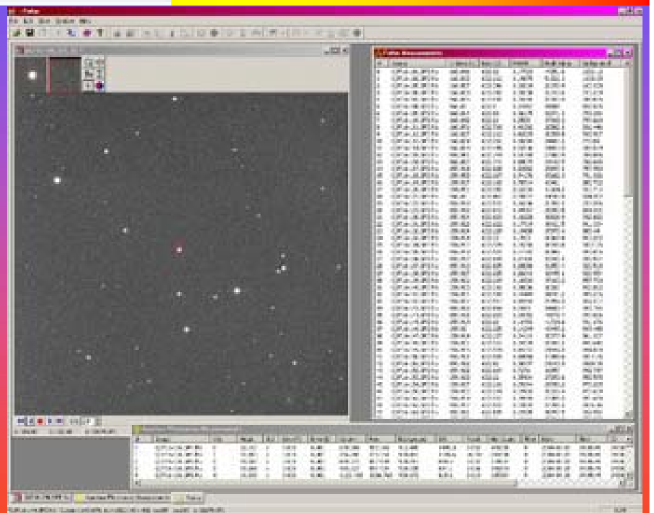

Data analysis

Aperture Photometry:

Entering the effective Radii of the
- Object
- Inner background
- Outer background

measuring aperture

ApRad = 1.5*FWHM/2

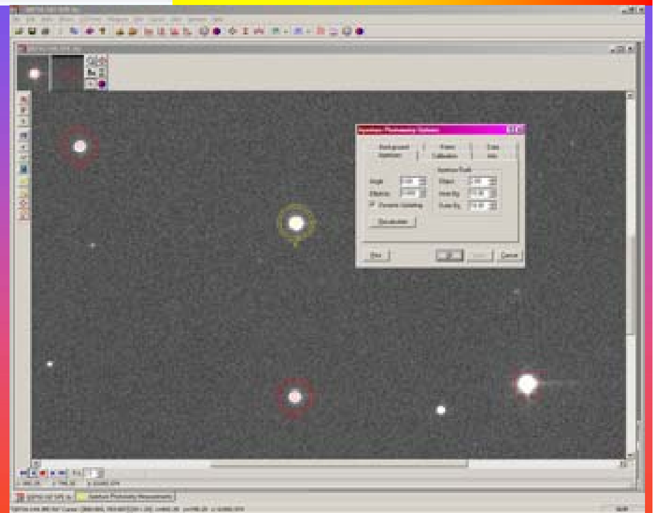

Data analysis

Aperture Photometry:

Zero point calculation
from the marked
standard stars

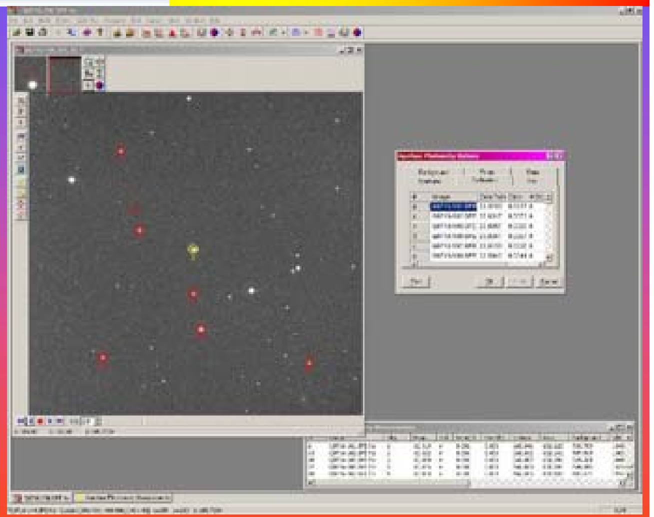

Data analysis

Aperture Photometry:

List of results
sorted by image

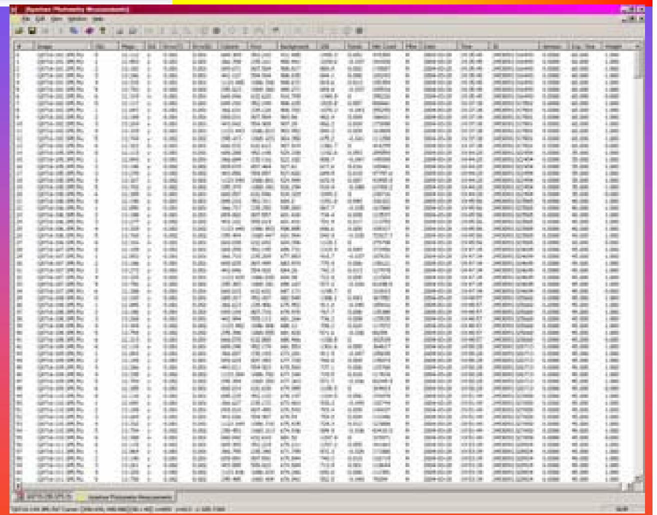

Data analysis

Aperture Photometry:

List of results
sorted into
ascending order by the
Object number column

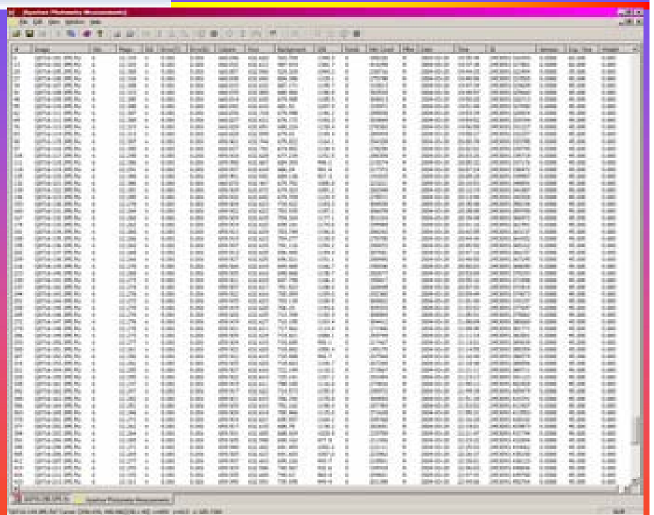

0716+714

Intra day
variability

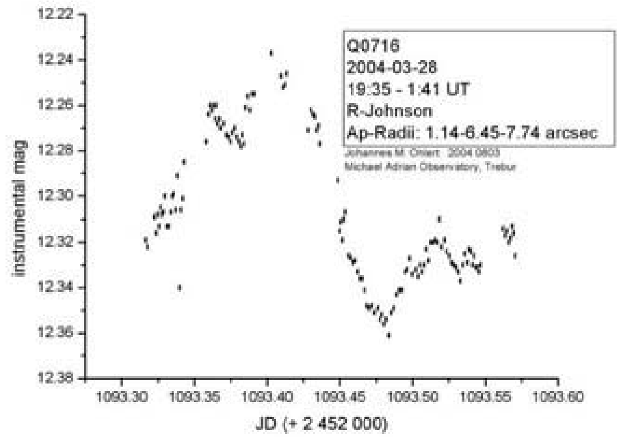

0716+714

Comparison
with 2 of 6
standard stars

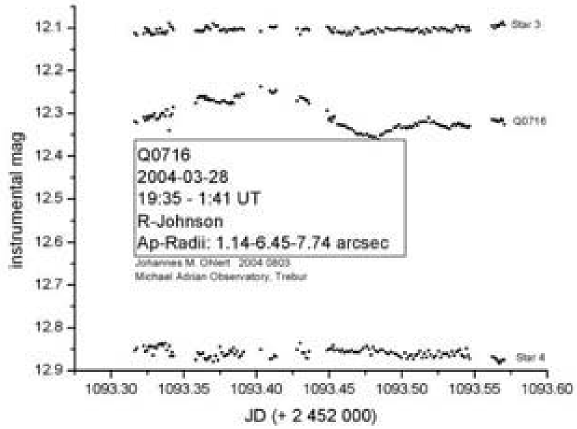

0716+714

Correlation
of the
instrumental mag
with
FWHM

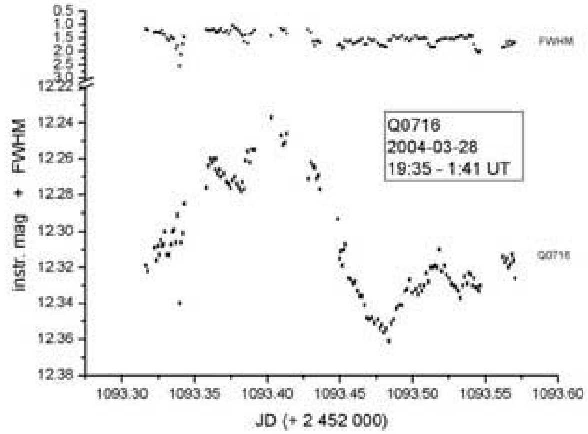

0716+714

Summary
Nov. 2003
→ May 2004

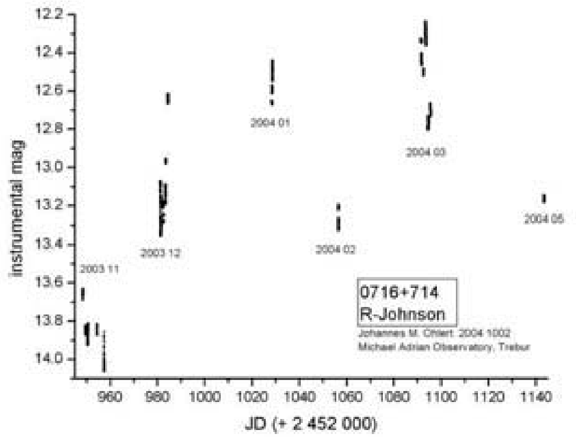

Calculation of the Photometry errors with MIRA

Dear Dr. Ohlert,

Answers to the photometry questions are given below.

1. Regarding photometry errors, they are calculated using the formulae in my paper from Pub Astronomical Society of the Pacific , Vol 103, No.659, January 1991, pp. 122--130. This is called "Signal to Noise Considerations for Sky Subtracted CCD Data" and it has turned out to be something of a seminal paper on the subject---much to my delight. I wrote this when I was on the staff at the University of Arizona. For aperture photometry, the theoretical and empirical error are respectively computed using equations 10 and 11(or 12), converted to magnitude error using the standard relation in equation 13. These values apply to the summed count inside the inner aperture and to the noise and pixels sampled in the annulus between the 2nd and 3rd apertures.

The uncertainty in magnitude is easily calculated from the S/N obtained through equations (7), (11), or (12) using the definition of a magnitude, m, corresponding to an observed count, C, viz., $m = \text{const} - 2.5 \log C$. Differentiating both sides to determine the dependence of a change in m on a change in C and substituting their respective uncertainties, $\sigma(m)$ and $\sigma(C)$, we obtain $\sigma(m) = 1.0857[\sigma(C)/C]$. Since the S/N is the inverse of the relative error in the net object count, we simply make the substitution $S/N = C/\sigma(C)$ and obtain

$$\sigma(m) = 1.0857\,(S/N)^{-1}\,, \qquad (13)$$

If we assume that p is large, then equation (7) can be written in the form

$$S/N = \frac{C_0^{1/2}}{[\ldots]^{1/2}} \qquad (10)$$

Two practical observational cases are illustrated by this form of the equation: the "sky-limited" case in which [illegible]

[illegible] the internal random error of the observation. Replacing the measured background ("sky") variance for the theoretical variance per sky pixel and allowing for spurious scatter [illegible] which leads to

$$S/N = \frac{C_0^{1/2}}{[1 + n\sigma_s^2 C_0^{-1}(1 + \frac{1}{p})]^{1/2}} \qquad (11)$$

$$S/N = \frac{C_0^{1/2}}{[\frac{1}{g} + n\sigma_s^2 C_0^{-1}(1 + \frac{1}{p})]^{1/2}} \qquad (12)$$

for a gain factor of g electrons ADU^{-1}. The assumption of

C_0: total signal for the object

Confidence test

Photometry of an exoplanet transit

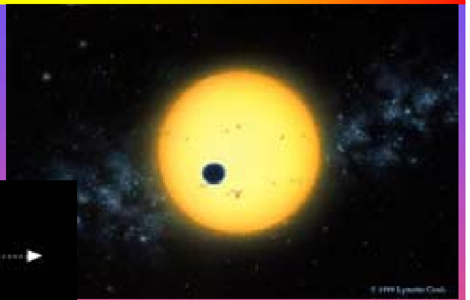

Brightness variability due to a transit

R. Alonso, T. Brown etal 23. Aug. 2004
Trans-Atlantic Exoplanet Survey
TrES-1:
The Transiting Planet of a Bright K0V Star

Parent Star: (0.88 +- 0.07) M_{Sun}
Planet: (0.75 +- 0.07) M_{Jup}
R_{Pl} = 1.08 R_{Jup} R_{Pl}/R_S = 0.130
P = 3.030065 d a = (0.0393 +- 0.0011) AU

TrES-1

1st Transit for T1T

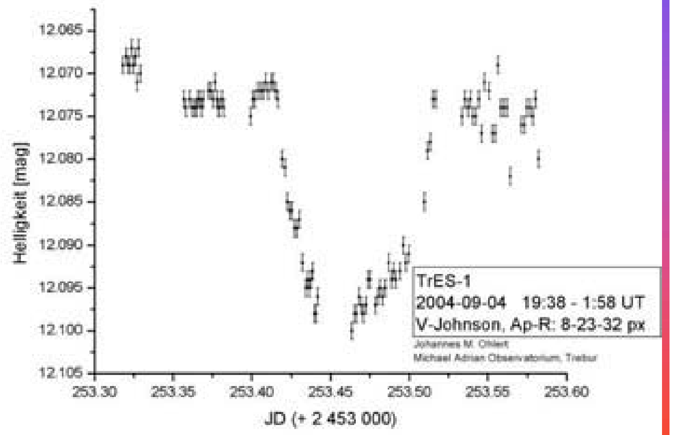

TrES-1

Comparison with GSC brightness

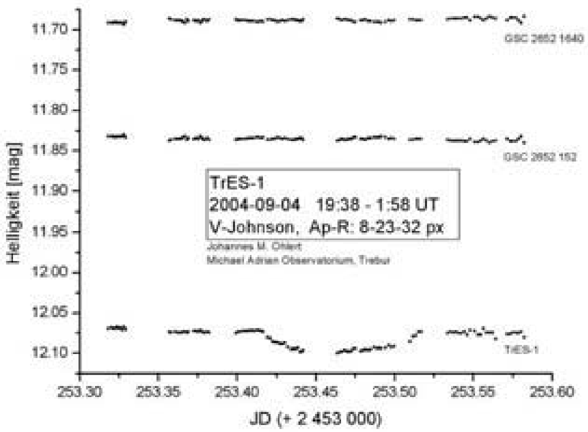

TrES-1

2nd Transit for T1T

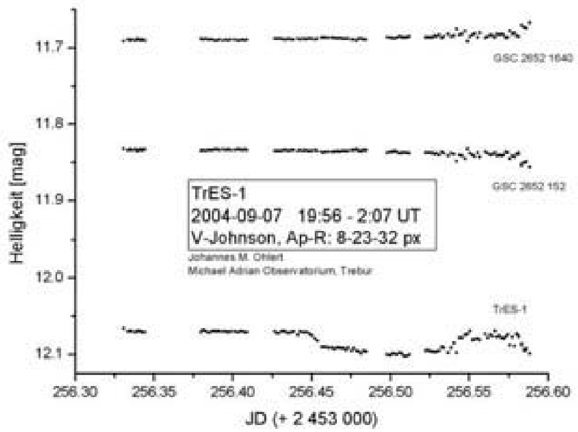

TrES-1

Comparision of
1st and 2nd
T1T-Transit

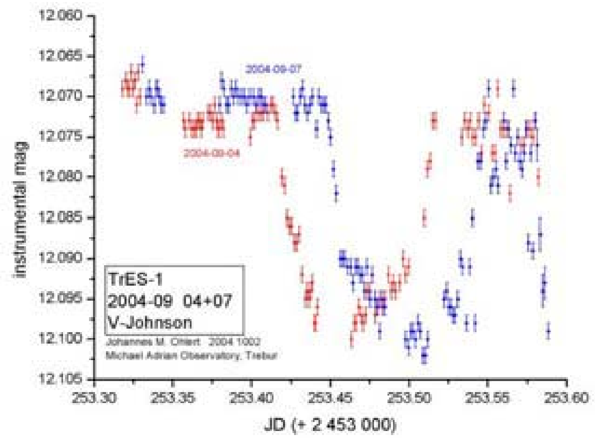

Other Multifrequency Campaigns

The multifrequency WEBT/ENIGMA campaign on AO 0235+16

C.M. Raiteri, M. Villata
for the WEBT and ENIGMA collaborations

BACKGROUND

(Raiteri et al., 2001, A&A 377, 396)

The analysis of the radio light curves from 1975 to 2000 revealed 5 major outbursts, almost equally spaced every 5.7±0.5 yr

The optical light curves are not in contradiction with this quasi-periodicity (radio-optical correlation with very short time delay)

Next outburst was foreseen to peak around February-March 2004

THE CAMPAIGN

The WEBT/ENIGMA campaign covers two observing seasons:

Part I : July 2003-April 2004
Part II: July 2004-April 2005

Main aims:

- confirm the quasi-periodicity (!)
- study both *short-term* and *long-term* multiwavelength variability and correlations

OBSERVATIONS

- Radio+near-IR+optical data from WEBT/ENIGMA → *PI: Raiteri*
- 3 XMM pointings (January 18-19 and August 2, 2004, late January 2005) → *PI: Raiteri*
- Dense radio monitoring with the 100 m antenna in Effelsberg during XMM pointings → *PI: Kadler*
- 15 VLBA epochs (6 already done from January 10 to August 28) → *PI: Wiik*
- Optical spectra from VLT and TNG, NTT → *PI: Raiteri*

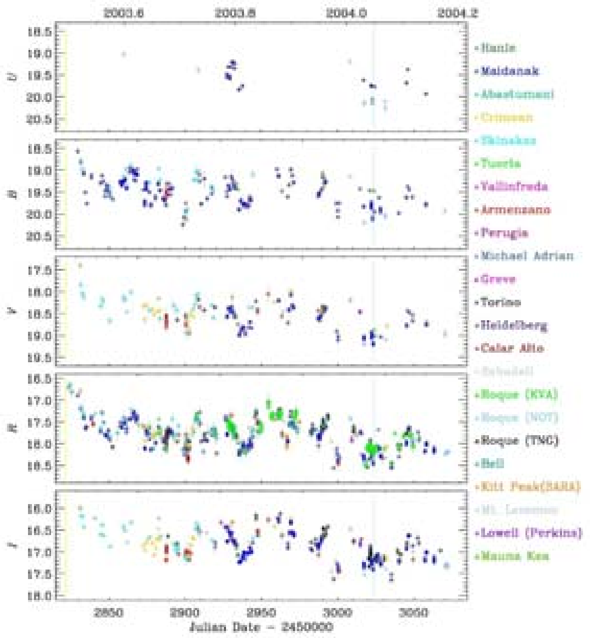

OPTICAL LIGHT CURVES

- 25 optical/IR telescopes from 35 to 358 cm
- 2690 data collected (major contribution from Maidanak team)
- many data discarded or binned

Pronounced variability - but faint state!

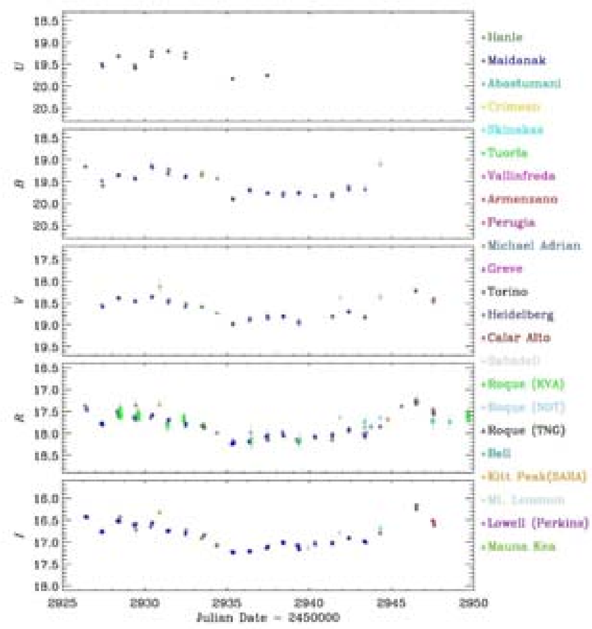

OPTICAL LIGHT CURVES

Variations of more than a mag in a few days

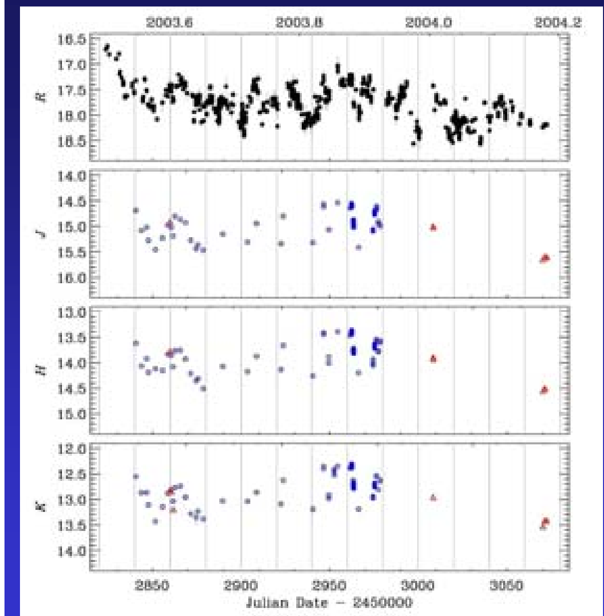

NEAR-IR LIGHT CURVES

Near-IR data were taken at Campo Imperatore (1.1 m) and at the NOT (2.56 m)

Close correlation with optical data

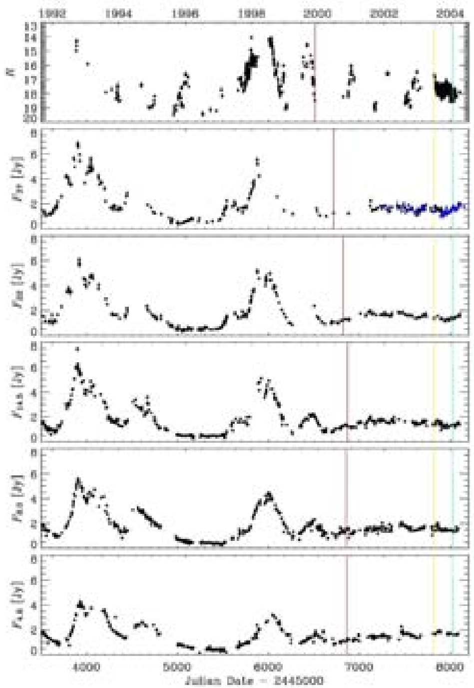

RADIO LIGHT CURVES

The last big radio-optical outburst occurred from late 1997 to late 1998

The radio state is low and quiescent since early 2000!

OPTICAL SPECTRA

A nice 900 sec VLT spectrum taken by Jochen on August 28, 2003

OPTICAL IMAGING

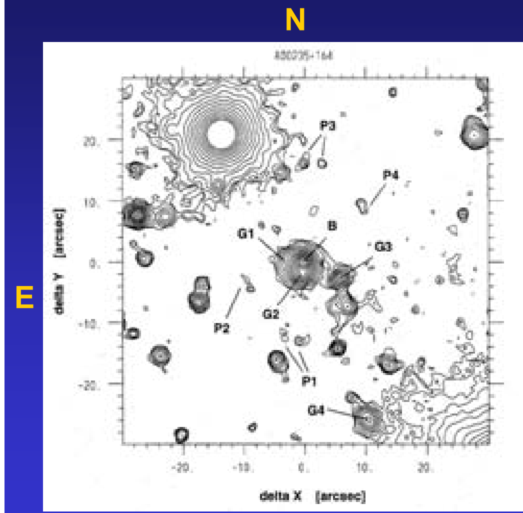

Nilsson et al. 1996, A&A 314, 754

R-band image at WHT showing the sorroundings of AO 0235+16

B is AO 0235+16

G1-G4 belong to the z=0.524 system

G1 is presumably the absorber (and possibly the microlensing galaxy)

XMM pointing of January 18-19: X-ray data

Exposure time: 30 ksec

EPIC pn, MOS1 and MOS2 analyzed together

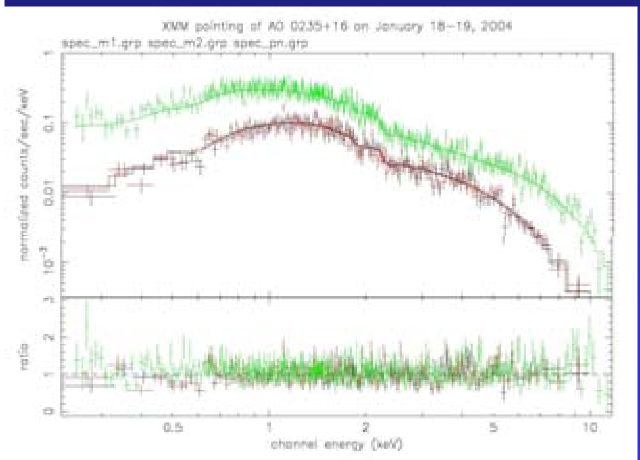

Model:

power law + galactic absorption + free absorption by the z=0.524 foreground galaxy

Results:

α=0.65±0.03

F(1 KeV)=0.31 μJy

No variability!

XMM pointing of January 18-19: optical-UV data

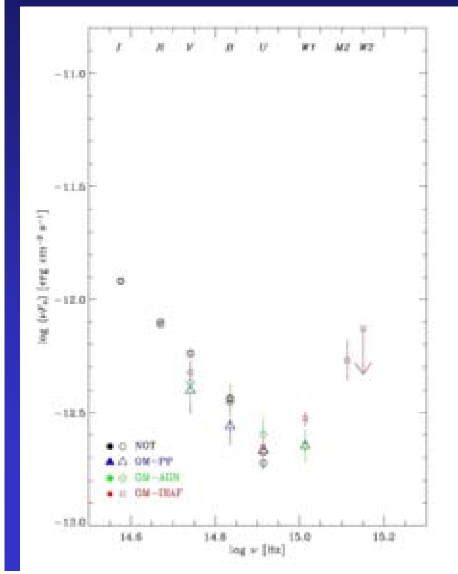

Correction for galactic extinction:

UBVRI → NED

W1, M2, W2 →

Cardelli et al. (1989) with E(*B-V*)=0.079 and R_V=3.1

Very steep optical spectrum ($\alpha \approx 3.3$) !

BUT: what about the *z*=0.524 absorber?

EXTINCTION

Extinction laws are known only for the Milky Way, the LMC, and the SMC: what is the best for the z=0.524 absorber?

Junkkarinen et al. (2004, astro-ph/0407281):

Analysis of an HST/STIS spectrum → graphite absorption at z=0.524 → Cardelli et al. (1989) gives the best fit for both galactic and foreground galaxy extinction

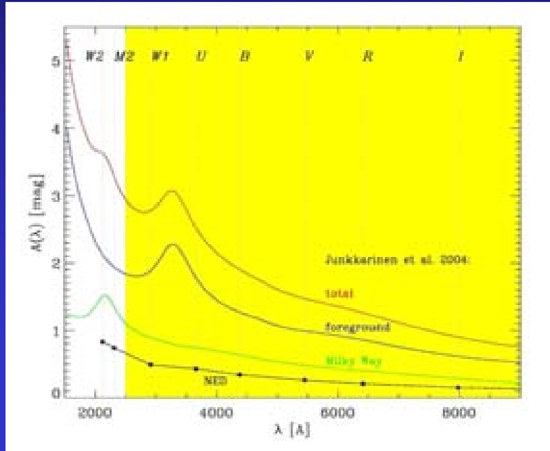

XMM pointing of January 18-19: optical-UV data

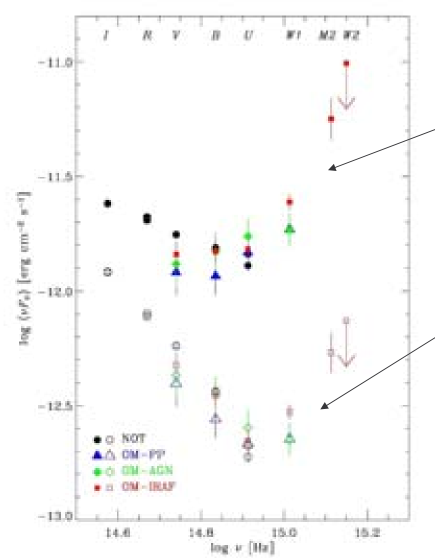

Extinction by both the Galaxy and the z=0.524 absorber according to Junkkarinen et al. (2004)

Galactic extinction only according to NED

Even if we neglect the uncertain *M2* datum, the UV rise is evident!

XMM pointing of August 2: X-ray data

Exposure time: 10 ksec

EPIC pn, MOS1 and MOS2 analyzed together

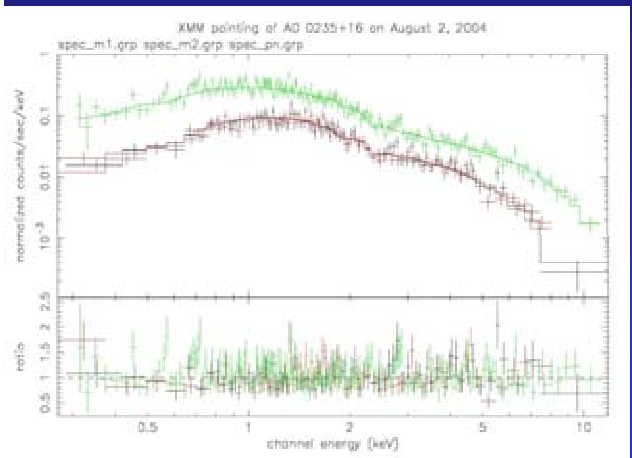

Model:

power law + galactic absorption + free absorption by the z=0.524 foreground galaxy

Results:

α=0.55±0.04

F(1 KeV)=0.26 μJy

No variability!

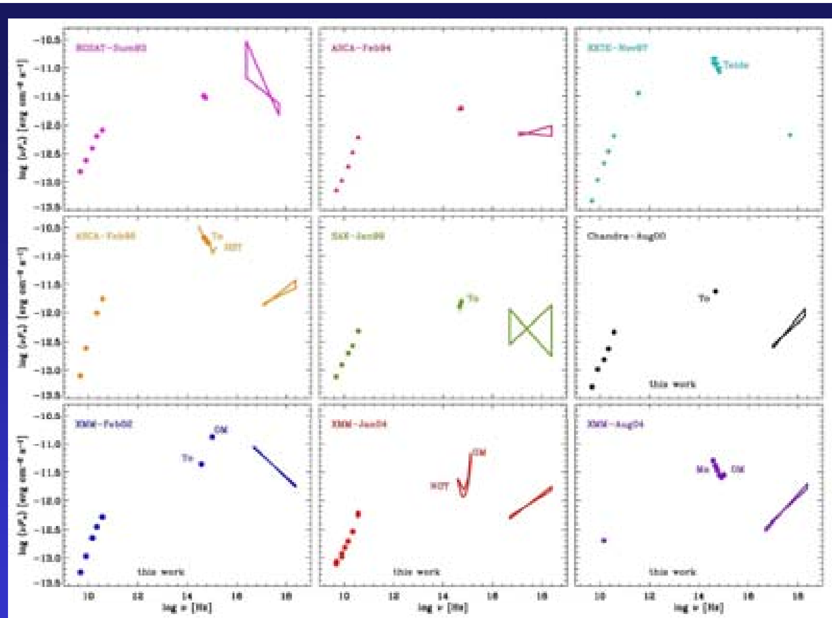

A bump in the far-UV cannot be avoided!

SUMMARY

- RADIO: faint and “quiescent” state
- OPTICAL/IR: faint state characterized by noticeable variability, with changes of more than a mag in a few days
- X-RAYS: both XMM pointings detected a faint state with hard spectra and no variability
- UV: the OM data show a UV rise in the SED suggesting a far-UV bump – if real, where does it come from?
- Still no sign of the predicted outburst…

We have 6 months and 1 XMM pointing left…

The multifrequency WEBT/ENIGMA campaign on 3C 66A

July 2003 - March 2004

Markus Böttcher – Ohio University
Claudia M. Raiteri, Massimo Villata
for the WEBT/ENIGMA collaboration

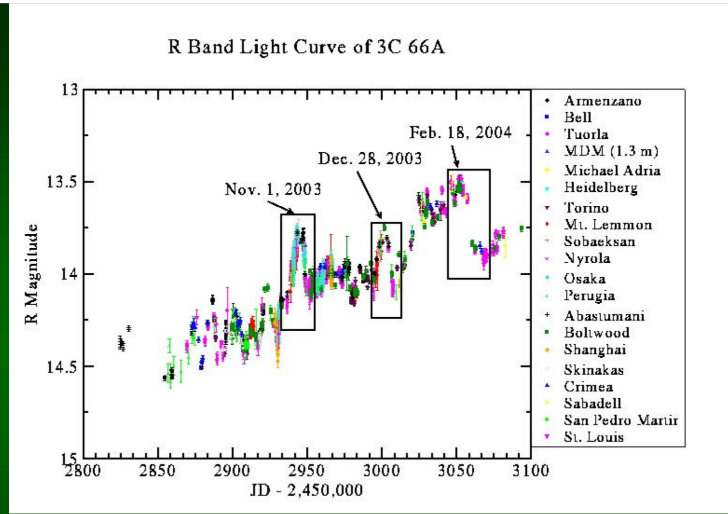

- Increasing trend; maximum brightness in February
- 2 pronounced flares with a ~ week timescale
- Moderate IDV

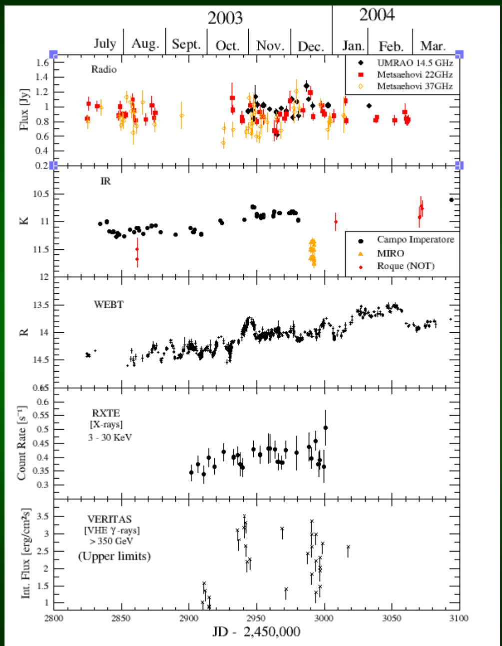

No correlation between radio and optical variations

RXTE data analysis complicated by 3C 66B best fit: $\alpha \approx 1.45$

Marginal det. (2.5 σ excess) by STACEE; no det. by Whipple/VERITAS

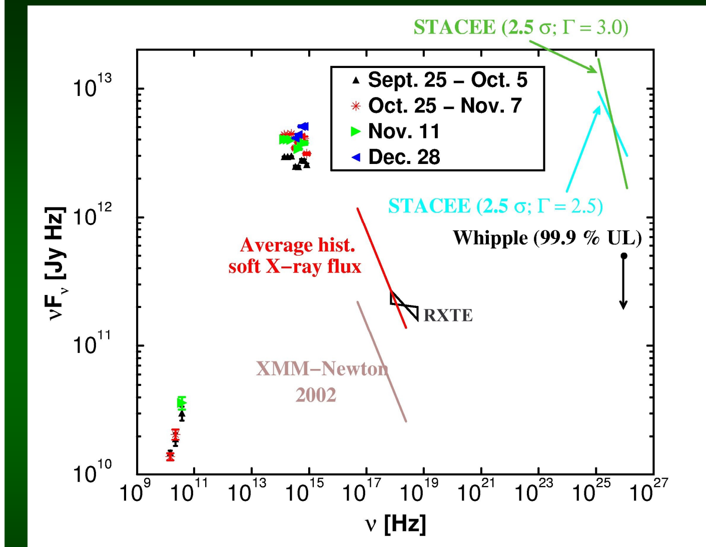

VLBA radio monitoring: 4 epochs done.
One (out of 6) jet component has SM of 11± 4.7 h^{-1} c

Stefano Ciprini

Tuorla Astronomical Observatory
University of Turku - Piikkiö, Finland

The ENIGMA Web Archive

IV ENIGMA Meeting
October 6-8, 2004 - Perugia, Italy

ENIGMA Archive: Criteria and Constraints

❑ **Primary function:** to make data of the ENIGMA multiwavelength observing campaigns and data collected by each team of the ENIGMA collaboration available within the collaboration.

❑ **Quick and easy access** through the web to data using any web browser.

❑ **Simple, simple, simple…** (simple means that it probably works; simpler means faster; simple means less errors and less time spent by users and constructors/maintainers…).

❑ **Avoid duplication:** (general Internet ethic rule to avoid useless duplication of information, errors, confusion, contradictions, obsolescence, exponential increasing of the web pages…). Huge public archives with AGN data existing yet: NED, CDS, HEASARC, IPAC…).

❑ **Manpower:** 1 person, 5-10% of his working time...

ENIGMA Archive: Approach and Layout

❑ **Html web pages:** easier consulting and more friendly with respect to mere FTP/SSH folders containing data.

❑ **Data:** simple ASCII text files, or direct links to other already existing web pages with data.

❑ **Format:** original sender-made format (no modification between the data producer/sender and the files of the archive).

❑ **Recommendations:**
- already reduced and "ready to do science" final data (e.g. flux densities)
- a short info-header (legends, units, instrument/detector, comments, references, Galactic extinction values, calibrations adopted, column densities, etc…).
- optional additional txt files with instructions to handle the data (e.g. magnitude/counts --> flux conversion, etc.).

The Archive Access Page

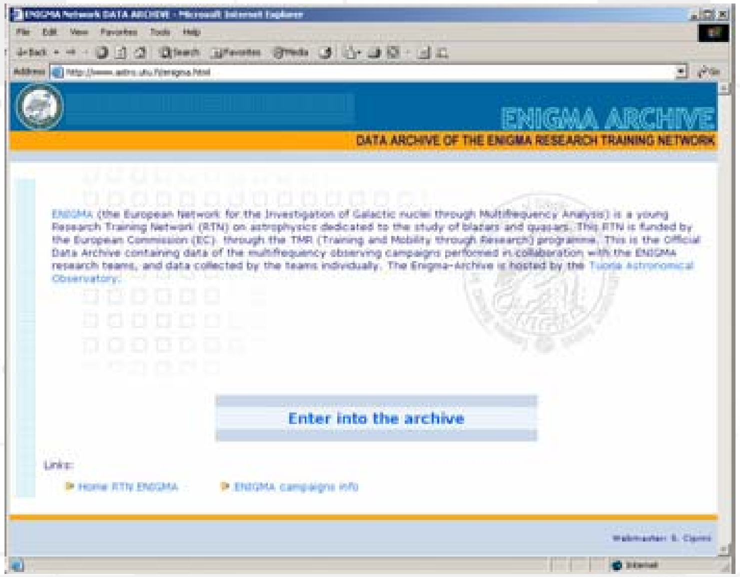

The Archive Homepage

The Archive Internal Pages

Example of a campaign/data internal page

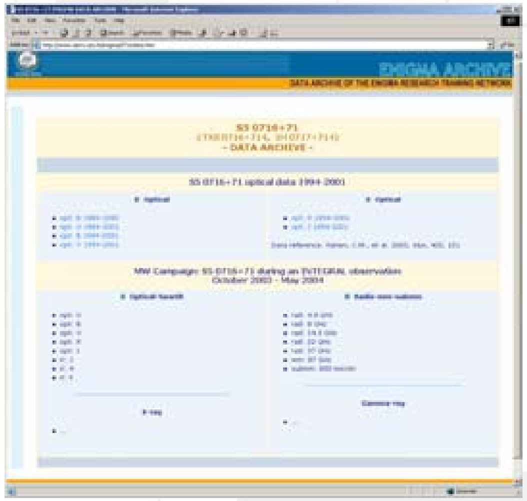

Example of a data file

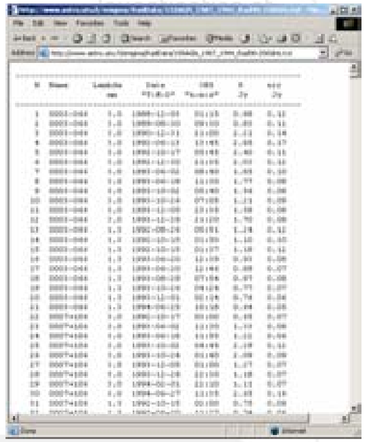

Archive Web Pages Structure

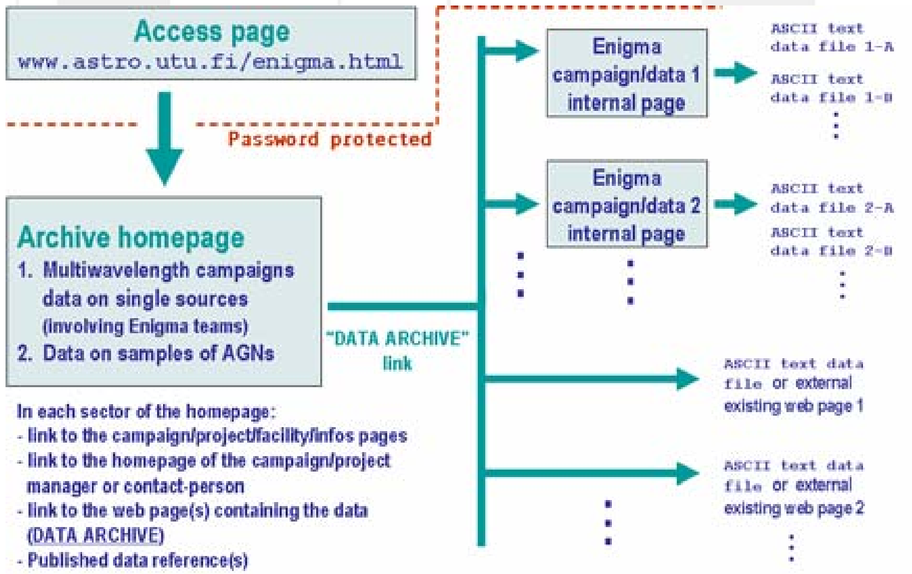

Current Data Content

The archive is online with already some data:

❑ **Data of single sources:**
0716+714: optical data 1989-2001 (published)
OJ 287: radio-optical data 1993-1997 (published, OJ94 project)

❑ **Data of source samples:**
85 AGN: Metsähovi radio data 1980-1995 (published)
155 AGN: SEST radio-mm data (1987-1994) (published)
157 AGN: BeppoSAX X-ray data (published)
Tuorla-Torino optical data 1994-1997 (published)

❑ **High energies (X-rays, gamma-rays):**
No data from any ENIGMA team yet.
(Please send data, this would be not only a radio-optical database).

Conclusion

❑ Archive primary function: to make the data (reduced, "ready-to-analyze" data) of the ENIGMA multiwavelength observing campaigns soon available.

❑ Despite of already existing databases (NED, CDS…), also published data could be useful in this archive (applying the minimal duplication principle).

❑ Extremely reduced manpower and time imply a very simple archive:
1. web based (quick and easy access, any interaction, pure html only);
2. data as ascii table files, provided directly by the data producer.

❑ Data (reduced, "ready-to-analyze" data only) and comments (constructive) are welcome. Help is welcome too.

❑ Procedures and use of the data, publication policy, ownership, relations with other collaborations/organizations (e.g. WEBT, EVN, GTN,…), need to be defined by the ENIGMA team leaders.

Radio and Optical Observations

2QZJ215454.3-305654: a radio-quiet BL Lac object or lineless QSO?

D. Londish[1,2], J. Heidt[3], B.J. Boyle[4,2], S.M. Croom[2], L. Kedziora-Chudzer[4,1]

1 University of Sydney

2 Anglo-Australian Observatory

3 Landessternwarte Heidelberg

4 Australia Telescope National Facility

MNRAS, 2004

2QZ BL Lac sample

45 BL Lac object candidates extracted from the 2dF QSO redshift survey (Londish et al. 2002) – now 52 objects by inclusion of 6dF

- 52 objects showing featureless spectra (2dF/6dF)
- No proper motion from sky survey plates (baseline 11 y), no thermal SED from SDSS-data => removal of (most) WD
- $< z > = 1.1$ predicted (QSO evolution model, Boyle 2000)
- High S/N spectra of a few candidates have shown redshifts between z = 0.3-1.7
- first optically selected sample, unbiased with respect to radio/X-ray properties

2dF spectrum of 2QZ...

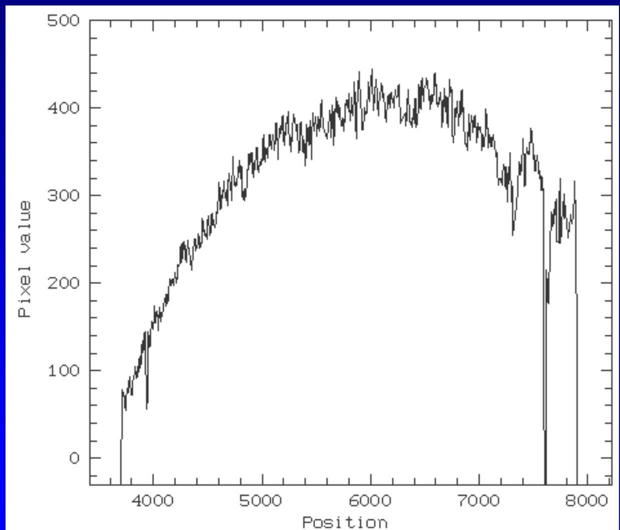

featureless...but not so good S/N

Properties (I)

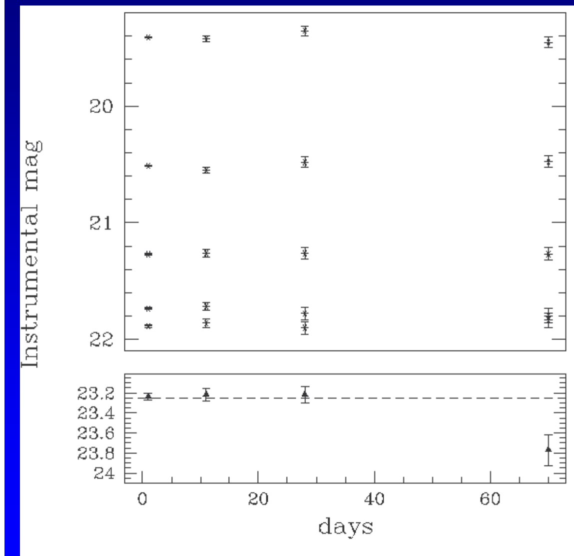

Variable: 0.5mag in 1 month

No optical polarization detected (0.5±0.2 %)

Properties (II)

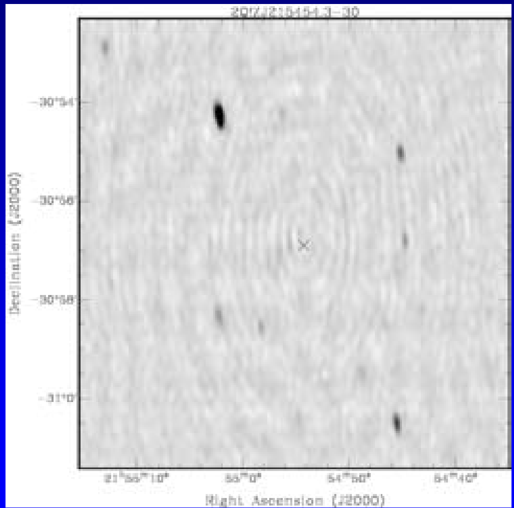

ATCA-image of 2QZ... at 1.4 GHz

No radio detection with Australia Telescope Compact Array at 1.4 GHz

➔3σ limit: 135 μJy

No radio detection with VLA (BnA conf) at 8 GHz

➔3σ limit: 300 μJy

No detection in NVSS and RASS

Need help from the VLT

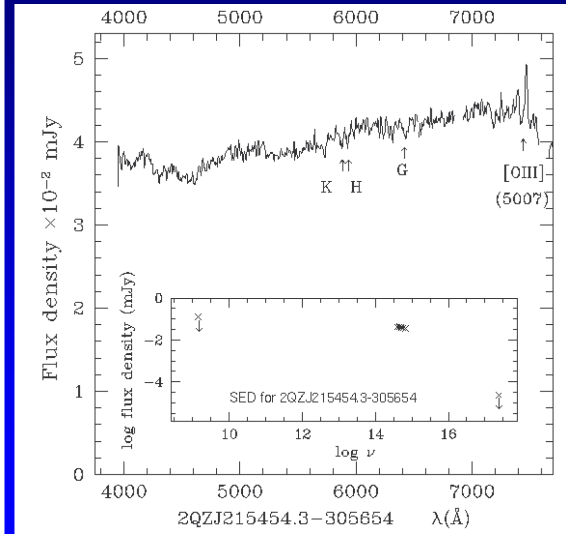

z = 0.495 from stellar absorption (Ca K+H, g-band) and weak [O III] in emission. Possibly also Hβ.

Optical spectral index (4500-7500Å) = -0.36 ($f_\nu \propto \nu^{-\alpha}$) typical for blue AGN (QSO)

Ca break contrast = 0.02

$$Br_{4000} = \frac{f^+ - f^-}{f^+}$$

➔ dominated by strong nonstellar continuum

Composition of the spectrum of 2QZ...

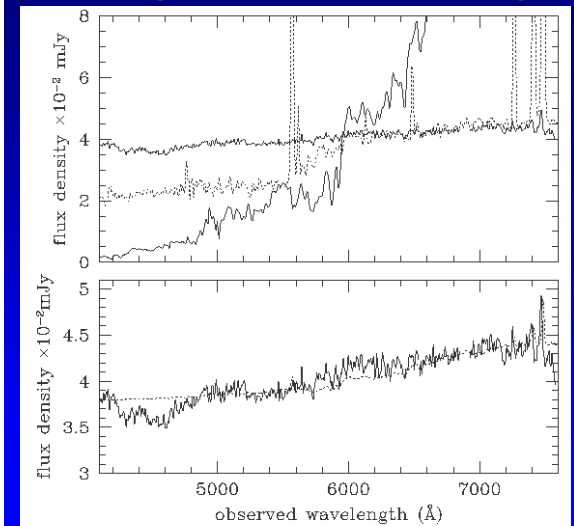

Decomposition of spectrum of 2QZ... in contribution of elliptical galaxy, starburst (from Kinney-Calzetti) + flat spectrum power law. Best ratio is:

0.015:0.045:0.94 (SB, Ell, power law) normalized at 5960 Å

➔ Nonstellar continuum dominates

Decomposition of the image of 2QZ...

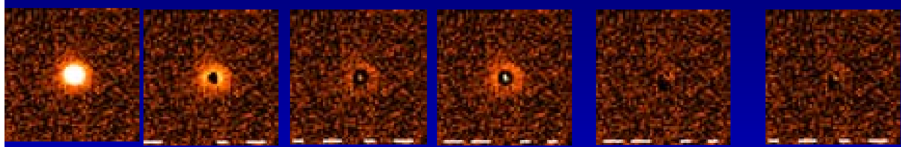

I-image - AGN - Ell. -Disk - AGN+Ell. - AGN+Disk

Fit	χ^2	m_{core} [mag]	M_{core} [mag]	m_{gal} [mag]	M_{gal} [mag]	r_e [arcsec]	r_e [kpc]	ϵ	PA [deg]
AGN	7.21	18.83	-24.06						
Ell.	2.39			18.59	-24.75	0.13	1.0	0.22	175
Disk	3.68			18.71	-24.43	0.18	1.4	0.27	171
Ell.+AGN	1.25	19.29	-23.60	19.08	-24.26	0.73	5.9	0.27	179
Disk+AGN	1.22	19.07	-23.83	19.56	-23.58	0.83	6.7	0.24	179

➔Best fit: AGN + galaxy. However, relative contribution differs from the one obtained from spectroscopy (even when correcting for slit losses). Reason unclear, ev. short integration time for image (30 sec).

2QZ...: what type of object?

- neither elliptical galaxy, nor combination of elliptical and starburst galaxy (can not reproduce the strong blue continuum)
- no type I QSO: lack of strong emission lines
- type II dust absorbed AGN unlikely: spectrum is too blue
- radio-quiet BL Lac dominated by optical synchrotron emission (object displays many features typical for a BL Lac) ?
- high-z version of narrow-line Sy I or high-z Sy II?

Radio-optical spectral index α_{ro}

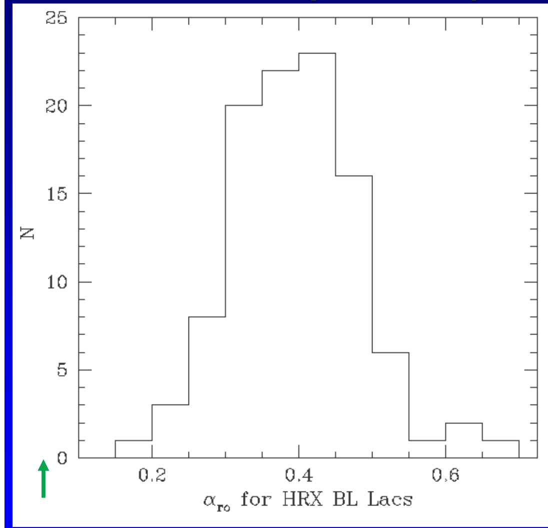

HRX BL Lacs from Beckmann et al. 2002

Using ATCA and VLT-data (separated by 6 weeks) one gets $\alpha_{ro} < 0.047$ or $\alpha_{ro} < 0.082$ depending on I-mag from fit used.

Comparison to the radio-weakest BL Lacs shows 2QZ.. to be even more extreme.

➔ Not a typical BL Lac but probably a member of a hitherto unrecognized population of radio-quiet continuum objects

Alternatives?

Narrow-line Sy I unlikely: [O III]/Hβ < 3 ➔ not observed

High-z Sy II: Maybe, objects with similar optical spectra have been found in deep x-ray fields (e.g. Chandra deep field) but they are normally dominated by stellar light

Possible explanations include:

- instability patterns in accretion disk (rather than dust obscuration) result in the lack of broad-line region in spectra
- very high accretion rate on central engine resulting in a strong UV-peaked continuum

➔➔ Key: X-ray observations (XMM-Newton/Chandra) to resolve puzzle!!!

Stefano Ciprini
Tuorla Astronomical Observatory
University of Turku - Piikkiö, Finland
S. Ciprini, L.O. Takalo, G. Tosti, C. M. Raiteri, M. Villata, A. Sillampaa

Optical behaviour of the blazar PKS 0735+178 from a ten-years observing monitoring

IV ENIGMA Meeting
October 6-8, 2004 - Perugia, Italy

PKS 0735+178 Characteristics

• PKS 0735+178 (z>0.424, Parkes radio catalog, other most used names: S3 0735+17, OI 158, DA 237, PG 0735+17, RGB J0738+177, VRO 17.07.02, 3EG J0737+1721) was classified as a classical BL Lac object by Carswell et al. (1974).

• Both radio (Kuhr et al. 1981) and X-ray selected (Elvis et al. 1992), it was detected as a gamma-ray source by EGRET (Nolan et al. 1996).

•Einstein, ROSAT, ASCA X-ray detection (early suggested to be inverse Compton emission operating in VLBI blobs, Madejski & Schwartz 1988).

• Optical-IR intraday variable blazar (Massaro et al. 1995; Heidt & Wagner 1996; Bai et al. 1998).

• Optical polarization: 1-30% (Valtaoja et al. 1993, Tommasi et al. 2001).

PKS 0735+178 characteristics

• Optical recurrent/periodic timescales claimed: 1.2, 4.8 years (Smith et al. 1987, Webb et al. 1988, Smith & Nair 1995); 14.2, 28.7 years (Fan et al. 1997), 8.6, 13.8, 19.8, 37.8 years (Qian & Tao 2004)… … low confidence.

• One of the most bent radio jet on the mas scale (Gabuzda et al. 1994).

• Several VLBI moving components (Kellermann et al. 1998, Gomez et al. 1999, Gomez et al. 2001, Homan et al. 2002).

• Early multifrequency radio measurements: very flat radio spectrum (superposition of incoherent synchrotron radiation from distinct components) → "cosmic conspiracy" prototype (Marscher 1980, Cotton 1980, Baath et al. 1991).

PKS 0735+178 characteristics

• Multi-epoch VLBI images: twisted jet with two sharp apparent bends of 90° within the inner 2 mas from the core, (a helix in projection): → jet precession, pressure gradients in the external medium (Gòmez et al. 2001), or plasma jet traveling inside a slowly moving curved funnel (Agudo et al. 2002).

• A large outburst observed in the radio bands during 1988-1994 (Aller et al. 1999, Terasranta et al. 2004).

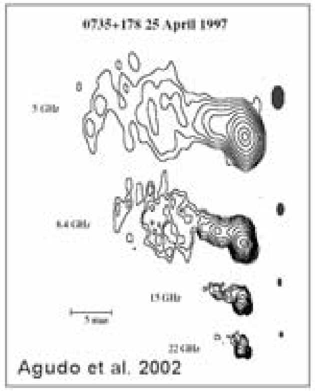

Fig. 1. 5, 8.4, 15 and 22 GHz (from top to bottom) VLBA images of 0735+178 in 25 April 1997. Contour levels increment by factor of 2 (plus 90 per cent contour). From top to bottom images, levels start at: 0.25%, 0.125%, 0.5% and 1% of the peak intensity of 0.684, 0.487, 0.445 and 0.321 Jy/beam. In the same order, convolving beams (shown as filled ellipses) are 2.55×1.38, 1.44×0.79, 0.85×0.48 and 0.58×0.32 mas, at position angles of 1.8°, 0.6°, -0.3° and -3.0° respectively.

PKS 0735+178 Characteristics

• Unusual radio morphology also described in Kellermann et al. (1998), Gòmez et al. (1999), Homan et al. (2002), Rector & Stocke (2003).

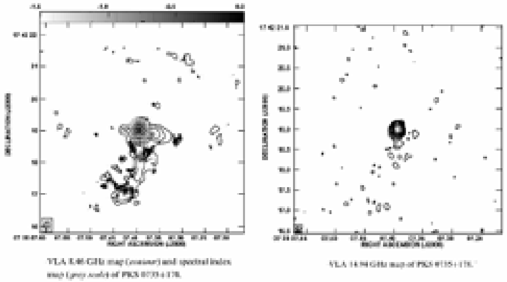

VLA 8.46 GHz map (contour) and spectral index map (grey scale) of PKS 0735+178. VLA 14.94 GHz map of PKS 0735+178.

PKS 0735+178: This object has a intervening absorption system at $z = 0.424$ (Carswell et al. 1974; Rector & Stocke 2001). The 8.46 GHz and spectral index maps are overlaid in Figure 1. The 14.94 GHz map is shown in Figure 2. The 8.46 GHz map shows an unusual jetlike morphology to the south and west. The spectral index map confirms that PKS 0735+178 consists of a flat-spectrum core ($\alpha^{8.46}_{14.94} = -0.24$) and steep-spectrum ($\alpha^{8.46}_{14.94} \lesssim -1$) jets, not multiple images of the core.

Rector & Stocke 2003

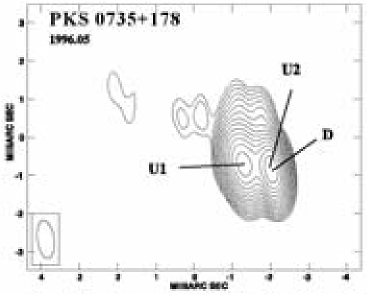

FIG. 9.—Total intensity image of J0738+17 at 15 GHz, epoch 1996.05. We see most of the flux in an east-west core jet, plus a faint parallel "bar" of emission, about 1.5 mas north of the main structure. This unusual morphology is also seen by Kellermann et al. (1998) and Gomez et al. (1999). Our fitting process yields one reliable jet component, U1 (K1), at $R \simeq 0.8$ mas and $\theta \simeq 80°$ (see Fig. 9), that is consistently fitted over all epochs at 15 GHz but only at the first two epochs at 22 GHz, probably because of the lack of sensitivity at the higher frequency. Gomez et al. (1999) propose that this component marks a bend in the jet. However, we find no evidence of anything other than the unaccelerated, essentially radial motion reported in Table 3 and Figure 10

Homan et al. 2001

PKS 0735+178 Characteristics

• Optical absorption line due to an intervening system identified with Mg II gives z>0.424. Imaging was presented by Bregman et al. (1981) Hutchings et al. (1988), Stickel et al. (1993), Scarpa et al. (2000), Falomo & Ulrich (2000), Pursimo et al. (2002) and other, but the host galaxy remain unresolved. On the other hand the companion galaxies are well resolved. The nearby environment has been shown by Pursimo et al. (1999).

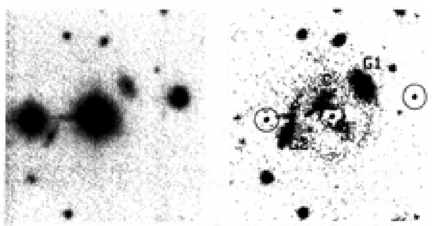

Figure 2. 35″ field around PKS 0735+178. Galaxies G1 and G2 are clearly visible in the original image (left). The circle around the object corresponds 15 kpc of a projected distance (z=0.424). Feature C is a faint companion and A is an artifact. The nearby stars, 1.1 and 2.7 magnitudes fainter than PKS 0735+178, have been subtracted perfectly.

Pursimo et al. 1999

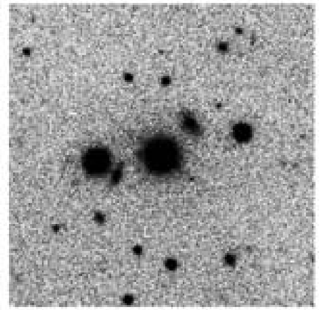

Fig. 4. The BL Lac object PKS 0735+17 (brightest object in the center) imaged by NTT+SUSI (R filter). The two bright objects at both sides of 0735+17 are stars. Field shown is 52 arcsec and North-East is at the top-left side.

Falomo & Ulrich 2000

PKS 0735+178: long-term data

• Historical flux light curve data:
- Optical: about 100 years (Qian & Tao 2004, Ciprini et al. in prep.).
- near-IR: about 20 years (Lin & Fan 1998, Fan & Lin 1999).
- radio-mm: 1980-2004 data (Metsähovi, good sampling), 1977-2004 data (University of Michigan UMRAO), 1987-1995 (SEST data).
- recent BVRI optical data (10 years): BVRI by Perugia, Torino, Tuorla.

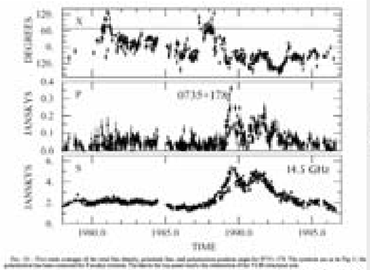

Aller et al. 1999

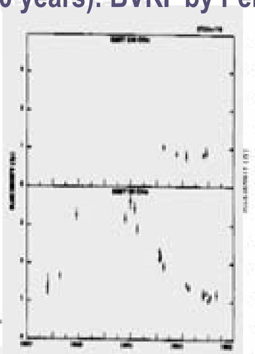

Tornikoski et al. 1996

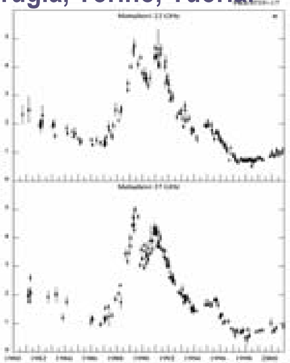

Teräsranta et al. 2004

PKS 0735+178: long-term data

• Optical data available since 1905 (~ 100 years data).
• Last 30-years data (1970-2004) show a well sampled B-light curve → sufficient level of confidence in the statistical analysis results.

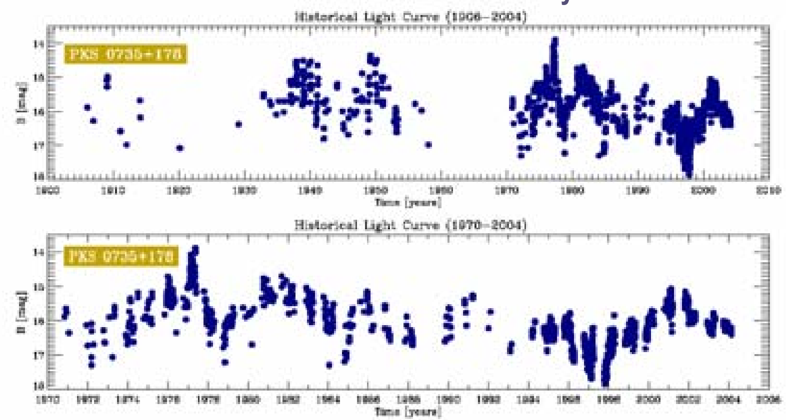

Fig. 3. The historical light curve of PKS 0735+178 in B band reconstructed from literature (data mainly from Qian & Tao 2004) and with our original B and R data added (magnitudes derived using mean colour index $B - R = 0.993$ for data sets homogeneity Fan et al. 1997; Qian & Tao 2004). The time series so obtained is composed of 1725 data

PKS 0735+178: long-term data

- Long-term trend of the light curve.

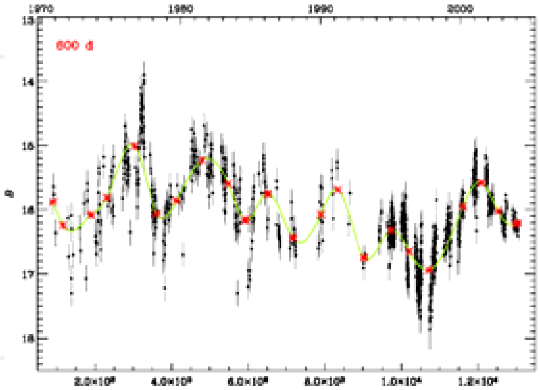

Example of cubic spline interpolation over the light curve binned at 600 days.

New comparison star calibration

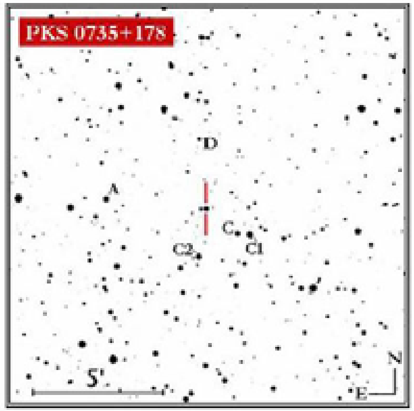

- Source magnitude is obtained with differential aperture photometry with respect to comparison stars in the same field. (Johnson-Cousins photometric system, Bessel 1979)
- New unpublished *VRI* calibration of comparison stars in the field of PKS 0735+178 (C1, C, D, C2).
- A C D stars calibrated by Smith et al. (1985). There is not any other recent photometric calibration of comparison stars in this field (see, e.g. Gonzalez-Perez 2001) .

New comparison star calibration

- Photometric calibrations derived from several photometric nights at the Perugia University observatory, using Landolt standards (for observing and reduction details see e.g. Fiorucci & Tosti 1996, Fiorucci et al. 1998).

Table 1. The new VR_cI_c Johnson-Cousins photometric calibration of comparison stars C1, C, D, C2, in the field of PKS 0735+178. A, C, D, stars were previously calibrated by Smith et al. (1985). C and D star magnitudes are in agreement within the uncertainties.

star	R.A. (J2000.0)	Dec. (J2000.0)	$U^{(1)}$ [mag]	$B^{(1)}$ [mag]	V [mag]	R_c [mag]	I_c [mag]
C1	07 38 00.5	+17 41 19.9	...	...	13.24 ± 0.06	12.91 ± 0.04	12.59 ± 0.07
C	07 38 02.4	+17 41 22.2	16.26 ± 0.08	15.48 ± 0.05	14.44 ± 0.05	13.84 ± 0.04	13.33 ± 0.06
D	07 38 08.3	+17 44 59.7	16.65 ± 0.12	16.48 ± 0.10	15.88 ± 0.05	15.44 ± 0.04	15.08 ± 0.04
C2	07 38 08.5	+17 40 29.2	...	...	13.30 ± 0.07	12.81 ± 0.05	12.37 ± 0.07

(1) U, B values by Smith et al. (1985).

10-years BVRI optical monitoring

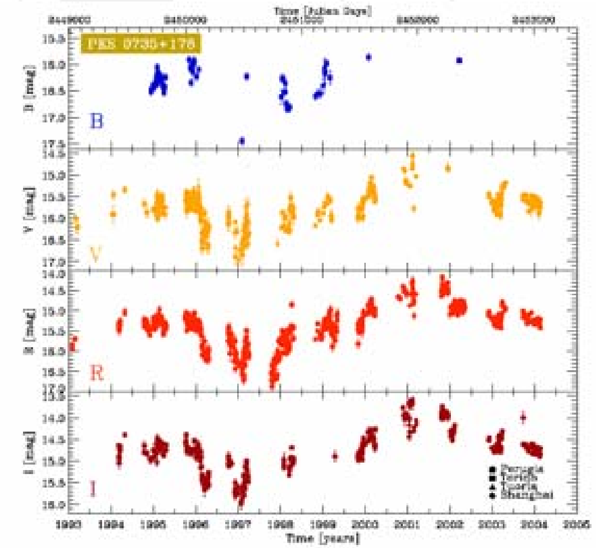

Fig. 2. *BVRI* magnitude light curves of PKS 0735+178 from 1993 to beginning of 2004. Data comes from our ten-years observing monitoring. Published observations from Shanghai Observatory (Qian & Tao 2004) are added in order to improve the sampling. Data sets of different observatories are in agreement within the uncertainties.

- 11 observing seasons, 10-years, 1621 final photometric data points.
- Our improved sampling recorded also the larger (and faster) optical flares.
- Moderate flux level and mild flaring. Rapid variations superimposed to slower variations.

10-years BVRI optical monitoring

• Optical long-term data: 10 years of optical monitoring (BVRI bands).
Data from:
Perugia University Obs. (Italy): unpublished;
INAF-Torino Obs. (Italy): unpublished;
Tuorla Obs. Turku Univ. (Finland): some data published in Katajainen et al. 2000.

DATA POINTS PER OBSERVATORY

Obs.	B	V	R	I	Tot.	Period
Perugia	0	226	490	282	998	Feb1993-Feb2004
Torino	75	38	150	0	263	Dec1994-Apr2002
Tuorla	0	55	0	0	55	Oct1995-Feb2001
Shanghai	0	115	52	138	305	Jan1995-Dec2001
Total	75	434	692	420	1621	

SAMPLING AND FLUXES

	B	V	R	I
Start date [JD-2449000]	698	45	21	420
End date [JD-2449000]	3354	4053	4053	4053
Mean gap in data [days]	35.9	9.3	5.8	8.7
Longest time gap [days]	780	352	375	356
Max flux [mJy]	2.21	6.1	7.3	9.9
Min flux [mJy]	0.51	0.67	0.60	1.1
Absorption coeff.† [mag]	0.152	0.117	0.094	0.068

† Values for the galactic extinction by NED database (Schlegel, Finkbeiner, & Davis 1998).

10-years BVRI optical monitoring

• Data from different obs. are in agreement within the uncertainties (in terms of long-term, moderate-precision photometry).

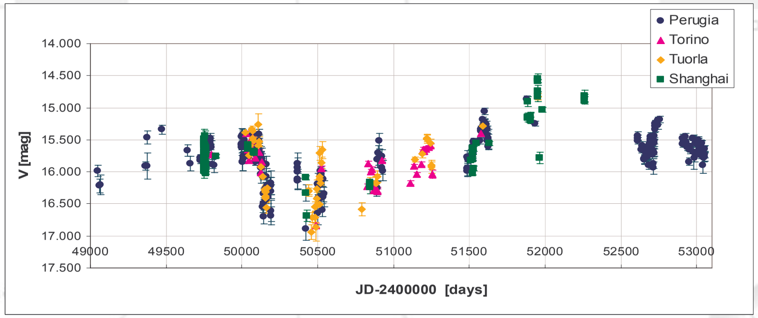

• The best sampled curve is in the R band.

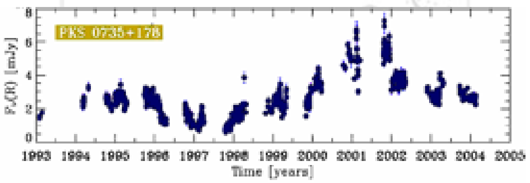

Optical spectral indexes

• Optical flux variations in blazars are usually accompanied by changes in the spectral shape. These changes can be determined computing and analyzing optical colour indexes and spectral indexes.

• The de-reddened spectral flux distribution in the optical range can be expressed conveniently by a power law for BL Lacs $F_\nu = k\nu^{-\alpha}$

(α = spectral index).

• In calculating flux spectral slopes, we selected data coupling frames with a lag of no more than 15 minutes, and using only the most precise data, possibly from the same telescope.

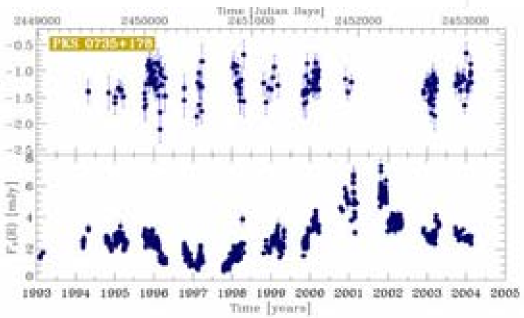

Optical spectral indexes

• Since the host galaxy of PKS 0735+178 is rather faint (Pesce et. al 1995, Scarpa et al. 2000, Falomo & Ulrich 2000, Pursimo et al. 2002), the galaxy color (thermal) interference was neglected in the observed continuum optical spectra.

• Positive hints of correlation between the spectral index and the brightness, but weak "flat-when-bright" trend.

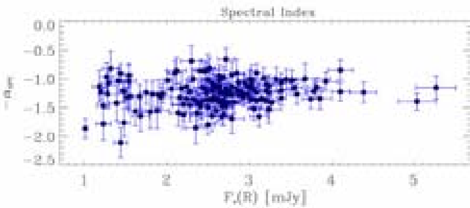

• Rather achromatic behaviour in long-term timescales.

• Optical flux in different bands well correlated

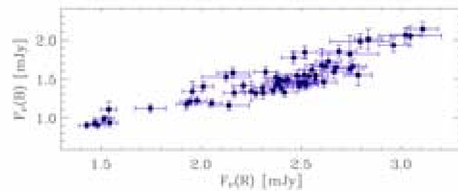

Searching for soft-hard-soft signature in optical flares

• Common pattern (not the unique one) in X-ray (usually well sampled data) flares.

• Spectral slope flattens when source luminosity increases. The more intense is the energy release, the higher is the particle energy. Loops, hysteresis cycles in the scatter plot between spectral index and flux density.

• Hysteresis cycles --> pure non-thermal cooling evolution of a single population of accelerated particles (see e.g., Kirk et al. 1998; Georganopoulos & Marscher 1998; Kirk & Mastichiadis 1999;…)

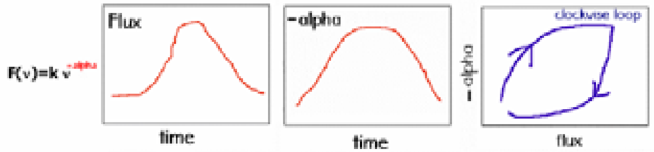

Soft-hard-soft signature

• PKS 0735+178 in these last 10-years showed relatively low optical brightness, moderate intensity fluctuations and mild flaring -> only few times the soft-hard-soft signature is clearly recognized in the optical variations.

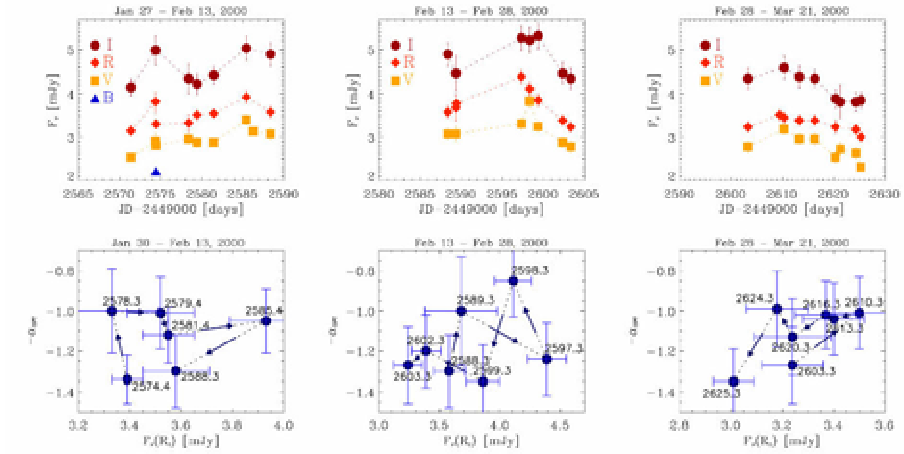

Temporal analysis methods

• Temporal analysis and statistical tools were applied to study the optical time variability in:
- the 1970-2004 historical light curve,
- our R-band (best sampled) light curve, for each observing season

• Applied methods:
- first order structure function (SF);
- discrete correlation function (DCF), and z-transformed DCF;
- discrete Fourier transform (DFT) in Lomb-Scargle implementation (periodogram);
- "cleaned" discrete Fourier transform;
- phase dispersion minimization (PDM);
- discrete wavelet transform power spectrum;

…in progress

1970-2004 B-flux light curve analysis

• Hints of recurrent time scales of variability (in particular a possible period of about 4.2-4.5, and 8.4-8.6, 12 years) comes out from the preliminary analysis.

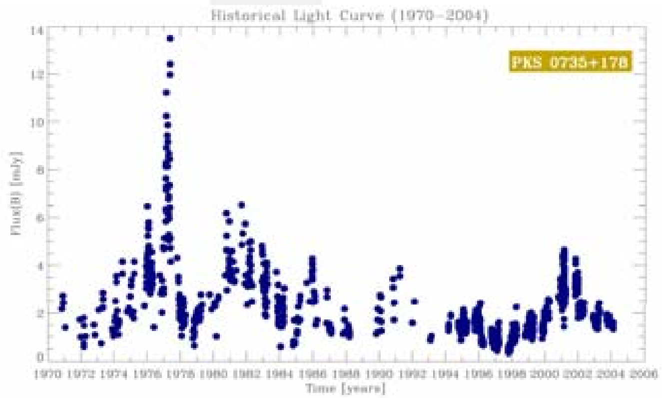

1970-2004 B-flux light curve analysis

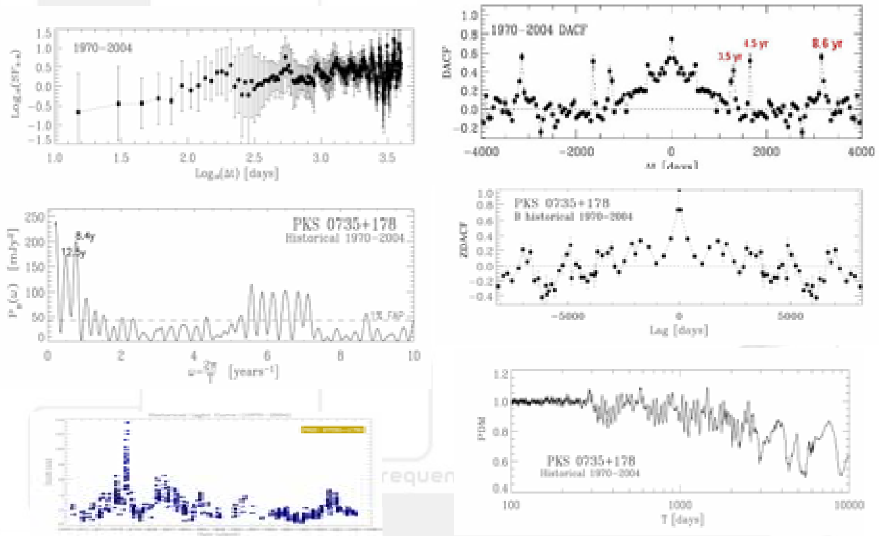

Discrete wavelet transform power spectrum

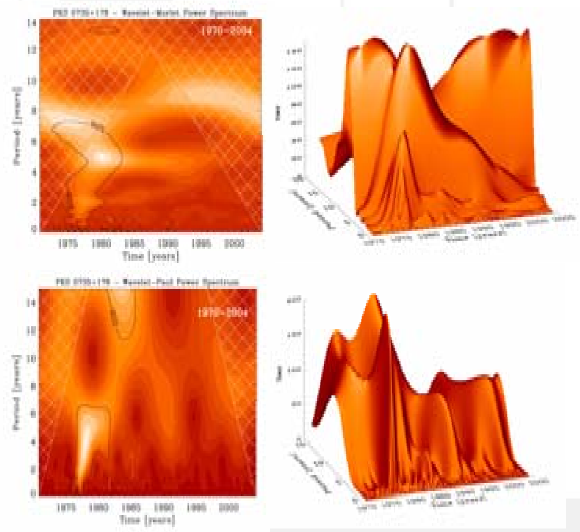

- Wavelets are used to transform a signal into another representation that present the information in a more useful form.
- Transform computed at different times in the signal with mother wavelet functions of different frequency convolved on each occasion.
- Location-frequency 2D plane.

R-band light curves: periodograms

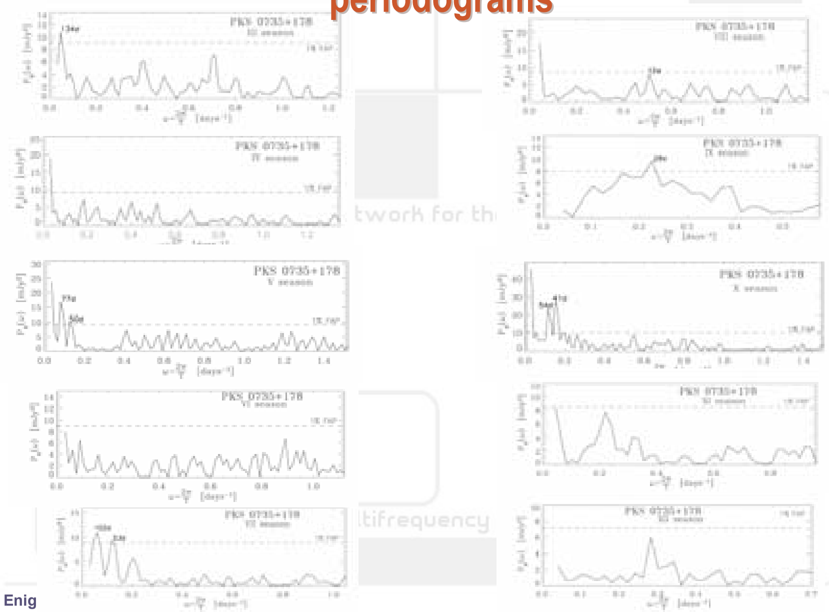

R-band light curves: structure functions

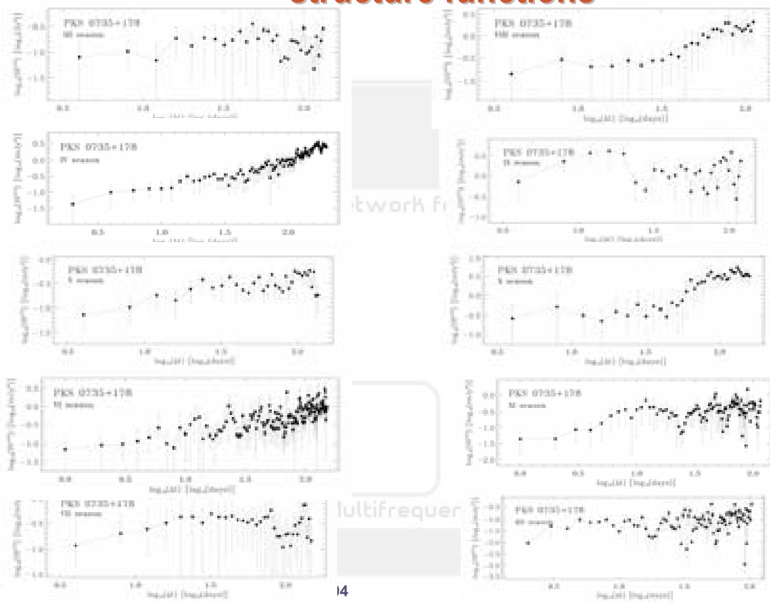

Timescales

• Preliminary computed time-scales

Observing season	Duration [days]	VE T [days]	$SF\ T_{dr}$ [days]	PSD slope α	$SF\ T_{hs}$ [days]	$DACF^{\dagger\dagger}\ T_{pe}$ [days]	$P(\omega)\ T$ [days]	C-DFT T_{pe} [days]	PDM T_{dr}
1906-2004†	.	..	---	----	.	..	.	..	.
1970-2004†	33.3y	..	4.2y,7.2y,8.1y,9.0y,10.0y,11.8y	1.5,2.0	210,1.5y	..	8.4y,12.5y	...	8.1y,12.6y,14.9y, *3.5y,6.1y
III Oct94-Apr95	191	..	12,73,79,124, *39,118	---	.	..	134	...	--
IV Sep95-Apr96	203	..	72,84,132, *46,146,182	1.97 ± 0.25	...	..	...	...	--
V Oct96-Apr97	178	..	16,50,79, *61,89,123	1.77 ± 0.2	36	..	50,77	...	--
VI Oct97-Apr98	189	..	29,66,122,*79	----	.	..	.	...	--
VII Oct98-May99	189	..	96,109	1.64 ± 0.09	31	..	53,102	...	--
VIII Nov99-Mar00	144	..	83 *53	1.84 ± 0.12	78	..	12	...	--
IX Oct00-Mar01	153	..	30,57,83, *71,112	----	.	..	28	...	--
X Oct01-May02	201	..	69,113	1.46 ± 0.17	65	..	41,54	...	--
XI Nov02-Apr03	144	..	24,60,81 *36,110	2.34 ± 0.12	12	..	...	...	--
XII Sep03-Feb04	148	..	18,55, *27	----	.	..	...	...	--

† Time scales followed by "y" are expressed in years.

†† Time scales calculated with both the DACF and ZDACF.

Optical variability mode

• Slopes in the *SF* were reliably determined, but the *SF* plateau can be recognized only for the best sampled observing seasons.

•The ZDACF and first-order SF shapes give a fluctuation mode similar to the shot noise: *P(f)* $=1/f^{\alpha}$, with $1.5 < \alpha < 2.3$.
This power spectrum is characteristic of a random walk, stochastic relaxation processes.

PKS 0735+178 SED

EGRET source. Synchrotron peak in the Near IR-optical bands. X-ray emission is likely inverse Compton emission.

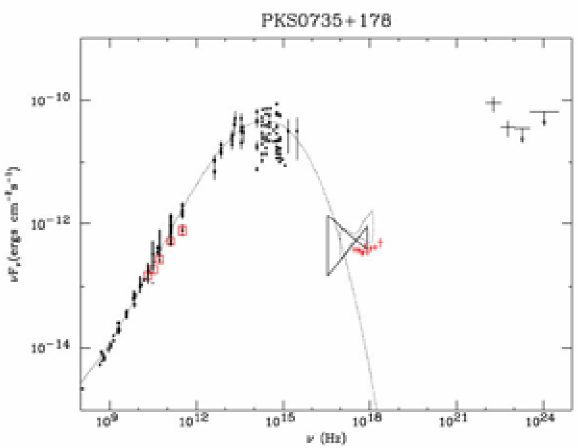

Conclusions

• Obtained, collected and analyzed the largest amount of optical data ever published on PKS 0735+178.

• Some preliminary results are found, but there are still open questions.

• 1993-2004 optical behaviour: rather achromatic long-term optical variations, moderate flux level, mild flaring and no outburst.

• Variability mode similar to the shot noise, (*P(f)* $=1/f^{\alpha}$, with $1.5 < \alpha < 2.3$, random walk).

• A first look suggests that it is difficult to correlate this optical variability with the radio one.

• The work is in progress…

Optical spectroscopy of BL Lacs with ESO VLT+FORS1

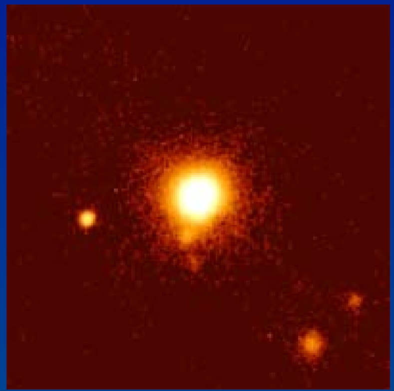

B. Sbarufatti, A. Treves, R. Falomo, J. Heidt, J. Kotilainen, R. Scarpa

Talk Outline

- BL Lac optical spectroscopy: the problem of line detection
- The VLT view on BL Lacs: program and observations
  - New redshift determinations:
    - emission lines properties
    - intervening absorptions
  - Featureless objects
  - Wrong ID

Optical spectra of BL Lac objects

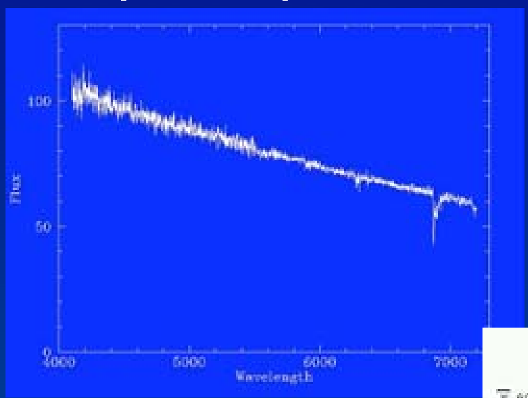

BL Lac optical spectra are often dominated by a non-thermal emission from a relativistic jet. Intrinsic spectral features are strongly diluted by the continuum.

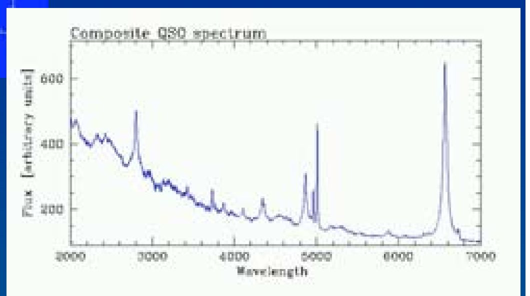

Redshift of many BL Lacs are still unknown.

Simulated spectra of BL Lacs.

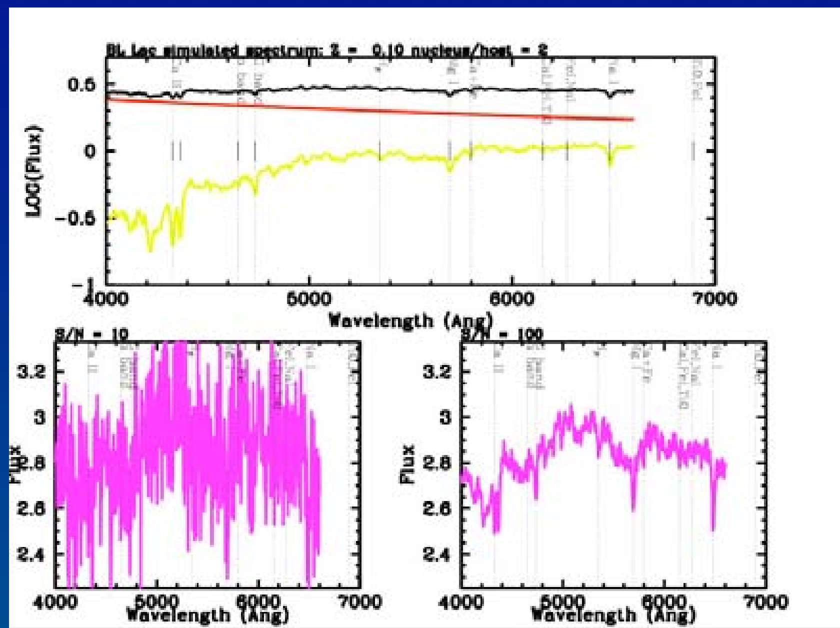

Detection of spectral features.

- To detect weak spectral features (EW~ 1 Å or less), high S/N spectra (>100) are required.
- With 4 m class telescopes such a S/N can be reached for objects with V 15.
- For fainter objects, an 8 m class telescope, is required.

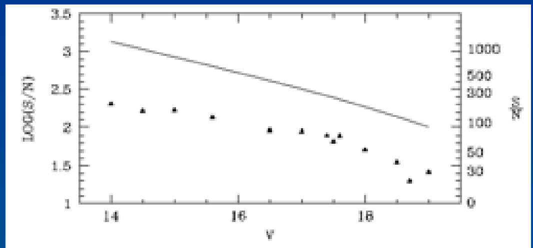

Program Objectives

- Redshift → Distance → Physical quantities.
- Search for weak broad emission lines.
- Statistics of intervening systems.
- Unveiling the nature of bright very featureless BL Lacs (underluminous host or extremely beamed nuclei).

The VLT view of BL Lac spectra

- High S/N (100-500) spectra of ~80 BL Lac with VLT+FORS1; obs. in service mode during poor seeing conditions.
- Selection:
  - ☑ Source classified as BL Lac in the main catalogues.
  - ☑ Redshift unknown or uncertain.
  - ☑ Bright lineless sources are preferred.
- 31 objects observed from April ‘03 to March ’04. Other 18 planned for Summer ‘04.

The VLT view of BL Lac spectra

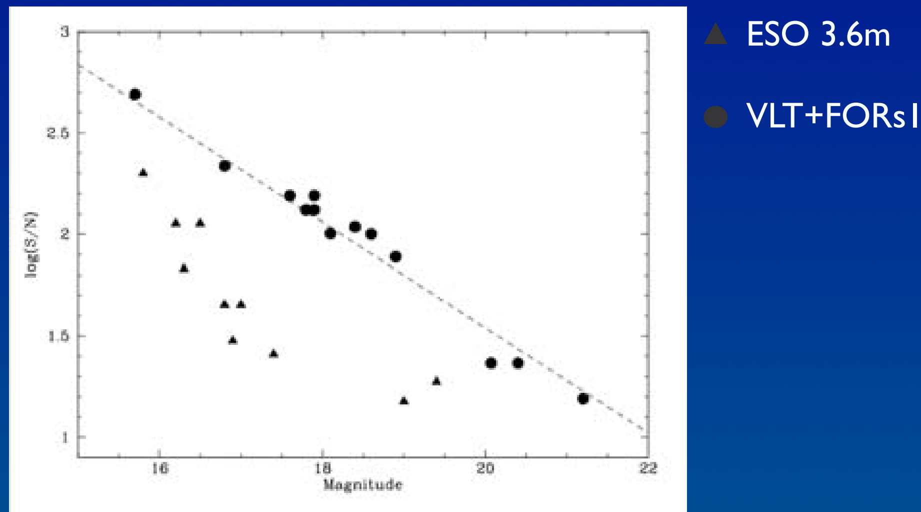

Results

We obtained new redshift estimates for 13/31 sources, in the range 0.2<z<1.2. The remaining sources are featureless BL Lacs (11) and misclassified objects (3 QSO, 2 galaxies, 2 galactic stars).

Object	RA J2000	Dec J2000	V	Class	S/N	z	line type
1RXS J022716.6+020154	02 27 16.6	+02 01 58.0	18.8	H	100	0.457	g
PKS 0306+102	03 09 03.6	+10 29 12.3	18.4	L	20	0.862	e
1RXS J031615.0−26074	03 16 15.0	−26 07 56.7	17.5	L	130	0.443	e,g
PKS 0338−214	03 40 35.5	−21 19 31.2	17.1	L	210	0.223	e
PKS 0426−380	04 28 40.4	−37 56 19.6	19.0	L	100	1.105	e,a
1RXS J055806.6−383829	05 58 06.2	−38 38 27.0	17.1	H	280	0.302	g
PKS 0808+019	08 11 26.7	+01 46 52.2	17.2	L	140	1.148	e
1WGA J1012.2+063	10 12 12.2	+06 31 01.0	16.8	L	200	0.727	e,a
PKS 1250−33	12 52 58.4	−33 19 59.3	21.5	L	30	0.856	e
PKS 1256−229	12 59 08.5	−23 10 38.7	16.7	L	170	0.481	e
PKS 1519−273	15 22 37.7	−27 30 10.8	17.7	L	170	1.297	e
MH 2136−428	21 39 24.1	−42 35 21.3	16.2	L	490	0.497	g
PKS 2354−021	23 57 25.1	−01 52 15.3	21.2	L	30	0.81	a

Note. — e: emission lines; g: host galaxy lines; a: intervening absorptions

Results: redshift distribution

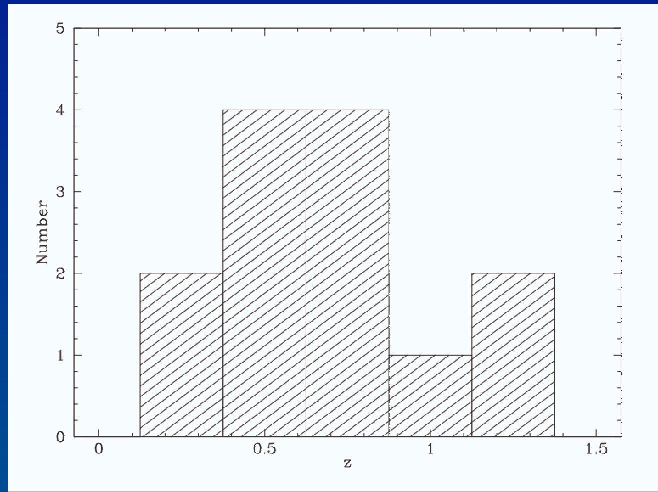

Results: new redshifts from emission lines.

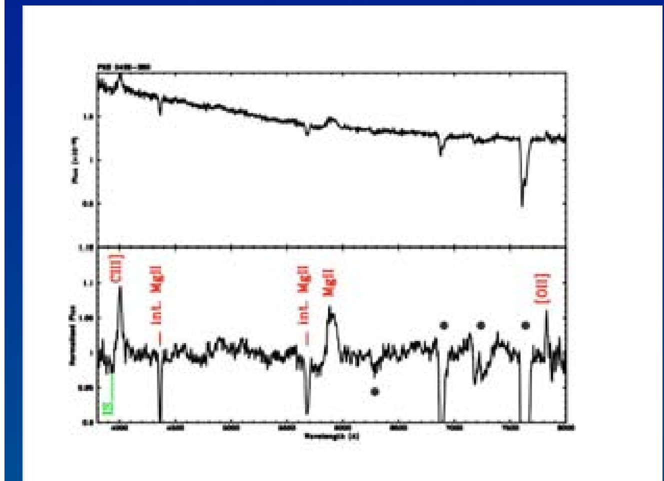

PKS 0426-380

- S/N = 100
- z_{em} = 1.105
- Intervening absorptions @ z = 0.56, 1.03.

Results: new redshifts from absorption lines.

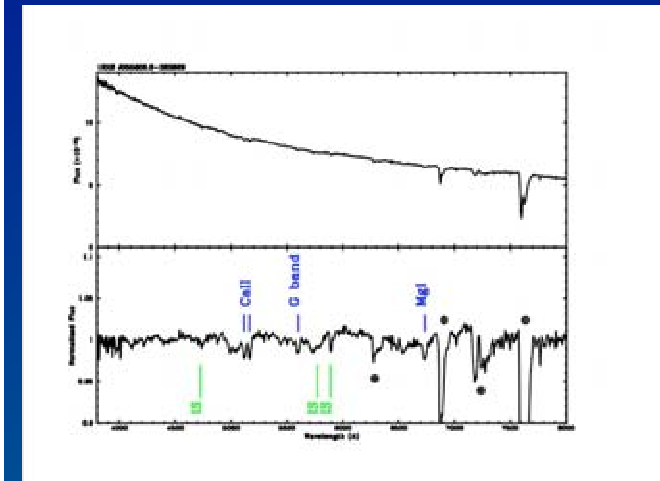

1RXS 055806.6-383829

- S/N = 280
- z_{abs}=0.302
- EW abs lines 0.7-0.9

Results: emission lines

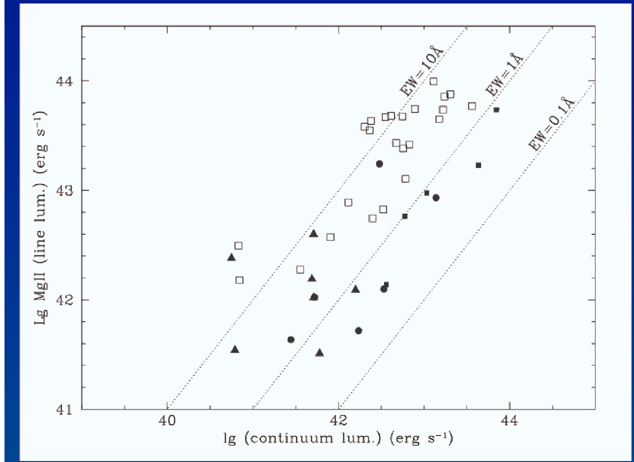

- Emission lines luminosities are somewhat lower respect to previous samples (Scarpa & Falomo '97), but conform to the behavior of the class.

▲ our sample
□ ■ HPQs and BL Lacs from Scarpa&Falomo'97
● BL Lacs from Stickel et al.'93

Results: BL Lacs and intervening systems

- Stocke & Rector '97 found intervening absorptions in 10 out of 37 BL Lacs in the 1Jy sample → intervening halos can be related to BL Lacs
- We find intervening absorptions in 2 objects over 13 new redshift estimates. If confirmed intervining halos probably are NOT related to BL Lacs

What about the featureless sources?

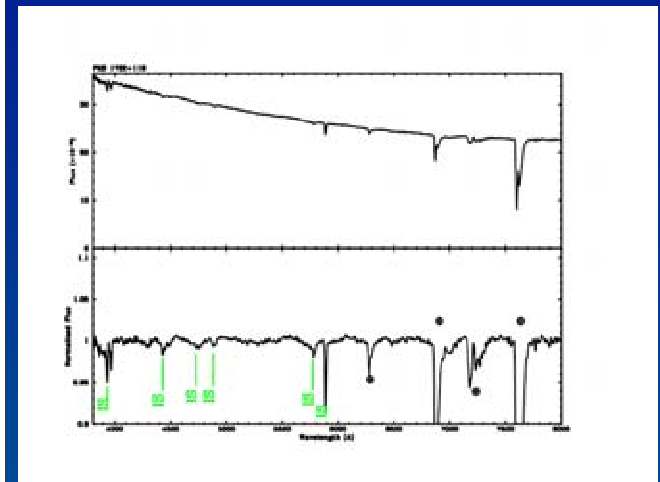

PKS 1722+119

- S/N 340
- EW upper limit on intrinsic features 0.02 Å
- Such an object could be useful to study the ISM, especially the Diffuse Interstellar Bands.

Wrong IDs

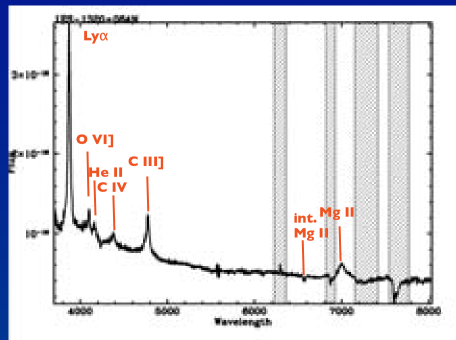

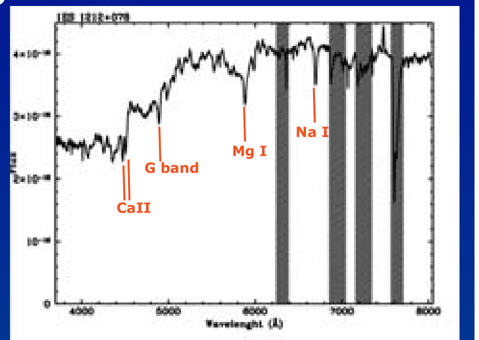

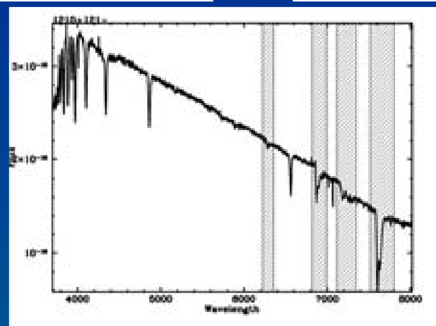

Summary

- S/N up to 500 reached with VLT+FORS1, which allows to detect features with EW ≤ 0.5 Å.
- New redshift for 13 objects (Sbarufatti et al. 2004, submitted to AJ).
  - ☑ Emission lines follow the expected distribution, covering the lower luminosity region.
  - ☑ Intervening systems may NOT be related to BL Lacs.
- 11 objects show spectra without any intrinsic feature; EW upper limits can be used to constraint Nucleus/Host ratio and z
- 7 wrong classifications (3 type 1 QSOs, 2 elliptical galaxies, 2 galactic stars).

Helical Magnetic Fields in Parsec-Scale Radio Jets

Andreas Papageorgiou

Current Post-doc at CIT, funded by the EU 5th Framework

Introduction

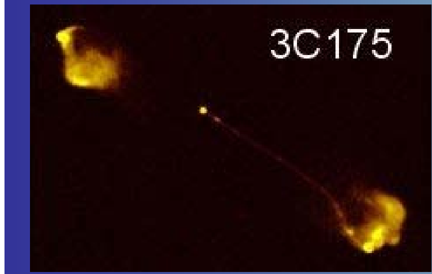

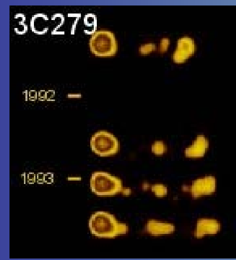

- Radio Jets: Collimated outflows powered by AGN
- A large fraction of their radiation due to synchrotron
- Observations on a range of Scales: Large scales (FRI & II), smaller scales (pc-scale jets)

Profiles

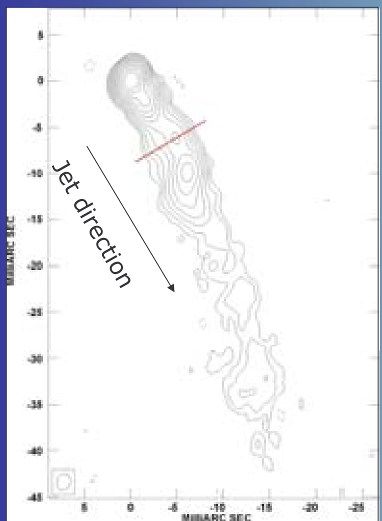

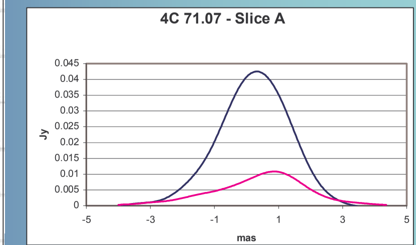

Observations

1055+018

(Attridge et al. 1999)

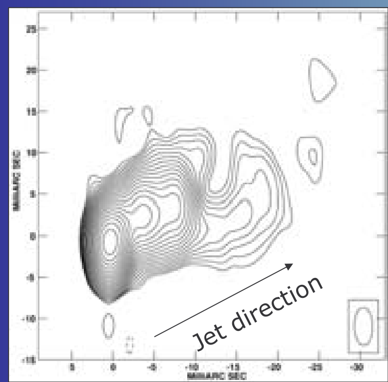

Total Intensity

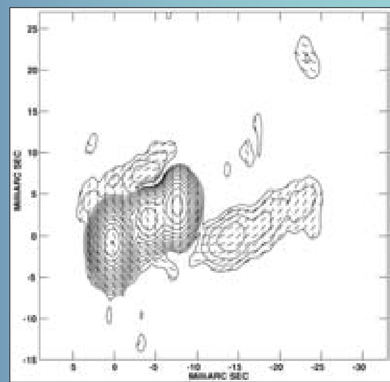

Polarized Intensity with B Vector Sticks

Observations

3C 353

(Swain, Bridle & Baum 1998)

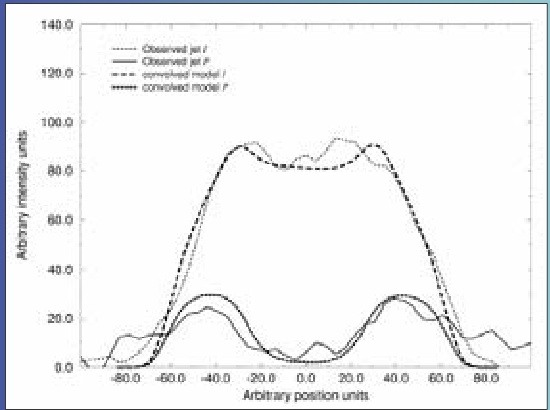

Observations

3C 380 & 4C 71.07

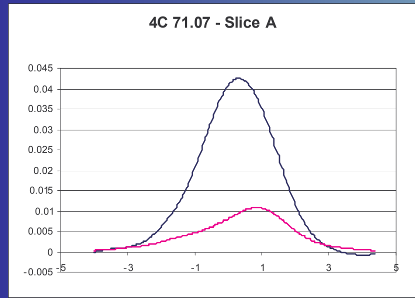

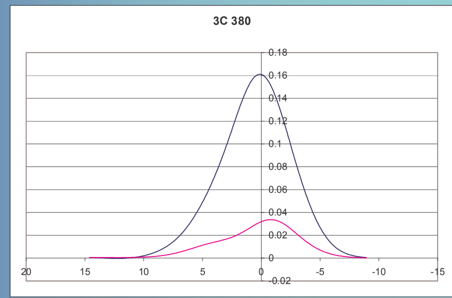

Summary of observed features

- Asymmetry in I and P across the jet
- I and P maxima not aligned
- Edge brightening
- Apparent Magnetic field distribution flips from longitudinal to transverse

All four features can be reproduced by helical magnetic field model

Why Helical Fields?

- Can give rise to asymmetries in polarization
- Can produce transverse B field in the middle and longitudinal at the edges
- Avoids physical asymmetries (eg, in density or pressure)

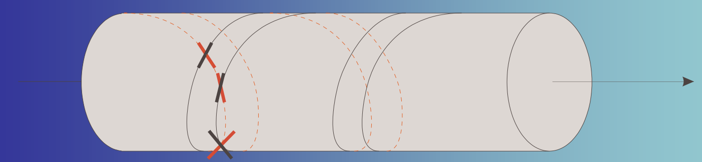

Are helical fields possible?

Variation of the Magnetic Anchoring Model (Nakamura et al. 2001)

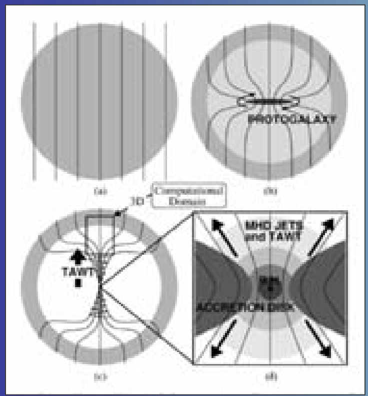

Results of 3D MHD Simulation (Nakamura et al. 2001)

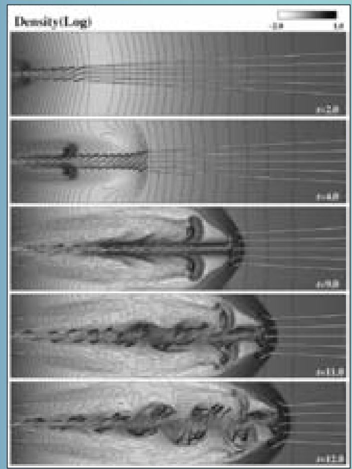

Helical Models

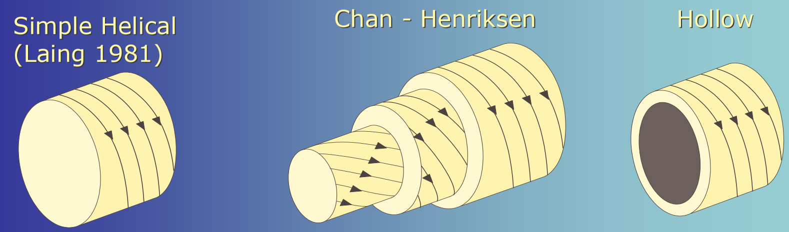

Additional Parameter: f
Tangled Magnetic Field Component

$$\frac{\langle B_t^2 \rangle}{\langle B_{Hel}^2 \rangle} = \frac{f}{1-f}$$

I and P profiles of Helical Model

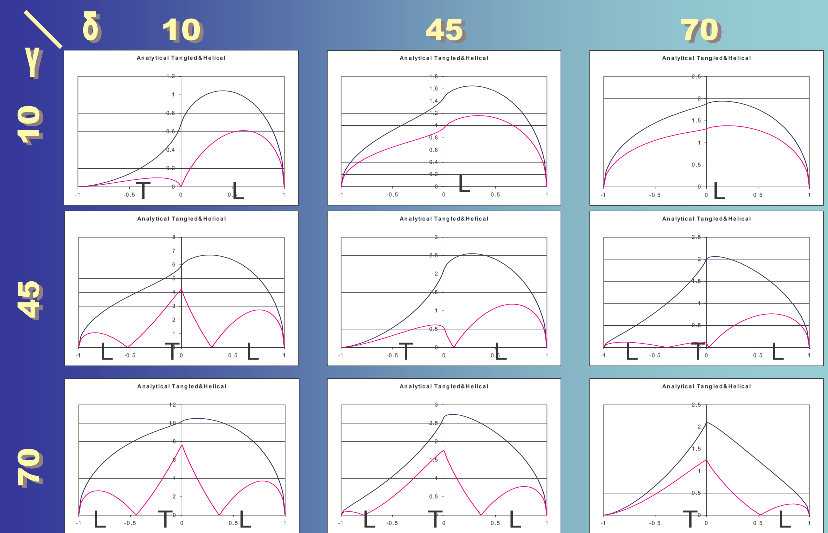

App. Magnetic Field Orientation

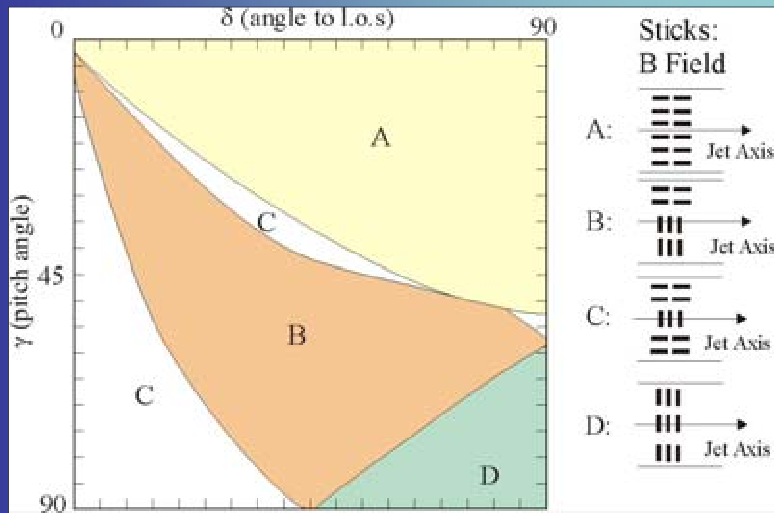

Comparison Helical & 4C71.07

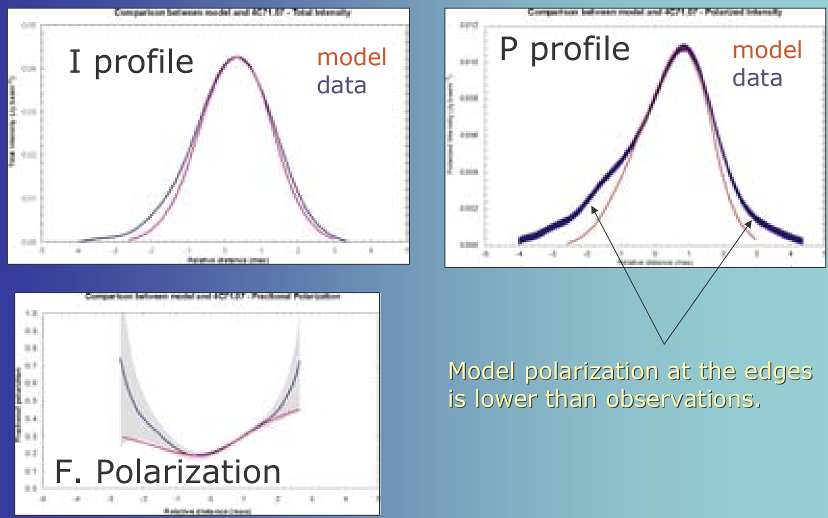

Model polarization at the edges is lower than observations.

Addition of Compression Shell

- Produces high Fractional polarization at the edges but not in the middle

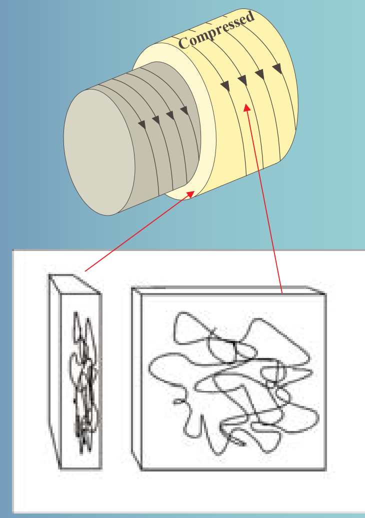

Fractional Polarization of Compressed Shell

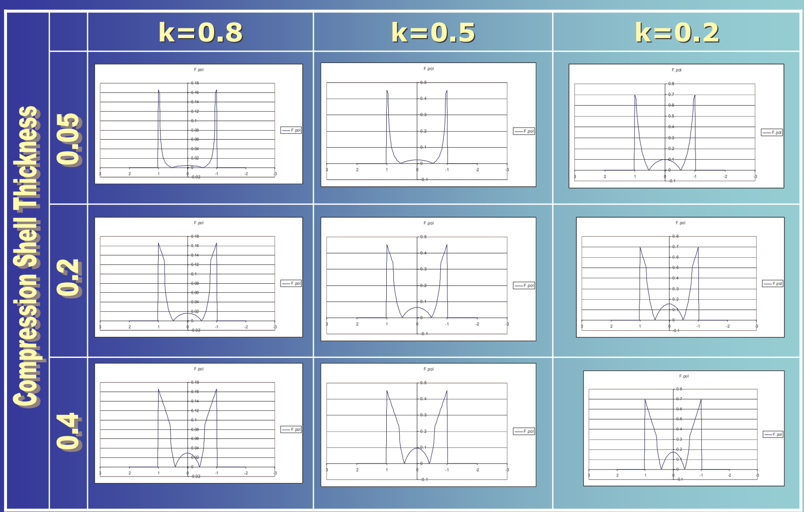

Comparison

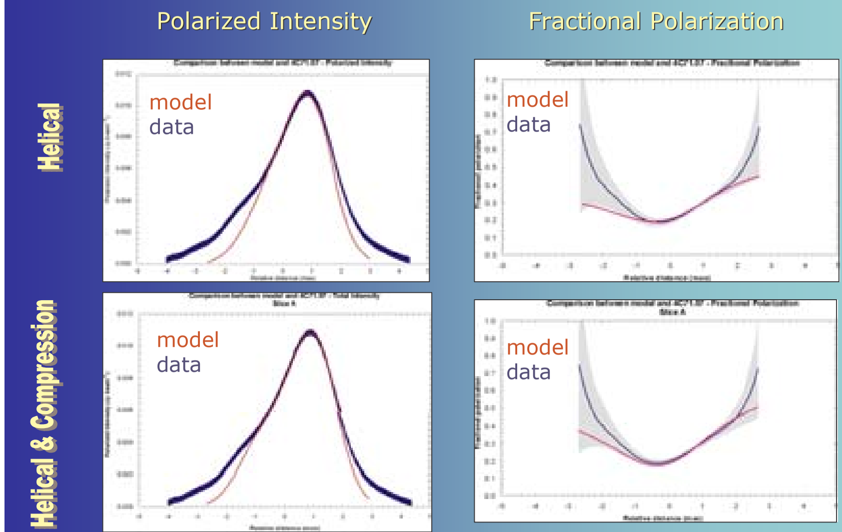

3C380

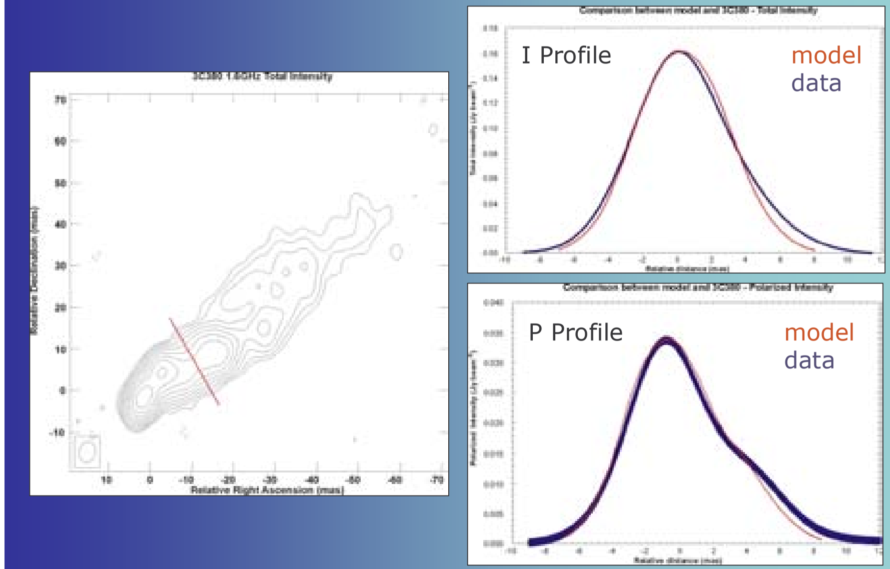

1928+738

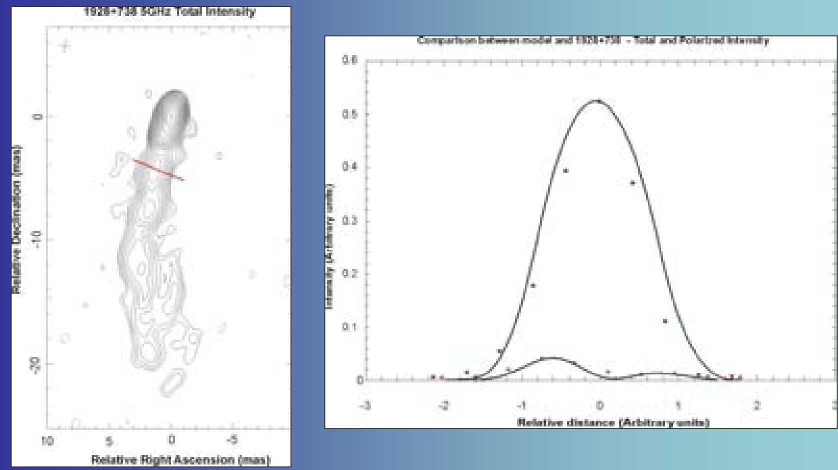

1055+018

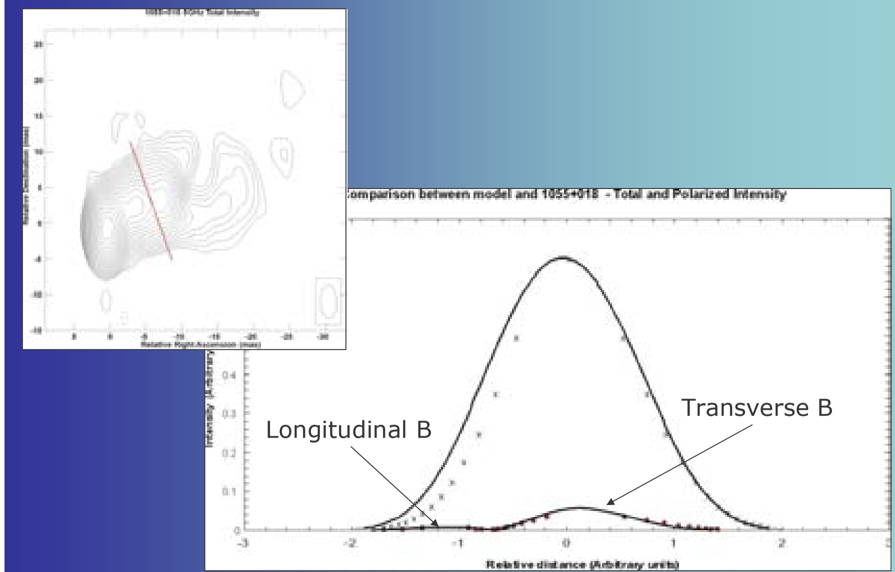

3C353

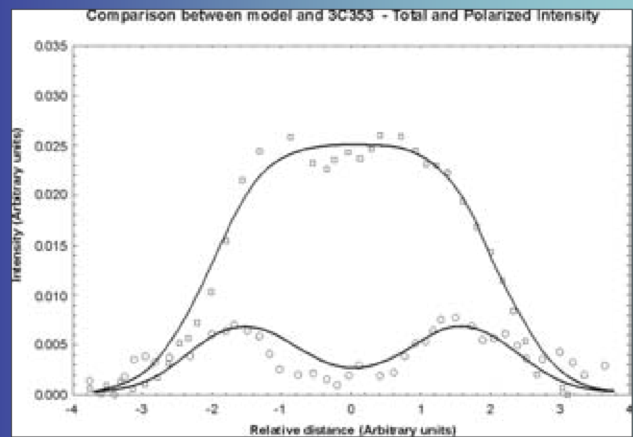

Other Techniques

3C 273

Asada et al. 2002

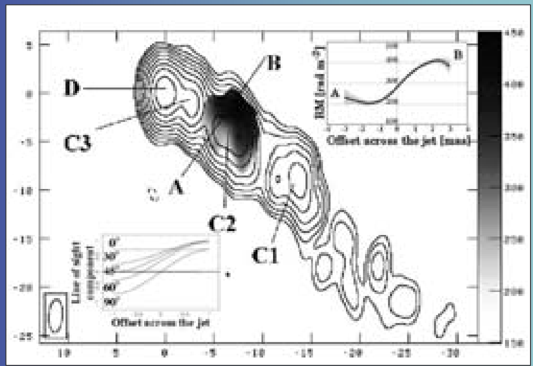

Total Intensity contours with Faraday Rotation grey scale

Rotation Measure in 4C71.07

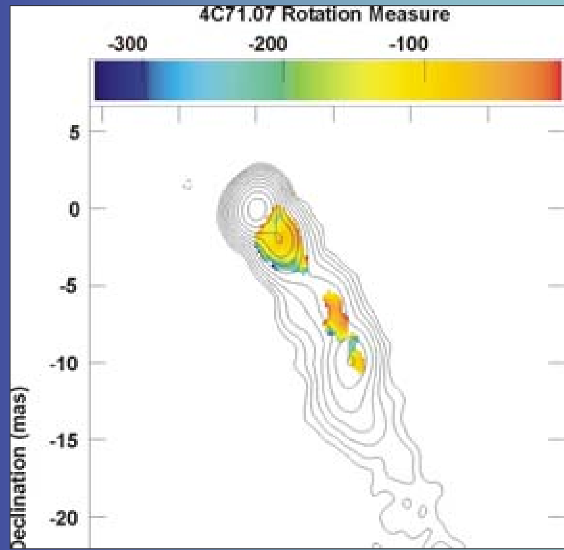

Summary

- Model qualitatively describes many of the observed features (Asymmetries, Peak displacement, B field orientation)
- If Helical fields are present, model could provide values on the angle to the line of sight
- Independent method (RM profiles) can be used to compare predictions of pitch angle and angle to l.o.s.

Further Work

- Examine more sources!! There are plenty in the archives that have not been reduced for polarization
- The model can be used to predict likelihood of observation of the four magnetic field behaviours (A,B,C & D). This can be compared with observations.

4th ENIGMA meeting in Perugia 2004

Long term variability of inverted-spectrum sources

Ilona Torniainen
Metsähovi Radio Observatory

Merja Tornikoski, Harri Teräsranta, Metsähovi Radio Observatory

Margo Aller & Hugh Aller, University of Michigan, Radio Astronomy Observatory

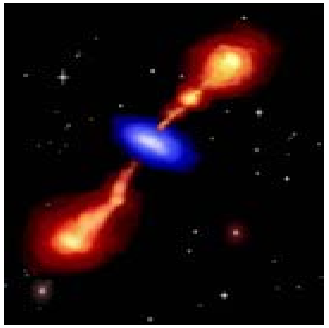

Extragalactic inverted-spectrum radio sources

- Active Galactic Nuclei (AGN) with special spectral shape in radio continuum

ordinary AGN

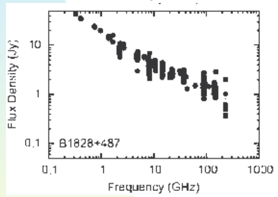

inverted-spectrum AGN

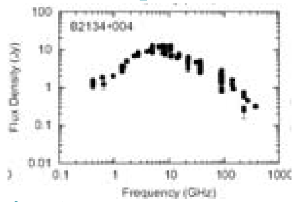

- Inversion due to free-free or synchrotron self-absorption
- Quasars and galaxies, here mostly quasars

Ilona Torniainen
Metsähovi Radio Observatory

Categories:

- **Compact Steep-spectrum (CSS) sources**
- **Gigahertz-peaked spectrum (GPS) sources**
- **High Frequency Peakers (HFP), extreme-GPS**

Common properties, classical approach

- **anticorrelation between turnover frequency and linear size**
- **low variability, sustained turnover frequency**
- **low polarization**

=> ? a) Evolution from compact to extended
b) Confined by dense environment
c) Recurrent activity

Ilona Torniainen
Metsähovi Radio Observatory

The study

- WHY:
  - To identify new high-peaking GPS sources
  - To study the variability of the known ones

  } Important for Planck mission
- HOW:
  - Sample of 60 sources: 16 new candidates, 44 known inverted-spectrum sources
  - Monitored in Metsähovi: 22, 37 GHz
  - Some observations at SEST in Chile: 90, 230 GHz
  - Monitoring data from Michigan: 4.8, 8, 14.5 GHz
  - Additional data from literature

  } Data spanning over three decades!

Ilona Torniainen
Metsähovi Radio Observatory

Results: New candidates (tot.16)

- 11 sources turned out to be flat spectrum sources with inverted spectrum during the bursts
- 1 inverted but very variable
- The rest had flat spectra
- No classical GPS sources found

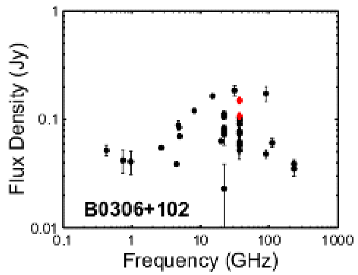

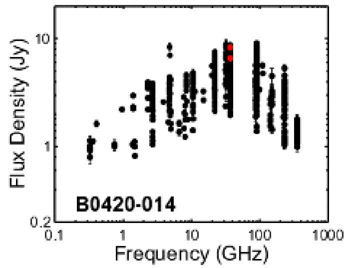

Ilona Torniainen
Metsähovi Radio Observatory

Results: Known GPS sources (tot. 44)

- **40 % of the bona fide inverted-spectrum sources turned out to be flat spectrum sources with inverted spectrum during bursts**

  => Classification has been made with too sparse data

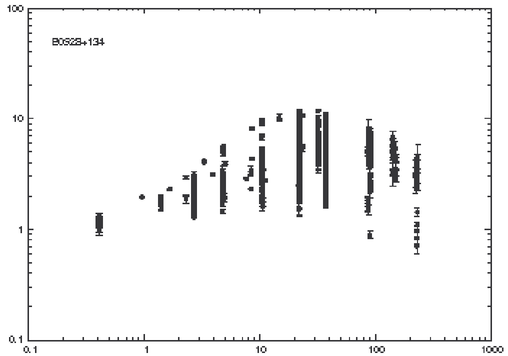

Ilona Torniainen
Metsähovi Radio Observatory

Results: Known GPS sources

- **31 % of the GPS sources retained inverted spectrum but exhibited variability**
  ⇏Original definition!

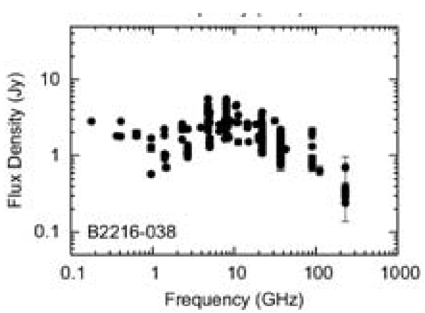

Ilona Torniainen
Metsähovi Radio Observatory

Results: Known GPS sources

- Only 4 genuine GPS sources with little variability and inverted spectrum
  - one had so poorly data that the interpretation is not reliable

  => more data needed to reveal the multi-epoch spectra

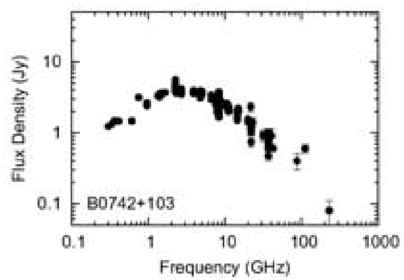

Ilona Torniainen
Metsähovi Radio Observatory

Results: conclusions

- The classification has been done with too little data
  - => It is possible that a considerable proportion of all GPS sources are not gigahertz-peaked
  - => The interpretation of the properties of the GPS class is based on a sample including a remarkable amount of non-GPS sources

=>The concept of GPS sources should be re-examined!

Planck foreground science

- (High-peaking) GPS sources
  - Their number even smaller than estimated??
- Variable sources with inverted spectra during outbursts
  - A remarkable share of bona fide GPS sources??
  - The effect on the Planck science depends on the state of activity
    - => the variability should be modelled to find out what proportion of time they are active = visible for Planck

The Future

- Monitoring continues at Metsähovi
  - => Multi-epoch data on high frequency variability of the sources
  - The sample extended to include also galaxy-type GPS sources: will they exhibit variability too?
- RATAN-collaboration: simultaneous spectra
- Statistical cluster analysis of the sources
- Development of variability models

Host Galaxies of Compact Steep Spectrum Radio Sources

Mirko Tröller
Metsähovi Radio Observatory

4th ENIGMA Meeting
Oct. 6-8, 2004
Perugia, Italy

in collab. with
Merja Tornikoski, Metsähovi
Esko Valtaoja, Tuorla Observatory

Outline

- Introduction
- The Sample
- Data Analysis
- Few First Results
- Summary

Properties of CSS Sources

- compact, small intrinsic size ≤15 kpc (radio)
- high luminosity (like 3CR doubles)
- steep spectra
- peaked around 100MHz
- turnover frequency varies with size
- low polarisation
- superluminal motion appears to be rare

Why are CSS Sources Important?

- their bright and symmetric radio structure probe the ISM of the host galaxies
- CSS sources may be younger stages of powerful large scale radio sources, giving insight into genesis and evolution

Why are the Hosts Important?

- optical identification to measure redshift
- radio and stellar evolution are quite different (10^{8}º10^{1} yr)
  -> host properties should be independent of radio size
- study environment which may trigger the radio activity

The Sample

Complete sample of 55 CSS

28 galaxies, 27 QSOs

broad-band images in R and V

t_{int} = 600 - 1800 sec

observed at the NOT

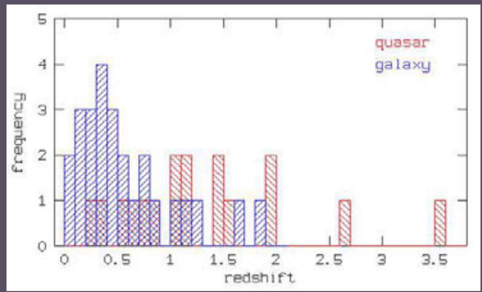

QSOs tend to be at higher redshift

Aim of the Work

- What are the hosts of CSS sources ?
- Probing the GPS-CSS-FR2 evolution scenario
- Effect of nearby environment on nuclear activity

Data Analysis

2-dim. surface brightness analysis

two-component model : ***core (AGN) + host galaxy***

core : scaled PSF

$$\text{host galaxy} : I(r) = I(r_e) dex \left\{ -b_n \left[\left(\frac{r}{r_e} \right)^{1/n} - 1 \right] \right\}$$

iterative χ^2-minimization with

n = 4 (de Vaucouleurs type E)
n = 1 (disk type S)

Models

1. Model : scaled PSF
   -> check if host is resolved or not

2. Model : galaxy + scaled PSF
   -> fit with nuclear component (AGN)

3. Model : pure galaxy
   -> fit without AGN component

Fit Parameter

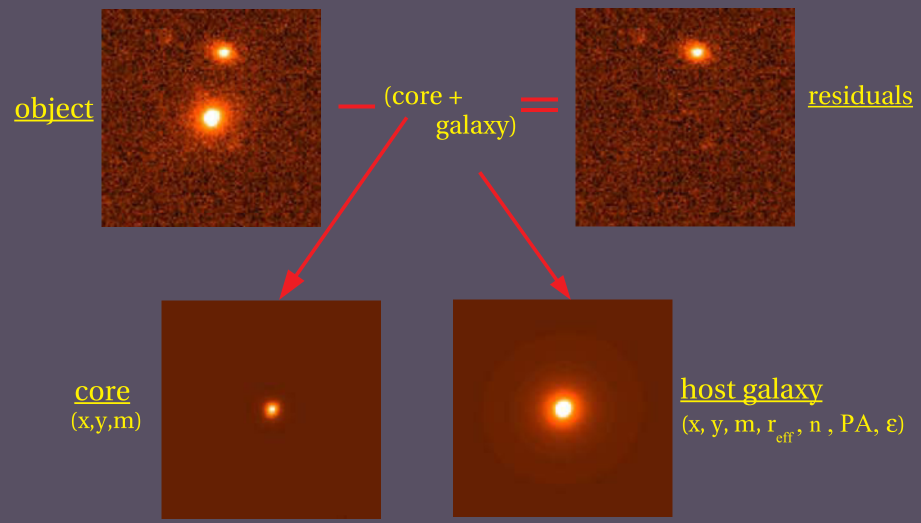

Resolved or Not Resolved ?

Host *resolved*

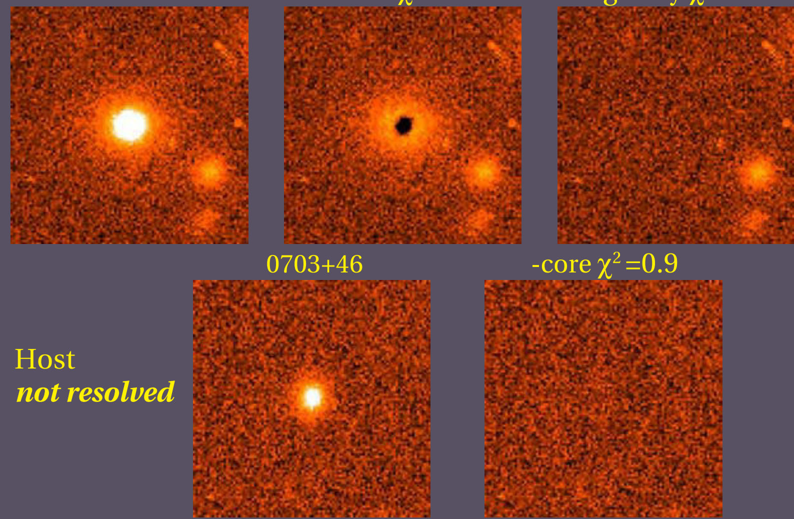

Host *not resolved*

Best Model

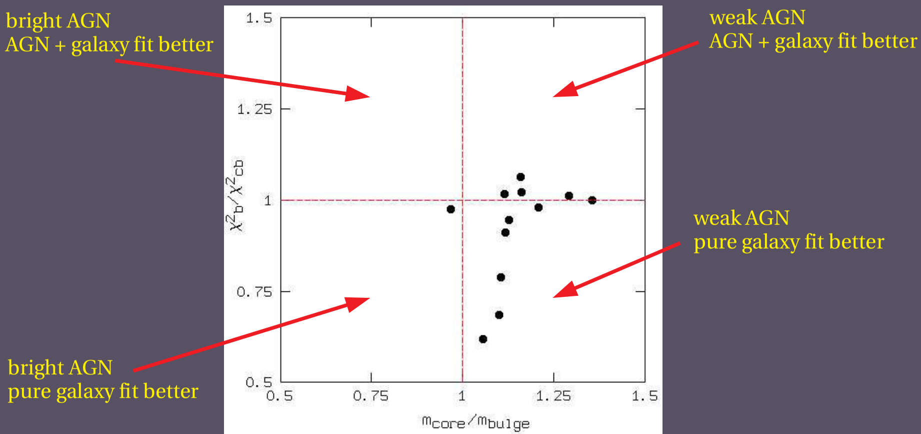

i) Pure galaxy model yields best fit
ii) AGN is faint in the AGN+galaxy model

Host Properties – Size

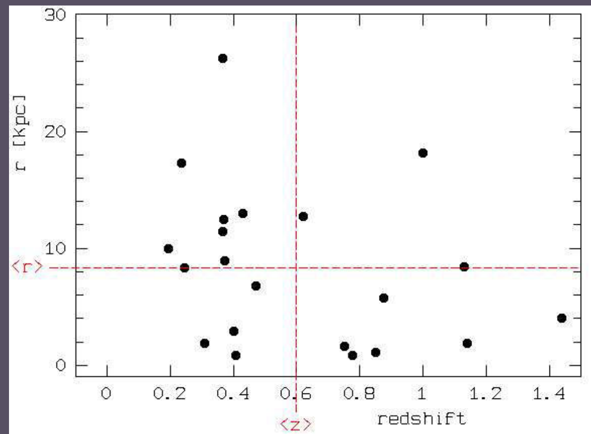

Resolved hosts :
$<r_{eff}> = 8.3$kpc @ $<z> = 0.6$

Host Properties – Type

$$\mu(r) \propto \left(\frac{r}{r_e}\right)^{1/n}$$

r<3kpc, n<4 :

ordinary-ellipticals

r>3kpc, n>4 :

bright-ellipticals

CSS hosts :

n=4.1
r=8.3kpc

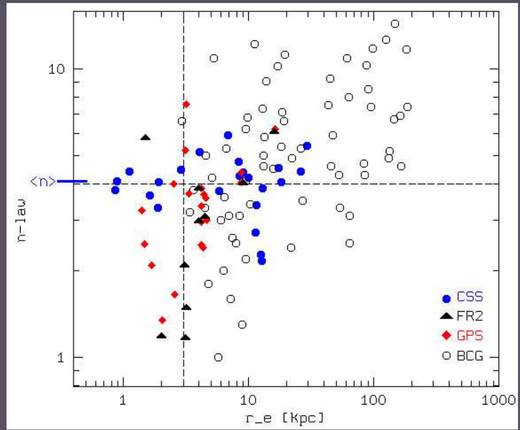

(deVries2000, Graham1996, Caon1993)

Kormendy Relation

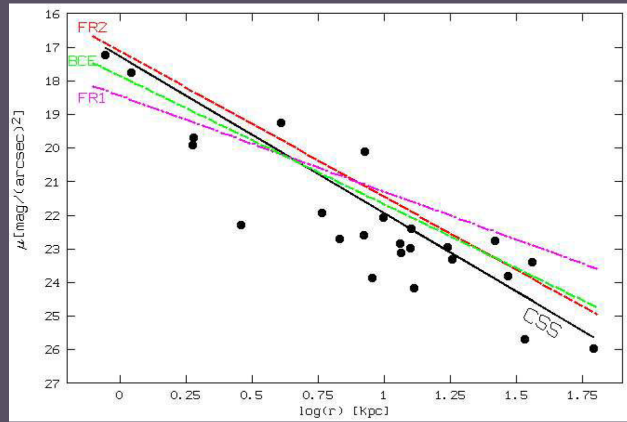

(Govoni2000, Lendlow1995)

Kormendy relation similar to FR2s not BCE-FR1s

Pre-Results

- CSS sources are bulge dominated with a weak or absent nuclear component (in R and V)
- Hosts are large ellipticals $\langle r_{eff} \rangle$=8.3kpc
- Kormendy relation resembles the one found for FR2's
  -> supports the GPS-CSS-FR2 sequence

To Do

- complete the photometry of the hosts
- compare R and V band (determine V-R color)
- determine local galaxy density
- compare optical and radio morphology

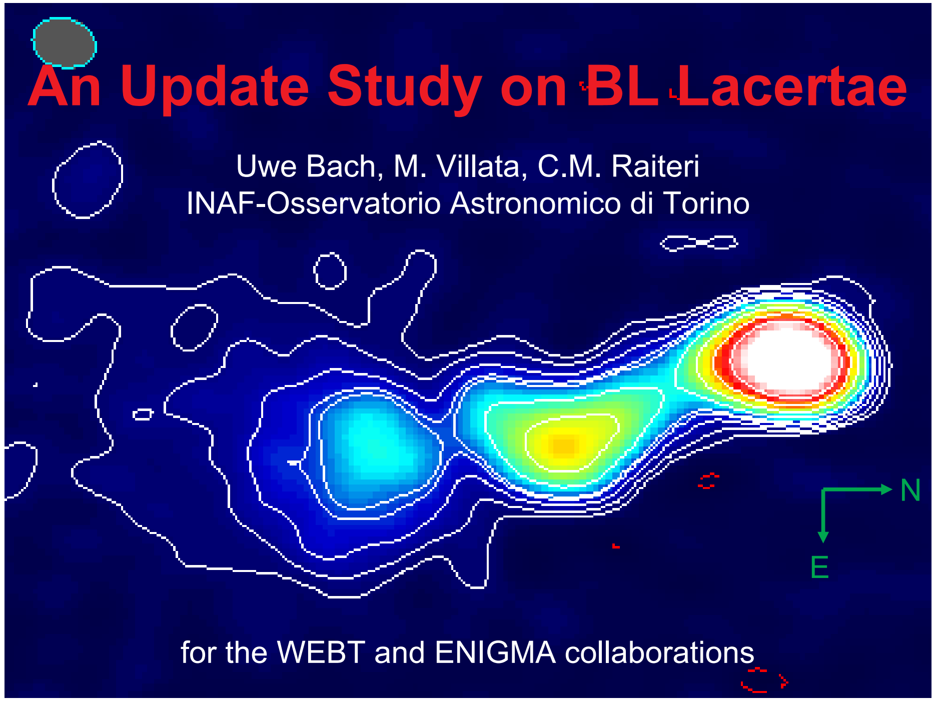

Contents

- Intro on BL Lacertae
- Variability
  - optical
  - radio
  - radio-optical correlation
- BL Lac on parsec-scales
  - jet kinematics
  - precessing jet?
- Outlook

BL Lacertae

- Eponym of the BL Lac objects.
- redshift = 0.069 ~ 300 Mpc.
- Highly variable at all wavelengths.
- Correlated variability:
  - radio and X-rays (Kawai et al 1991).
  - radio-spectrum and optical (Villata et al. 2004b).

VLBI observations show:

- Compact core and a bent parsec-scale jet.
- Nearly no kpc-scale structure.
- Regular ejections of superluminal jet components.

BL Lacertae

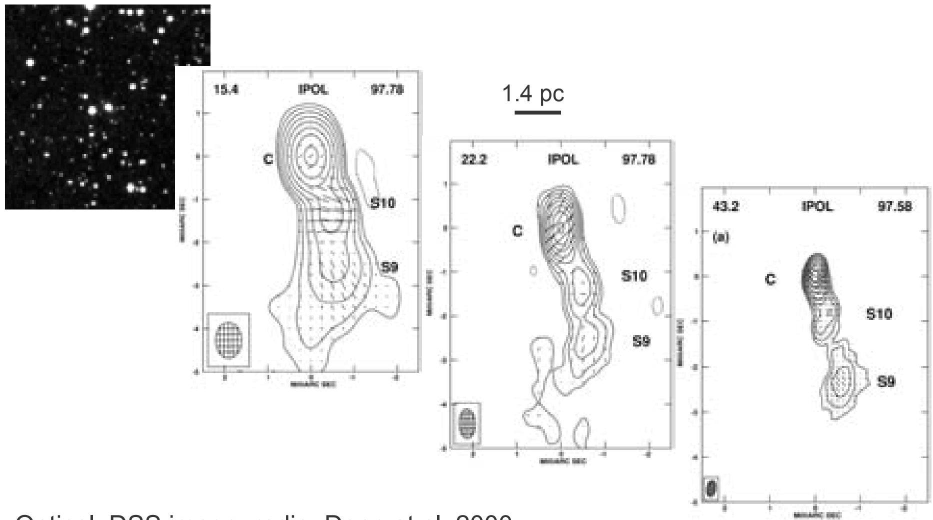

Optical: DSS image; radio: Denn et al. 2000

Optical Variability (UBVRI)

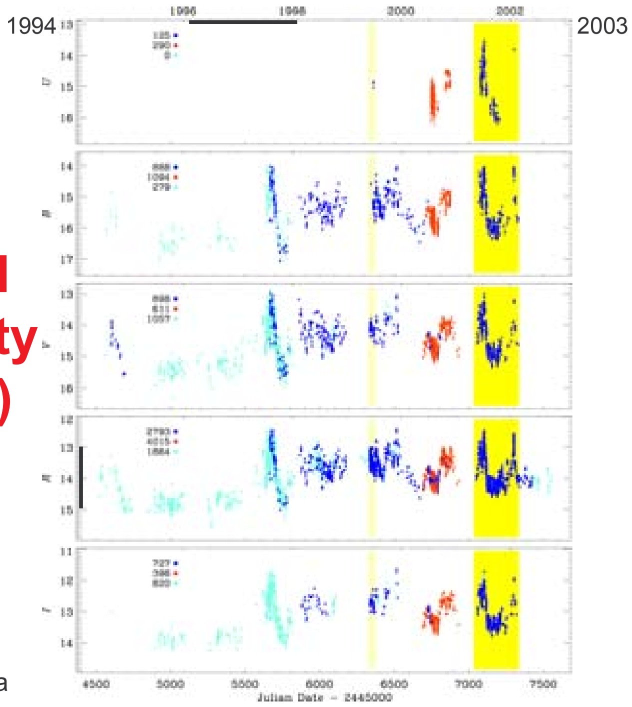

Villata et al. 2004a

Optical Variability (R-band)

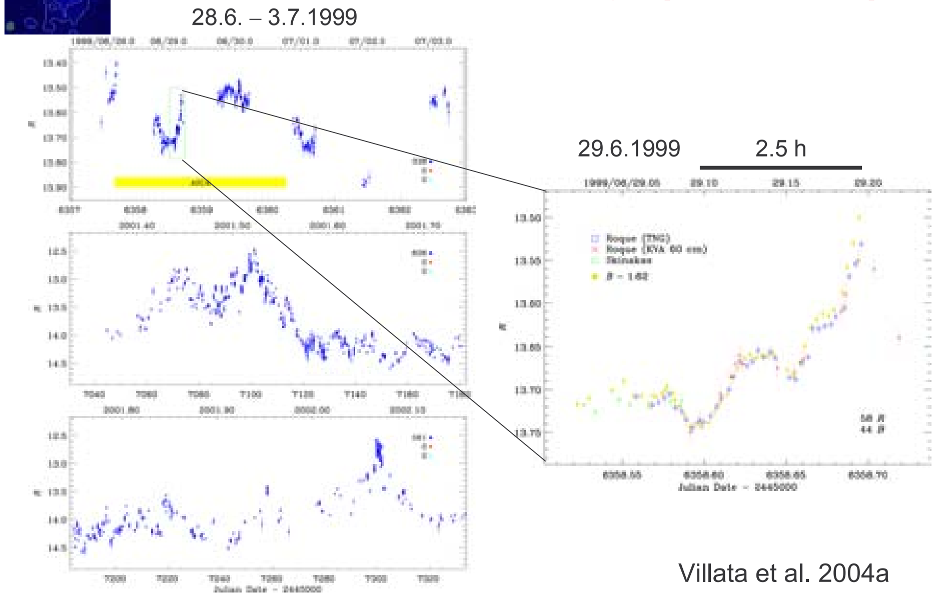

Villata et al. 2004a

Bluer when Brighter

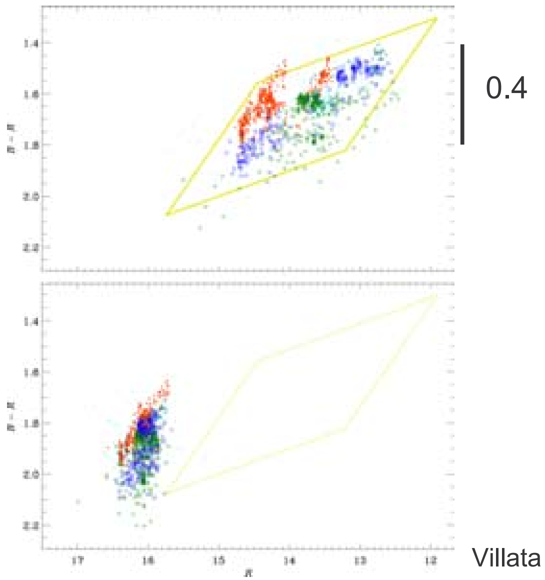

Villata et al. 2004a

Radio Variability (5-37 GHz)

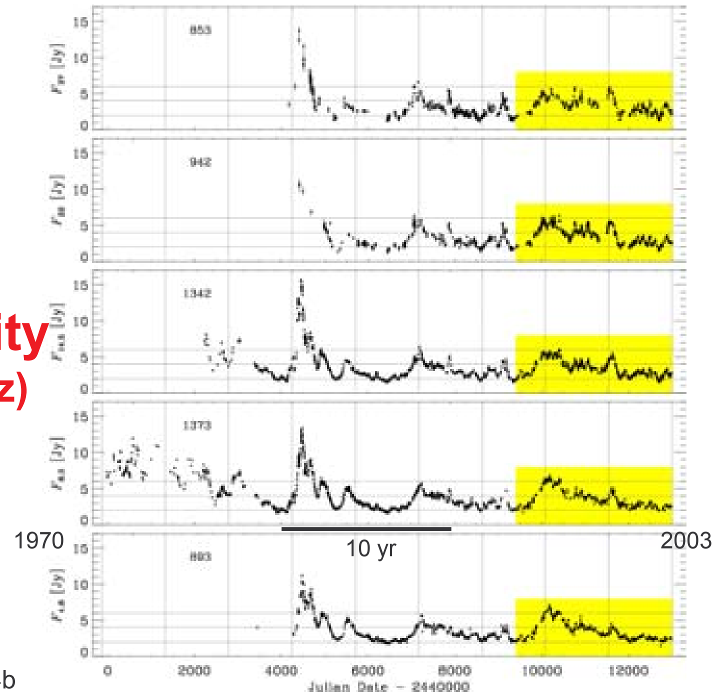

Villata et al. 2004b

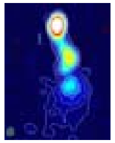

Correlated variability

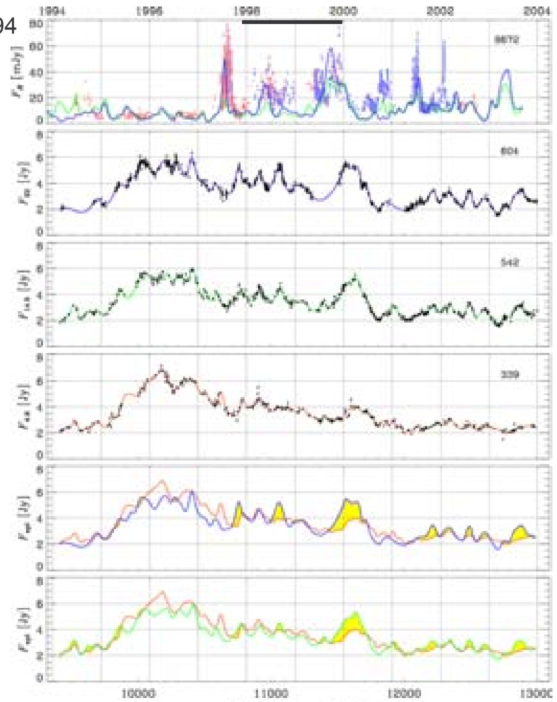

Villata et al. 2004b

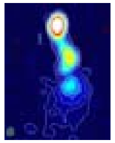

Very Long Baseline Interferometry (VLBI)

- 118 epochs of VLBI data since 1994 (~ 1 obs./month):
  - 41 at 43 GHz.
  - 21 at 22 GHz.
  - 22 at 15 GHz.
- 7 superluminal components with bend trajectories (Denn et al. 2000; Reynolds et al. 2004; Stirling et al. 2004).

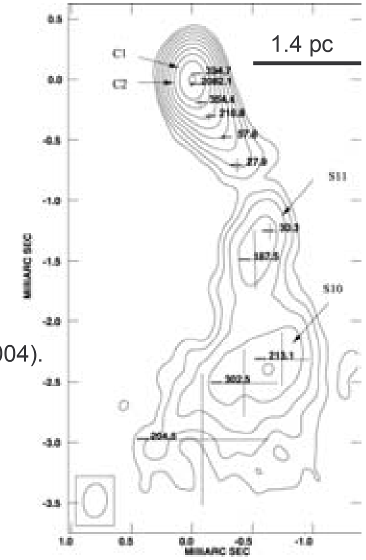

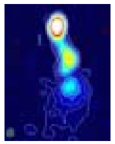

Jet Trajectories

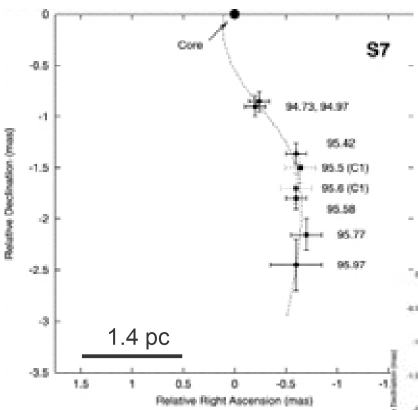

β_{app} = 2 - 6 c

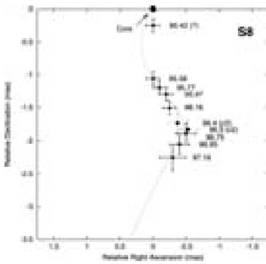

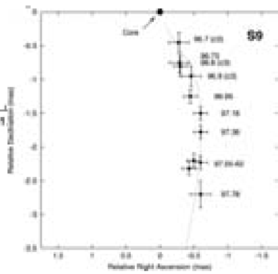

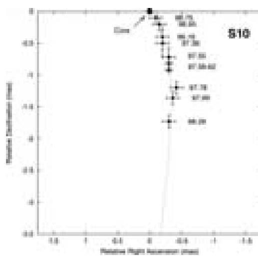

Denn et al. 2000

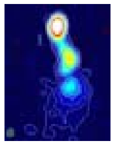

Ejection Dates

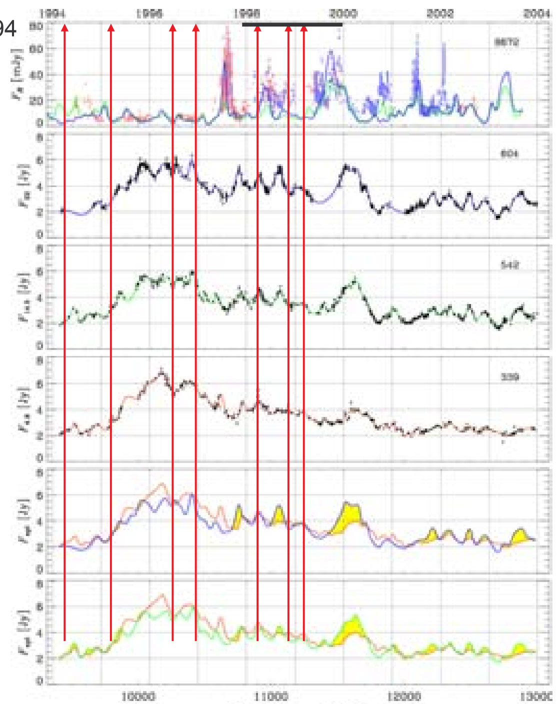

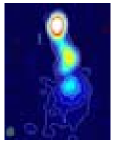

Precessing Jet?

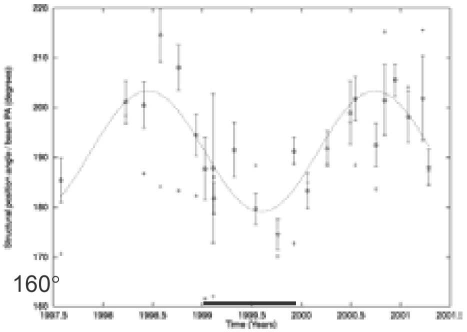

- Sinusoidal variation at the base of the radio jet (~2.3 yr).
- Same period was found in the EVPA at 7mm (VLBI) and at 1mm (single dish, HHT).
- A precessing jet model with β = 0.989 *c* and I = 9.2 ° can predict the component positions in the jet.

Stirling et al. 2004

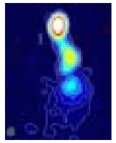

Summary

- Periodicities in the radio bands of about 3-4 yr and **8 yr** and a possible 8 yr period in the R-band.
- Optical variability:
  - a longer (few days) with mild chromatism (Doppler factor variations)
  - intra day variations with strong chromatism (particle acceleration or shocks)
- Radio variability:
  - mainly "soft" flares that propagate towards lower frequencies.
  - "harder" radio flares which show optical counterparts (optical leads by ~100 d).
- VLBI reveals:
  - superluminal jet with speeds of 2-6 *c*
  - precessing jet nozzle with a period of ~2.3 yr

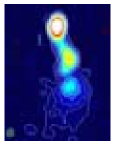

Outlook

- Update the optical and radio light-curves.
- Include IR and mm data.
- Comparison of the VLBI component data with the optical and radio light-curves:
  - ejection dates vs. flares.
  - ejection angle vs. flares.
  - polarization angle variability (VLBI vs. single-dish).
  - jet component light-curves vs. optical/radio l.-c.
  - …
- If necessary: Ask for archival VLBI data or propose new observations.

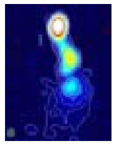

Outlook

- We proposed a multi-frequency radio monitoring of blazars between 1.6 GHz and 32 GHz at the antennas in Medicina and Noto including: 3C66A, 0235+16, 0716+714, OJ287, 0917+62 0954+658, 3C273, 3C279, 1633+38, 3C345, BL Lac, 3C454.3

Emmanouil (Manolis) Angelakis
Max-Planck-Institut für Radioastronomie

Elimination of Foreground Sources in the CBI Fields: Status Report and Results

In collaboration with:
MPIfR: A. Kraus , T. Krichbaum, A. Zensus
CALTECH: A. Readhead, T. Pearson, R. Bustos, R. Reeves

Supported by the RTN ENIGMA

Abstract

- **6000 point sources** (from the NVSS catalogue at 1.4 GHz)
  - At 4.85 GHz (6 cm) and 10.45 GHz (2.8 cm)

Do these sources contaminate the CMB data observed with the Cosmic Background Imager (CBI)?

➢ CBI FOREGROUND SUBTRACTION
➢ DISCOVER NEW CANDIDATES FOR VARIABILITY STUDIES etc.

The Cosmic Background Imager (CBI)

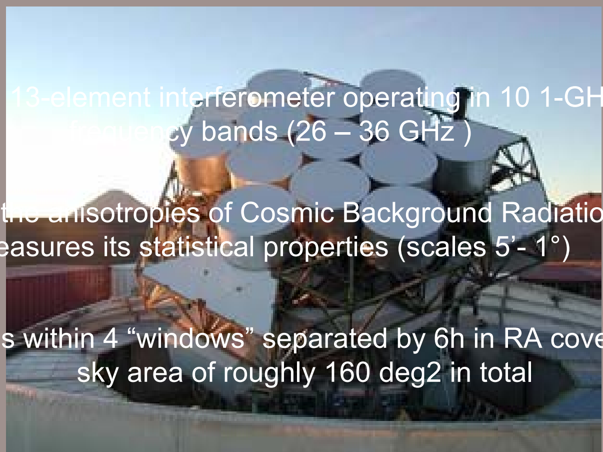

Is a 13-element interferometer operating in 10 1-GHz frequency bands (26 – 36 GHz)

Images the anisotropies of Cosmic Background Radiation and measures its statistical properties (scales 5'- 1°)

Observes within 4 “windows” separated by 6h in RA covering a sky area of roughly 160 deg2 in total

The target fields

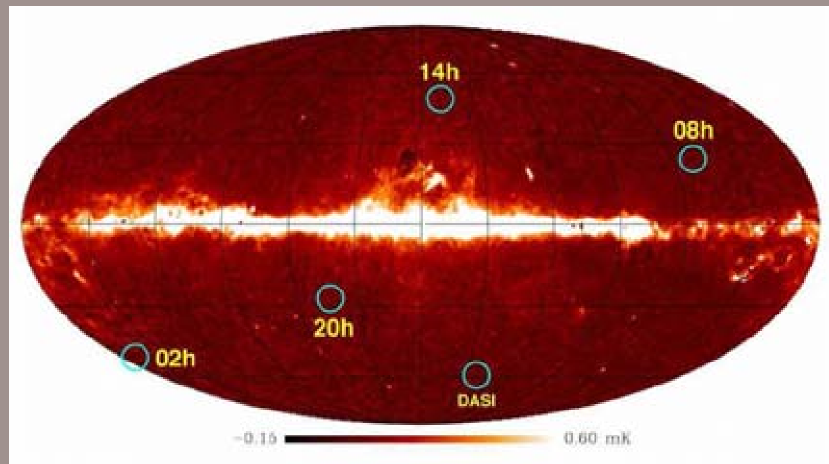

Motivation: The problem

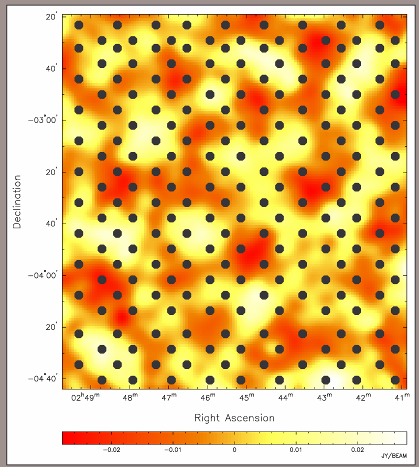

Motivation: The solution

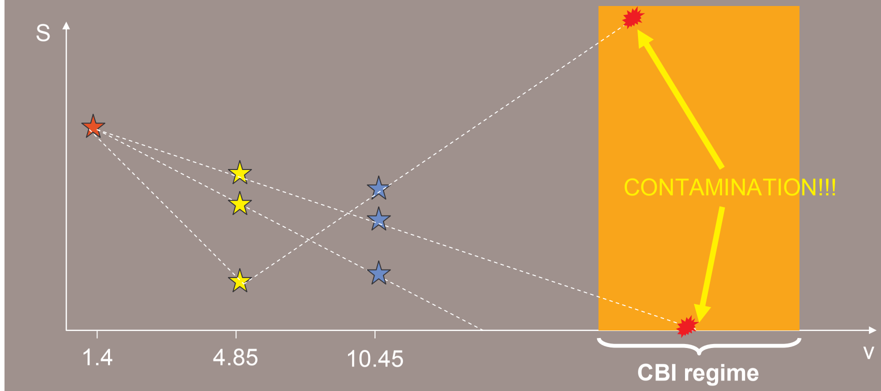

The solution

The 100-m telescope at Effelsberg

The “differential” observing method

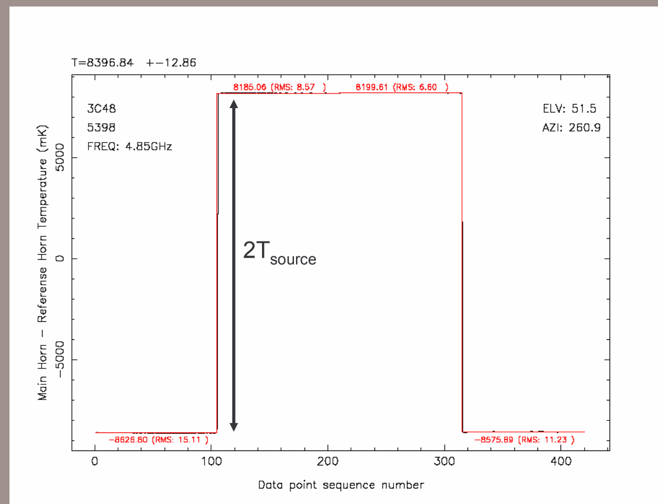

The “differential” observing method

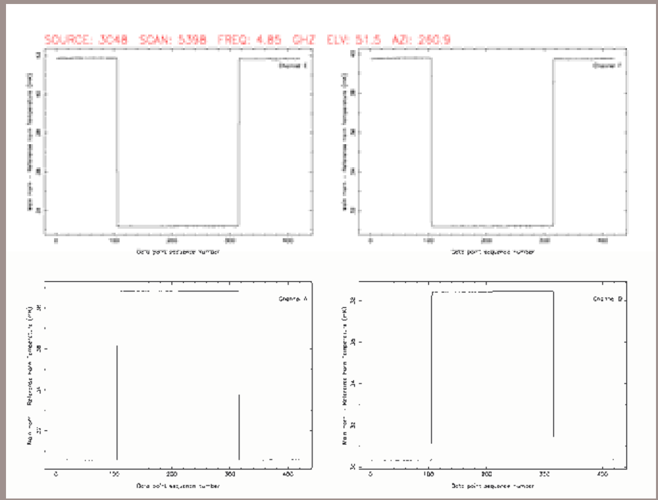

The efficiency of the observing method

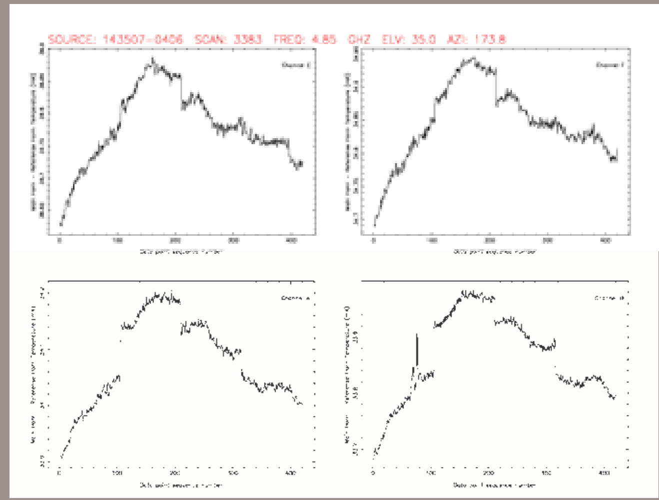

The efficiency of the observing method

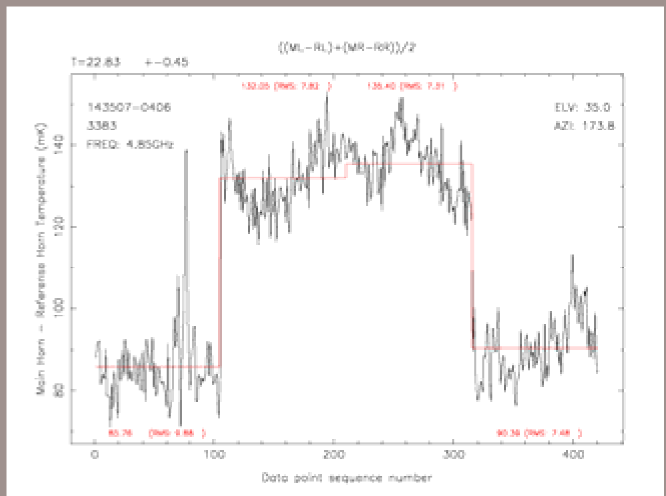

Problems: Weather

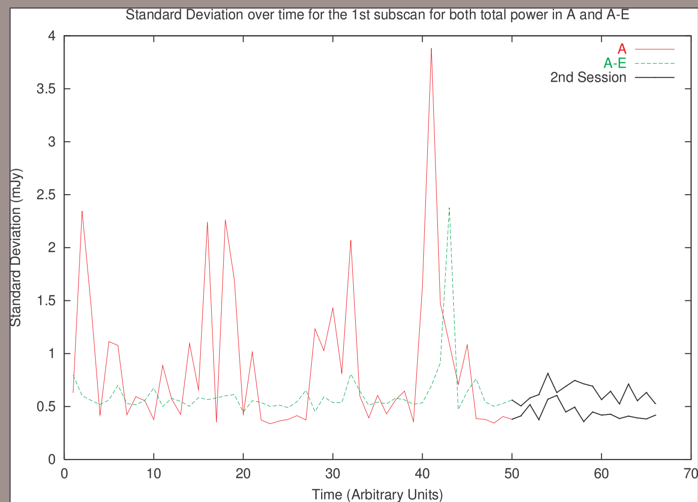

Problems: "Confusion"

It is estimated that at 4.85 GHz 50% of sources are confused!

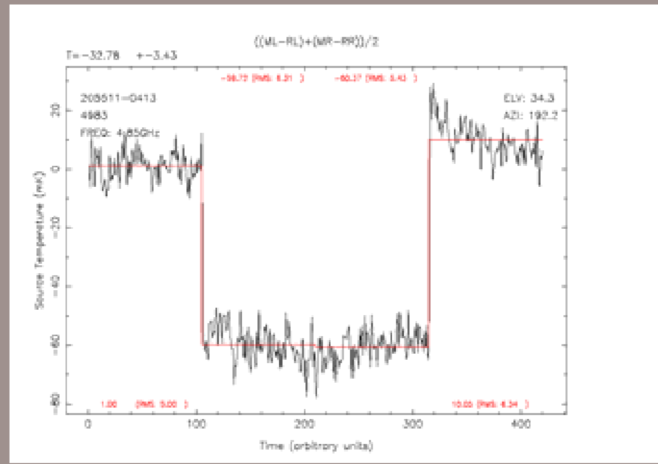

Problems: "T_{cal}" problem

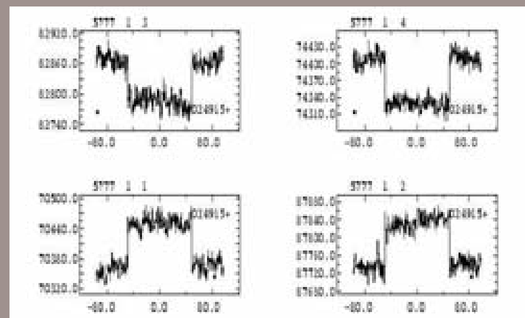

Problems: "T_{cal}" problem

$$CalibratedSignal = T_{cal}\frac{Sig}{Cal}$$

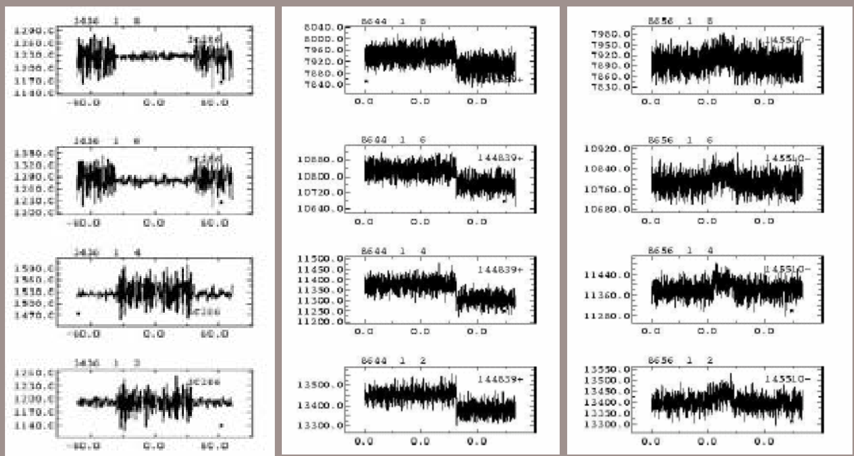

Problems: “T_{cal}” problem

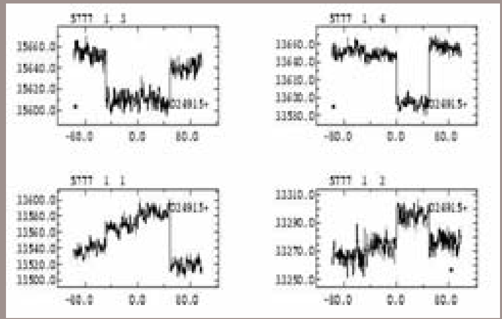

Problems: different T_{sys} over different channels

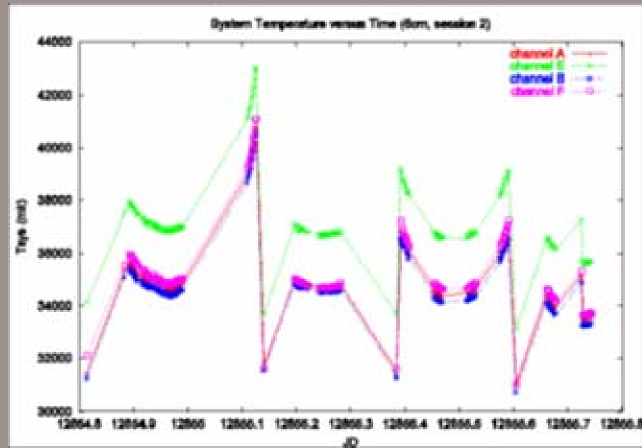

Problems: sensitivity

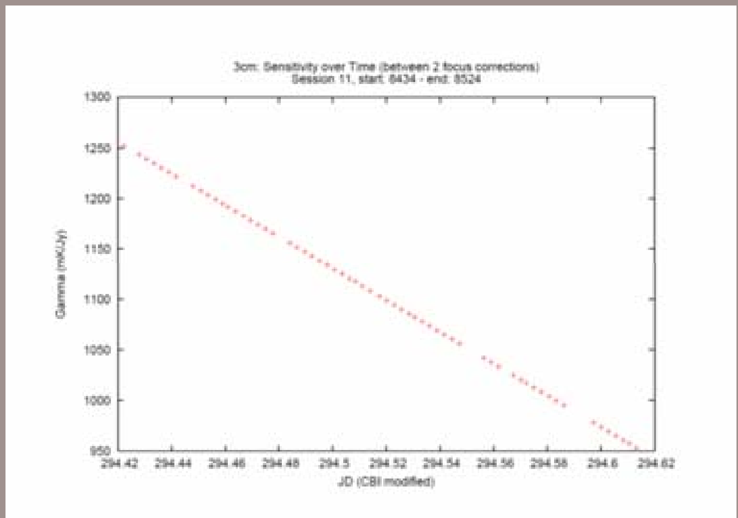

Observing strategy

1. Focus corrections
2. Pointing Corrections
3. Calibration
4. “Repeaters”

5. Loop of 12 target sources
6. Pointing check

7. Calibration with “blind” telescope

Data analysis

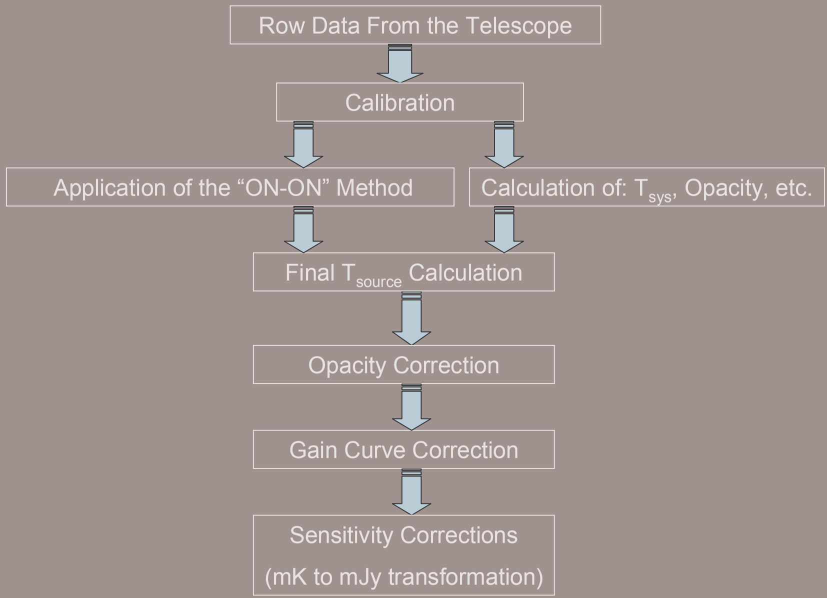

A "deep" observation

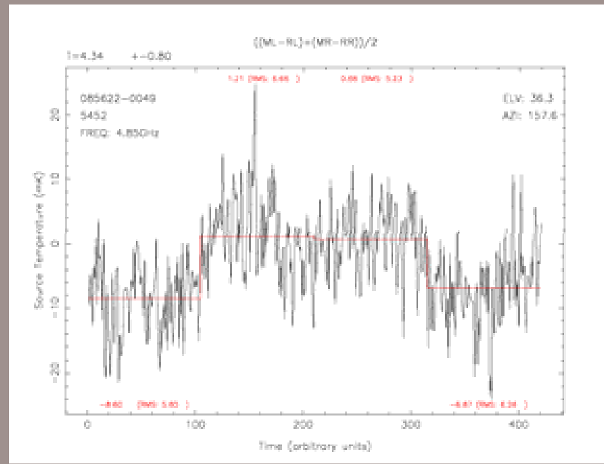

Field coverage

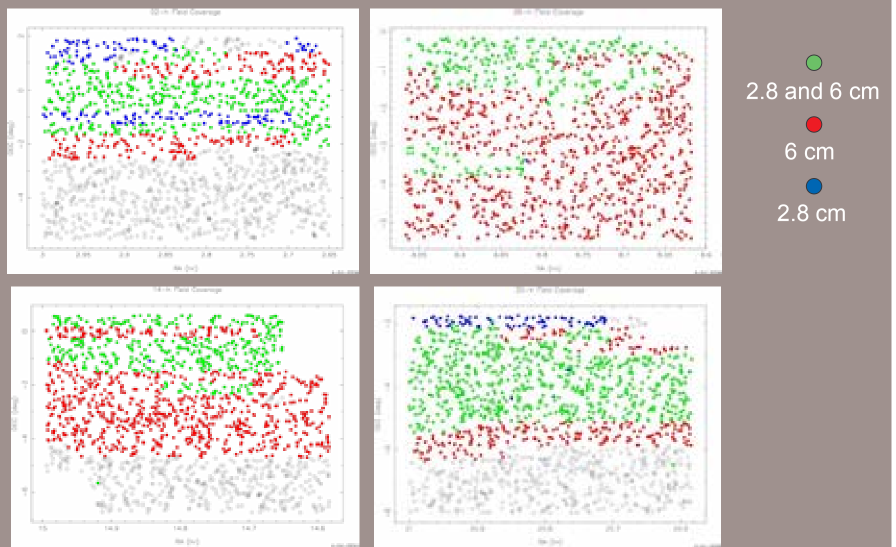

Recent results: Flux Density Distribution

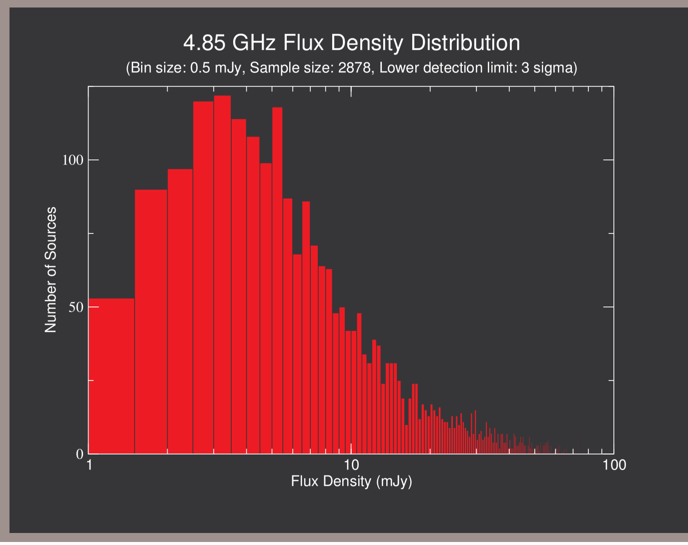

Recent results: Flux Density Distribution

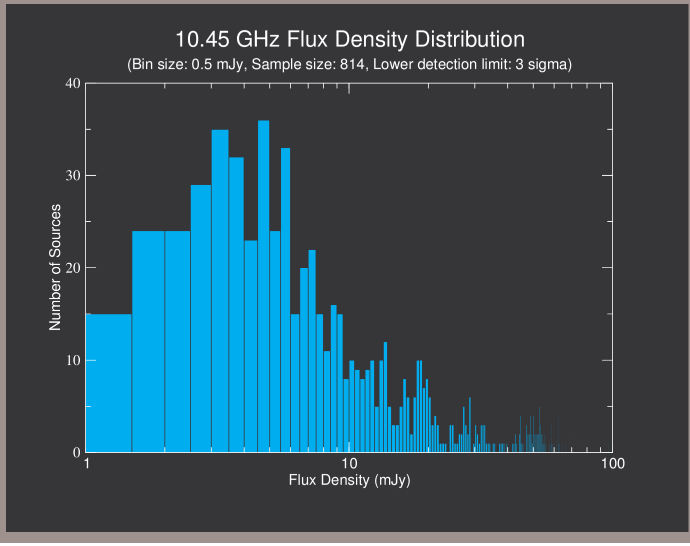

Recent results: Spectral Index Distribution

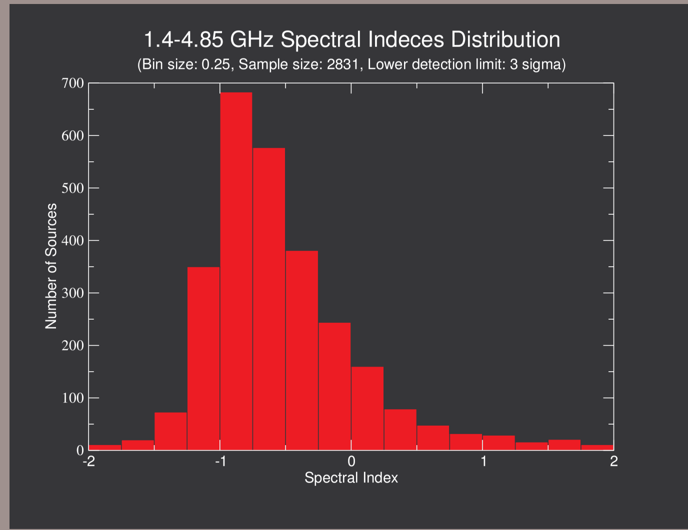

Recent results: Spectral Index Distribution

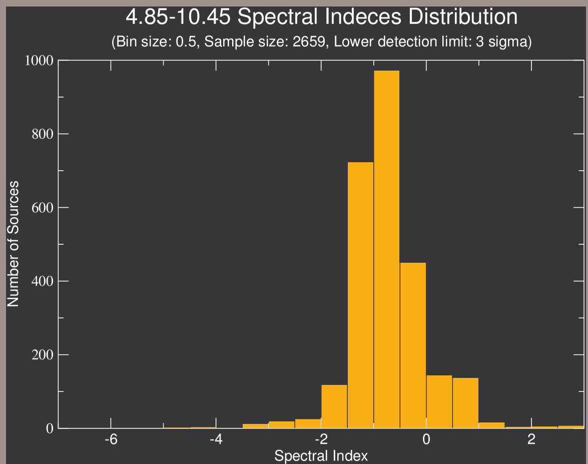

Recent results: Spectral Index Distribution

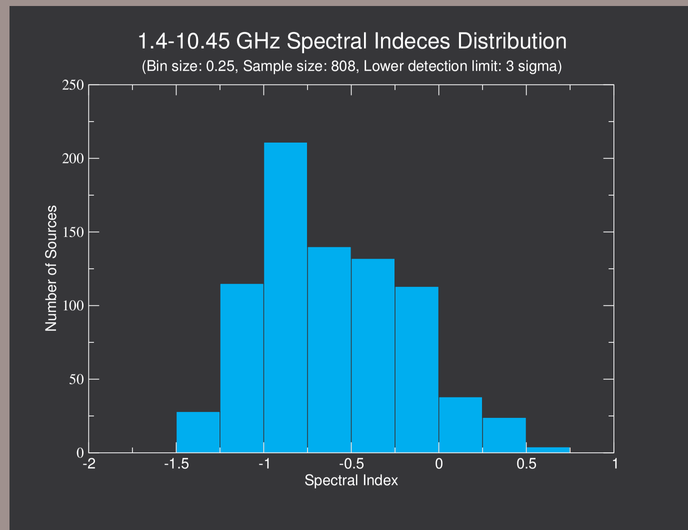

Recent results: Summary

- The ambition of reaching 1-3 mJy seems approachable
- Most sources (~70%) display a “steep” spectrum (α<-0.5)
- Significant number of sources (~30) display a “flat” or “inverted” (α>-0.5) spectrum being possible candidates for variability studies

Recent results: Flat and/or Inverted Spectra

Source	S_{22} (mJy)	S_6 (mJy)	$S_{2.8}$ (mJy)	α_6^{22}	$\alpha_{2.8}^{22}$	$\alpha_{2.8}^{6}$
022923+0105	22.6	42.7	-	0.512	-	-
024050-0138	5.0	42.0	-	1.713	-	-
024138+0027	5.1	32.5	-	1.489	-	-
024203-0128	14.9	49.6	-	0.969	-	-
024342-0103	5.6	15.2	-	0.805	-	-
025156+0057	6.3	21.5	-	0.988	-	-
025233+0101	5.4	10.5	-	0.533	-	-
084025-0321	9.4	18.2	-	0.534	-	-
084031-0315	12.2	12.2	-	0.637	-	-
084050-0046	12.8	73.4	-	1.405	-	-
084549-0052	10.8	29.0	-	0.795	-	-
085031-0016	6.1	12.2	-	0.555	-	-
085212-0404	9.2	20.8	-	0.655	-	-
085630-0400	20.5	45.6	-	0.643	-	-
145002+0016	10.9	23.1	-	0.606	-	-
145202+0033	14.0	79.0	-	1.392	-	-
203511-0518	12.0	65.7	-	1.369	-	-
203641-0507	5.2	39.0	-	1.622	-	-
203742-0505	6.1	14.7	-	0.708	-	-
203807-0527	17.3	55.2	-	0.933	-	-
204038-0536	7.7	20.1	-	0.770	-	-
204235-0535	8.6	21.6	-	0.740	-	-
204250-0546	8.9	35.9	-	1.122	-	-
204305-0549	8.7	53.0	-	1.454	-	-
204740-0246	5.1	19.3	-	1.071	-	-
205157-0206	5.5	21.8	2.68	1.109	(-0.358)	(-2.722)
025333+0024	17.4	-	53.0	-	0.554	-
025515+0037	30.5	28.9	47.1	(-0.043)	(0.216)	0.635
025528+0144	27.7	31.3	52.2	(0.099)	(0.315)	0.666

Immediate future plans

“CBI” PROJECT:

- Completion of the observations and data reduction
- Detailed study of the stability of the system (repeatability)
- Development of sophisticated algorithms to check the confusion problem
- Data Publication within summer 2004
- On-line database development

“INVERTED SPECTRA” PROJECT:

- Further study of the inverted spectrum sources: Simultaneous observations at 6, 2.8, 0.9 cm and high frequency mapping of their vicinities

I appreciate your attention!

On behalf of:

MPIfR: A. Kraus , T. Krichbaum, A. Witzel, A. Zensus

CALTECH: A. Readhead, T. Pearson, R. Bustos, R. Reeves

Seasonal Cycles in IDV Blazar Cores and new Projects as ENIGMA Post-doc

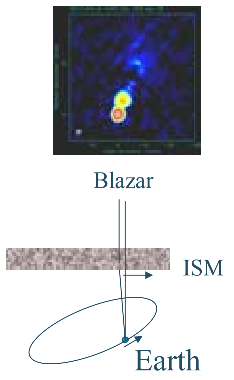

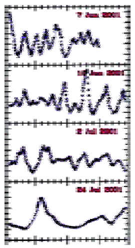

Lars Fuhrmann,
Perugia Team

T.P. Krichbaum, A. Witzel, T. Beckert,
G. Cimò, A. Kraus, S.J. Qian,
J.A. Zensus, MPIfR
and
B. Rickett, U. C. San Diego
and
G. Tosti, Perugia Team

ENIGMA meeting, Oct. 2004

Overview

- **Part I:** Seasonal Cycles in IDV Blazars - Model Predictions vs. Observations
- The Case of Quasar 0917+624: Effelsberg 4.85 GHz IDV Monitoring and 15 GHz VLBI Observations
- A new Candidate: The BL Lac 0954+658
- **Part II:** New projects as ENIGMA Post-doc

Explanations for radio IDV

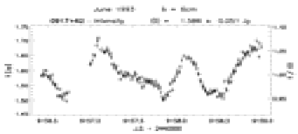

0917+624 @ 5 GHz

intrinsic or extrinsic or both ?

Source intrinsic IDV:

- relativistic beaming requires extremely high Doppler factors: D ~ 100 – 1000
  observed: D ~ 10 – 40

$$T_B^{obs} \simeq \left(\frac{D}{1+z}\right)^3 \cdot T_B$$

- 'fine-tuning' of shock-in-jet models towards IDV time scales: special source geometries and small viewing angles

Interstellar Scintillation (ISS):

- IDVs are small ! → must scintillate through the ISM
- local screen: irregularities in the electron density driven by turbulence

Explanations for IDV (cont.)

- new IDV type (?): "extreme" IDV sources with $\Delta S \sim 300\%$ and $t_{IDV} \sim 0.5$ hrs (e.g. Dennett-Thorpe & de Bruyn 2000)
  PKS 0405-385, PKS 1257-326 and J1819+3845
- time delay measurements (e.g. Jauncey et al. 2000) and annual modulation: ISS origin for extreme IDV sources

Part I Annual Modulation in IDV

- Seasonal Cycles due to the Earth orbital Motion: Model Predictions vs. Observations
- Effelsberg 4.85 GHz IDV Monitoring
- VLBI Observations of quasar 0917+624

- new phenomenon in IDV studies Dennett-Thorpe & de Bruyn (2000, 2003):

➔ seasonal cycle in the extreme IDV source J1819+3845

- relative velocity v changes as earth evolves around Sun
- $t_{ISS} = s_0 / v$, spacial scale $s_0 \sim D \cdot \theta_S$

J1819+3845

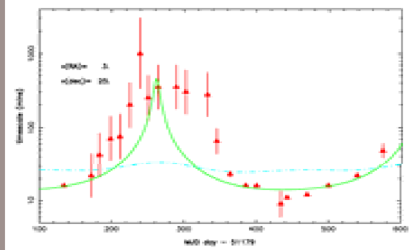

Westerbork 5 GHz

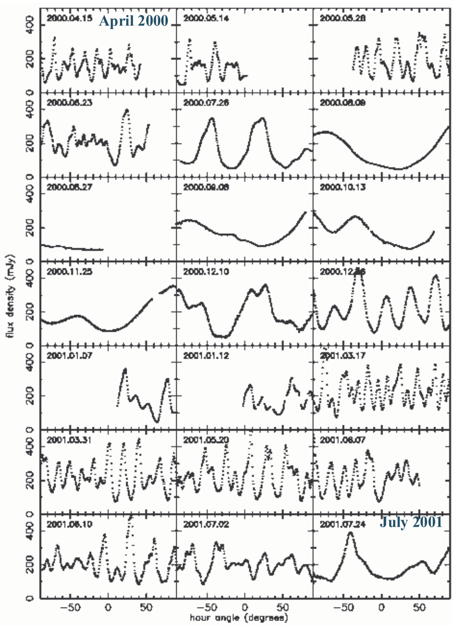

Applications to the medium and the source structure:

- the detection and fitting of seasonal cycles reveal:
  - ISS origin of IDV !
  - θ_S, LSR velocity of the medium (V_{RA} , V_{Dec}) and distance D; anisotropy in source structure and/or scattering medium (axial ratio, orientation)

➔ PKS 1257-326 (Bignall et al. 2003):

V_{RA} = 5 km/s, V_{Dec} = 0 km/s;
D = 10–15 pc; θ = 30–37 µas
axial ratio < 0.5; orientation: 25°

Model Predictions vs. Observations

The Case of 0917+624

- Quasar 0917+624 at z = 1.446
- always strong IDV since 1987 (10 - 20%, 0.5 – 1.6 days)
- September 1998: dramatic change in IDV properties (Kraus et al. 1999)

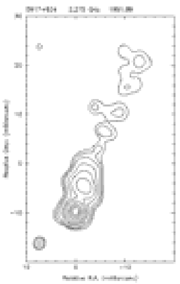

Standke et al. 1996

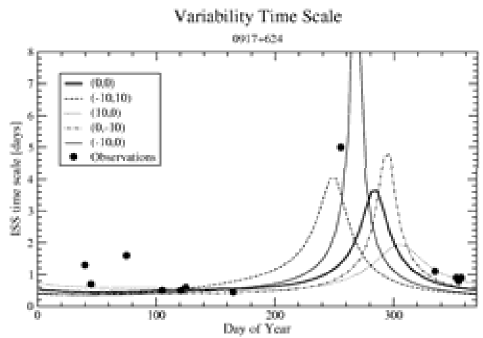

4.85 GHz data obtained between 1989 - 2000 (Effelsberg, VLA)

D = 150pc
θ = 70 µas

Effelsberg 4.85 GHz IDV Monitoring

- 2.5 years monitoring between 2000 and 2003 (28 sessions, duration between 5 and 65 hrs)
- main targets: 0917+624, 0716+710, 0954+658
- cross-scans with dense time sampling (~ 2 scans every 1.5 h)
- equal duty cycle for secondary calibrators 0836+710 and 0951+699
- primary calibrators every 2 – 3 hrs (3C286, 3C48, 3C295, NGC7027)
- final measurement errors: in the range of 0.5 – 1 %

Effelsberg 4.85 GHz IDV Monitoring

- IDV analysis: modulation index m, variability amplitude Y, χ^2 – test

$$Y[\%] = 3\sqrt{m^2 - m_0^2} \qquad \chi^2 = \sum_{i=1}^{N} \left(\frac{S_i - \langle S \rangle}{\Delta S_i} \right)^2$$

- time scale analysis: structure functions

$$SF(\tau) = \langle (S(t) - S(t+\tau))^2 \rangle_t$$

$$t_{IDV} = \left(\frac{\rho_0}{a} \right)^{1/\beta}$$

$$m = (0.5 \cdot \rho_0)^{1/2}$$

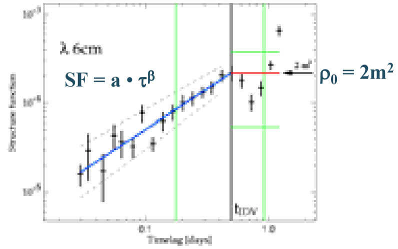

0917+624

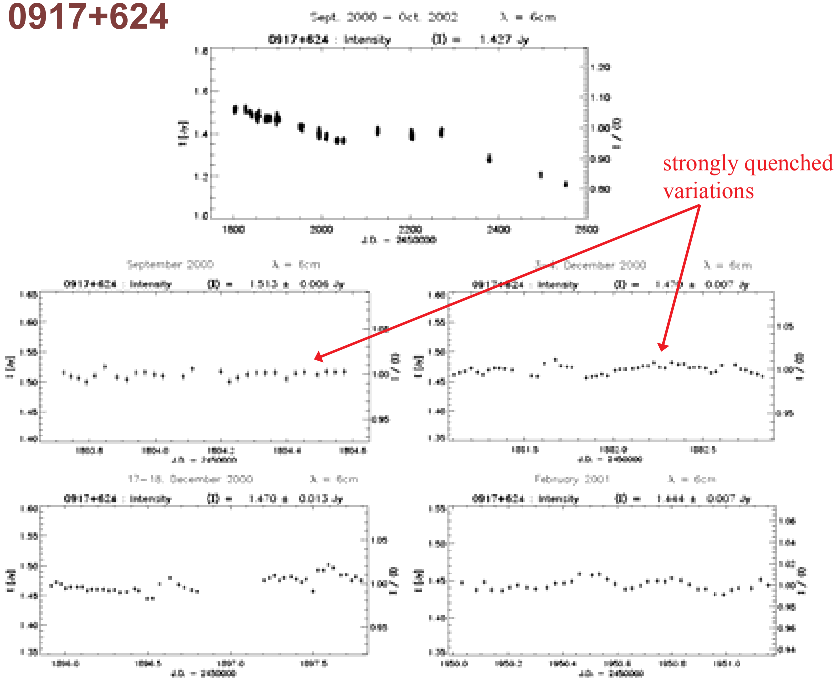

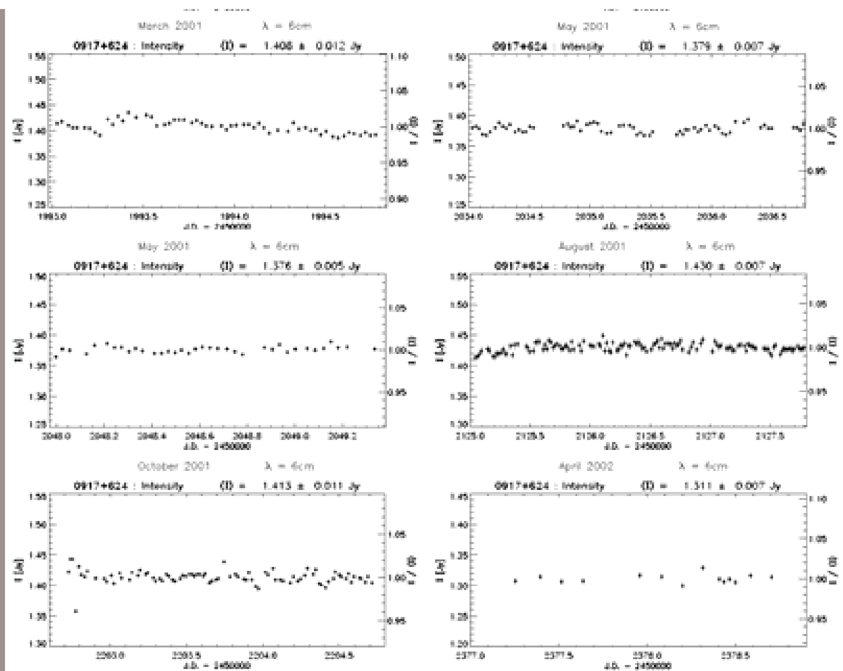

Summary for 0917+624

- dramatic change of IDV properties
- since 2000, pronounced IDV completely missing
- only low amplitude variations: m ≤ 0.8 % (past: m = 4 – 5 %)

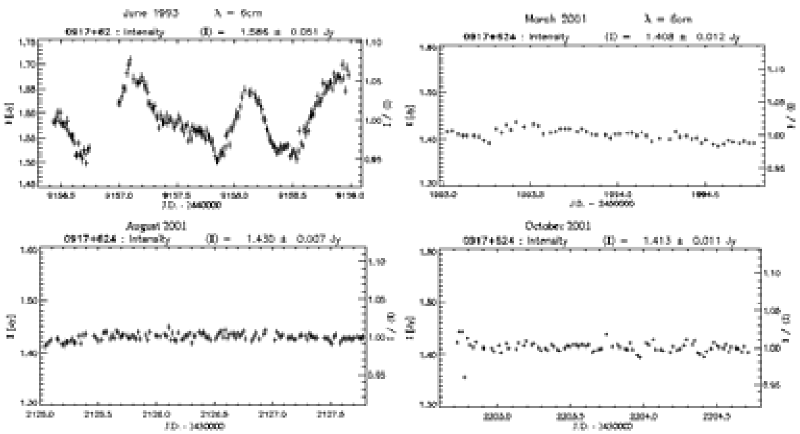

Summary for 0917+624 (cont.)

- annual modulation ? problems:
  - no restart of rapid IDV
  - m appears to be strongly variable
- two possible scenarios:

i) Changes in the scattering medium

- ISM much more complex: decrease in the strength of turbulence or increase in distance

$$m^2 \sim D^{-0.3} < C_n^2 >$$

- m ~ 0.5 % (present): requires decrease of $<C_n^2>$ by factor ~ 130 or increase in distance ~ kpc

➔ moving foreground layer?

Summary for 0917+624 (cont.)

ii) Intrinsic changes in the source structure

- disappearance of the scintillating component(s) or increase in size

➔ e.g. blend of core with newly ejected jet component
➔ extremely quenched scintillations
➔ new VLBI observations

VLBI observations of 0917+624 at 15 GHz

- strongly quenched scintillations due to structural changes in the core region ?

➔ new jet component(s) and thus temporary larger size of scintillating component

- VLBI observations should reveal new jet component(s) ejected shortly before 0917+624 ceased varying
- Krichbaum et al. (2000): first 3 epochs (VLBA + Effelsberg) at 15 GHz between 1999 and 2000
- 3 new epochs between December 2001 and July 2002

VLBI observations of 0917+624 at 15 GHz

Epochs 1 – 3: 1999 – 2000

Krichbaum et al. (2000)

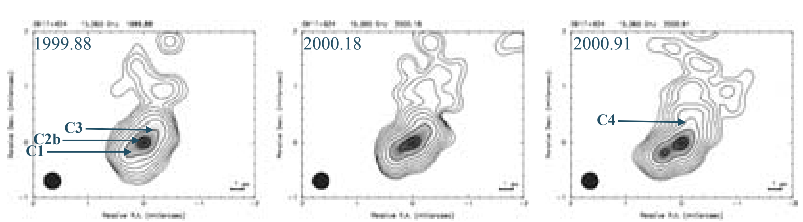

- bent core-jet morphology
- 2 central components: separating with ~ 0.17 mas/yr (β_{app}= 5.8)
- ejection date of C2b: 1998.1

VLBI observations of 0917+624 at 15 GHz

Epochs 4 – 6: 2001 – 2002

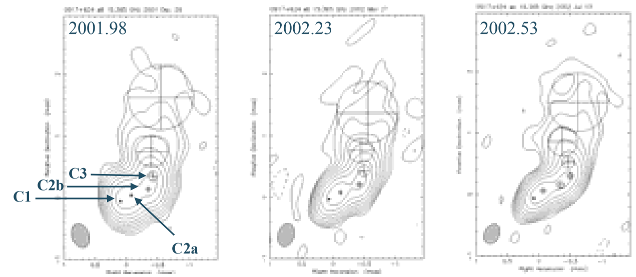

- bent core-jet structure
- new component C2a
- cross-identification with epochs 1 - 3

VLBI observations of 0917+624 at 15 GHz

Component Motion

- ejection of components during flux density outbursts
- C2b: ejection date 1998.3
- Sept. 98: core separation of 0.07mas
- blend of core with component C2b:

➔ ISS model yields m_{6cm}= 2.3%, t_{IDV} = 7 days for screen at 150pc observed: m_{6cm}= 1.8%, t_{IDV} > 5 d

➔ strongly quenched scattering rather than seasonal cycle !

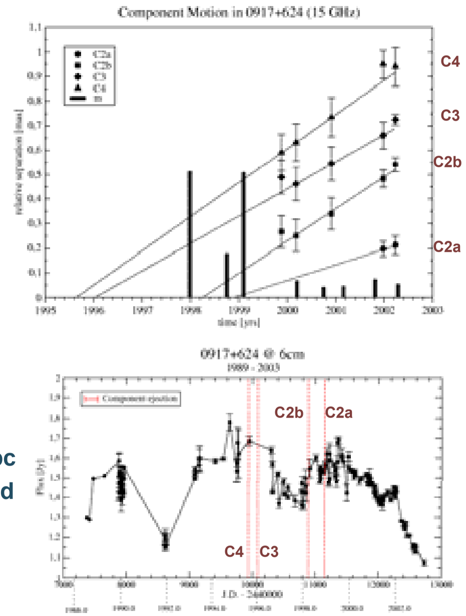

VLBI observations of 0917+624 at 15 GHz

- C2a: ejection around 1999.0
- similar scenario likely for present inactivity, but:

more components are needed !

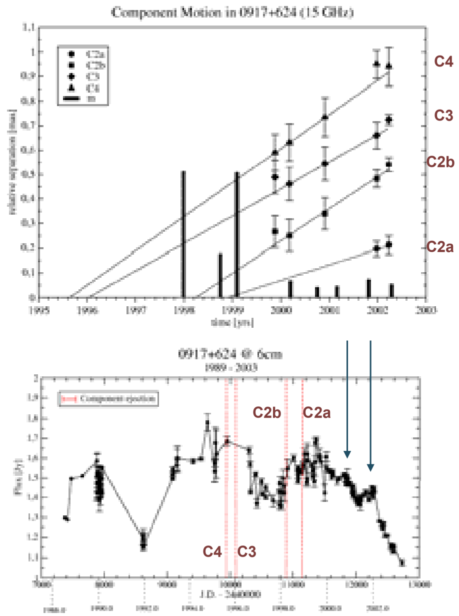

0954+658

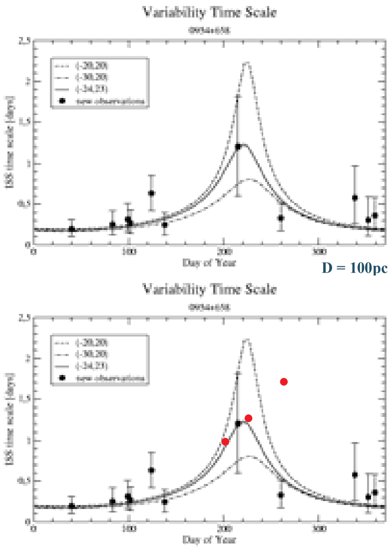

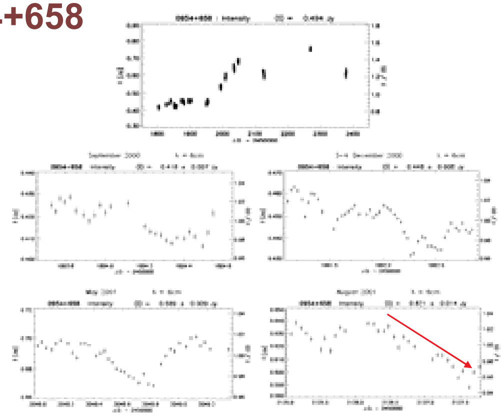

- scatter of m low (m ~ 1.1 – 2.4 %)
- t_{IDV} ~ 0.3 days, but August 2001: ~ 1.2 days !

➔ seasonal cycle ! ???

new IDV observations in July, August and September 2004

New Projects as ENIGMA Post-doc

- Multi-frequency monitoring of Blazars with Medicina and Noto @ 1.6 – 32 GHz
  (Torino + Perugia Team)

  - simultaneous broad band radio spectra and their evolution
  - Data will complement other campaigns/observations (X-ray, optical, radio, VLBI, WEBT…)

  ➔ multi-frequency studies

- REM telescope: optical monitoring of a Blazar sample (+ high energy satellite targets)

  - schedule and data reduction

- ongoing IDV projects

High Energies and Theory

High Energy observations and multifrequency campaigns

Leo Takalo

- Campaigns 2003-2004:
- S5 0716+714 (INTEGRAL; 5/5; S. Wagner)
- AO 0235+164 (XMM; 6/15; C. Raiteri)
- 3C 66A (RXTE; 7/9; M. Böttcher)
- PKS 2155-304 (HESS; S. Wagner)

PKS 2155-304 campaign: KVA observations

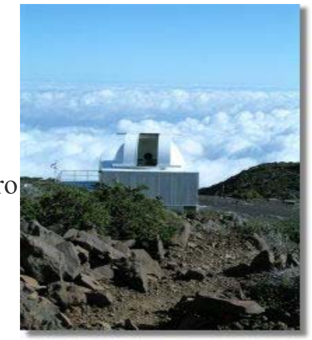

- Observers: Elina Lindfors, Stefano Ciprini, Luisa Ostorero
- Data reduction and analysis: Kari Nilsson
- 12 intra-nights, 404 total photometric data points in R-band obtained during the RXTE and HESS pointings

August 02./03., 10 R-band frames, telescope: KVA, Observer: Luisa Ostorero
August 9./10., 50 R-band frames, telescope: KVA, Observer: Stefano Ciprini
August 13./14., 50 R-band frames, telescope: KVA, Observer: Luisa Ostorero
August 17./18., 45 R-band frames, telescope: KVA, Observer: Stefano Ciprini
September 07./08., 32 R-band frames, telescope: KVA, Observer: Elina Lindfors
September 08./09., 40 R-band frames, telescope: KVA, Observer: Elina Lindfors
September 09./10., 45 R-band frames, telescope: KVA, Observer: Elina Lindfors
September 10./11., 35 R-band frames, telescope: KVA, Observer: Elina Lindfors
September 11./12., 40 R-band frames, telescope: KVA, Observer: Elina Lindfors
September 13./14., 20 R-band frames, telescope: KVA, Observer: Elina Lindfors
September 21./22., 12 R-band frames), telescope: KVA, Observer: Elina Lindfors
September 22./23., 25 R-band frames, telescope: KVA, Observer: Elina Lindfors

PKS 2155-304 campaign: KVA total binned light curve in R-band

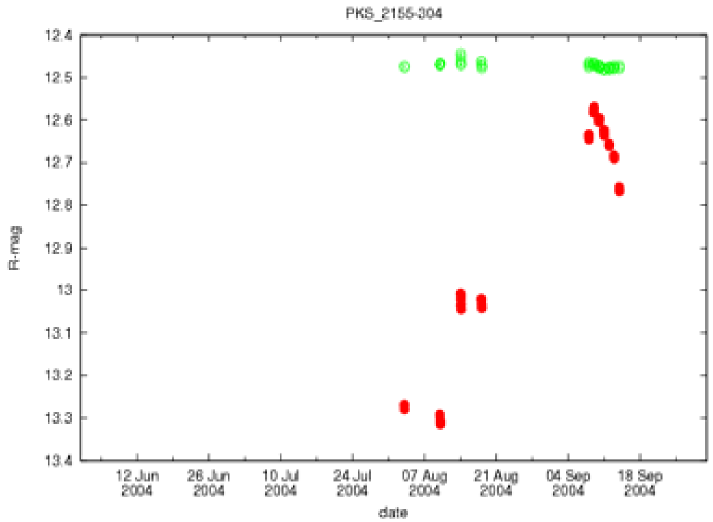

PKS 2155-304 campaign: example of two KVA intra-nights

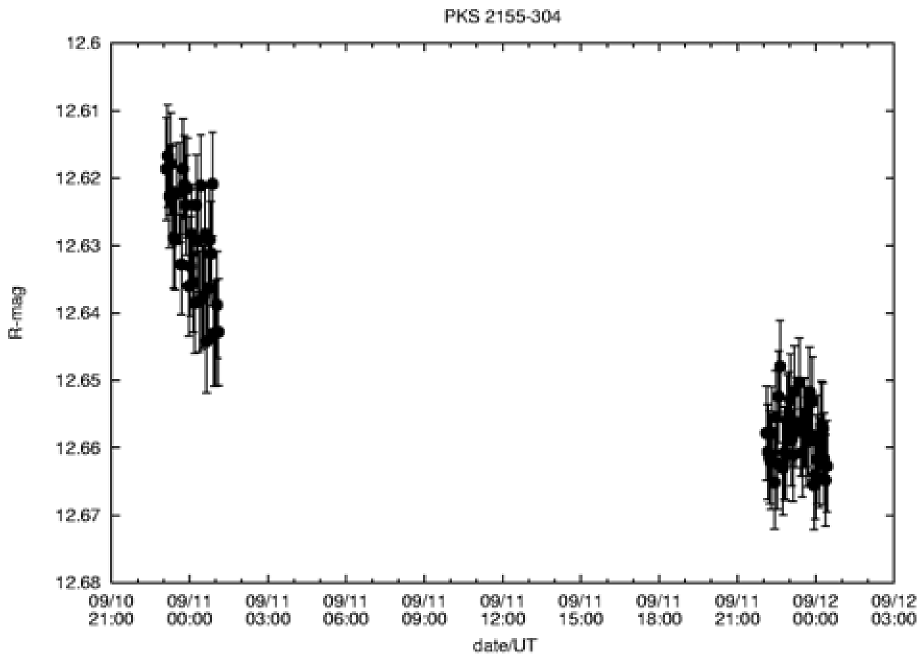

Multiwavelength Observing Campaign on 3C 66A

Sept. 20 - Dec. 15, 2003

First Results

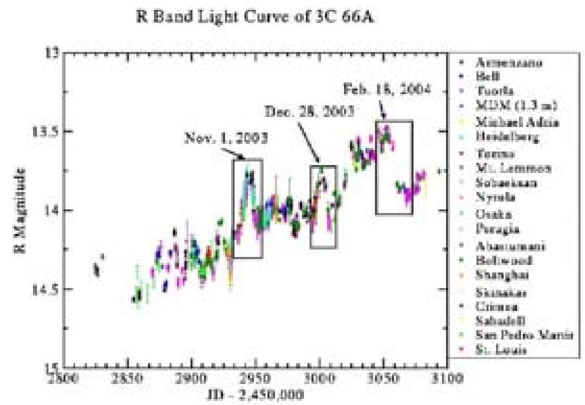

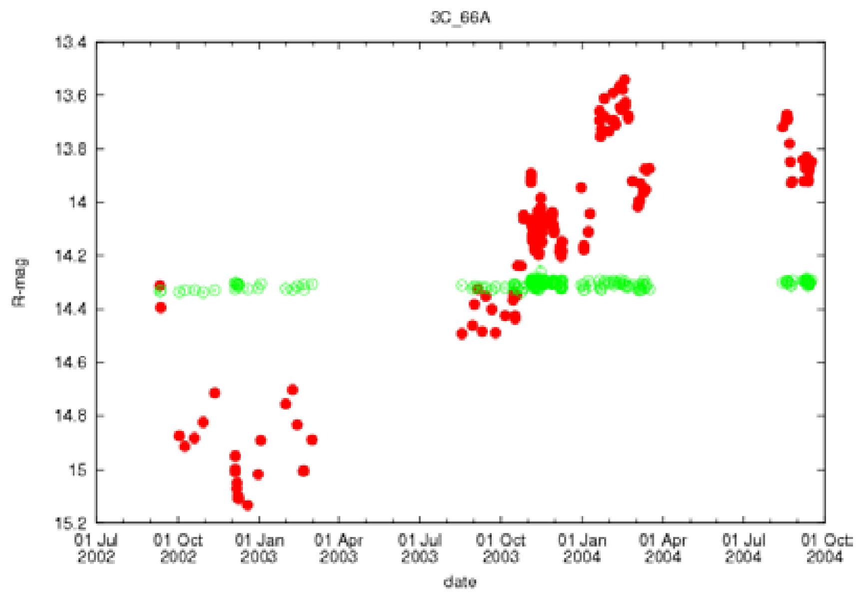

VLBAobservations

- Frequences: 2,5,8,22,43,86 Ghz
- Polarization
- 9 Epochs (so far 7 observed)
- Some results by Tuomas Savolainen

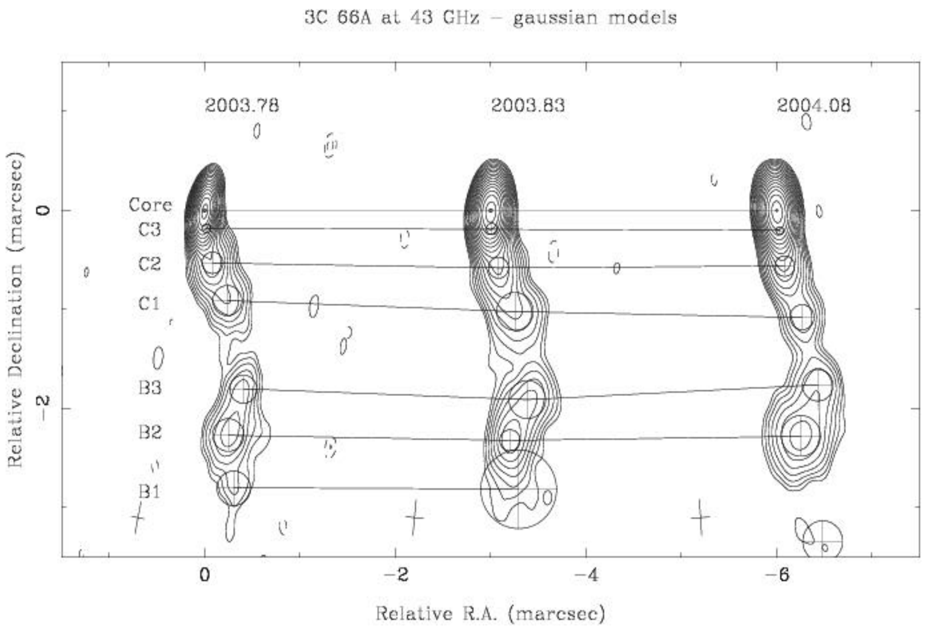

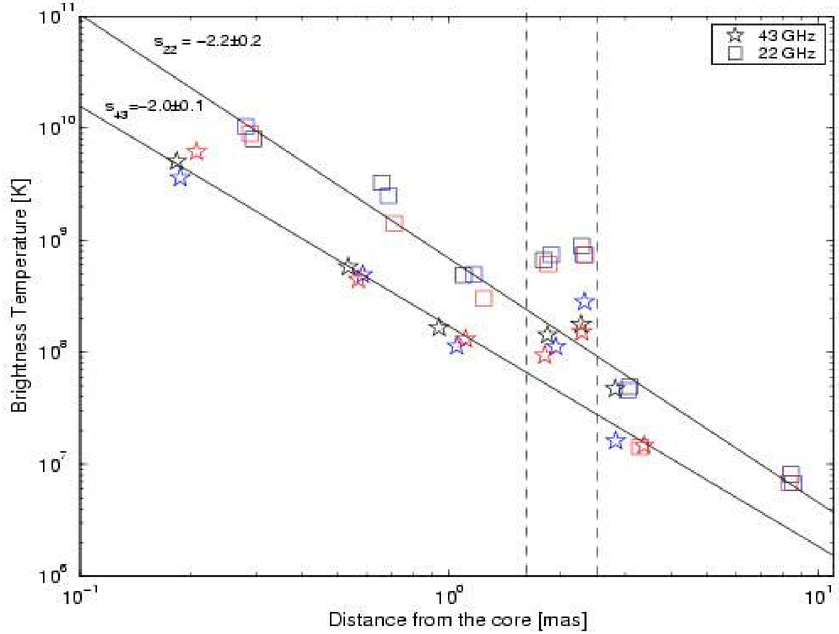

- New Campaigns:
- AO 0235+164 (Continued from last season)
- OJ 287 (L. Takalo?)
- From 11.2004 to 5.2008!!!
- VLBA; WEBT; XMM; INTEGRAL; MAGIC;
- SWIFT; AGILE; CHANDRA; ?????
- Outbursts September 2006 and November 2007!!!
-

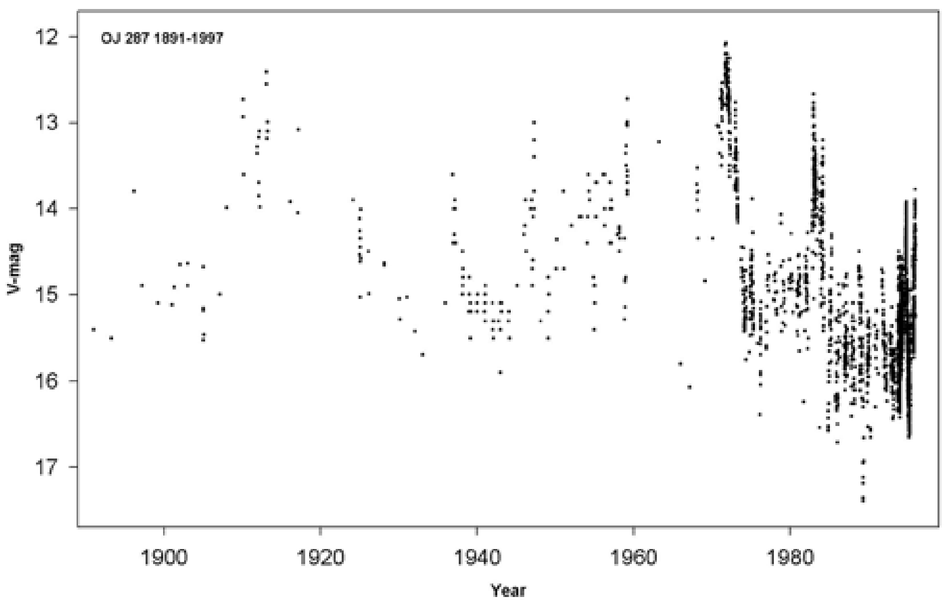

Prediction by Aimo

OJ287 with a strict outburst periodicity of 11.86 year

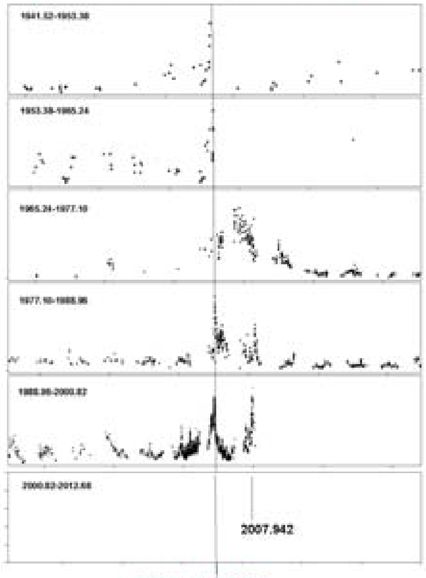

2006.742 (28.9.2006)

- Archive: www.astro.utu.fi/enigma.html
- user: **********
- password:********
- Tuorla/KVA light curves: http://users.utu.fi/kani/1m/index.html

X-Ray Variability Studies of TeV Blazars.

Dimitrios Emmanoulopoulos
Stefan Wagner

ENIGMA meeting Perugia, October 6-8 October 2004

Landessternwarte Heidelberg

Overview

- Final lightcurve for MKN421 from 1996-2003 (PCA results).
- Direct comparison PCA and ASM.
- Structure Function Analysis.
- Characteristic Time Scales.

Short update on the October-November 2003 X-ray observations of PKS2155-304

Final results for MKN421

The PCA archive consists of 11 observations (1996-2003)

Final results for MKN421

Proposal number	Earliest obs.	Latest obs.
10345	**15/3/96 13:18:24**	19/4/96 02:01:04
10341	1/3/96 06:08:00	1/3/96 06:46:56
20341	2/4/97 03:30:24	3/6/97 06:34:40
30261	24/3/98 00:52:16	13/4/98 07:37:36
30262	18/4/98 11:36:00	8/5/98 20:58:40
30269	26/2/98 13:27:44	25/7/98 22:40:48
40182	5/2/00 03:33:52	8/5/00 22:23:34
50190	24/01/01 01:04:48	6/2/01 16:10:08
60145	18/3/01 03:30:24	1/4/01 09:07:44
70161	2/12/02 04:33:04	14/1/03 13:10:08
80172	26/02/03 14:49:36	**6/3/03 11:24:32**

Final results for MKN421

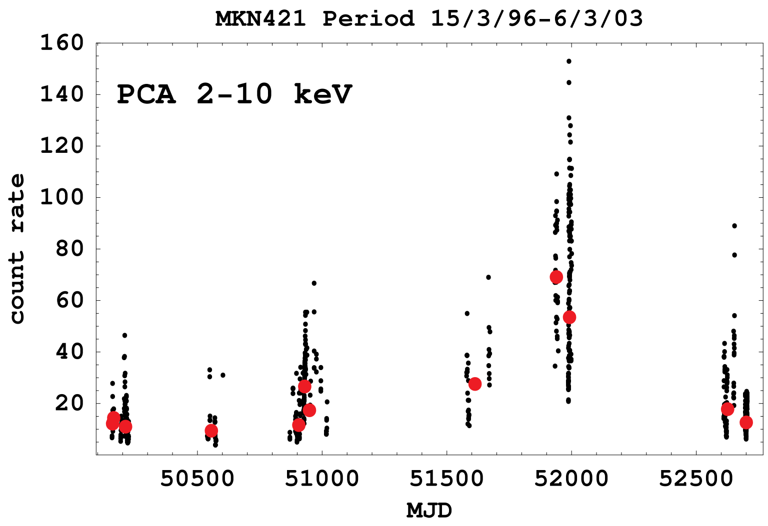

Final results for MKN421

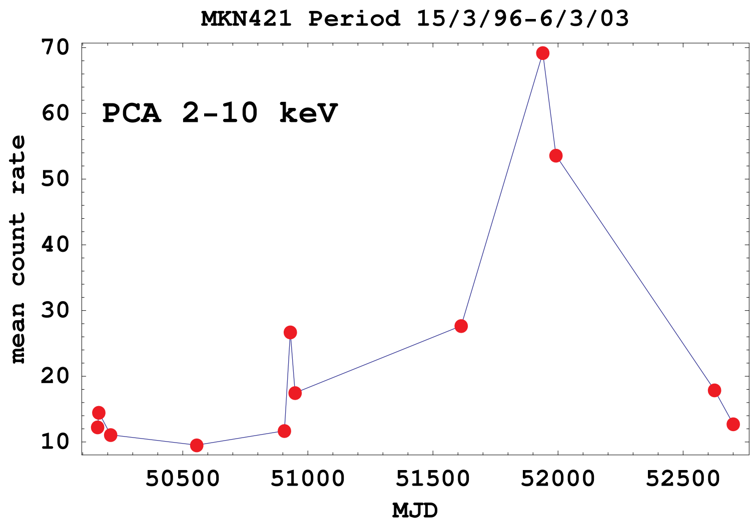

Final results for MKN421

1) We have an extended excitation of the source which lasts $\sim$ 1500 days.

2) The activity of the source before and after this excitation may represent a “quiescent” period of MKN421.

3)Variability patterns on short time scales (minutes, hours, days) are superimposed on a bigger and slower variable pattern.

Direct comparison ASM and PCA

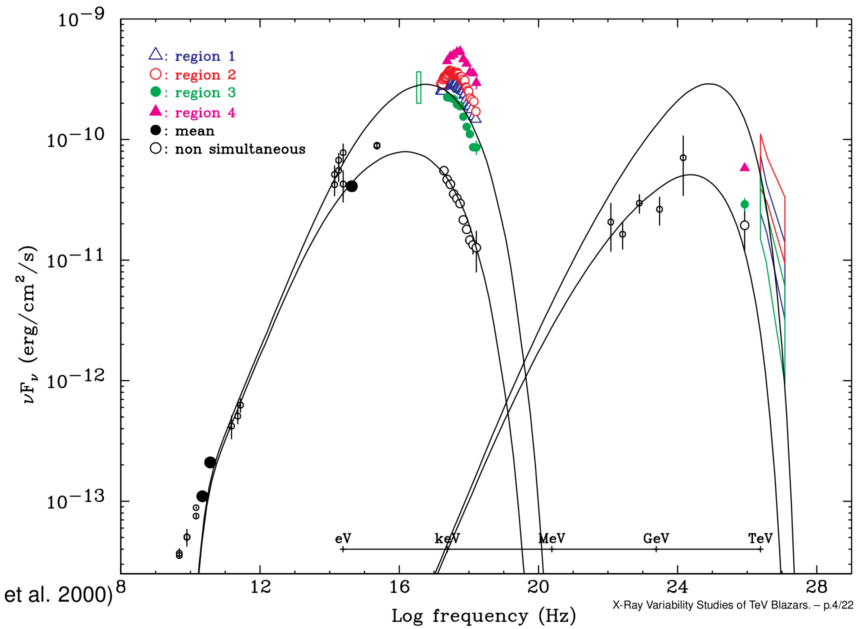

(Takahashi et al. 2000)

Direct comparison ASM and PCA

Motivation

1)X-ray band lies between the two broad band components of the SED.
2)X-ray regime unlike the optical regime is not affected by the host galaxy and fast moving ionized clouds near the center of AGN $\Longrightarrow$ Ideal band for variability studies.

a)ASM provides us with regular sampling and homogeneous data.

b) ASM archive covers a time period of more than ~ 8 years.

M and PCA

ıstrument.

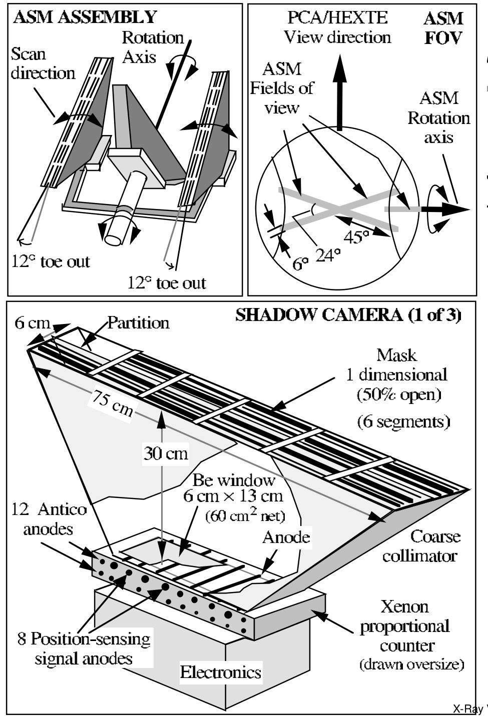

Direct comparison ASM and PCA

ASM is not as sensitive as a pointing instrument.

a)A lot of X-ray studies have been carried out based on ASM data. (e.g. Takahashi et al. 2000, Aharonian et al.1999)

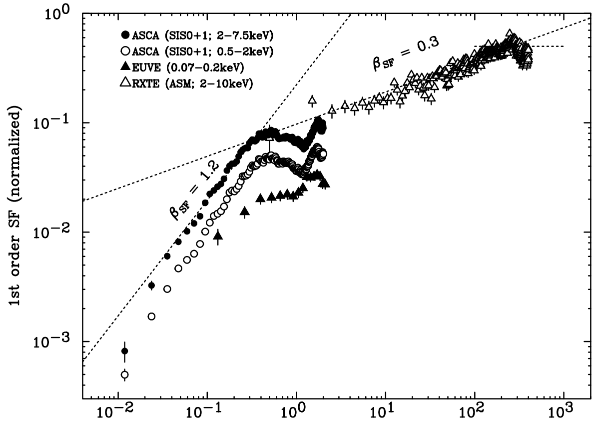

Direct comparison ASM and PCA

ASM is not as sensitive as a pointing instrument.

a)A lot of X-ray studies have been carried out based on ASM data. (e.g. Takahashi et al. 2000, Aharonian et al.1999)

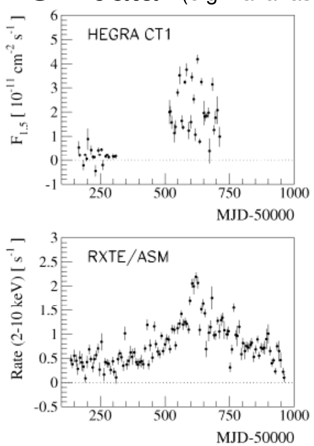

Direct comparison ASM and PCA

ASM is not as sensitive as a pointing instrument.

a) A lot of X-ray studies have been carried out based on ASM data. (e.g. Takahashi et al. 2000, Aharonian et al.1999)

b) Negative comments concerning ASM observations. (e.g. Uttley et al. 2002, Kataoka et al. 2002)

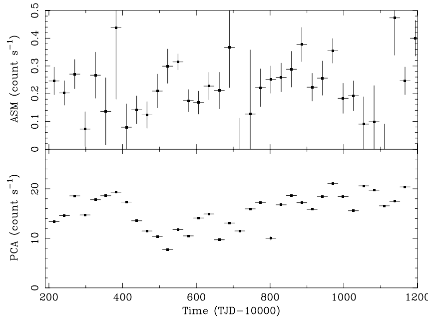

NGC 3516

Direct comparison ASM and PCA

ASM is not as sensitive as a pointing instrument.

a) A lot of X-ray studies have been carried out based on ASM data. (e.g. Takahashi et al. 2000, Aharonian et al.1999)

b) Negative comments concerning ASM observations. (e.g. Uttley et al. 2002, Kataoka et al. 2002)

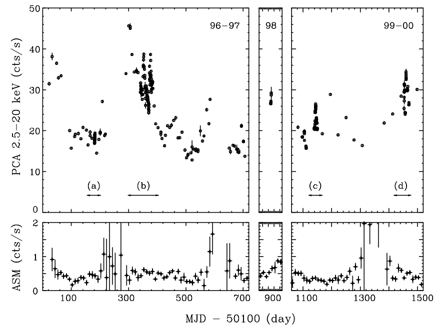

3C273

Direct comparison ASM and PCA

ASM is not as sensitive as a pointing instrument.

a) A lot of X-ray studies have been carried out based on ASM data. (e.g. Takahashi et al. 2000, Aharonian et al.1999)

b) Negative comments concerning ASM observations. (e.g. Uttley et al. 2002, Kataoka et al. 2002)

Assesment of the sensitivity level ⟶ Comparison between ASM and PCA measurements, taken at the same periods for the case of MKN421.

Sensitivity levels of ASM

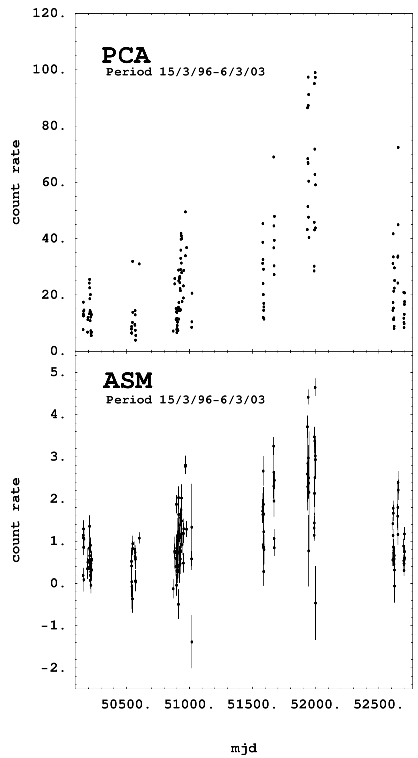

Sensitivity levels of ASM

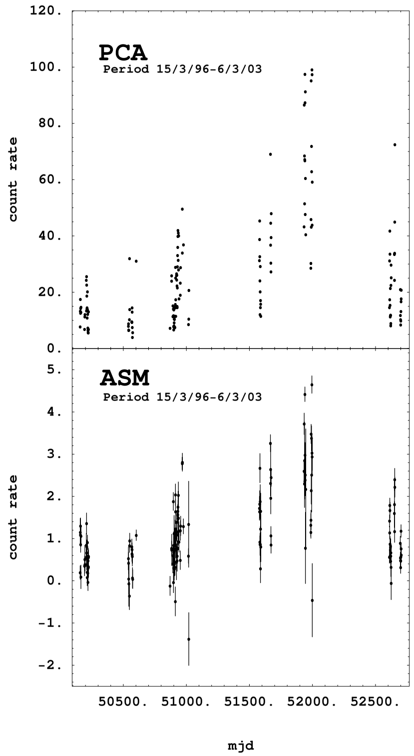

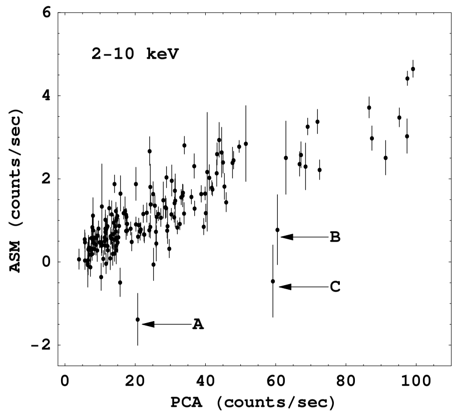

A,B,C "Binning affected" values

Sensitivity levels of ASM

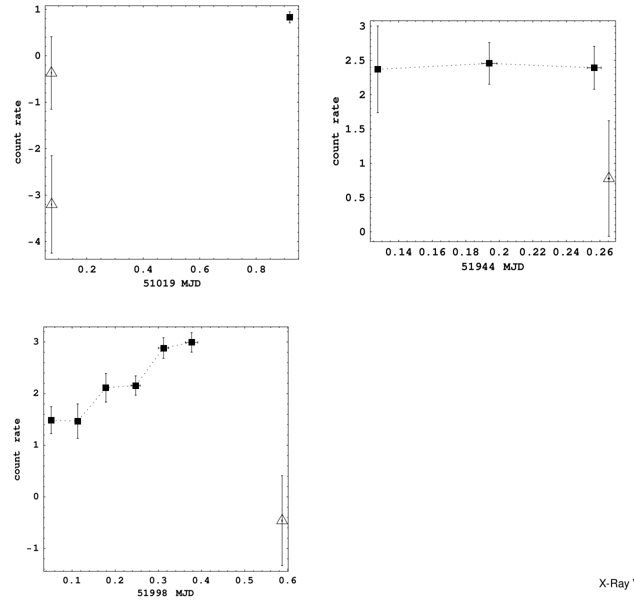

Sensitivity levels of ASM

Truly simultaneous measurements

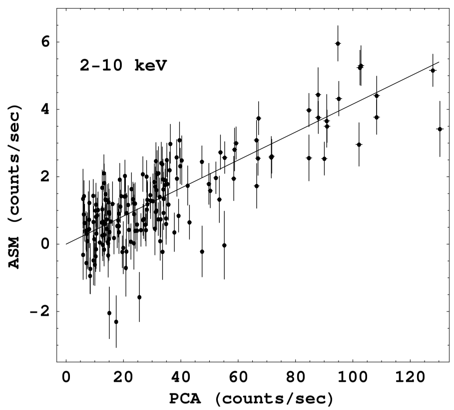

$Y_{ASM} = aX_{PCA}$
$a = 0.0416 \pm 0.0014$
Reduced χ^2=1.8781 for 172 D.O.F.

Sensitivity levels of ASM

Truly simultaneous measurements
reveal that
VARIABILITY on time scales of 100-100000 sec CAN
be traced with ASM for the case of MKN421.

SF analysis and Characteristic Times

SF of PCA and ASM

$$S_x^{sf}(\tau) = \frac{1}{N(\tau)} \sum [x(t+\tau) - x(t)]^2$$

SF analysis and Characteristic Times

SF of PCA and ASM

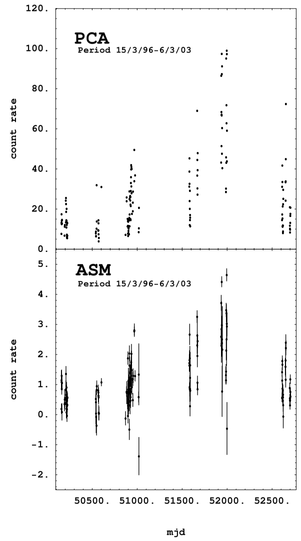

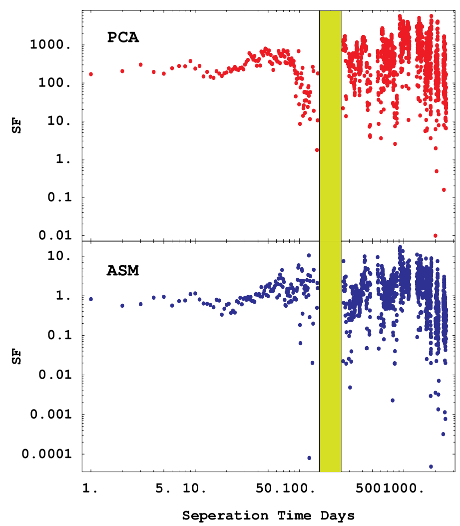

SF analysis and Characteristic Times

Error Determination

- Statistical Errors

$$\sigma^2_{stat}(\tau_k) = \sum_{i,j} \frac{\left[(x_i - x_j)^2 - \overline{(x_i - x_j)^2}\right]^2}{n_k(n_k - 1)}$$

SF analysis and Characteristic Times

Error Determination

- Statistical Errors
- Flux Measurements Errors

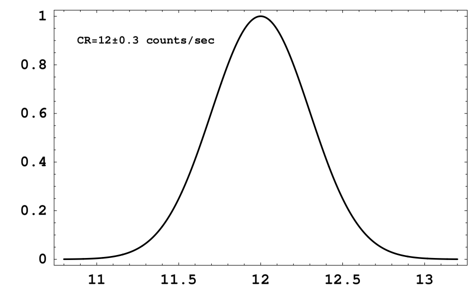

We repeat this process 300 times.

SF analysis and Characteristic Times

Error Determination

- Statistical Errors
- Flux Measurements Errors
- Observational Sampling Errors

We consider a randomly selected subset from the original "parent" data set and calculate the SF. We perform this procedure 300 times.

SF analysis and Characteristic Times

Error Determination

- Statistical Errors
- Flux Measurements Errors
- Observational Sampling Errors

Total uncertainty of the SF for the k^{th} bin:

$$\sigma^2_{SF}(\tau_k) = \sigma^2_{stat.}(\tau_k) + \sigma^2_{fl.}(\tau_k) + \sigma^2_{sampl.}(\tau_k)$$

SF analysis and Characteristic Times

Structure Functions

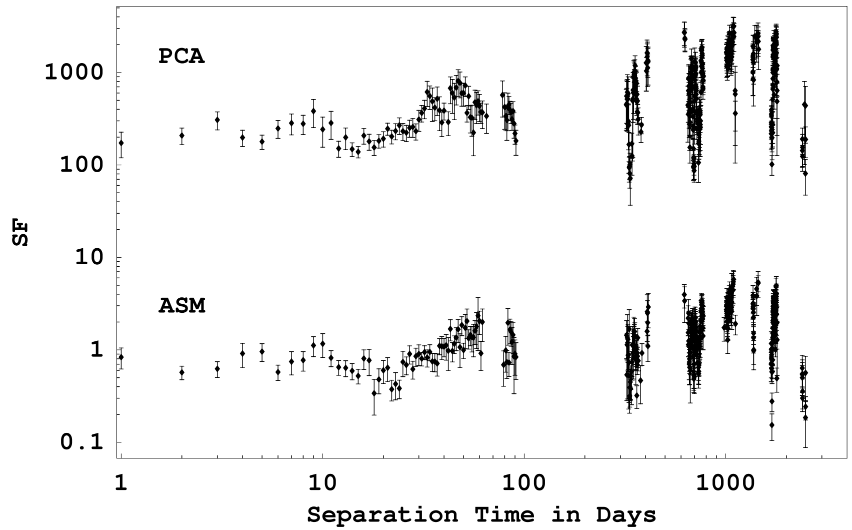

SF analysis and Characteristic Times

Structure Functions

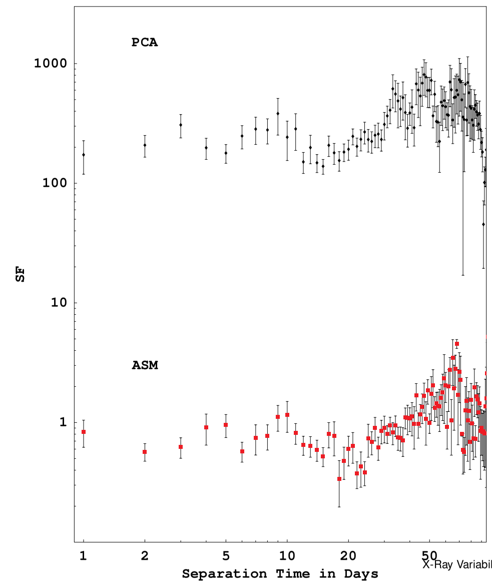

SF analysis and Characteristic Times

Structure Functions

Correlation Coefficient ~ 0.74 $\longrightarrow$ We can study Characteristic Variability Time Scales with ASM for time intervals bigger than a day.

Time Scales for long time periods (ASM)

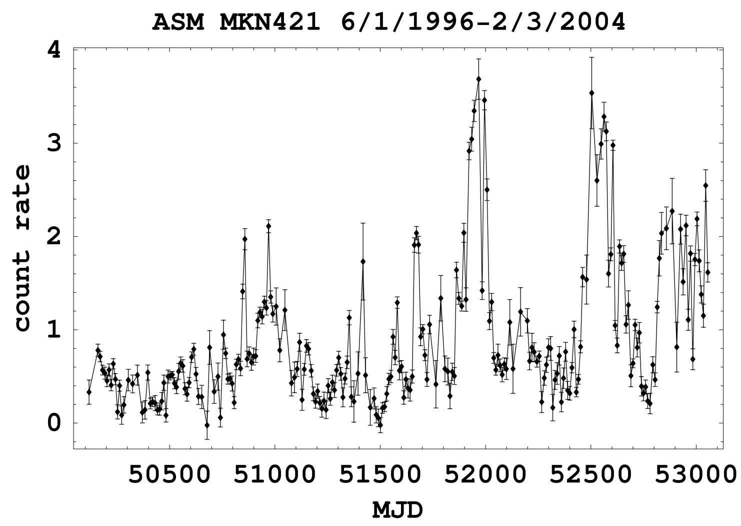

Time Scales for long time periods (ASM)

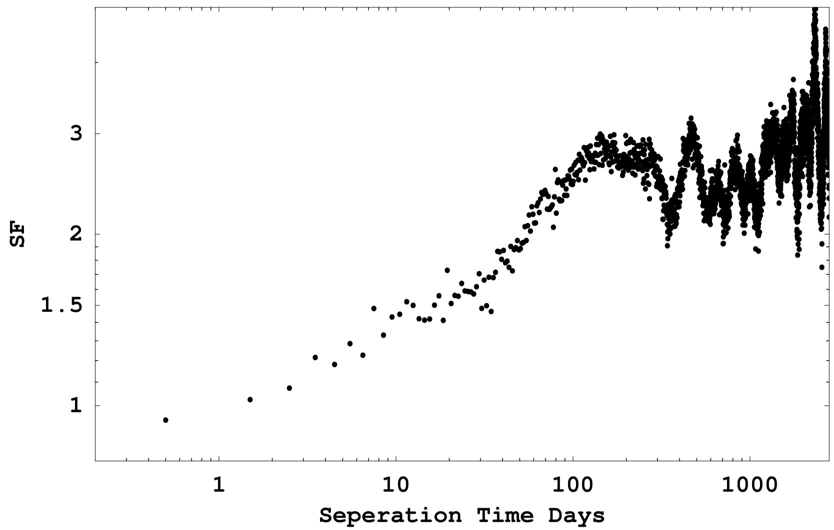

Time Scales for long time periods (ASM)

Determination of the break

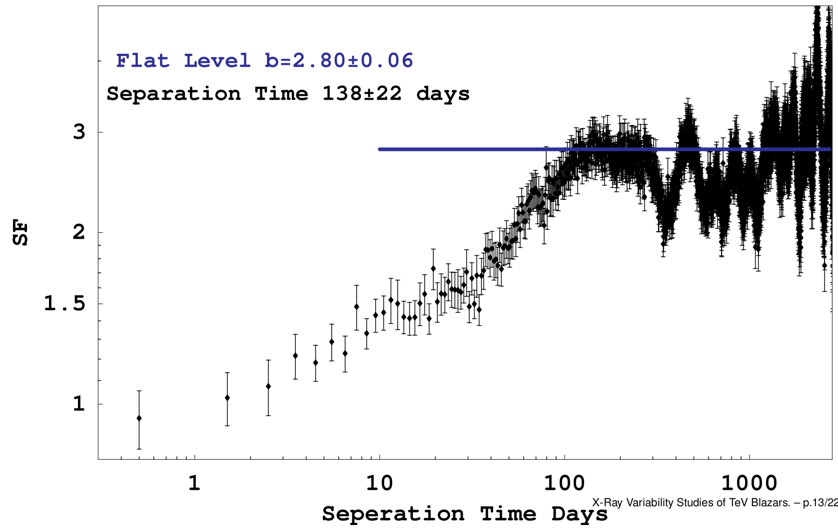

Time Scales for long time periods (ASM)

Determination of the break

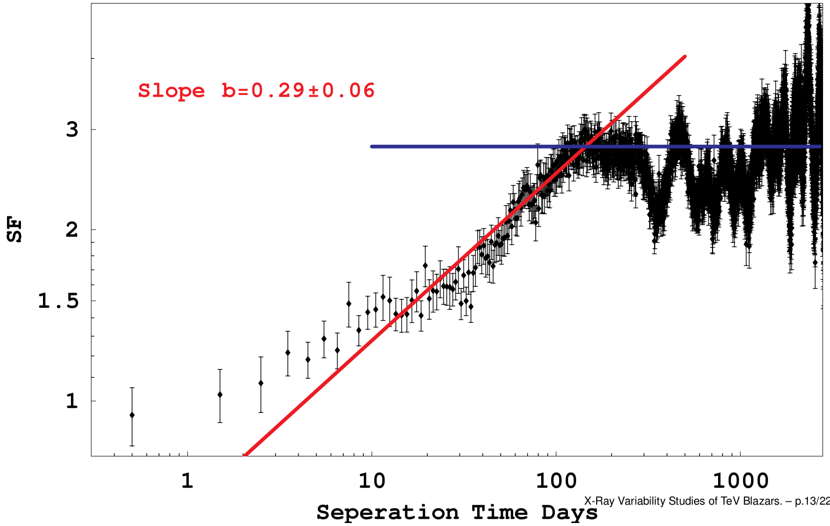

Time Scales for long time periods (ASM)

Determination of the break

We have a break $\sim$ 140 days
What does it tell us?

It gives us the maximum time-scale of correlated signals.

$$S_x^{sf}(\tau) = 2V \times (1 - ACF(\tau))$$

Time Scales for short time periods (PCA)

For daily variations we use PCA

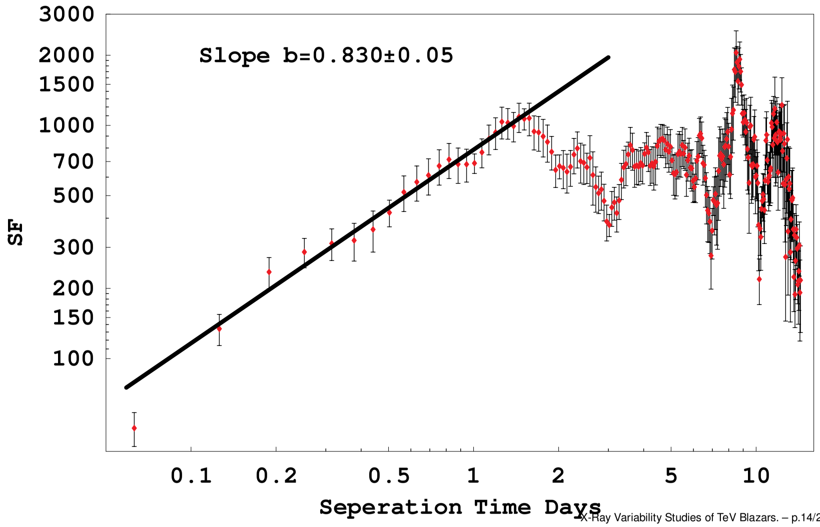

Time Scales for short time periods (PCA)

- We have an additional intraday time-scale of $\sim 1.4 \pm 0.1$ days.

$$SF(\tau) \propto \tau^b \rightarrow P(\nu) \propto \nu^{-(b+1)}$$

- For b=0.83 we get $P(\nu) \propto \nu^{-1.83}$ which is flatter than the "random walk" case (b=1) and steeper than "flicker" noise (b=0)
- We have a decrease in variability amplitude with temporal frequency.

Combination of SF

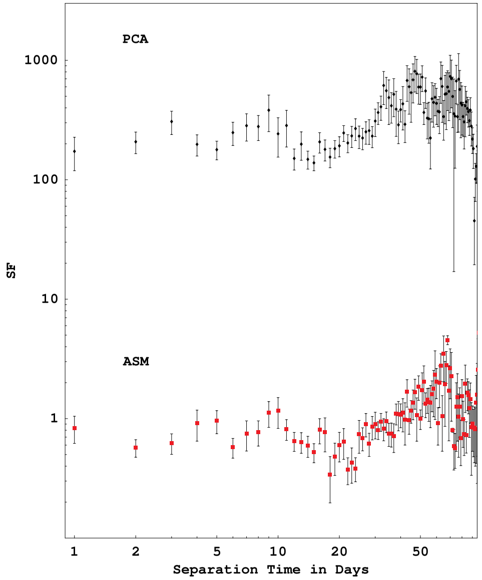

Combination of SF

Scaling the SFs

Scaling factor$= 331 \pm 5$

Combination of SF

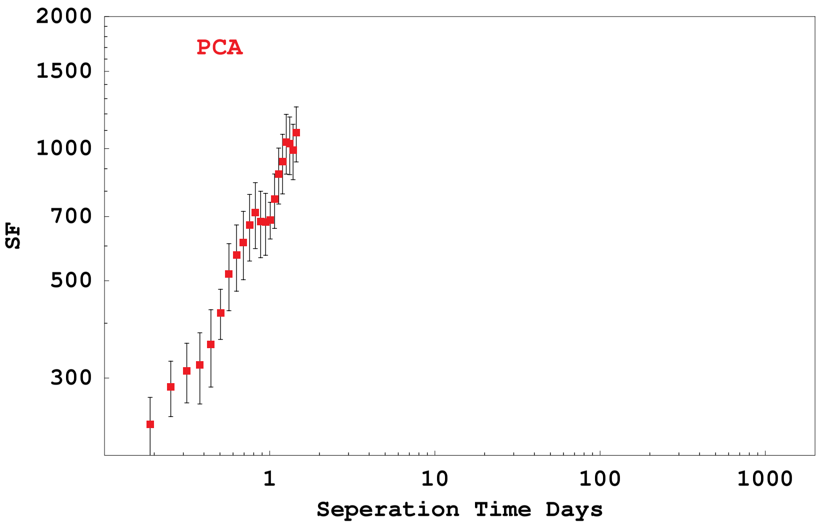

Combination of SF

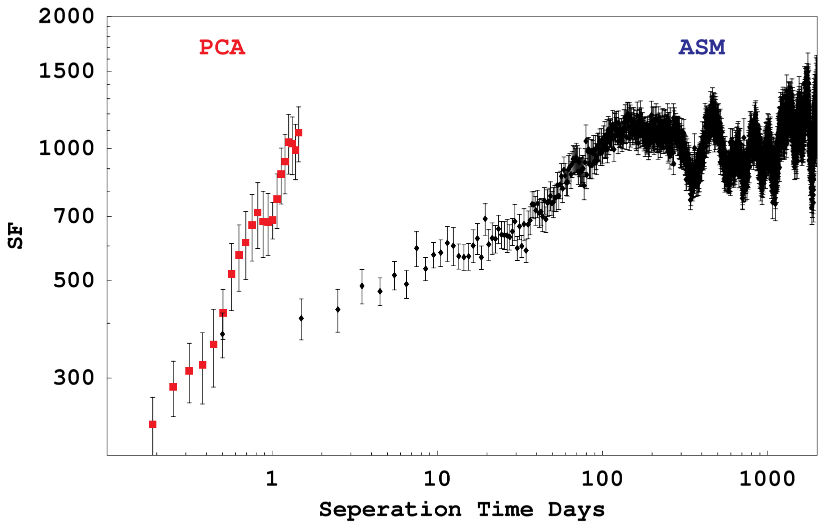

Combination of SF

Scaling the SFs

Difference in the inclination

Combination of SF

Scaling the SFs

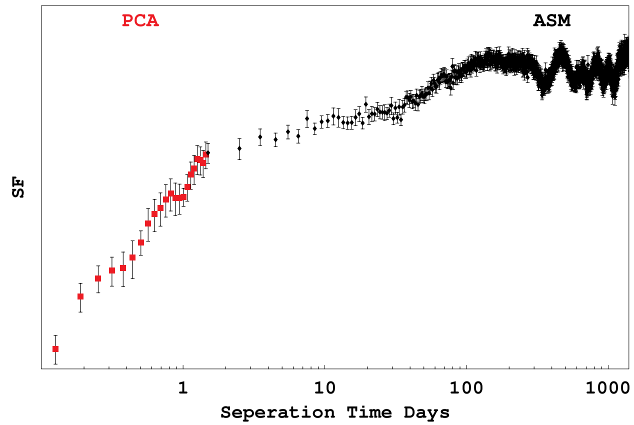

Arbitrary units in the SF axes

Conclusions

- MKN421 exhibits at least two characteristic time scales ~ 1.5 and ~ 140 days.
- Variability on shortest time scale could be interpreted with shock fronts (Tanihata et al. 2000). A "blob" of plasma passes through a region in the jet where shock fronts are formed and electrons are accelerated.
- Variability on longer time scales (??). Maybe it reflects the lifetime of a blob (??)

Update on the October-November 2003 X-ray observations of PKS2155

The observations lasted from 22-10-04 till 31-10-04 and from 14-11-03 till 24-11-03.

Update on the October-November 2003 X-ray observations of PKS2155

PRELIMINARY results for the X-ray observations of October-November 2003

XTE – HESS light curves

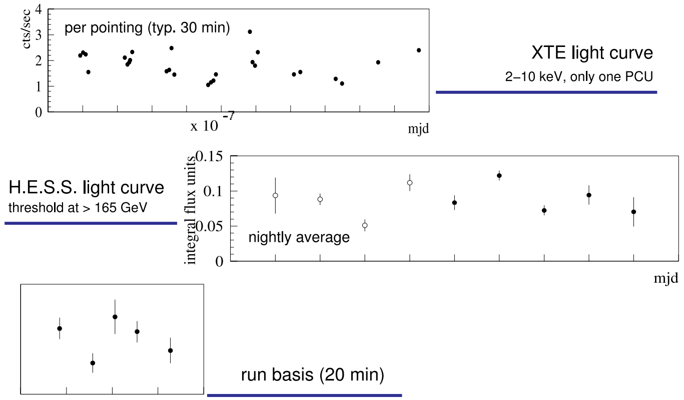

Update on the October-November 2003 X-ray observations of PKS2155

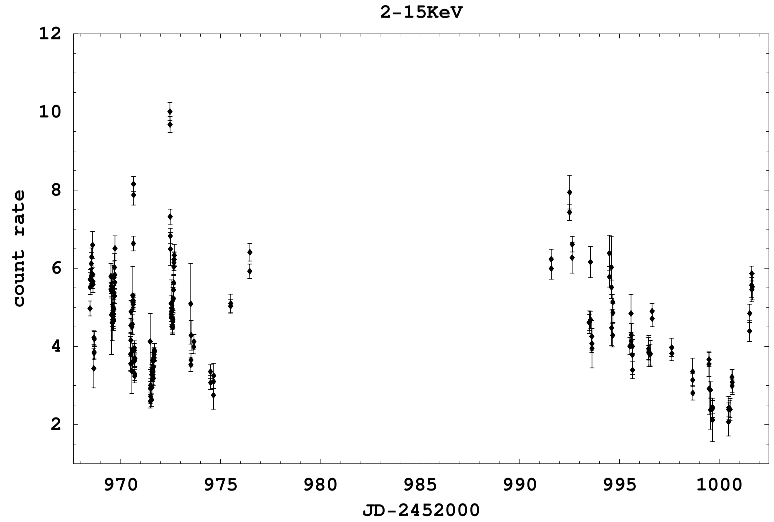

Update on the October-November 2003 X-ray observations of PKS2155

The October observations 2003 (9 days).

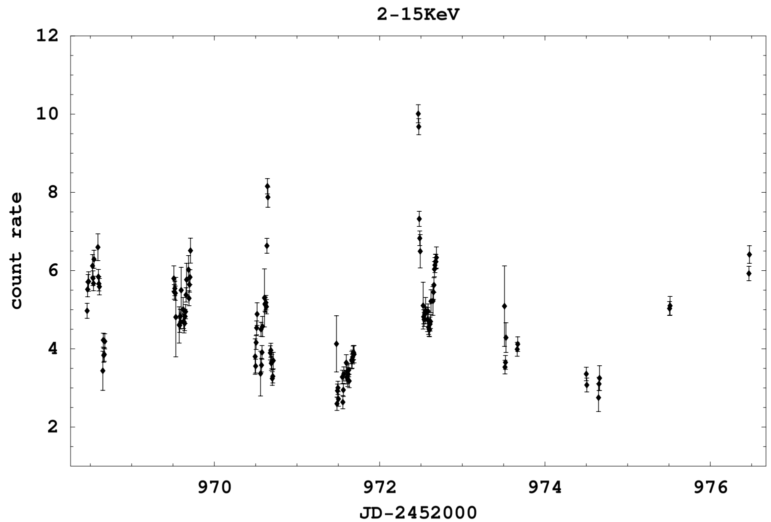

Update on the October-November 2003 X-ray observations of PKS2155

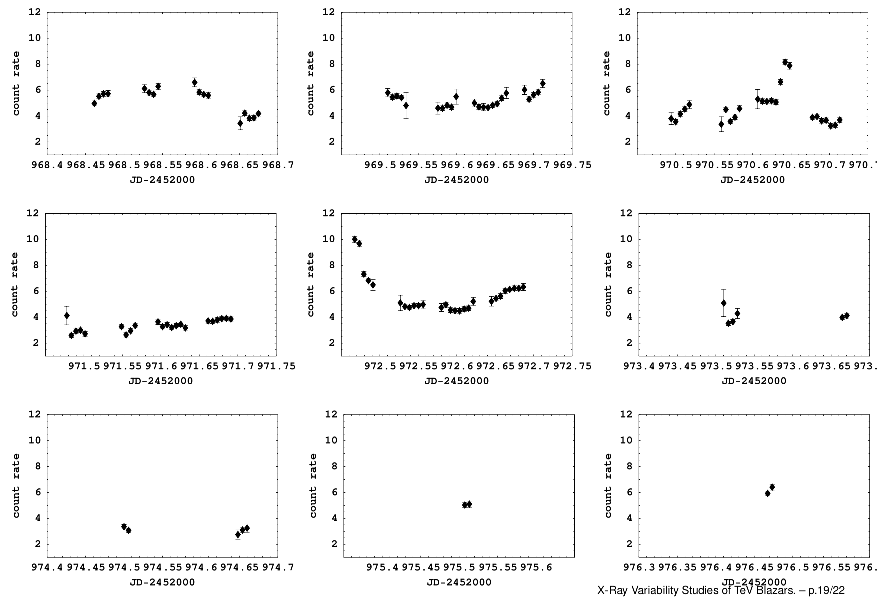

Update on the October-November 2003 X-ray observations of PKS2155

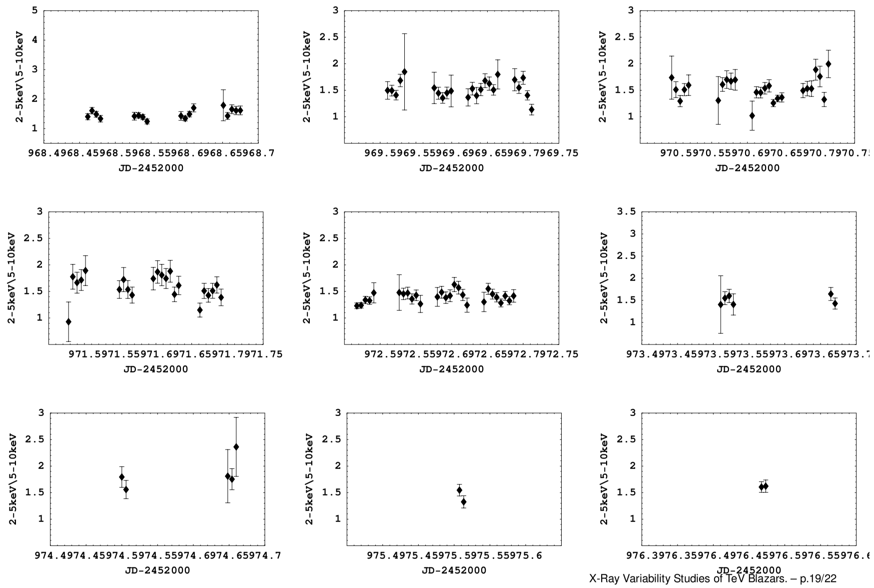

Update on the October-November 2003 X-ray observations of PKS2155

Hardness Ratio $\frac{2-5}{5-10}$ vs 2-15kev.

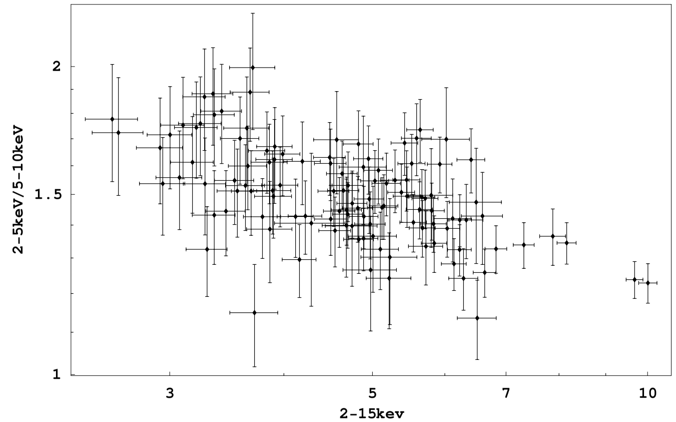

Update on the October-November 2003 X-ray observations of PKS2155

The November observations 2003 (11 days).

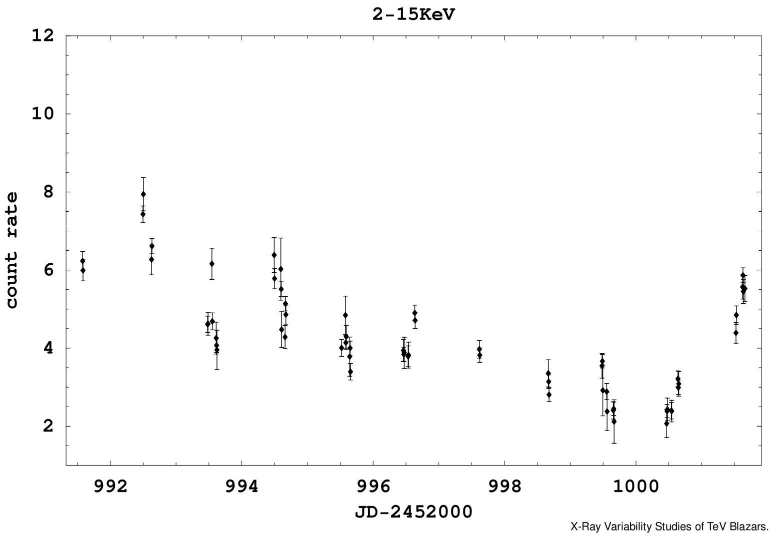

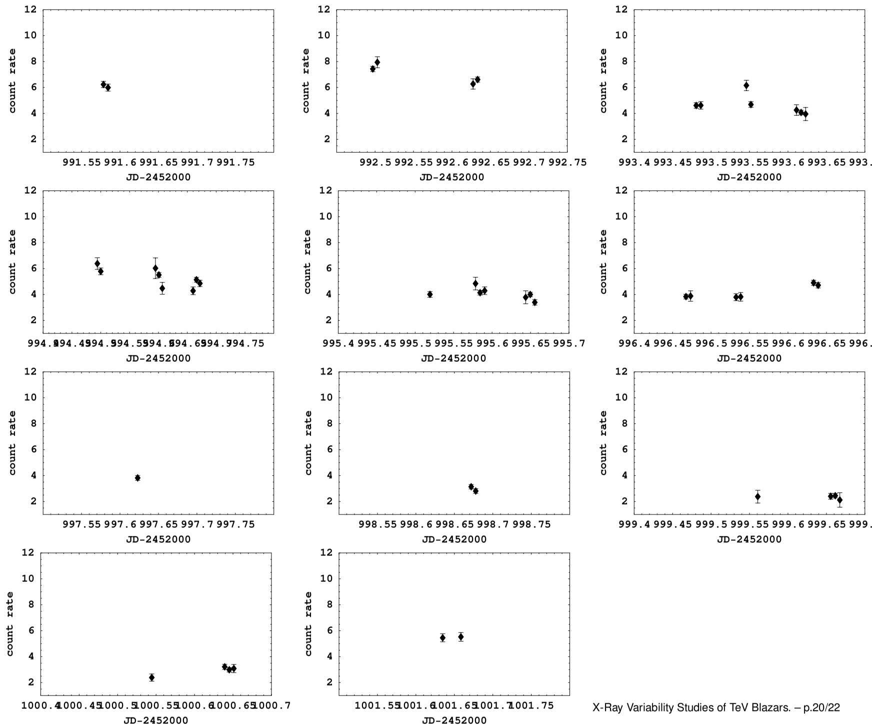

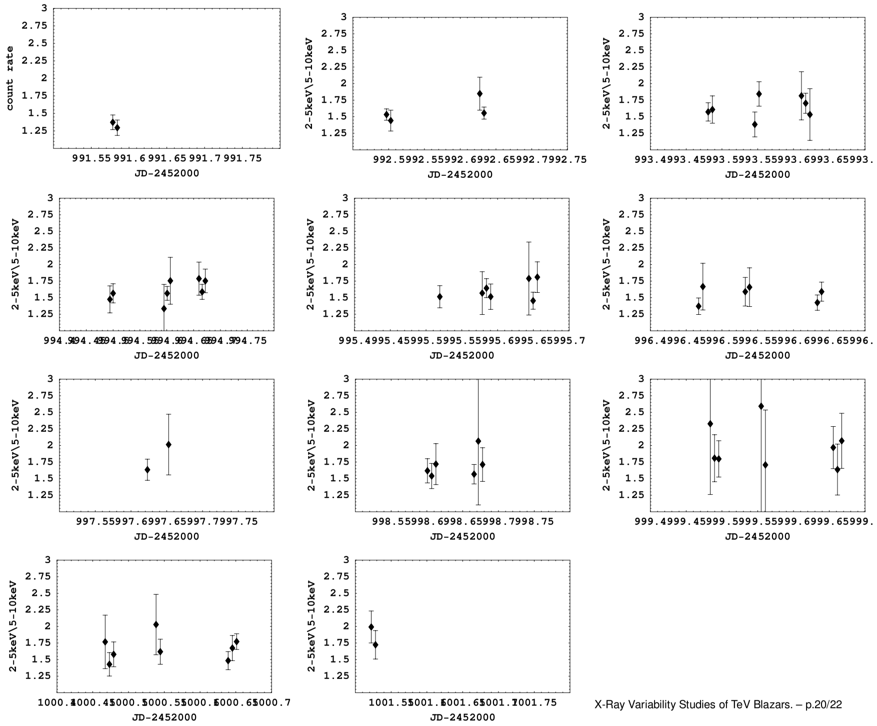

Update on the October-November 2003 X-ray observations of PKS2155

Hardness Ratio $\frac{2-5}{5-10}$ vs 2-15kev.

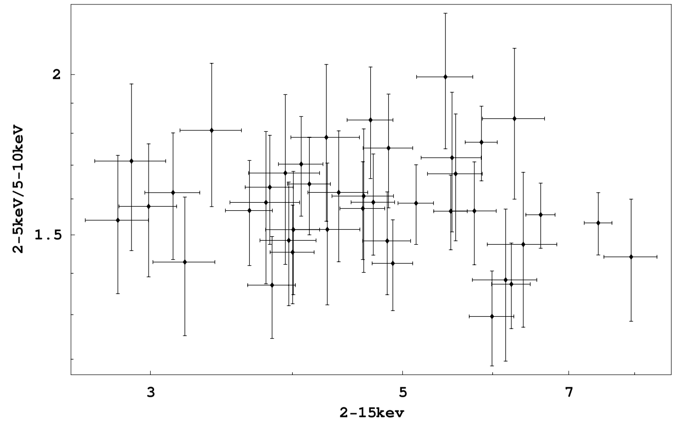

Update on the October-November 2003 campaign of PKS2155

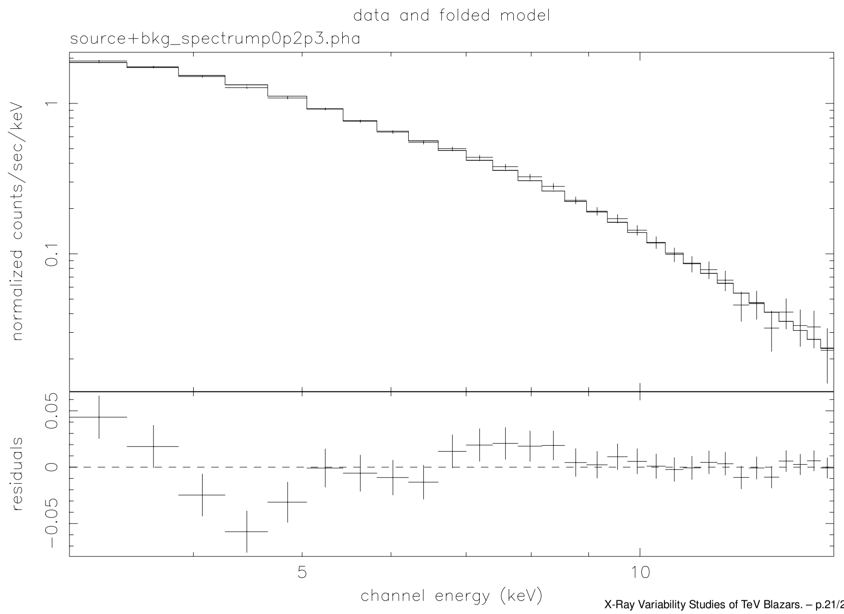

Update on the October-November 2003 campaign of PKS2155

The spectrum

- Steep spectrum with inclination $2.71^{+0.03}_{-0.03}$
- $F_{2-15keV} = 3.134 \cdot 10^{-11} ergs\ cm^{-2}\ sec^{-2}$

Evolution of the synchrotron peak in the TeV blazars.

Krzysztof Katarzyński[1,2]

[1]Osservatorio Astronomico di Brera (OAB, Italy),
[2]Nicolaus Copernicus University -
Toruń Centre for Astronomy (TCfA, Poland)

Introduction

- what does it mean the synchrotron peak?
- correlation between the position of the peak and the level of the emission at the peak - the results of the observations
- a few examples of the light curves observed in the X-rays
- how to explain the observed light curves and what about the peak correlation?
- the expected evolution of the source vs the results of the observations

Mrk 501 - example of synch. & IC peaks

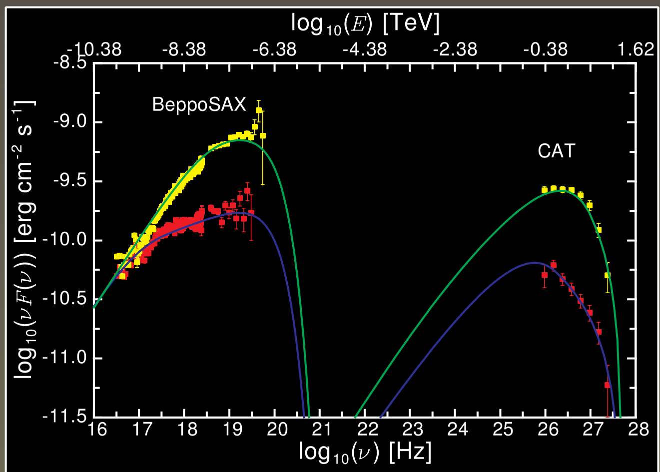

(BeppoSAX - Pian et al. 1998, CAT - Djannati-Atai et al. 1999)

Mrk 421 - evolution of the synch. peak

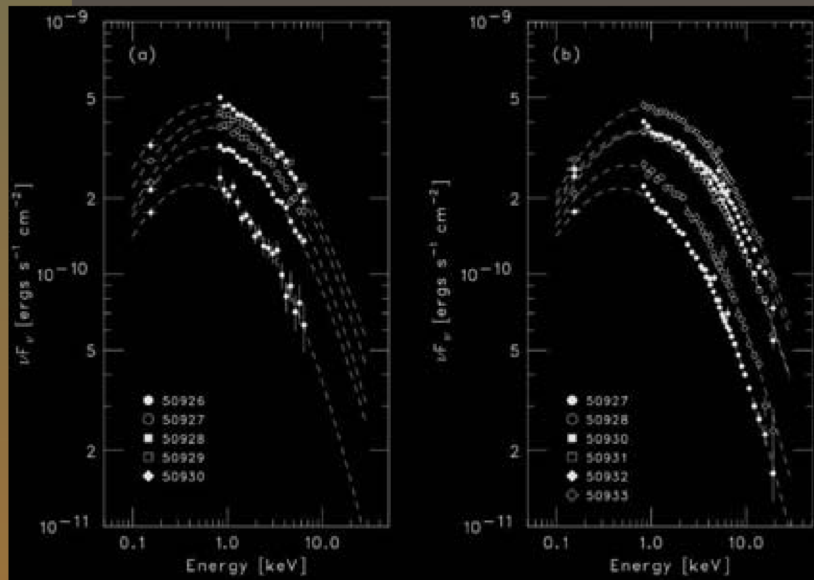

(Tanihata et al. 2004)

Mrk 421 - the peak correlation

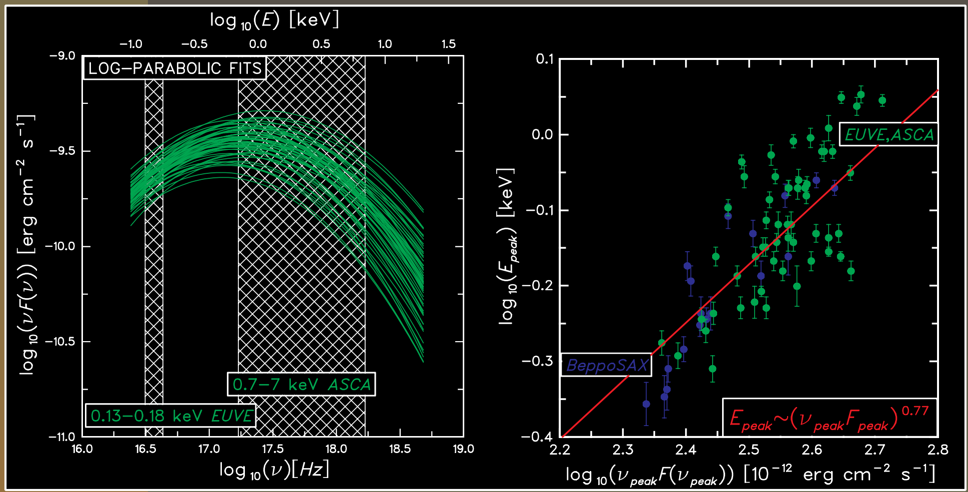

(Tanihata et al. 2004)

Mrk 421 - the peak correlation

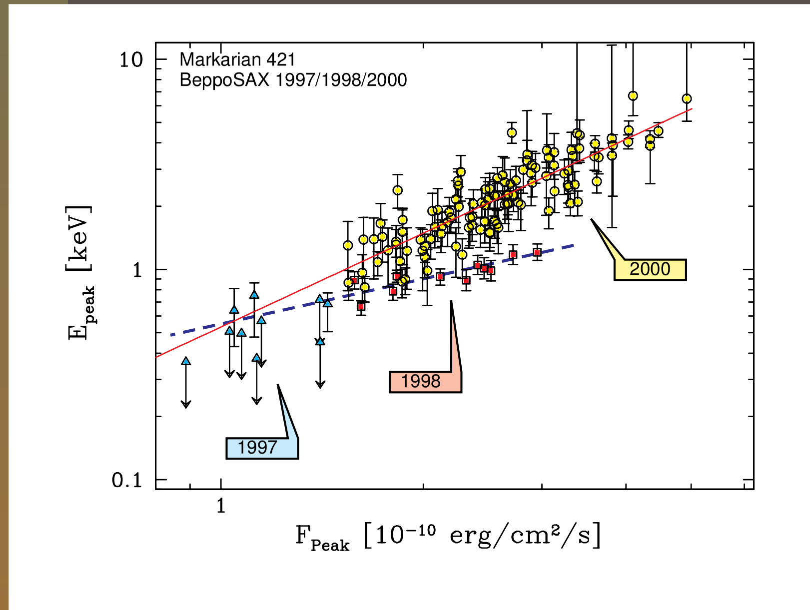

(Fossati et al. in preparation)

Mrk 421 - activity observed in 2001

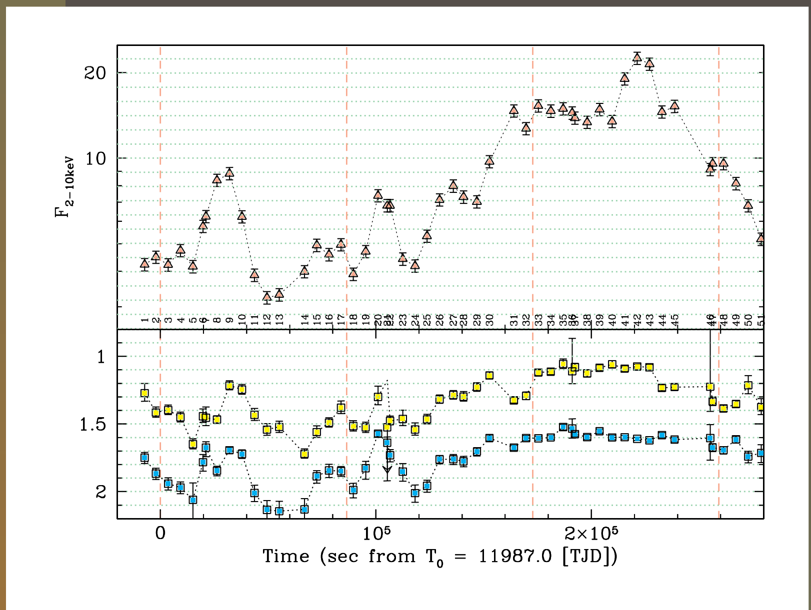

(RXTE-PCA, Fossati et al. in preparation)

Mrk 421 - activity observed in 2001

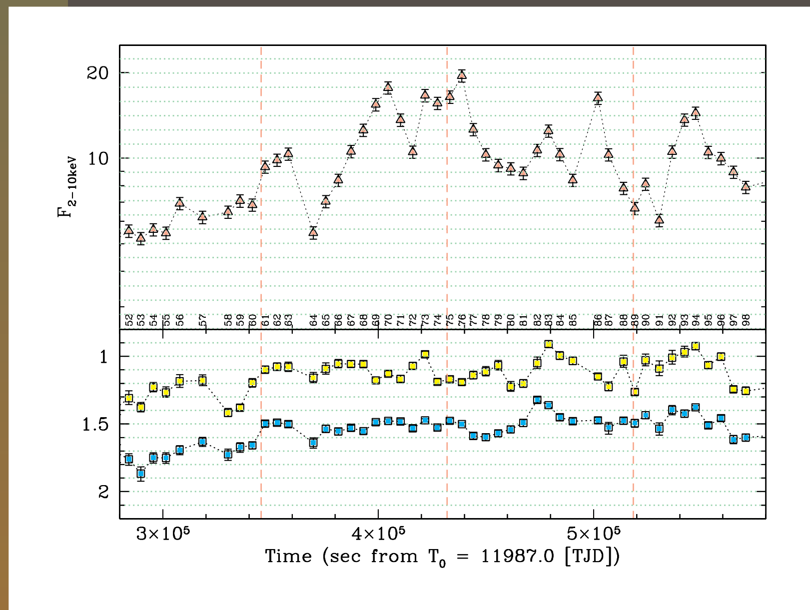

(RXTE-PCA, Fossati et al. in preparation)

conclusions from the obser. of Mrk 421

- we observe clear correlation in the evolution of the synchrotron peak
- the value (x) of the correlation ($\nu_{peak} \propto [\nu_{peak} F_{peak}]^{x}$) is constant for a period of several days at least
- the value of the correlation may change in a longer time scales (e.g. $x_{1998} \sim 0.7$, $x_{2000} \sim 1.5$)
- typical duration time of a single flare is about a few hours
- during a few days we may observe several flares but we may observe also a longer activity events with the plateau at the top of emission and the duration time longer than one day

structure of a blazar

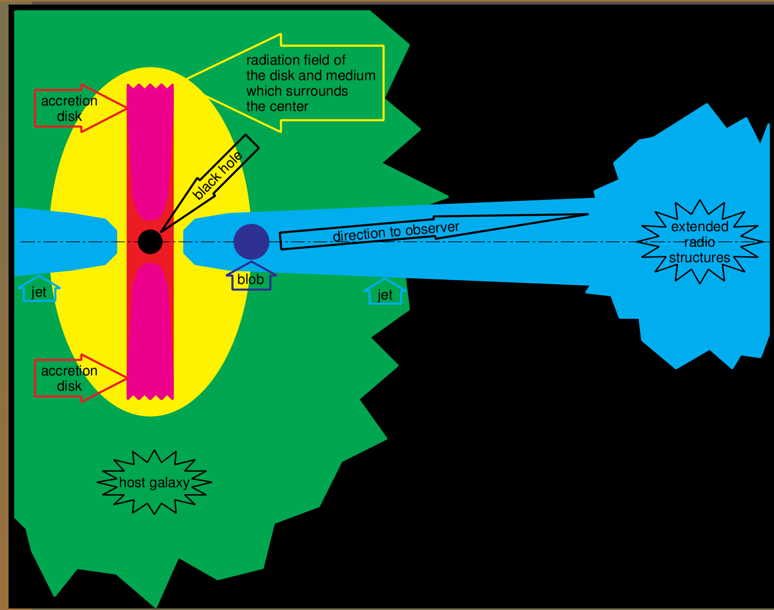

a single blob or many blobs?

- If we assume that the observed peak correlation is generated by a single source then we have to explain how such source can survive for a relatively long time (at least a few days). Note that usually we connect the duration time of a single flare with the size of the emitting region...
- If the observed variations a related to the rise and decay of a several components the peak correlation should be almost identical for all of the observed flares. Is this condition enough to explain the observed correlations?

evolution of a single flare

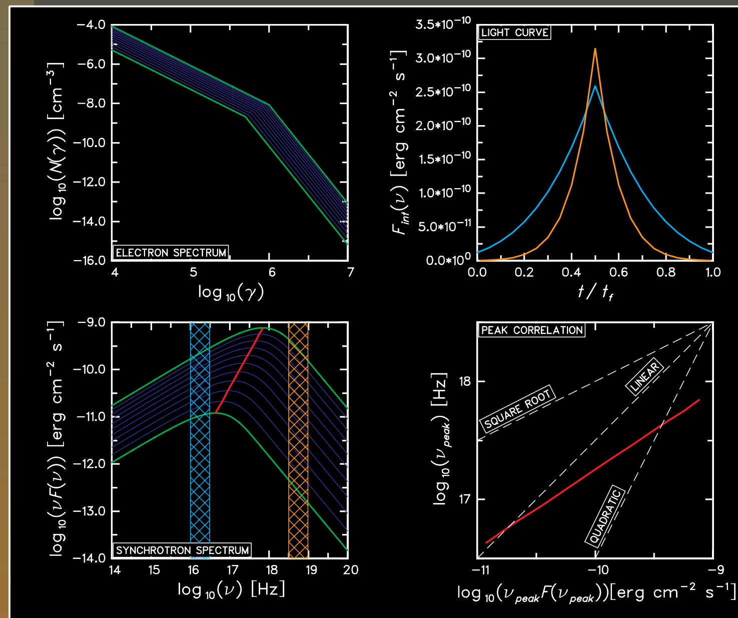

flares well separated in time

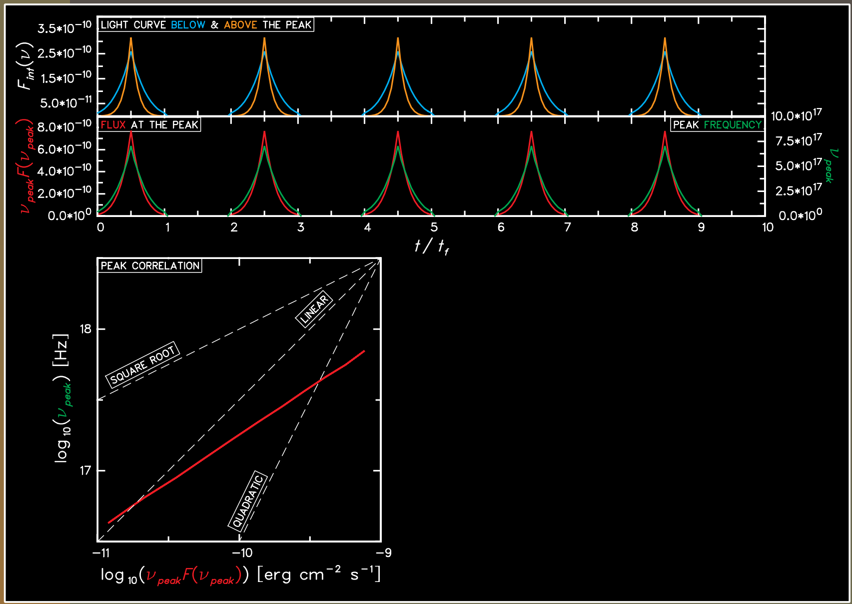

OAB-Italy

superposition of equally distributed flares

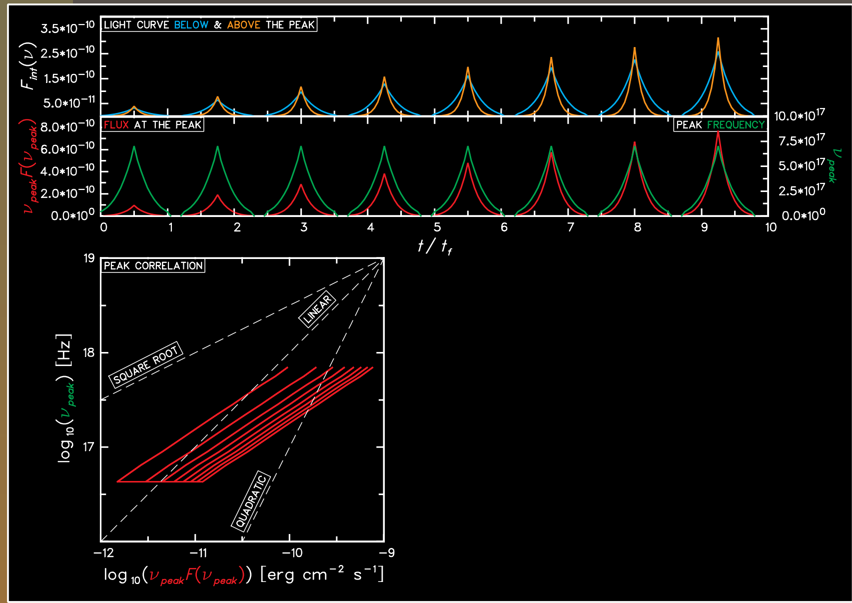

OAB-Italy

two combined flares

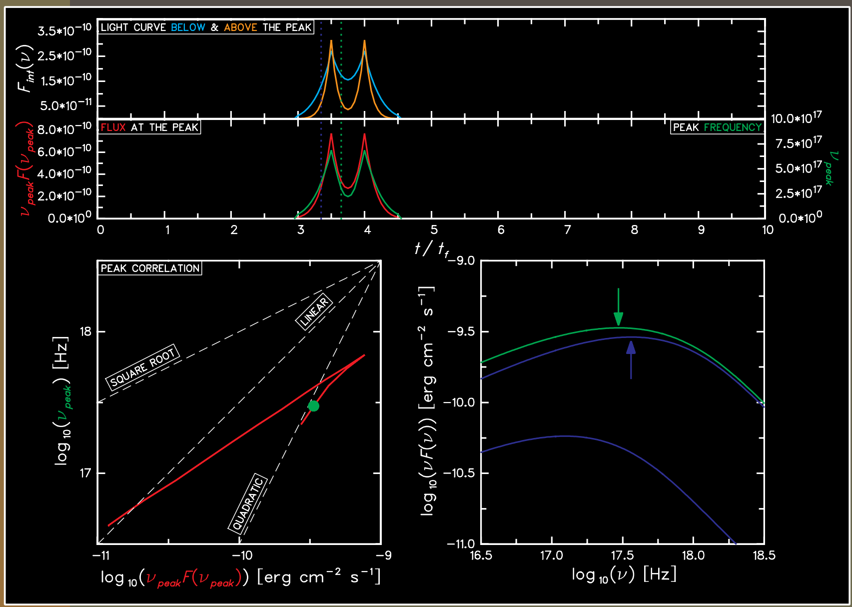

OAB-Italy

two combined flares

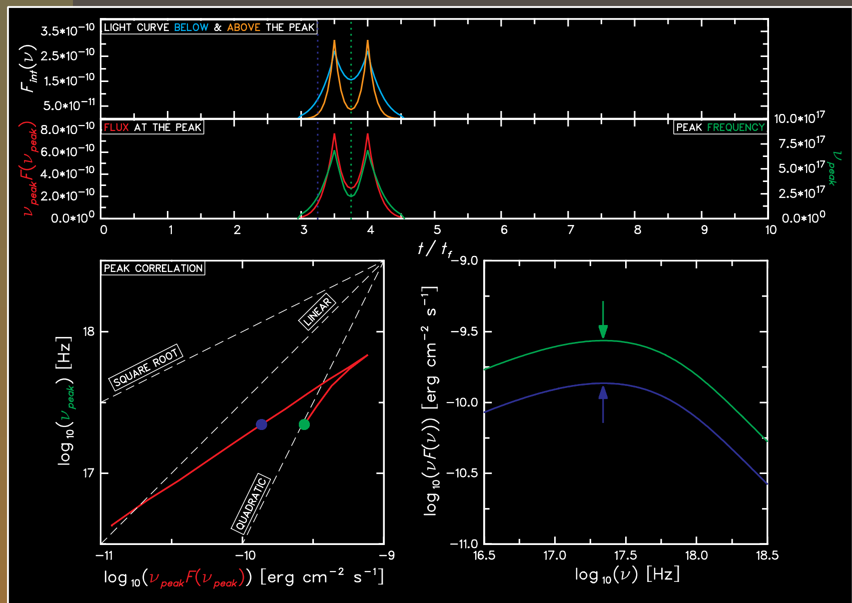

OAB-Italy

20 randomly distributed flares

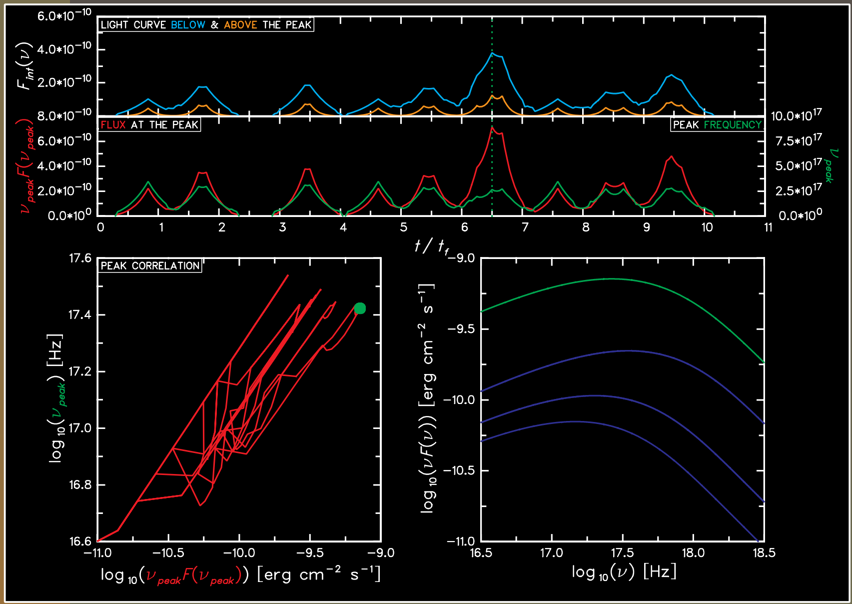

OAB-Italy

20 randomly distributed flares

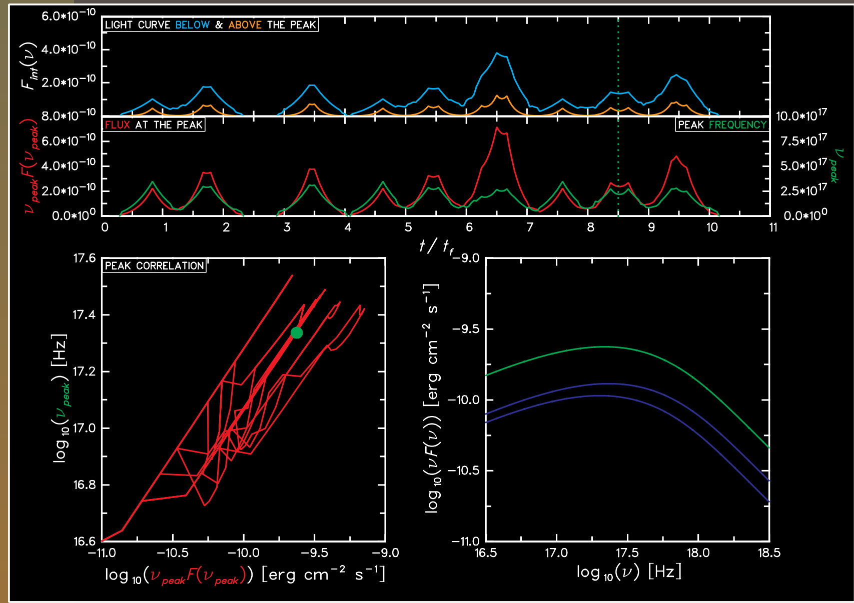

OAB-Italy

50 randomly distributed flares

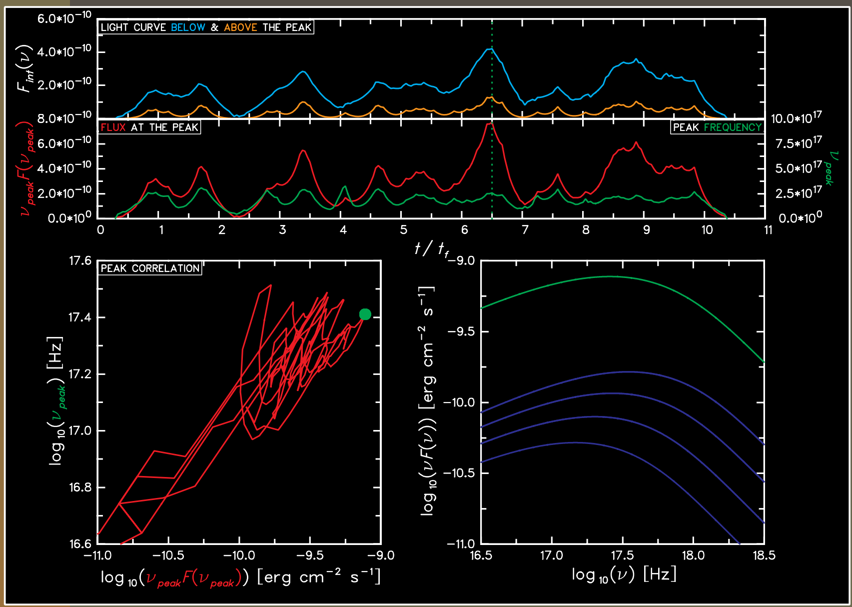

OAB-Italy

simulation vs observations

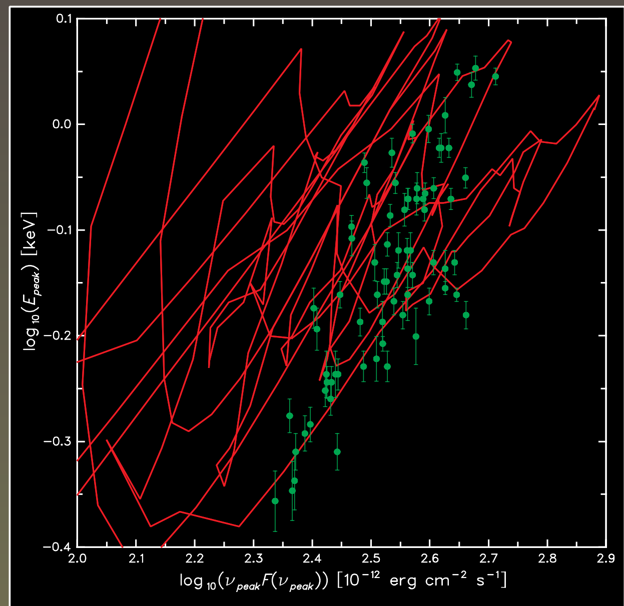

OAB-Italy

what we should observe...

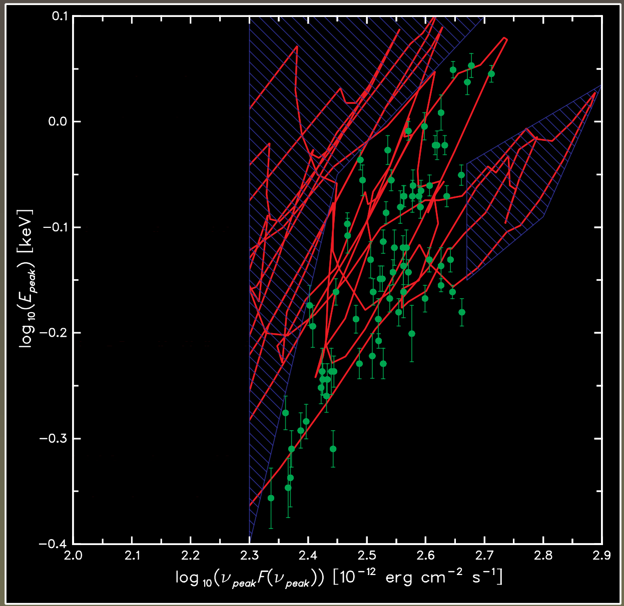

randomly sampled correlation

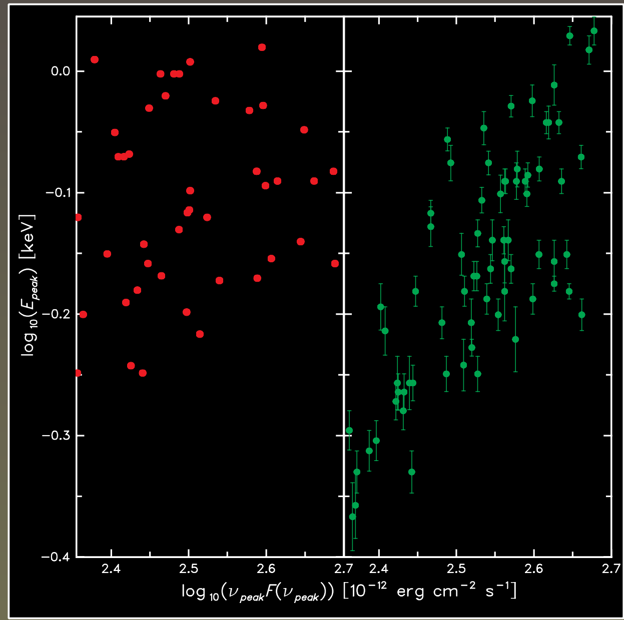

conclusions

- If we assume that the observed light curves are generated by many independent flaring events then it's quite difficult (or even impossible) to explain the peak correlation.
- Note that in the simulations we have assumed perfect symmetry for the rising and decaying phase of a single flare in order to obtain the peak correlation for this basic activity. What if there is difference between the evolution in the rising and decaying phase?
- Does this result mean that the long term activity (at least a few days) can be generated by a single component (e.g. Sokolov, Marscher & McHardy 2004)?

References

- Djannati-Atai, A., Piron, F., Barrau, A., et al., 1999, A&A, 350, 17
- Pian, E., Vacanti, G., Tagliaferri, G., et al., 1998, ApJ , 492, L17
- Sokolov, A., Marscher, A., P., & McHardy, I., M., 2004, astro-ph 0406235
- Tanihata, C., Kataoka, J., Takahashi, T., et at., 2004, ApJ, 601, 759

Small/large scale jet connection

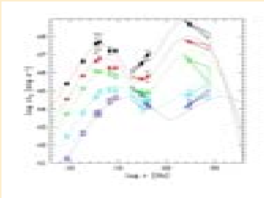

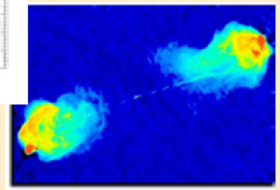

Fabrizio Tavecchio
(INAF – Osservatorio Astronomico di Brera)

L. Maraschi, R. Sambruna, T. Cheung, J.Gambill

1

Outline

Blazars

Large scale jets

Put everything together!

2

Blazars:
Inner jet <0.1 pc

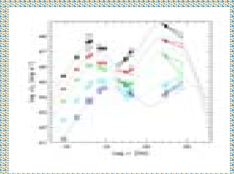

3

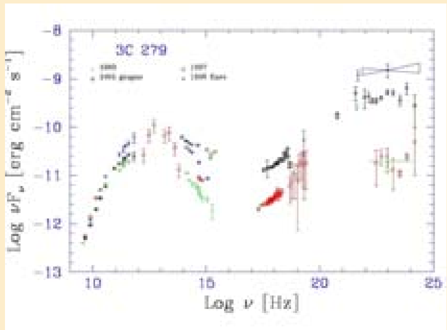

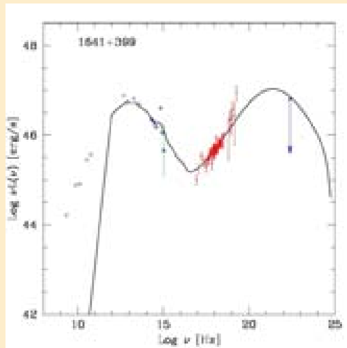

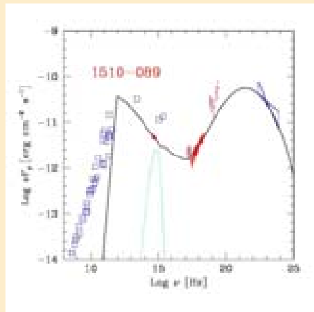

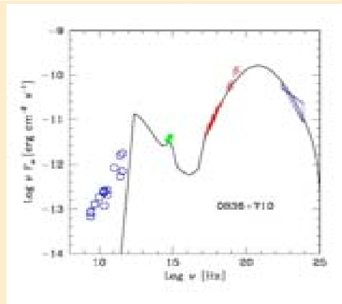

We derive B, R, Ne, Γ and the jet power P

Large-scale jets

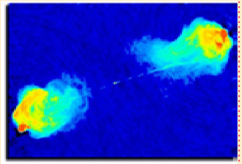

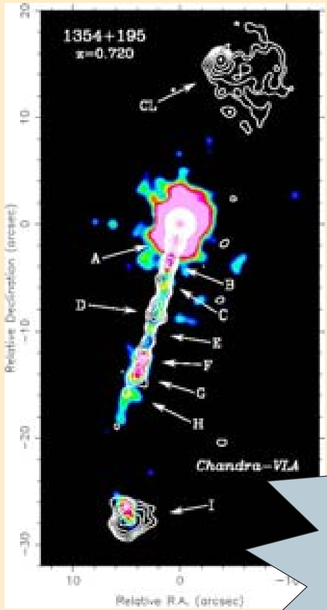

From Sambruna et al. 2002

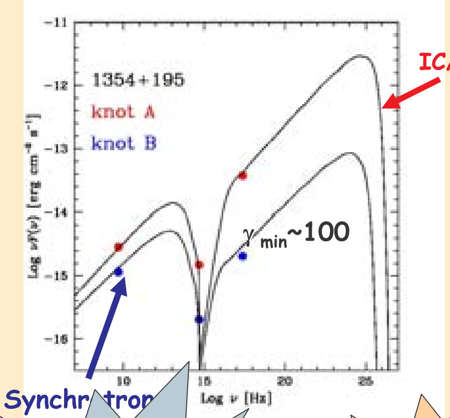

Γ ~ 5-10
Θ ~ 5°

δ=5–10
at >100 kpc

Sample of well studied BeppoSAX blazars (Maraschi & Tavecchio 2003)

Blazars:
Inner jet <0.1 pc

1510-089
1641+399 ?

Large scale jets

Sample of Chandra/HST jets (Sambruna et al. 2002, 2004)

Chandra and radio images

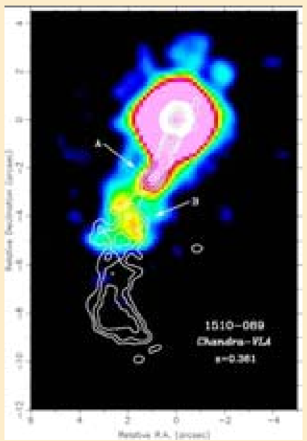

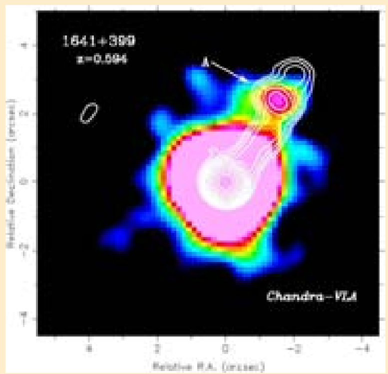

1510-089

blazar

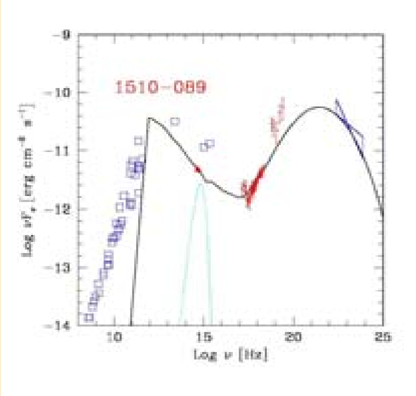

knot

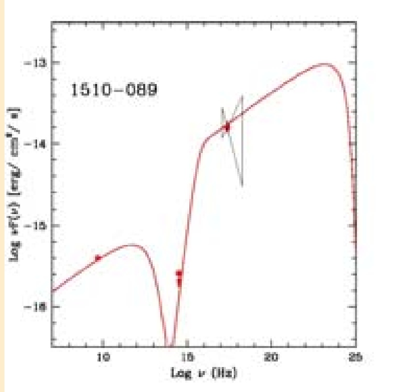

Tavecchio et al., in press

1641+399

blazar

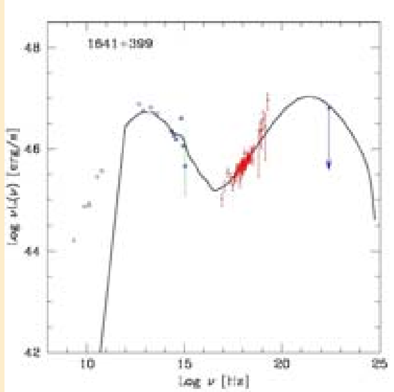

knot

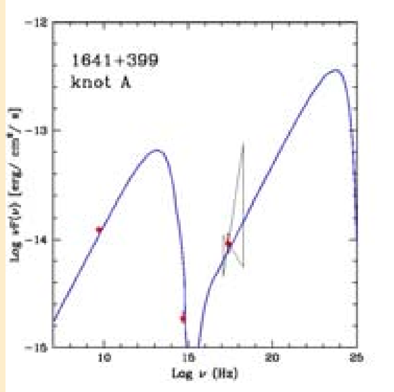

Tavecchio et al., in press

Comparing physical parameters

		Log r	U_B	Γ	P (10^{47} erg/s)
1510	in	17.5	8e-2	19-10	5-1
	out	24	4e-13	16-9	4-1.3
1641	in	17.5	0.3	10-5	1.2-0.3
	out	23.4	5e-12	8-4	4.2-1.1

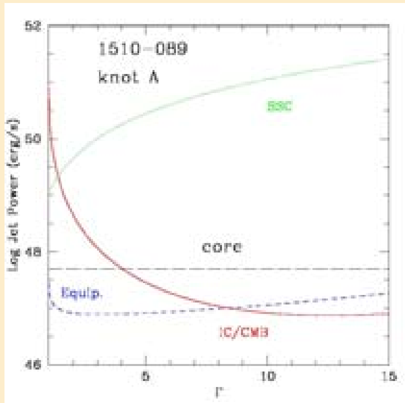

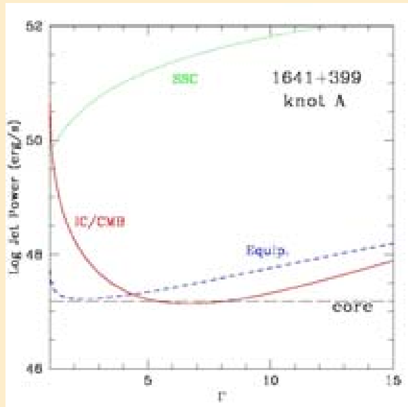

A simple general scenario?

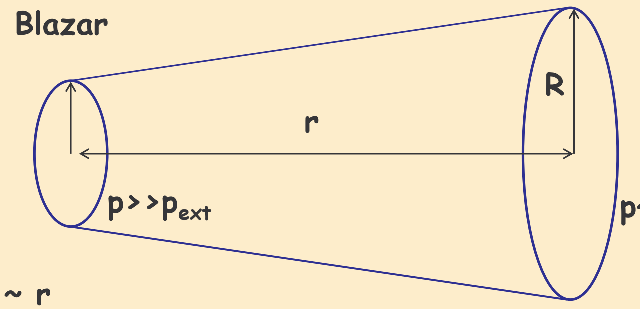

$R \sim r$

$B \sim r^{-1}$

Γ~const

P~const

No dissipation
No deceleration

(e.g. the free jet model of Blandford & Konigl 1979)

Conclusions

Comparison between parameters derived in small and large scale regions of the <u>same jet</u>

The power and the Lorentz factor do not substantially change: free, dissipationless flow

Consistent with conical jet. B decreses as r^{-1}

Other 3 blazars with Chandra/HST data are under study…

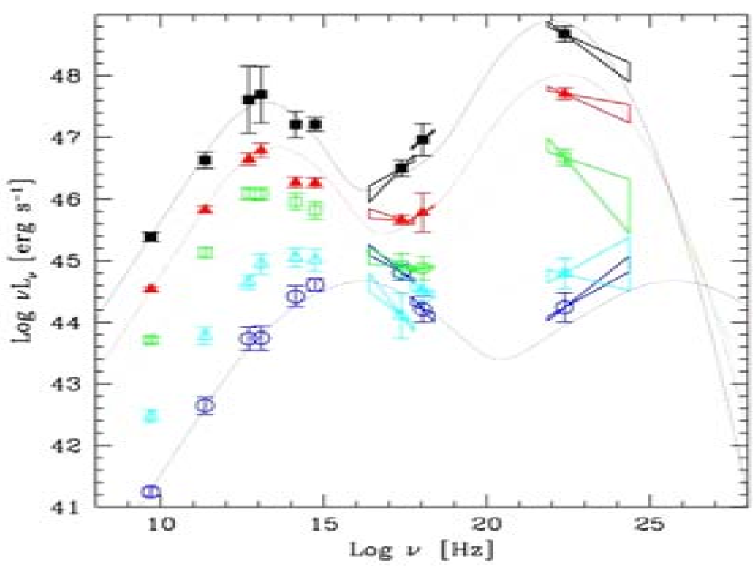

Ghisellini et al. 1998

Producing X-rays in large-scale jets

Powerful (aligned) QSOs

~~Synchrotron~~ ~~SSC~~ ~~thermal~~ → IC/CMB

Schwartz et al. 2000

Tavecchio et al. 2000
Celotti et al. 2001

Radiogalaxies

FRIs: Synchrotron — e.g Worrall et al. 2001, 2002

FRIIs: Synch? SSC? — e.g Wilson et al. 2001

very energetic electrons

Amplification of the CMB energy density

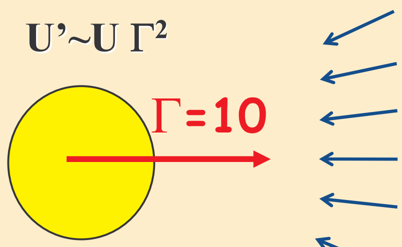

Photons will appear more concentrated in time and with an energy $\varepsilon_1 = \varepsilon\,\Gamma$

IC/CMB model: problems, criticisms

{ Large power requirements (~10^{48} erg/s)
Close alignement (small probability) } Bias!

Cooling: how to produce X-ray knots?

Stawarz et al. (2004), Dermer & Atoyan (2004)

Why X-ray knots?

Problem: the X-ray emitting electrons ***cannot cool*** inside the knot

t_{cool}~10^7 yrs

even including adiabatic losses!

→ Continuous strem of X-rays

A possible solution

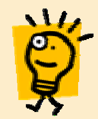

Several compact regions overpressured with respect to the external plasma (instabilities, clouds, entrained material, reconnection sites)

Tavecchio, Ghisellini & Celotti 2003

→ expansion

→ very efficient adiabatic losses

But problems (Stawarz et al. 2004)

Moving blob?

A *Chandra-HST* survey of jets

Sambruna et al. 2002
Sambruna et al. 2004

17 “radio selected” jets

Short (10 ks) Chandra exp
1 HST orbit (1 filter)

10 with X-rays (59%)

10 with optical

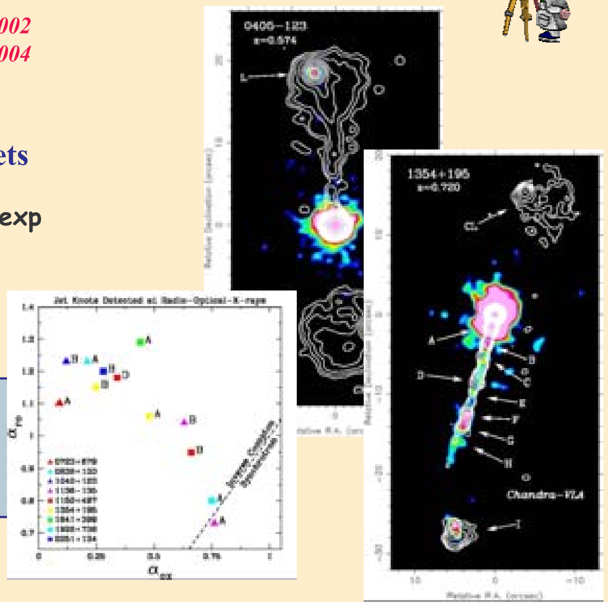

Speed and power

The model allows us to __constrain the physical parameters__ of jets at kpc scale

Γ~3-10 $\qquad$ P~10^{47} -10^{48} erg/s

Supported by recent numerical simulations (Scheck et al. 2002), but see Wardle & Aaron 1997

Increasing radio-to-X-ray flux along the jet

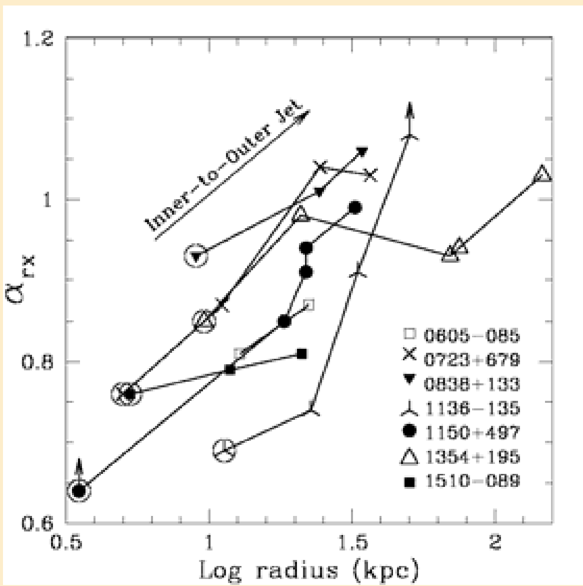

Sambruna et al. 2004

or, better…

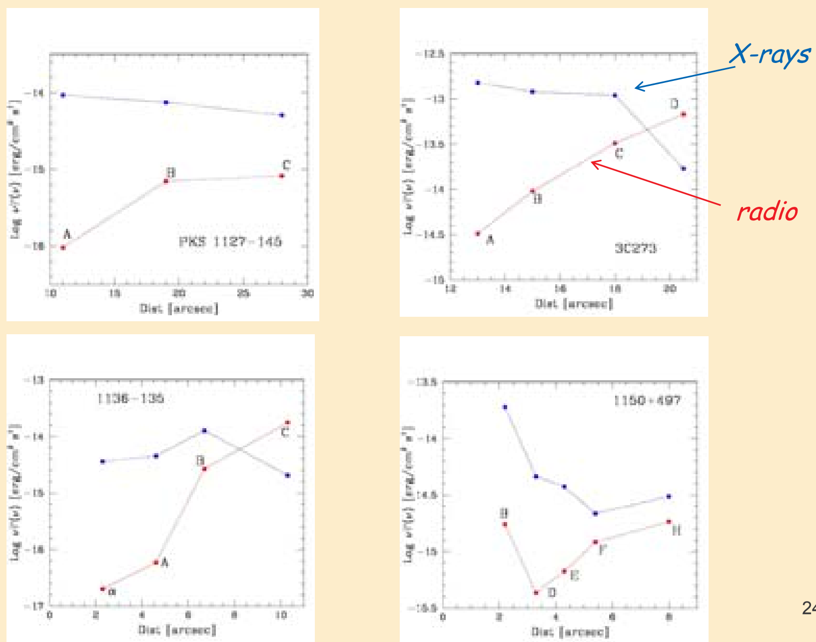

Evidence for deceleration?

Georganopoulos & Kazanas (2004):

- the jet is continuously decelerating
- particles end fields evolves through adiabatic compression/expansion

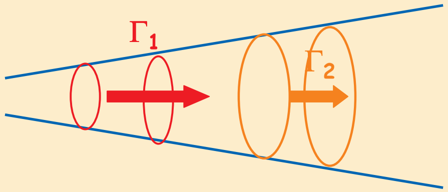

25

3C 273

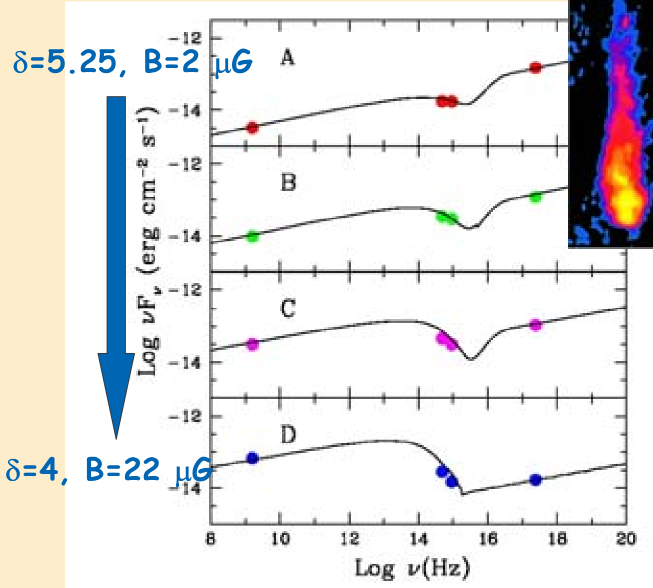

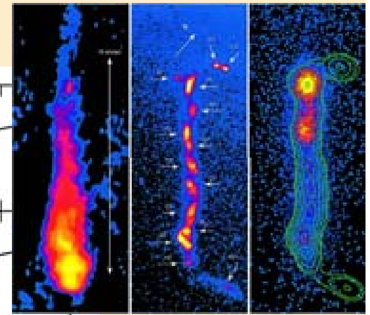

Sambruna et al. 2001

26

Deeper exposures

(in progress)

1136-135
1150+497

80 ksec Chandra

Multicolor HST (3 filters)

New 22 GHz radio maps

27

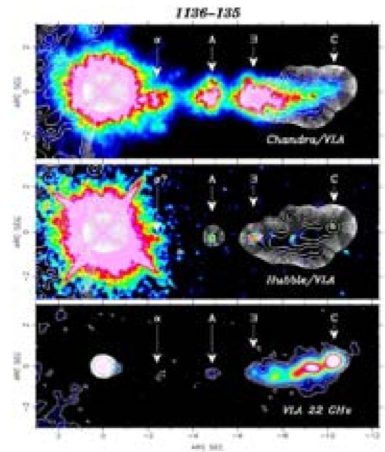

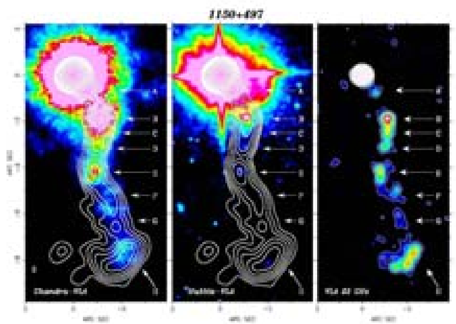

28

Synchrotron to Compton transition?

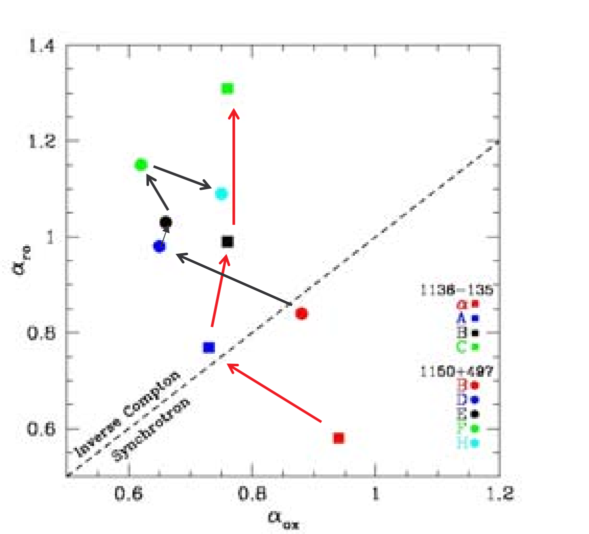

SEDs:

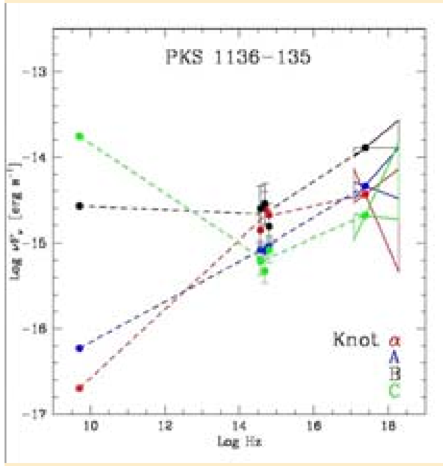

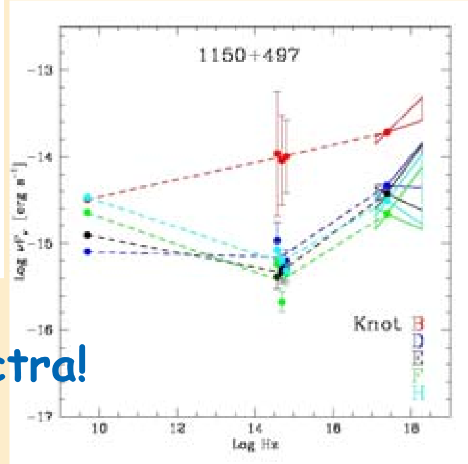

X ray-spectra!

Summary

The survey confirms the IC/CMB interpretation for powerful jets

<u>Global behavior</u> along the jet:

Increasing α_{rx}

Synchro-IC transition?

3C371: a synchrotron jet

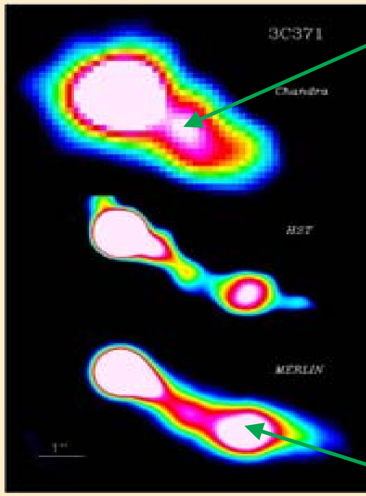

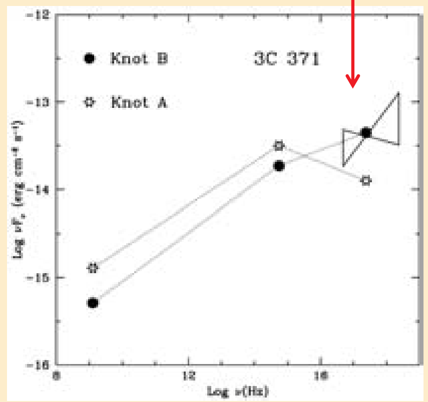

Knot B

Knot A

$\gamma_e \sim 10^7$

Pesce et al. 2001

"Weakening" of the acceleration process?

$$t'_{\rm cool}(\gamma) = \frac{3mc}{4\sigma_T U_{\rm CMB}\Gamma^2(1+z)^4\gamma}$$

$$t'_{\rm acc} = \frac{\Delta R}{c\Gamma}$$

$$\gamma_{\rm max} = \frac{3mc^2}{4\sigma_T U_{\rm CMB}\Gamma(1+z)^4\Delta R}.$$

$$\gamma_{\rm max} = \frac{3mc^2}{4\sigma_T U_{\rm CMB}\Gamma(1+z)^4\,\theta d}$$

$$\gamma_{\rm max} = \frac{10^7}{\Gamma_1\theta_{-1}d_2(1+z)^4}$$

Continuous or discrete flow?

GK04 assume a continuous flow

BUT

….

Alternatives to the IC/CMB:

Synchrotron from complex electron distributions:

From cooling…

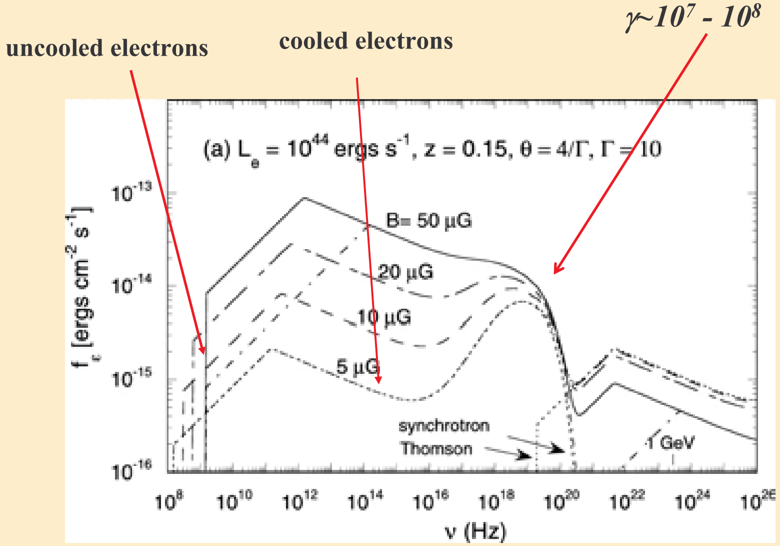

Dermer & Atoyan 2002

…or from acceleration

Multiple shocks or turbulence (Stawarz et al. 2004):

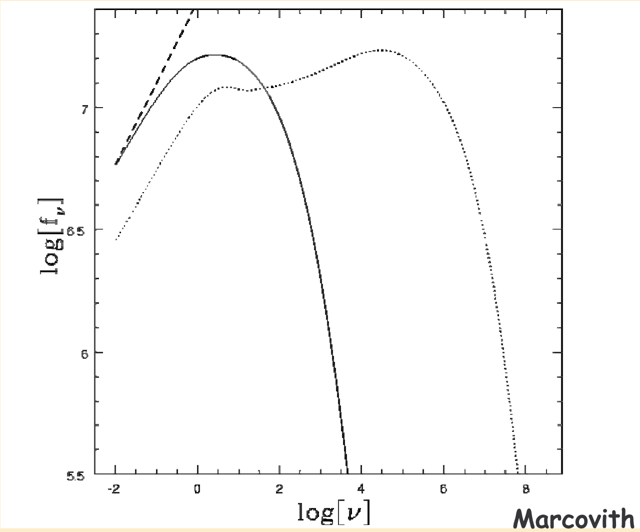

Marcovith & Kirk 1999

Synchrotron from another electron component or from HE protons…

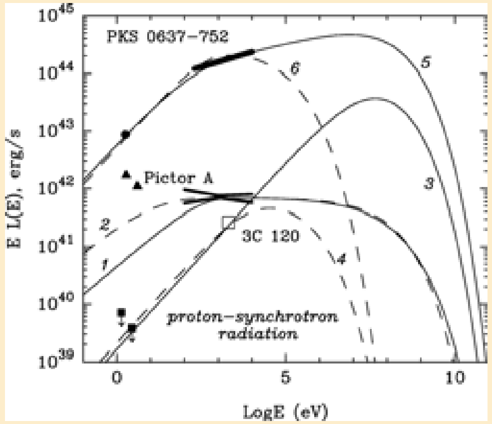

Aharonian 2002

Secondary electrons could be produced through $p-\gamma$ or p-p

inefficient, Urad quite small

a density of ~1 part/cm^3 is necessary

Aharonian 2002

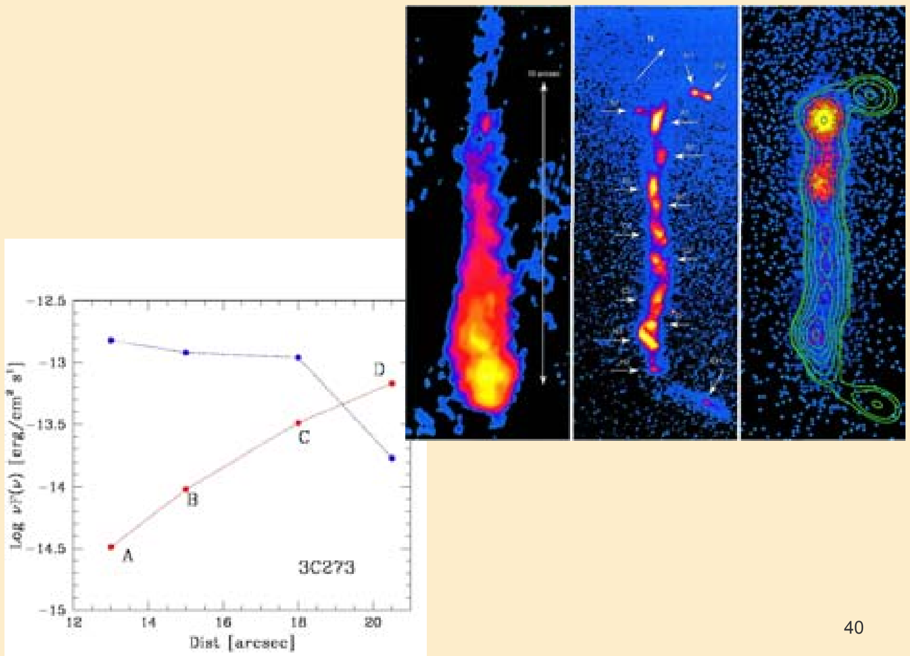

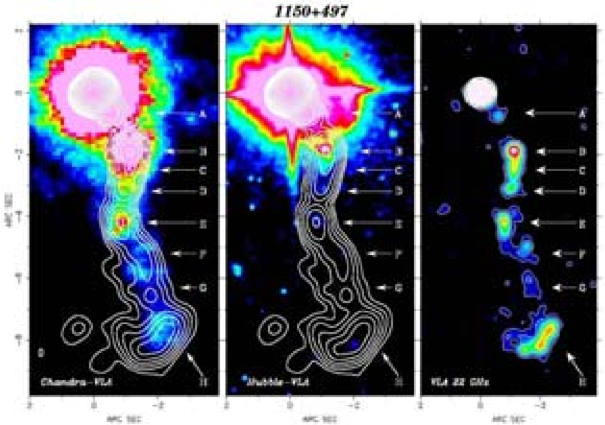

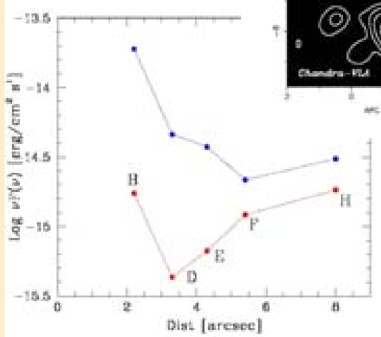

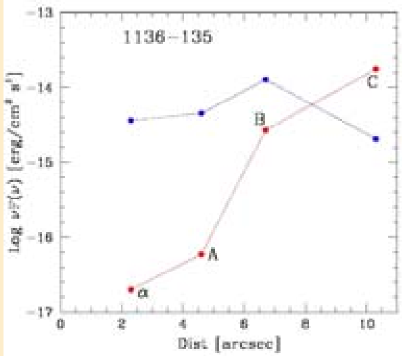

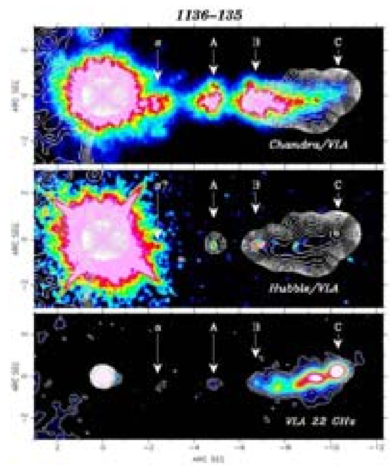

Amplification of the emission

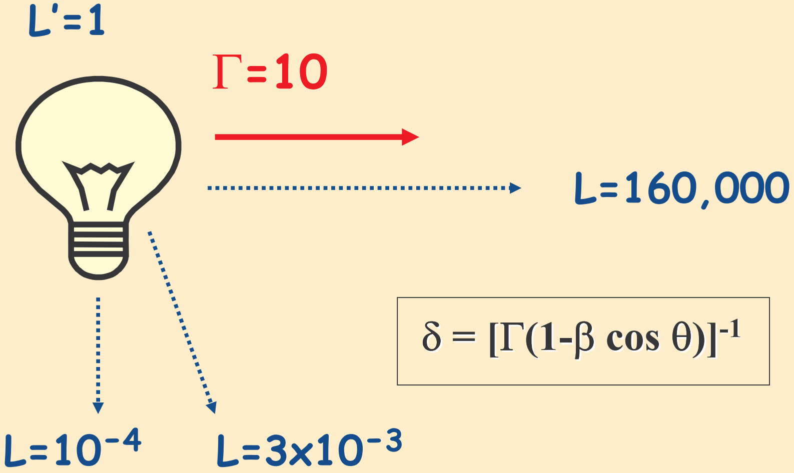

$$\delta = [\Gamma(1-\beta \cos \theta)]^{-1}$$

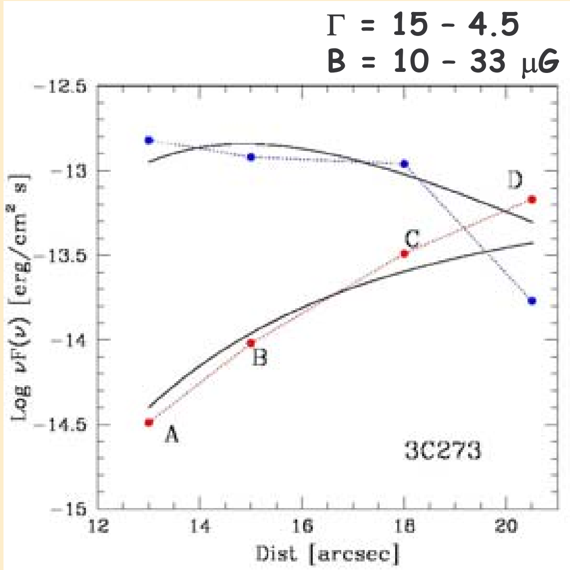

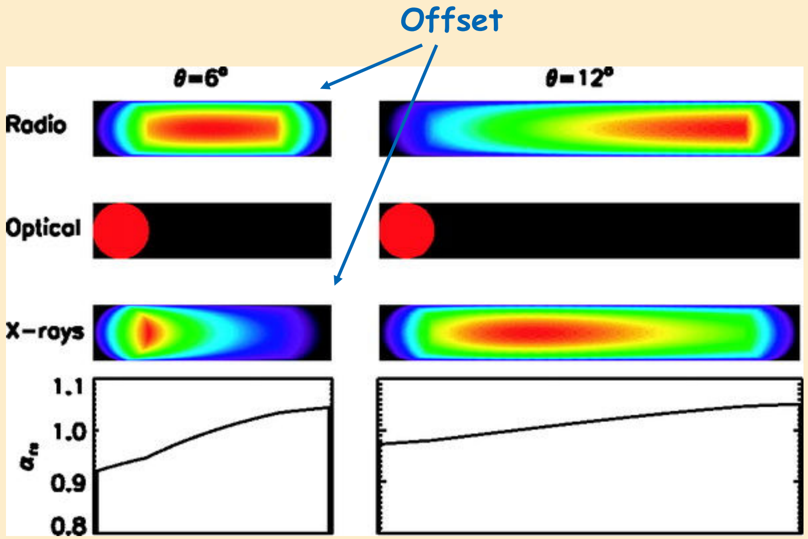

G&K04

But not in all the cases...

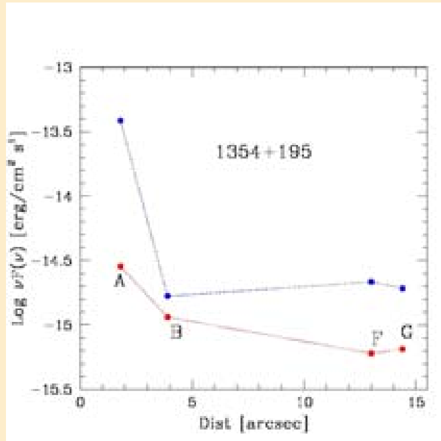

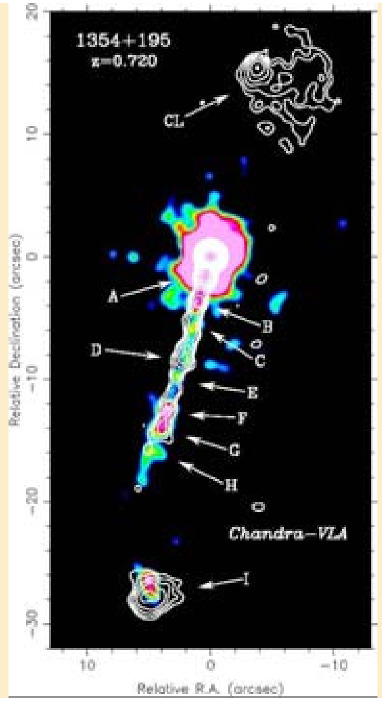

PKS1127-145 *Siemiginowska et al. 2002*

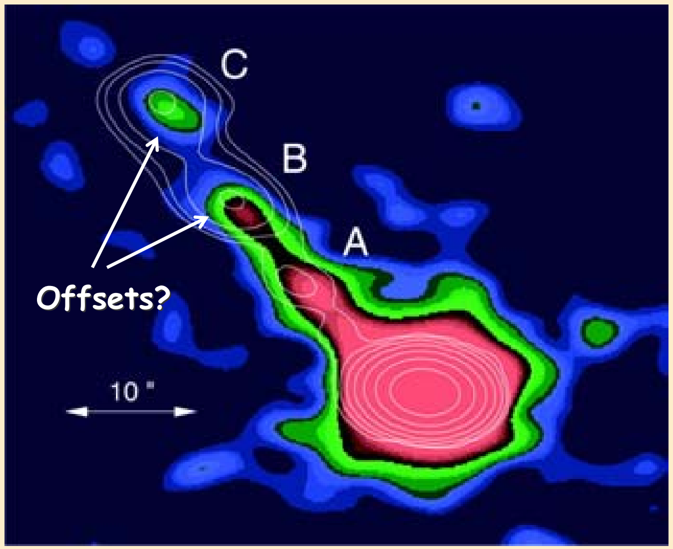

Is 10^{47-48} erg/s too large?

Blazars:

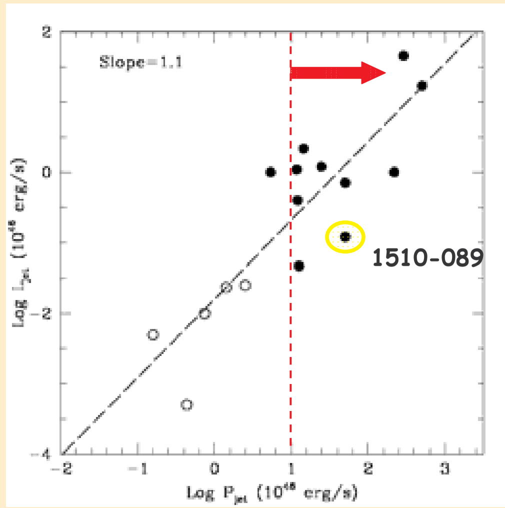

Maraschi & Tavecchio 2003

Evidence for *small angles* from superluminal motions:

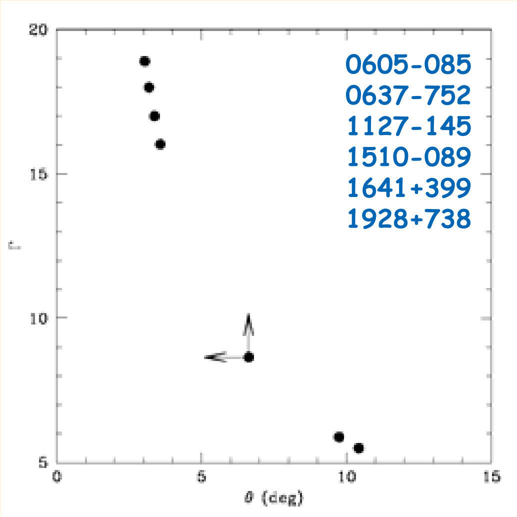

Parameter space

$\delta \sim 10$ → small θ~5 deg, Γ~10

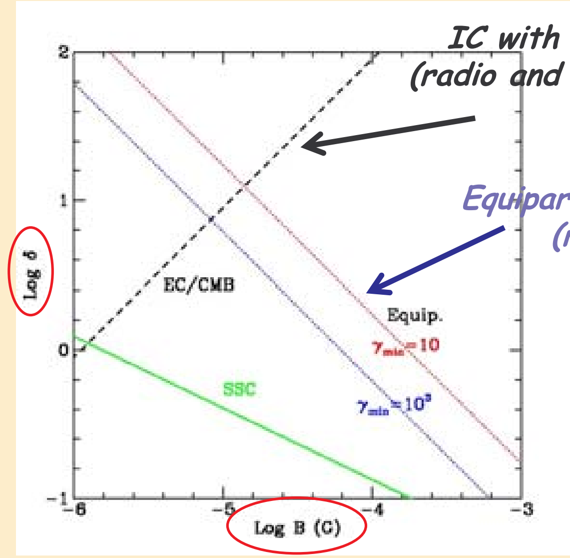

Jets: from the BH to large scale

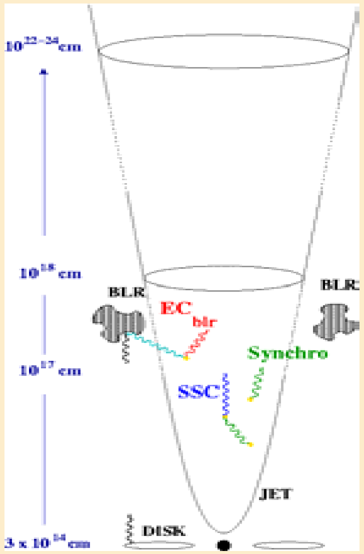

Resolved X-ray jet

VLBI region

Blazar emission region

Accretion region

Enigmas from Jet Formation Processes

or A Jet Formation Cookbook

José Gracia, IASA Athens
Kanaris Tsinganos, Univ Athens
Nektarios Vlahakis, Univ Athens
Theory Gang @ LSW, Heidelberg

Enigma Meeting 6-8 Oct 2004, Perugia

Outline

The ingredients

Ingredients for successfull(?) jet formation

- collimation
- acceleration
- mass loading
- *compatible with accretion flow*

The tools

- large-scale ordered magnetic field
  - magneto-centrifugal mechanism
  - Blandford & Payne 1982 (Heyvaerts, Krasnopolsky, Bogovalov, Tsinganos, Vlahakis, Camenzind, etc)
- small-scale turbulent magnetic field
  - magneto-rotational instability
  - outflows only by-product
  - Balbus & Hawley (Mineshige et al, Shibata et al, Theory@LSW)
- other
  - thermal pressure
  - radiation

The Blandford-Payne recipe

- take large-scale magnetic field in vertical direction
- anchor field lines at base
- stirr the base $\rightarrow$ rotation $\rightarrow B_\phi$
- hoop-stress (B_ϕ-loops) $\rightarrow$ magnetic pinching $\rightarrow$ **collimation**
- conversion of magnetic poynting-flux to kinetic energy $\rightarrow$ **acceleration**

Does it taste like collimation?

Simple model (Bogovalov & Tsinganos 1999):

- anchor radial magnetic field at spherical shell
- inject plasma with velocity V_0 along field lines
- *appropriate* boundary conditions at $R = R_0$
- at $t = 0$, start stirring with Ω_0

MOVIE1

- magnetic Alfven waves communicate base with flow upstream
- rapid **collimation** of magnetic field

Does it taste like acceleration?

Not so simple model (Vlahakis et al 2000)

- describe MHD solution in terms of $v(R, \theta) = f(R) \times g(\theta)$
- assume simple self-similar scaling for $f(R)$
- *appropriate* boundary conditions at $\theta = \theta_0$
- solve (numerically) for $g(\theta)$

MOVIE2

- steady state MHD flow crossing all critical points
- conversion of poynting-flux to kinetic energy $\rightarrow$ **acceleration**

Different tastes of mass loading

- ideal MHD: mass-flux proportional to magnetic flux
- need to concentrate large number of mgn field lines in small volume
- but for Blandford-Payne type mass-flux only $< 5\%$ of wind

two simple ideas:

- Two-zone models (Tsinganos & Bogovalov, etc)
  - inner region rotates slower $\rightarrow$ not collimated
  - high mass-load of $> 25\%$
  - collimation by outer standard solution
- high pressure inner region
  MOVIE3 (Stute, JG, Camenzind, submitted)

Different tastes of mass loading

- ideal MHD: mass-flux proportional to magnetic flux
- ield lines in small
- y < 5% of wind

two s

- , etc)
  ed

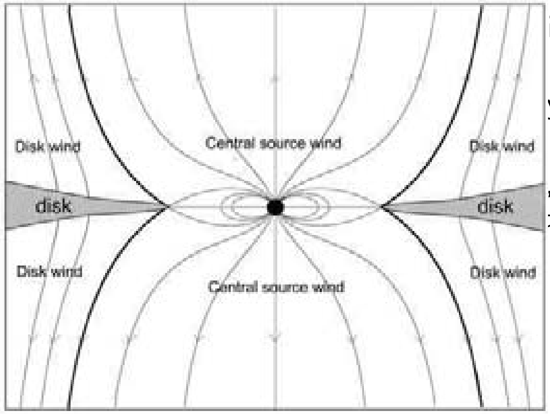

The dessert: accretion flows

so far treated only as *appropriate* boundary condition

- correct ideal MHD relations
- compatible with accretion flow theory

But:

- accretion flows *not* ideal MHD (need field line slipping) $\longrightarrow$ ressistive MHD description
- accretion flows poorly understood
- poor communication between communities

The "Global Model" menu

Casse & Keppens 2002, 2004

- resistive MHD accretion flow
- inner sink region (BH, NS, central engine)
- ideal MHD outflow region

But:
We cannot reproduce the results!
MOVIE4

The "Global Model" menu

Casse & Keppens 2002, 2004

- resistive MHD accretion flow
- inner sink region (BH, NS, central engine)
- ideal MHD outflow region

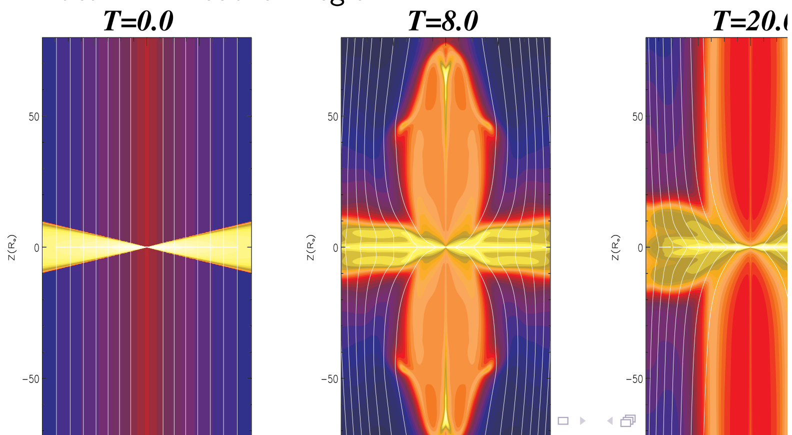

Missing enigmatic spice?

global model does not work

- error in our numerical code?
- some ingredient missing?
- composition not good enough?
- wrong paradigm? We have been cooking this to long

Magnetohydrodynamic Interpretation of Superluminal Jet Kinematics

Nektarios Vlahakis, University of Athens
in collaboration with Arieh Königl, University of Chicago

Outline

- what observations infer
- MHD model
- results

The quasar 3C345

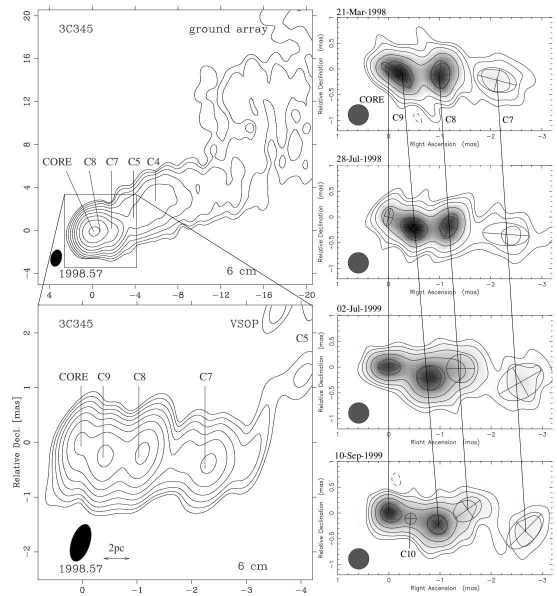

(credit: Klare et al)

The plasma components move with an apparent speed of 3-20c

These plasma components travel on curved trajectories

These trajectories differ from one component to the other

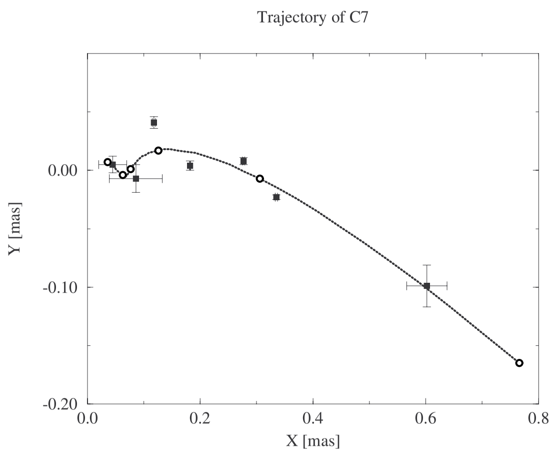

(credit: Lobanov's thesis)

- Superluminal apparent motion $\Rightarrow \beta_{\rm app}$
- Compare radio- and X-emission (SSC) $\Rightarrow \delta$

From $\delta(t_{\rm obs}) \equiv \dfrac{1}{\gamma\,(1-\beta\cos\theta_V)}$ and $\beta_{\rm app}(t_{\rm obs}) = \dfrac{\beta\sin\theta_V}{1-\beta\cos\theta_V}$
we find $\beta(t_{\rm obs})$, $\gamma(t_{\rm obs})$ and $\theta_V(t_{\rm obs})$.

For the C7 component of 3C 345 Unwin et al. (1997) inferred that it accelerates from $\gamma \sim 5$ to $\gamma \sim 10$ over the (deprojected) distance range (measured from the core) $\sim 3-20\ {\rm pc}$. Also the angle θ_V changes from ≈ 2 to $\approx 10^o$ and the Doppler factor changes from ≈ 12 to ≈ 4. ($t_{\rm obs} =$ 1992 – 1993.)

- pc-scale acceleration → nonthermal origin
- Polarization → magnetic fields

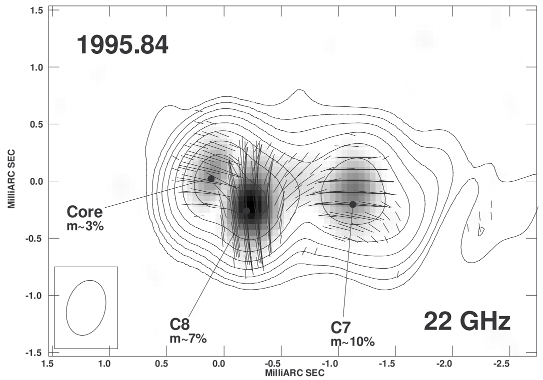

(credit: Ros et al)

- collimation

The MHD model

- We examine outflows taking into account
  - matter
  - large-scale electromagnetic field
- Assumptions:
  - axisymmetry
  - steady-state
  - special relativity
  - ideal MHD
  - r self-similarity (all quantities on the conical disk surface are power laws in r)

(details of the model can be found in Vlahakis & Königl 2003, ApJ, 596, 1080)

First results (Vlahakis & Königl 2004, ApJ, 605, 656)

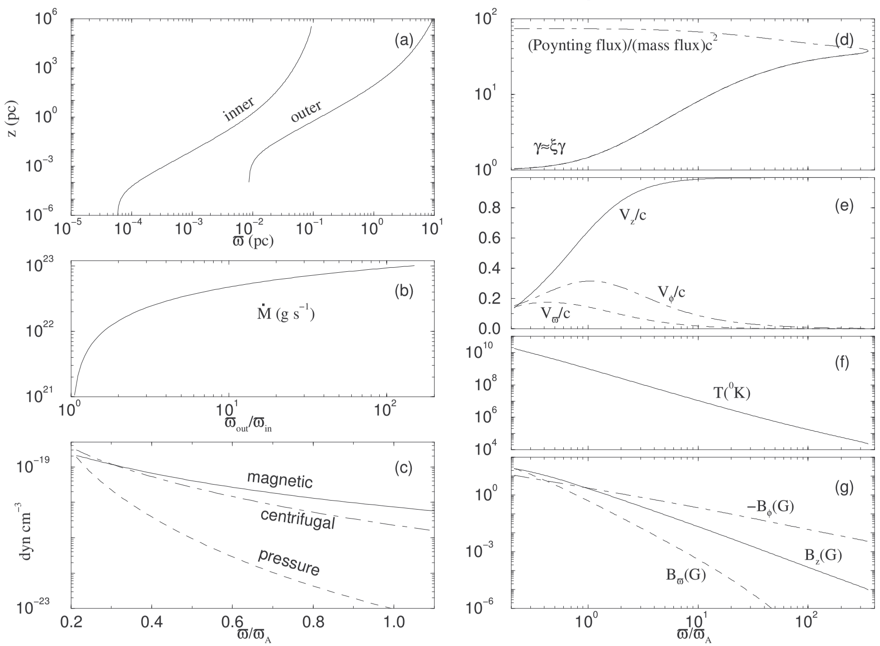

Next step: For given $\theta_{\rm obs}$ (angle between jet axis and line of sight) and ejection area on the disk (r_o, ϕ_o) project the trajectory on the plane of sky and compare with observations. Find the best-fit parameters r_o, $\theta_{\rm obs}$, ϕ_o.

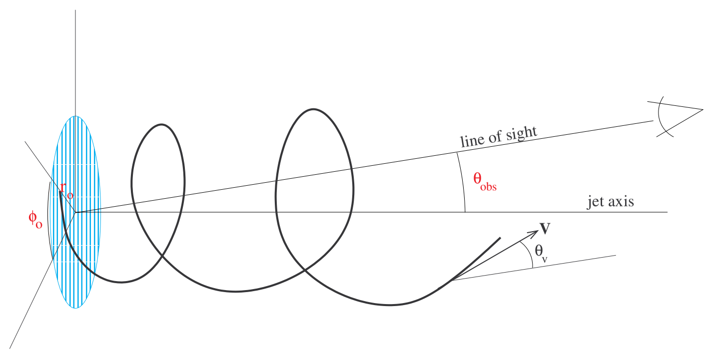

Preliminary results

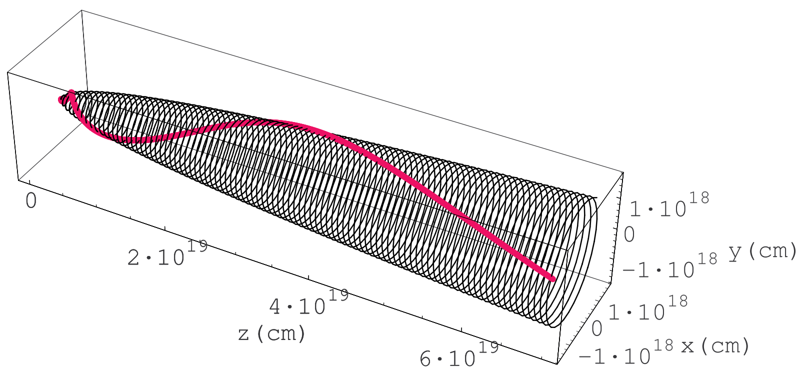

best-fit: $r_o \approx 2 \times 10^{16}$cm, ϕ_o=180^o and $\theta_{\rm obs}$=9^o

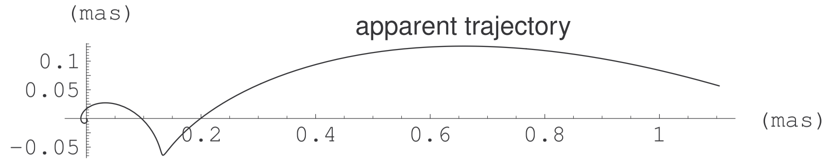

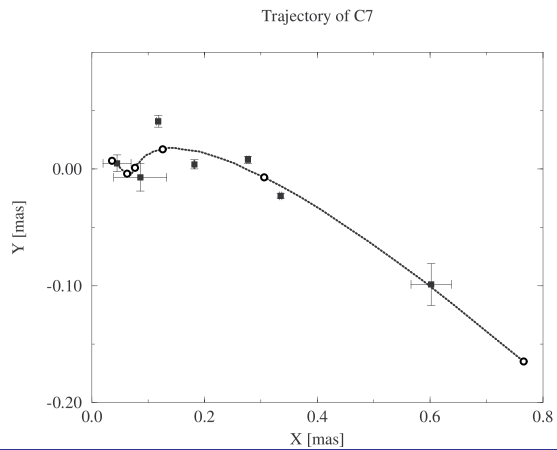

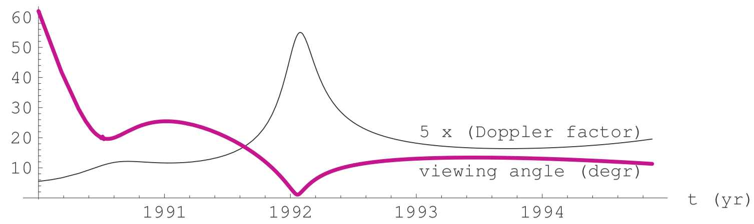

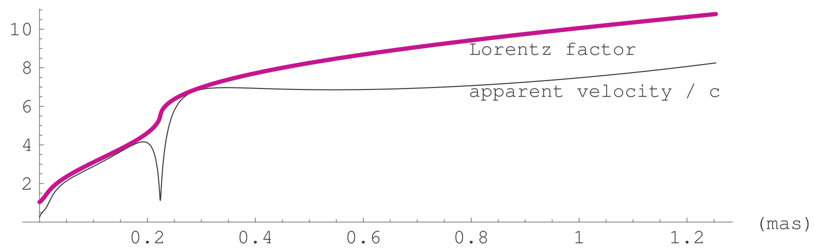

Discussion

- generalization of Camenzind & Krockenberger (1992) (we solve the momentum equation, address the acceleration and collimation)
- other interpretations of the helical trajectories: K-H instabilities (Hardee 2000), binary black hole (Caproni & Abraham 2003) may have contributions, but cannot explain the acceleration
- Next steps:
  - complete the analysis for the kinematics of C7 and the other components in 3C 345 (new data – Klare's thesis)
  - polarization
  - other sources (e.g., 3C 279, 0735+178) show similar behavior

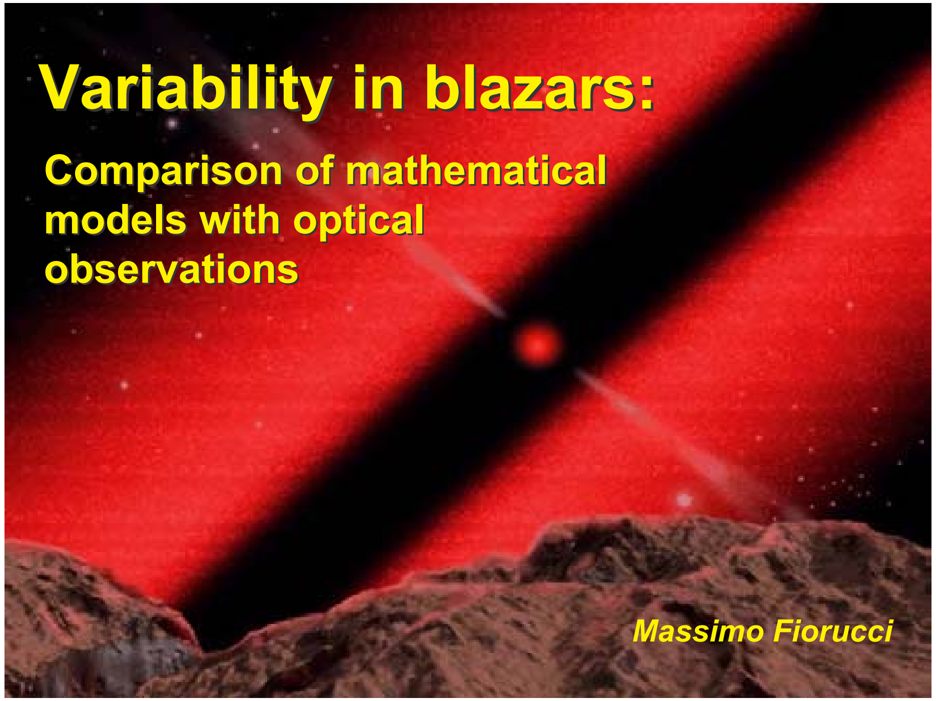

1) introduction

- Blazars are characterised by rapid and large variability at all frequencies
- The study of variability is considered one of the most important tools for exploring the physics of the jet and the AGN central engine
- In the last years, many efforts have been done to establish the presence of periodicity or regularities in the light curves

- However, light curves of blazars often appear to behave "randomly" at all the frequencies and in a large range of time-scales

2) analysis of variability

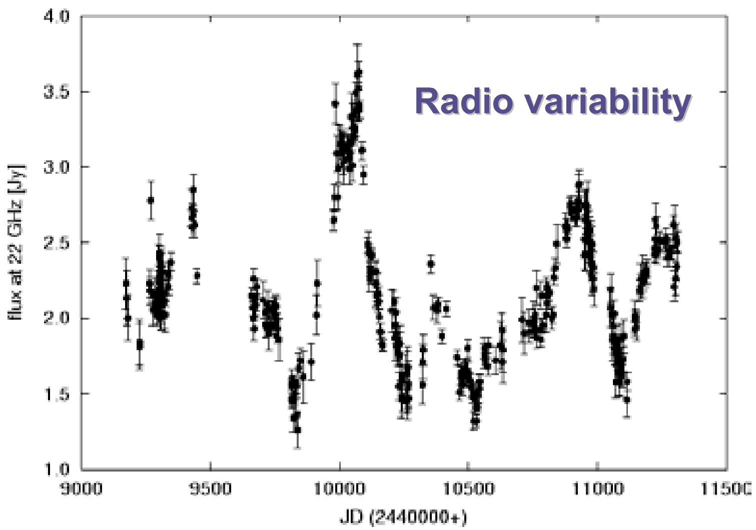

OJ94 Coll. - http://astro.utu.fi/oj94/

2) analysis of variability

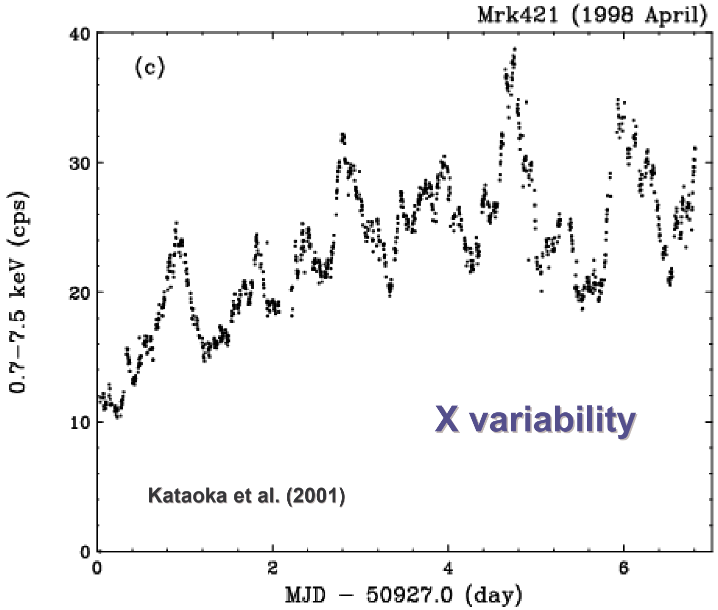

2) analysis of variability

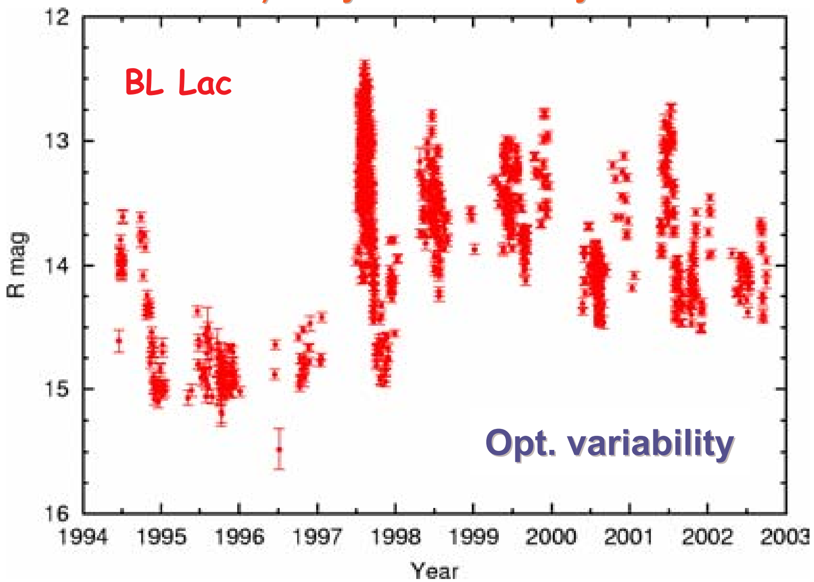

2) analysis of variability

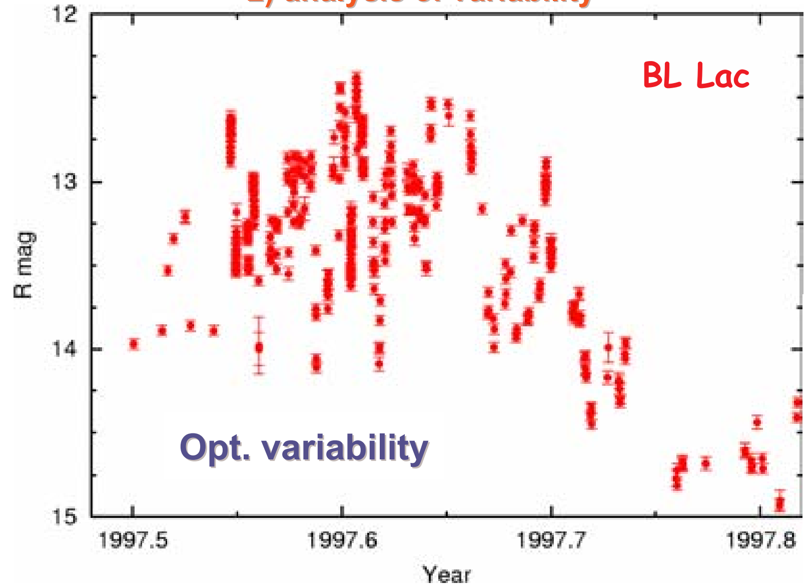

2) analysis of variability

Blazars observed with the AIT since 1994 :

S2 0109+22	PKS 0829+046	3C 345
3C 66A	OJ 287	Mrk 501
AO 0235+164	S4 0954+65	H 1722+119
4C 47.08	Mrk 421	I Zw 187
NGC 1275	OM 280	3C 371
2E 0323+0214	W Com	1ES 1959+650
2E 0414+0057	3C 273	PKS 2032+107
PKS 0422+00	3C 279	BL Lac
S5 0716+71	OQ 530	PKS 2254+074
PKS 0735+17	PKS 1424+24	1ES 2344+514
1ES 0806+524	MS 14588+2249	

2) analysis of variability

Marchili, Fiorucci & Tosti (A&A submitted):

Power Spectral Density (Periodogram)	Scargle (1982)
Discrete Auto-Correlation Function	Edelson & Krolik (1988)
Structure Function (first order)	Simonetti et al. (1985)

work in progress:

Detrended Fluctuation Analysis	Peng et al. (1995)
Wavelet Scalegram	Scargle et al. (1993)

2) analysis of variability

- 23 of the 32 selected blazars show strong variability in the optical bands.
- LBLs show a more pronunced variability with respect to HBLs.
- It is rare to find clear and stable periodicities.
- The amplitude of variability usually increases on time-scales from days to months.

- **Blazar variability seems to be characterised by a power law $PSD \propto f^{-\alpha}$, with the slope within the range α = 1.3-1.9**

2) analysis of variability

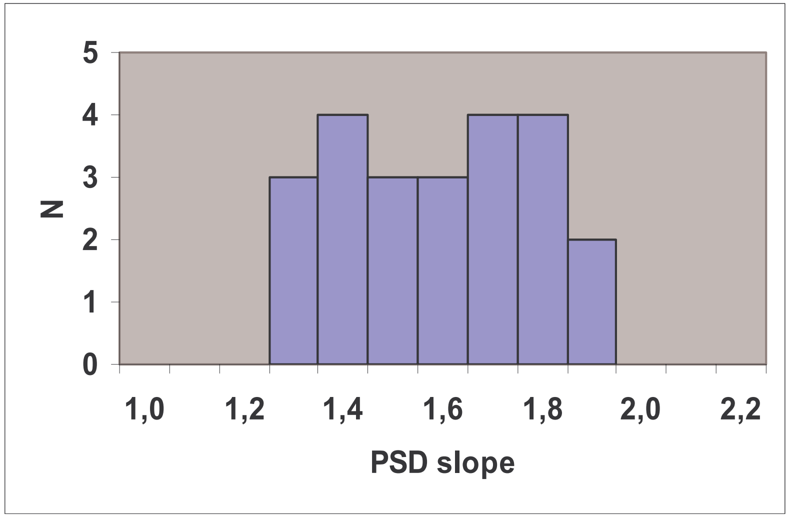

2) analysis of variability

Blazar variability seems to be characterised by a power law $PSD \propto f^{-\alpha}$

Optical:	α = 1.3-1.9	(Marchili, Fiorucci & Tosti, 2004)
Radio:	$\alpha \approx$ 2.0	(Lainela & Valtaoja 1993)
X-rays:	α = 2-3	(Kataoka et al., 2001)
X(AGN):	α = 1-2	(Lawrance & Papadakis, 1993)
GRB:	$\alpha \approx$ 1.6	(Beloborodov et al., 1998)

2) analysis of variability

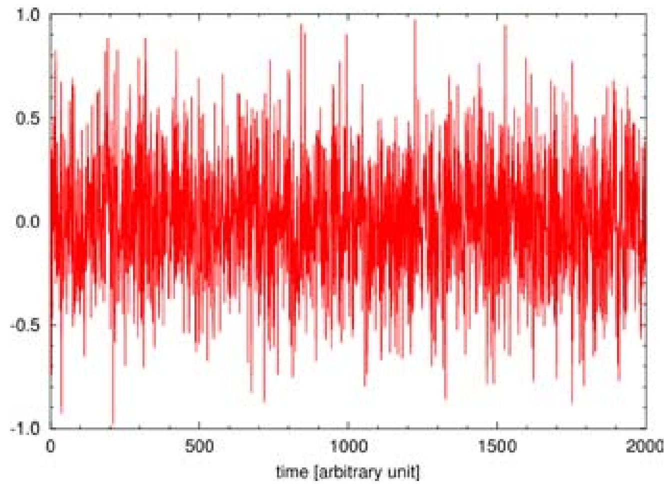

white noise

2) analysis of variability

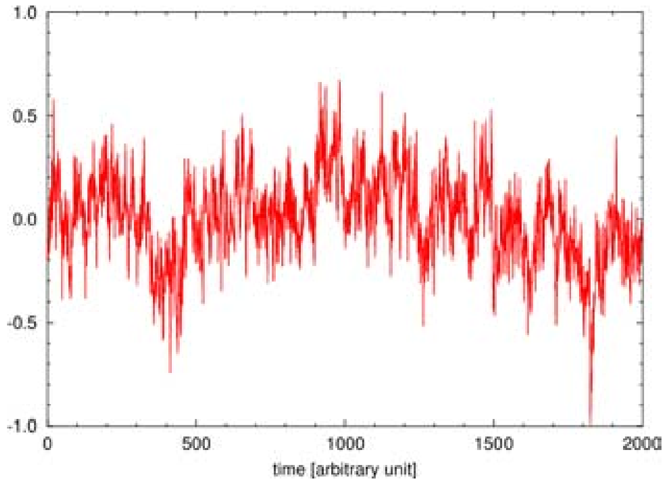

1/f noise

2) analysis of variability

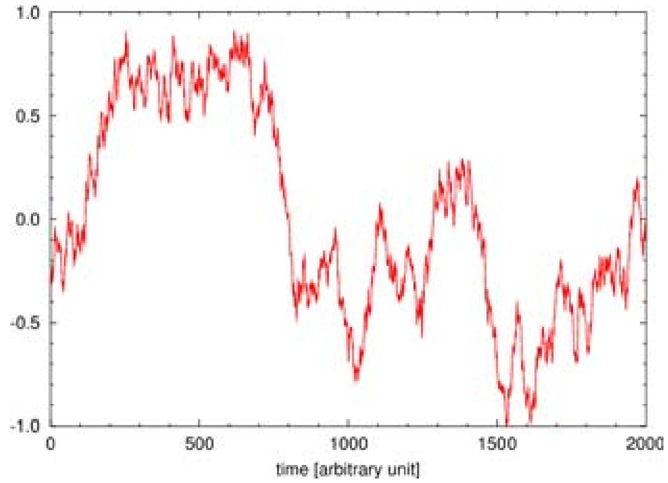

$1/f^2$ noise

2) analysis of variability

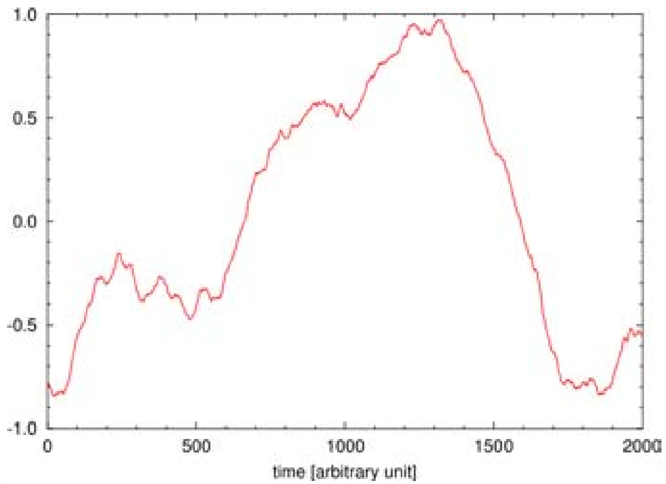

$1/f^3$ noise

3) mathematical models

1) Fractional Brownian motion

Mandelbrot & Wallis (1968)

2) Multiscaled randomness

Hausdorff & Peng (1996)

3) Superposition of relaxation processes

Review of Milotti (2001)

3) mathematical models

1) Fractional Brownian motion

- Consecutive steps in Brownian motion are indipendent of one another. FBm is a generalization of Brownian motion to include memory (history).
- The increments are normally distributed, but they are no longer indipendent.
- FBm is characterized by a parameter H, 0<H<1, that gives the standard deviation of each increment. The power spectral density is $PSD \propto 1/f^{(2H+1)}$
- The "Hurst" exponent (H) characterises the "persistence" of each increment:

1) H<1/2 gives anti-persistent fBm
2) H=1/2 gives standard Brownian motion
3) H>1/2 gives persistent fBm

3) mathematical models

2) Multiscaled randomness

- The output is the summation of multiple random inputs.
- Each input is associated with two parameters: the characteristic time scale and the amplitude.
- If model parameters are unconstrained, the likelihood of generating $1/f^{\alpha}$ noise is quite small.
- If the time scales of the inputs are "structured" and if there is a large number of inputs, then it is very likely that the output will be self-similar over an extended region, with the Power Spectral Density (PSD) that shows:

1) white noise at very low frequencies
2) $1/f^{\alpha}$ noise ($\alpha < 2$) intermediate region
3) $1/f^2$ region at high frequencies

3) mathematical models

3) Superposition of relaxation processes

- A train of random pulses
- Each pulse is modeled by simple exponential relaxation law:

$$N(t,t_k) = N_0 \exp(-\lambda (t-t_k)) \quad \text{for } t \geq t_k$$
$$= 0 \quad \text{for } t < t_k$$

- If the relaxation rate is uniformly distributed between two values λ_1 and λ_2, there are three characteristic regions for the Power Spectral Density (PSD):

1) white noise at very low frequencies
2) $1/f^{\alpha}$ noise ($\alpha < 2$) intermediate region
3) $1/f^2$ region at high frequencies

3) mathematical models

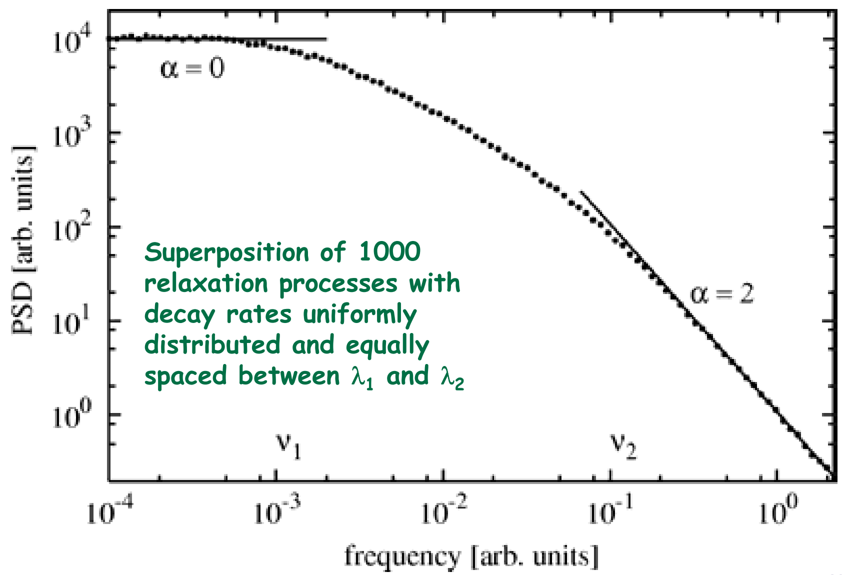

3) mathematical models

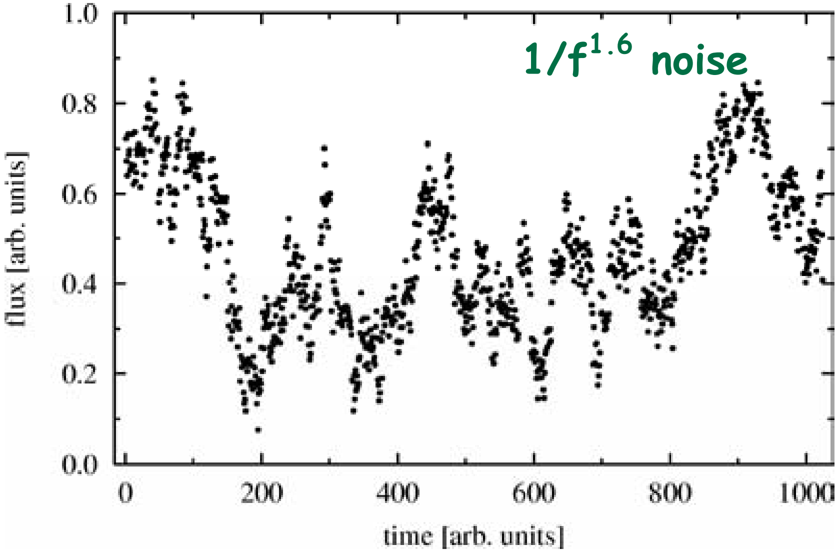

3) mathematical models

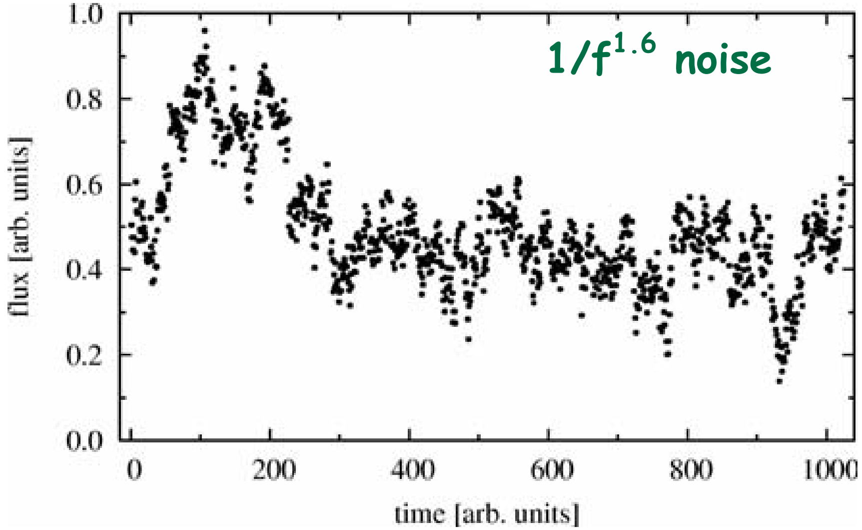

Conclusions

– Many mathematical models are able to reproduce the typical features of blazar variability
– They are all characterized by the presence of a large number of weakly correlated elements which appear at random, live only a short time and decay
– Some basic rule has to be present, otherwise only a $1/f^2$ signal has to be expected
– Many physical scenarios can be called in cause: shocks, blobs, magnetic reconnections, etc.
– It is possible to simulate blazar variability starting from a phenomenological model.

References

- Edelson R. A., Krolik J. H., 1988, ApJ 333, 646
- Grassberger P., Procaccia I., 1983, Phys Rev Lett 50, 346
- Hausdorff J.M., Peng C.-K., 1996, Phys. Rev. E 54, 2154
- Hufnagel & Bregman, 1992, ApJ 386, 473
- Kataoka J., et al., 2001, ApJ 560, 659
- Lomb N. R., 1976, Ap. Space Sci. 39, 447
- Lainela & Valtaoja, 1993, ApJ 416, 485
- Lawrance & Papadakis, 1993, ApJ 414, 85
- Mandelbrot B., Wallis J., 1968, Water Resources Research 4, 909
- Marple S. L., 1987, "Digital Spectral Analysis", Prentice-Hall Inc.
- Peng C. K., et al., 1995, CHAOS 5, 82
- Press W. H., et al., 1992, "Numerical Recipes", Cambridge Univ. Press
- Scargle J. D., 1982, ApJ 263, 835
- Scargle J. D., et al., 1993, ApJ 411, L91
- Simonetti J. H., Cordes J. M., Heeschen D. S., 1985, ApJ 296, 46

Composed in October 2004 by S. Ciprini
Tuorla Observatory, Finland